CRC Press
Taylor & Francis Group

Civil Engineering Innovations for Sustainable Communities with Net Zero Targets

EDITED BY

Sreevalsa Kolathayar, N Vinod Chandra Menon
and Sreekeshava K S

Civil Engineering Innovations for Sustainable Communities with Net Zero Targets

This volume on civil engineering innovations for sustainable communities with net zero targets aligns with the United Nations sustainable development goals in the context of civil engineering innovations. Major topics covered include hydrological alterations under climate change, smart water management, sustainable slope stability solutions, sustainable water management and climate-smart agriculture, conservation of wetlands, influence of phase change materials on thermal properties, building information modeling (BIM) for sustainable and affordable construction, and so forth.

Features:

- Combines concepts of civil engineering and sustainable development for future infrastructures
- Includes hydrological alterations under climate change impacts
- Covers prudent fiduciary discipline and effective cost management in the construction of buildings and critical infrastructure
- Discusses BIM and cost-effective sustainable construction
- Reviews hybrid artificial intelligence in civil infrastructure to attain SDGs #9 (industry, innovation and infrastructure) and #11 (sustainable cities and communities)

This book is aimed at graduate students and researchers in civil engineering, sustainable development, risk management, GIS, and water.

Civil Engineering Innovations for Sustainable Communities with Net Zero Targets

Edited by Sreevalsa Kolathayar, N Vinod Chandra Menon and Sreekeshava K S

CRC Press
Taylor & Francis Group
Boca Raton London New York

CRC Press is an imprint of the
Taylor & Francis Group, an **informa** business

Designed cover image: Shutterstock

First edition published 2025
by CRC Press
2385 NW Executive Center Drive, Suite 320, Boca Raton FL 33431

and by CRC Press
4 Park Square, Milton Park, Abingdon, Oxon, OX14 4RN

CRC Press is an imprint of Taylor & Francis Group, LLC

ISBN: 978-1-032-66201-5 (hbk)
ISBN: 978-1-032-84971-3 (pbk)
ISBN: 978-1-032-68689-9 (ebk)

DOI: 10.1201/9781032686899

Typeset in Times
by Apex CoVantage, LLC

The electronic version of this book was funded to publish Open Access through Taylor & Francis' Pledge to Open, a collaborative funding open access books initiative. The full list of pledging institutions can be found on the Taylor & Francis Pledge to Open webpage.

Contents

SECTION 2: Climate Change

SECTION 4: Sustainable Construction

SECTION 5: Frugal Innovations

Editor Biographies

Dr. Sreevalsa Kolathayar is professor-in-charge of the Institute Innovation Council (IIC) and Associate Professor in the Department of Civil Engineering, National Institute of Technology, Karnataka (NITK) Surathkal, India. He pursued an M.Tech. from IIT Kanpur, Ph.D. from IISc, and served as International Research Staff at UPC Barcelona Tech, Spain. He has authored five books, edited twelve, published over 150 research articles, and holds two patents. He is on the editorial board of several international journals. He is on the roster of two technical committees of the ASCE Geo-Institute and is an Expert Member of the Working Groups of BIS CED 39 for three IS codes. Dr. Sreevalsa has eight funded R&D projects and completed over 100 civil engineering consultancy projects. Dr. Sreevalsa's research interests include earthquake hazard assessment, site characterization, liquefaction, disaster risk reduction, soil reinforcement, slope stabilization, landslide mitigation, and water geotechnics.

Prof. N Vinod Chandra Menon has worked as Professor in the Centre for Disaster Management at the Yeshwantrao Chavan Academy of Development Administration (YASHADA), Pune. He has worked in charge of Emergency Preparedness and Response in the UNICEF India Country Office in New Delhi. He is currently Adjunct Professor at Amrita Vishwa Vidyapeetham, India; President of RedR India; and Regional Director of Asia of the International Emergency Management Society (TIEMS), Oslo. Prof. Menon has over 37 years of working experience, out of which more than a quarter century has been in the fields of disaster risk reduction, climate change adaptation, and public policy analysis. He was a member of the High-Powered Committee (HPC) on Disaster Management established by the Government of India in 1999.

Dr. Sreekeshava K S is currently working as Associate Professor and Head of the Department of Civil Engineering, Jyothy Institute of Technology, Bengaluru. He obtained a Ph.D. from BMS College of Engineering, Visvesvaraya Technological University, Belagavi, in the year 2020. His research interests are in the field of masonry structures, bio-composites, and structural design. He has published more than 30 research articles in reputed journals. He has successfully coordinated funded AICTE-ISTE and AICTE Teaching and Learning (ATAL) Academy Sponsored Faculty Development Programme. He has the honors of life member of the ISET, ISTE, ICI, INSC, NICEE, and IAENG. He has successfully completed the research funding grant under a competitive research funding scheme initiated under the scheme of TEQIP by Visvesvaraya Technological University, Belagavi. Dr. Sreekeshava is the organizing chair of the G20 C20 International Conference on Interdisciplinary Approaches in Civil Engineering for Sustainable Development (IACESD 2023).

Contributors

Minu Treesa Abraham
Instrumentation and Live Monitoring
Norwegian Geotechnical Institute
Oslo, Norway

Md Imran Ahmed
Department of Civil Engineering
R V College of Engineering
Bengaluru, Karnataka, India

K K Akheel
Structural Engineer, OEDEC
Dubai, UAE

S M Basutkar
Department of Civil Engineering
R V College of Engineering
Bengaluru, Karnataka, India

Namratha Bharadwaj
BMS College of Architecture
Bengaluru, Karnataka, India

Deepak M D
School of Construction
NICMAR University, Pune
Maharashtra, India

G Deepika
Centre for Incubation Innovation Research and Consultancy
Department of Food Technology
Jyothy Institute of Technology
Bengaluru, Karnataka, India

Sagnik Dey
Centre for Atmospheric Sciences and
Centre of Excellence for Research on Clean Air
Indian Institute of Technology (IIT) Delhi
New Delhi, India

Dhanush S
Centre For Incubation, Innovation, Research and Consultancy (CIIRC)
Jyothy Institute of Technology
Bengaluru, Karnataka, India

Jagdish H Godihal
Presidency University
Bengaluru, Karnataka, India

Gaurav Jagtap
Department of Civil Engineering
Indian Institute of Technology (IIT) Delhi
New Delhi, India

Deva Jefflin A R
Centre for Incubation, Innovation, Research and Consultancy (CIIRC)
Jyothy Institute of Technology
Bengaluru, Karnataka, India

Ashwin M Joshi
Sustainability, Gleeds Consulting (India) Pvt. Ltd.
Bengaluru, Karnataka, India

Ravi-Kumar Kadeppagari
Centre for Incubation Innovation Research and Consultancy
Department of Food Technology
Jyothy Institute of Technology
Bengaluru, Karnataka, India

Keerthana Kirupakaran
Department of Civil Engineering
Indian Institute of Technology Madras
Chennai, Tamil Nadu, India

Venkatesh Kodur
Department of Civil and Environmental Engineering

Michigan State University
East Lansing, Michigan (MI), USA

Sreevalsa Kolathayar
Department of Civil Engineering
National Institute of Technology
Surathkal, Karnataka, India;
Secretary,
India Chapter IACRR & IGS Surathkal Chapter
Karnataka, India

Lekshmi M S
Department of Civil Engineering
Cochin University of Science and Technology
Kochi, Kerala, India

Mahesh B
Centre for Incubation, Innovation, Research and Consultancy (CIIRC)
Jyothy Institute of Technology
Bengaluru, Karnataka, India

Rajib Maity
Department of Civil Engineering
Indian Institute of Technology Kharagpur
Kharagpur, West Bengal, India

Vasant Matsagar
Department of Civil Engineering
Indian Institute of Technology (IIT) Delhi
New Delhi, India

N Vinod Chandra Menon
Amrita Vishwa Vidyapeetham,
Kollam, India;
International Coordinator,
G20 C20 Working Group on Sustainable and Resilient Communities;
Programme Officer (Emergency),
UNICEF India Country Office;
Founder Member,
National Disaster Management Authority (NDMA), Government of India

Mithun Mohan
Department of Civil Engineering
National Institute of Technology Karnataka
Surathkal, Karnataka, India

Tulika Mondal
Energy & Wetlands Research Group, Environmental Information System
Center for Ecological Sciences [CES]
Indian Institute of Science
Bangalore, Karnataka, India

Paras Negi
Energy & Wetlands Research Group, Environmental Information System
Center for Ecological Sciences (CES)
Indian Institute of Science
Bangalore, Karnataka, India

Muhamed Safeer Pandikkadavath
Civil Engineering
National Institute of Technology Calicut
Calicut, Kerala, India

Geetha Priya M
Centre for Incubation, Innovation, Research and Consultancy (CIIRC)
Jyothy Institute of Technology
Bengaluru, Karnataka, India

Raghavendra K R
Centre for Incubation, Innovation, Research and Consultancy (CIIRC)
Jyothy Institute of Technology
Bengaluru, Karnataka, India

Rakshita C
Centre for Incubation, Innovation, Research and Consultancy (CIIRC)
Jyothy Institute of Technology
Bengaluru, Karnataka, India

T V Ramachandra
Energy & Wetlands Research Group, Environmental Information System
Center for Ecological Sciences (CES), Centre for Sustainable Technologies (astra)
Centre for Infrastructure Sustainable Transportation and Urban Planning [CiSTUP]
Indian Institute of Science
Bangalore, Karnataka, India

Narendra Reddy
Center for Incubation, Innovation, Research and Consultancy (CIIRC)
Jyothy Institute of Technology Campus
Bengaluru, Karnataka, India

M V Renukadevi
Department of Civil Engineering
R V College of Engineering
Bengaluru, Karnataka, India

Kusum Saini
Department of Civil Engineering
Indian Institute of Technology (IIT) Delhi
New Delhi, India

Manoj P Samuel
KSCSTE – Centre for Water Resources Development and Management
Kozhikode, Kerala, India

Thottathil Sarathkumar
Offshore Structures
National Institute of Technology Calicut
Calicut, Kerala, India

Neelima Satyam
Department of Civil Engineering
Indian Institute of Technology Indore
Indore, Madhya Pradesh, India

G Sethulakshmi
Department of Civil Engineering
National Institute of Technology Karnataka
Surathkal, Karnataka, India

Bharath Setturu
Energy & Wetlands Research Group, Environmental Information System
Center for Ecological Sciences (CES)
Indian Institute of Science
School of Mathematical and Natural Sciences
Chanakya University
Bangalore, Karnataka, India

Jiten Shah
Department of Civil Engineering
Institute of Infrastructure, Technology Research and Management (IITRAM)
Ahmedabad, Gujarat, India

Gunwant Sharma
Department of Civil Engineering
Malaviya National Institute of Technology
Jaipur, Rajasthan, India

Poonam Shekhawat
Department of Civil Engineering
Jyothy Institute of Technology
Bangalore, Karnataka, India

Rao Martand Singh
Department of Civil and Environmental Engineering
Norwegian University of Science and Technology
Høgskoleringen, Trondheim, Norway

Sreekeshava K S
Department of Civil Engineering
Jyothy Institute of Technology
Bengaluru, Karnataka, India

J S Sudarsan
School of Energy and Environment
NICMAR University, Pune
Maharashtra, India

U Surendran
KSCSTE – Centre for Water Resources Development and Management
Kozhikode, Kerala, India

Priyank Trivedi
Department of Civil Engineering
Institute of Infrastructure, Technology Research and Management (IITRAM)
Ahmedabad, Gujarat, India

Subha Vishnudas
Cochin University of Science and Technology
Kochi, Kerala, India

Jitendra Singh Yadav
Department of Civil Engineering
National Institute of Technology
Kurukshetra, Haryana, India

Foreword

I am very delighted that CRC Press of the Taylor & Francis Group has decided to publish *Civil Engineering Innovations for Sustainable Communities with Net Zero Targets* edited by Dr. Sreevalsa Kolathayar, Associate Professor, Department of Civil Engineering, National Institute of Technology Karnataka (NITK), Suratkal; Prof. N Vinod Chandra Menon, Founder Member, National Disaster Management Authority (NDMA), Government of India and International Coordinator, C20 Working Group on Sustainable and Resilient Communities: Climate, Environment and Net Zero Targets; and Dr. Sreekeshava K S, Associate Professor and Head of the Department of Civil Engineering, Jyothy Institute of Technology (JIT), Bengaluru. The chapters in this publication have been contributed by eminent academics, domain experts and practitioners from Indian Institutes of Technology (IITs), National Institutes of Technology (NITs), engineering colleges, private sector firms and universities in India. I am sure that this publication will be useful for faculty members, research scholars and students in engineering colleges, technical institutions and universities in India and other countries.

Recently, the people of Türkiye, Libya and Syria began their long road to recovery from disasters. The tragic circumstances of these disasters could have been avoided or the impacts reduced through innovative measures provided by the civil engineering community. We need to ensure that the solutions in the academic world reach the practitioners and the policy makers, so they can be fully integrated into development plans, and all kinds of risks can be avoided or reduced. I am sure this publication is an example of the way forward to enhance sharing of knowledge among sectors and among countries.

International cooperation is the foundation on which we can build an all-of-society approach to strengthen resilience at all levels and across all sectors, to help and support the neediest and the most vulnerable. A recent midterm review of the implementation of the Sendai Framework makes for sober reading. It calls for a major 'course correction' that will be deeply challenging in order to prevent and reduce the negative impacts of disasters and climate change. I am happy to note that this publication can contribute to make the 'course correction' possible.

I hope that this publication by CRC Press will encourage more cross-border collaboration between academics and practitioners in India and in the G20 member countries, promote multi-country research and consulting in areas of mutual interest and facilitate wider dissemination and outreach across the institutions in the G20 member countries, G77 member countries and G7 member countries and the member states of the United Nations. Most developing countries in the Global South can benefit through the experience sharing of professional expertise with institutions in the Global North. As the world is becoming increasingly multipolar, the interactions by G20 engagement groups have helped in sharing the innovations in development pathways by countries in the Global South and the exemplars from the best practices in reducing the greenhouse gas emissions, improving the transition to new and renewable energy sources, and identifying opportunities for reducing the carbon footprint by countries in the Global South.

I wish to convey my appreciation and congratulations to the editors of this very timely and needed publication and wish the publication all success by reaching out through the libraries of the academic and technical institutions and universities in India and the world. I also hope that this publication will receive the attention of policy makers, decision makers and technical education experts, and that this book will be considered as a valuable reference book and included in the syllabus of technical courses in India and around the world.

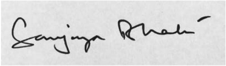

Sanjaya Bhatia

Incheon, Republic of Korea Head of Office,
UNDRR Global Education and Training Institute (GETI)
25 September 2023

Preface

I am very pleased that CRC Press of the Taylor & Francis Group is publishing *Civil Engineering Innovations for Sustainable Communities with Net Zero Targets* edited by Dr. Sreevalsa Kolathayar, Associate Professor, Department of Civil Engineering, National Institute of Technology Karnataka (NITK), Suratkal; Prof. N Vinod Chandra Menon, International Coordinator, C20 Working Group on Sustainable and Resilient Communities: Climate, Environment and Net Zero Targets & Founder Member, National Disaster Management Authority (NDMA), Government of India; and Dr. Sreekeshava K S, Associate Professor and Head of the Department of Civil Engineering, Jyothy Institute of Technology (JIT), Bengaluru. Eminent academics who are faculty members and research scholars in Indian Institutes of Technology (IITs), National Institutes of Technology (NITs), engineering colleges and universities in India have contributed their insights through their chapters. The increasing frequency of disasters, extreme events and climate change in recent years have posed enormous damage to buildings, infrastructure and assets. I am confident that the civil engineering innovations covered in this publication will be very valuable to teachers and students of engineering in India and abroad.

Frugal innovations and disruptive technologies adopted by engineers in the construction practices in several countries have demonstrated the strength of new building materials, which offer nature-based solutions. Construction of houses, roads, flyovers, bridges and critical infrastructure like installations for power supply, water supply etc. must be multi-hazard resilient and agile in responding to changes in weather patterns. I hope that this publication will provoke reflection among researchers and practitioners to search for sustainable development pathways and transition to new and renewable energy sources. I hope this publication will receive the attention it highly deserves. I want to convey my best wishes to the editors and authors of chapters in this publication for wider dissemination of their ideas.

Ambassador Vijay K Nambiar, IFS (Retd),
1 September 2023

Former Under Secretary General, United Nations
Former Indian Ambassador to China and Pakistan

Section 1

Sustainable Development

Taylor & Francis
Taylor & Francis Group
http://taylorandfrancis.com

1 Sustainable Communities with Net Zero Targets
An Introduction

Sreevalsa Kolathayar, N Vinod Chandra Menon and Sreekeshava K S

1.1 INTRODUCTION

No other field has received so much attention from scientific specialists and philosophical speculators than the field of disaster management, which has gained prominence because of the increasing frequency of disasters, climate change, conflicts and extreme events and the economic damage caused by them. The field of disaster management (DM) has evolved in the past few decades as a multi-disciplinary, trans-disciplinary and inter-disciplinary field by bringing together several streams in the Arts, Sciences, Humanities, Engineering, Technology, Law, and even Spirituality and Compassion. In July 1979, the United Nations Disaster Relief Coordinator convened the meetings of an International Expert Group to take stock of the work in the field of disaster management by the United Nations and other stakeholder groups. The deliberations of the International Expert Group provided the impetus for the formulation of the International Framework for Action for the International Decade of Natural Disaster Reduction (IDNDR) from 1990 to 2000 and the establishment of the United Nations International Strategy for Disaster Reduction (UNISDR) as the predecessor of the United Nations Office for Disaster Risk Reduction (UNDRR). Even though the United Nations Decade 1990 to 2000 was declared as the IDNDR, it took several years for disaster management practitioners to argue that the term "natural disasters" is a misnomer as most disasters happen because of human interference with nature and human activities such as construction in floodplains, unstable slopes and river banks etc., without recognizing the multi-hazard nature of geographical areas. There have been efforts by agencies like the UNDRR in the recent years of the 21st century to argue that while natural hazards exist in different geographies, they can be prevented from becoming disasters. However, there is a felt need for creating greater public awareness among stakeholder groups who erroneously use the term natural disasters without recognizing the human origins of most disasters.

Even though Rachel Carson wrote her much acclaimed book *Silent Spring* in 1962, it became recognized as a book giving the early warning signals of the climate

DOI: 10.1201/9781032686899-2

emergency only much later (Carson, 1962). The relationship between disaster management and climate change was understood, and efforts to ensure that development planning initiatives must be sensitive to the multi-hazard risks of the ecosystems and the risk and vulnerability faced by the geographies to climate change were argued by multi-disciplinary professionals only in recent years. Earth Day was first observed on April 22, 1970, six years after her death. The domestic production of DDT was banned in the United States much later, after a series of investigations into the harmful effects of DDT on human beings and the environment at large highlighted the adverse effects of DDT.

1.2 SUSTAINABLE DEVELOPMENT

The choice of Gro Harlem Brundtland, former Prime Minister of Norway, who also had served several years as the Environment Minister of Norway, by the United Nations Secretary General in 1984 to chair the World Commission on Environment and Development (WCED) was very strategic. The WCED was mandated to formulate a global agenda for change, which will address the following objectives:

- "to propose long-term environmental strategies for achieving sustainable development by the year 2000 and beyond;
- to recommend ways concern for the environment may be translated into greater co-operation among developing countries and between countries at different stages of economical and social development and lead to the achievement of common and mutually supportive objectives that take account of the interrelationships between people, resources, environment, and development;
- to consider ways and means by which the international community can deal more effectively with environment concerns;
- and to help define shared perceptions of long-term environmental issues and the appropriate efforts needed to deal successfully with the problems of protecting and enhancing the environment, a long term agenda for action during the coming decades, and aspirational goals for the world community."

(WCED, 1987)

The WCED Report aptly titled "Our Common Future" became very popular for its profound definition of sustainable development as "development that meets the needs of the present without compromising the abilities of future generations to meet their needs" (WCED, op. cit.).

India has overtaken China as the country with the largest population in the world, and the world population has crossed the 8 billion mark now. The challenges posed by poverty, deprivation, unemployment, malnutrition and the dwindling doubling time of populations of countries in the world have serious implications for poverty reduction and the achievement of the other Sustainable Development Goals (SDGs) formulated by the United Nations in 2015.

1.3 CLIMATE CHANGE

One of the major outcomes of the WCED Report was the United Nations Conference on Environment and Development (UNCED), popularly known as the Earth Summit, in Rio de Janeiro in 1992, to create greater awareness among world leaders on the importance of policy agenda to protect the environment through conscious development pathways which highlight preservation, conservation and regeneration of resources. The Earth Summit resolved to establish the United Nations Framework Convention on Climate Change (UNFCCC) to combat dangerous human interference with the climate system and to stabilize greenhouse gas emissions in the atmosphere. The Rio Declaration in 1992 at the Earth Summit and later the Kyoto Protocol became the guiding principles for the Paris Agreement on Climate Change, which was drawn up in 2015 and endorsed by several national governments.

1.4 DISASTER MANAGEMENT

The disaster management initiatives at the global level received further impetus in the World Conference on Natural Disaster Reduction at Yokohama, Japan, in May 1994. The outcome of the Yokohama Conference was the consensus on the Yokohama Strategy for a Safer World: Guidelines for Natural Disaster Prevention, Preparedness and Mitigation. The Yokohama Strategy consisted of the Principles, the Strategy and the Plan of Action, which was endorsed by the governments attending the World Conference on Natural Disaster Reduction. The establishment of the United Nations International Strategy for Disaster Reduction (UNISDR) in 1999 as the Secretariat for the IDNDR helped in creating greater awareness among national governments, donor agencies and civil society organizations working in humanitarian assistance across the world.

The Indian Ocean Tsunami in December 2004 became a watershed event because of the enormous loss of lives, damage and destruction of houses, public infrastructure and assets in the affected countries. The "Hyogo Framework for Action: Building the Resilience of Nations and Communities to Disasters" (HFA 2005–2015) was drawn up as a global strategy for disaster reduction, which was endorsed by the governments at the World Conference on Disaster Reduction held at Hyogo, Kobe, Japan. One of the major departures from the IDNDR approach was the recognition that disasters are caused by human interference with nature, so anthropogenic factors must be considered while drawing up disaster management plans to prepare for, respond to and recover from disasters.

The Hyogo Framework for Action identified five priorities:

- Ensure that disaster risk reduction (DRR) is a national and a local priority with a strong institutional basis for implementation
- Identify, assess and monitor disaster risks and enhance early warning
- Use knowledge, innovation and education to build a culture of safety and resilience at all levels
- Reduce the underlying risk factors
- Strengthen disaster preparedness for effective response at all levels

1.5 MILLENNIUM DEVELOPMENT GOALS (MDGs) 2005–2015

The United Nations formulated the Millennium Development Goals (MDGs) to address the major challenges facing humanity, and the time period for implementation of the MDGs was also to coincide with the HFA period of 2005–2015. The eight MDGs were the following:

1. Eradicate extreme poverty and hunger
2. Achieve universal primary education
3. Promote gender equality and empower women
4. Reduce child mortality
5. Improve maternal health
6. Combat HIV/AIDS, malaria and other diseases
7. nsure environmental sustainability
8. Global partnership for development

1.6 RIO+20 OR UNITED NATIONS CONFERENCE ON SUSTAINABLE DEVELOPMENT (UNCSD)

The United Nations Conference on Sustainable Development (UNCSD) was convened as a Rio+20 event after two decades since the Earth Summit in Rio de Janeiro. The UNCSD resolved to start working towards the SDGs, which were to be drawn up to accelerate the efforts made on the MDGs.

In spite of the efforts by national governments, donor agencies and civil society organizations and other stakeholder groups, the slow progress in the achievement of the MDGs compelled the United Nations to forge a consensus among world leaders for working towards the achievement of 17 SDGs during the period 2015–2030.

1.7 SUSTAINABLE DEVELOPMENT GOALS (SDGs) 2015–2030

The 17 SDGs are the following:

1. No Poverty
2. Zero Hunger
3. Good Health and Well Being
4. Quality Education
5. Gender Equality
6. Clean Water and Sanitation
7. Affordable and Clean Energy
8. Decent Work and Economic Growth
9. Industry, Innovation and Infrastructure
10. Reduced Inequalities
11. Sustainable Cities and Communities
12. Responsible Consumption and Production
13. Climate Action
14. Life Below Water

15. Life on Land
16. Peace, Justice and Strong Institutions
17. Partnerships

The 15-year timeframe for the initiatives for the achievement of targets of the SDGs from 2015 to 2030 coincides with the 15-year time frame from 2015 to 2030 of the Paris Agreement on Climate Change, Sendai Framework for Disaster Risk Reduction (SFDRR) and the New Urban Agenda. These four frameworks have a very close relationship with each other, as the underlying context of multi-hazard risk, vulnerability and exposure of communities in disaster-prone countries make it a critical imperative to ensure that disaster risk reduction is integrated with the development efforts while designing and implementing proposals for the construction of houses, public infrastructure and assets.

The UNESCAP Report on the midterm review of the SDGs in Asia Pacific found that all of the SDGs except SDG 13 on Climate Action have shown progress, while SDG 13 showed that it has regressed from the 2015 baseline figures (ESCAP, 2023).

The United Nations Secretary General Antonio Guterres has called on world leaders to accelerate efforts to achieve the targets of the SDGs, because the SDGs have succeeded in achieving only some of the goals in some countries, and the SDGs have regressed from the baseline figures of 2015 in some cases. At the high-level political forum on sustainable development convened at the 78th Session of the General Assembly of the United Nations, the political declaration adopted by the member states resolved to accelerate the efforts for working to achieve the targets of the SDGs and to contribute funds to strive for getting the efforts on track in the member states. The member states of the United Nations will have to make conscious efforts to pursue the Agenda 2030 and accelerate the efforts to achieve the targets of the SDGs in the coming years.

1.8 NATURAL RESOURCE MANAGEMENT

The United Nations Environment Program (UNEP) has declared the decade 2022 to 2032 as the United Nations Decade for Eco-system Restoration to promote Nature-based Solutions (NbS) in fragile ecosystems. It has been found that several communities are developing innovative solutions for conserving and regenerating ecosystems with good practices and disruptive frugal innovations. Traditional knowledge systems of Indigenous communities are being applied to develop seed banks of traditional varieties, promote the cultivation of millets and encourage the utilization of low-cost building materials which are eco-friendly. The documentation of oral traditions on natural resource management by elders is also being attempted, as these traditions have been found to have coping mechanisms to address desertification, drought and famines by communities.

1.9 FOUR GLOBAL FRAMEWORKS 2015–2030

The year 2015 saw the member states of the United Nations endorse four global frameworks to be implemented during the timeframe 2015 to 2030: UNDESA's

Sustainable Development Goals (SDGs); UNFCCC's Paris Agreement on Climate Change; UNDRR's Sendai Framework for Disaster Risk Reduction (SFDRR); and the UNHABITAT's New Urban Agenda. At the mid-point of the 15-year period of these frameworks, the review reports on these frameworks found that the countries have to redouble their efforts to achieve the targets of these framework agreements, because most of them have woefully failed in implementation of the policies needed to achieve the targets. Most targets were off-track, and the global pandemic COVID-19 or SARS Cov-2 had worsened the vulnerability of weaker sections in most countries impacted by the pandemic. Poverty, unemployment, malnutrition and access to water security, energy security and food security of the weaker sections had been adversely affected in several developing countries during the pandemic years.

1.10 WOMEN-LED DEVELOPMENT

Affirmative action through policies promoting gender equality and women empowerment is essential to ensure inclusive development pathways. It has been found that women-led development strategies are likely to achieve promising results by ensuring participation, ownership and effective implementation of empowering development initiatives as women show empathy and compassion to promote inclusive and participatory processes. As the world is facing increasing frequency of disasters, extreme events, climate change and conflicts, there is a greater need to explore approaches which facilitate engagement with local communities and stakeholder groups. Documentation of good practices of women empowerment will also be helpful to widely disseminate them among communities to strengthen their resilience to face shocks like disasters, extreme events, climate change and conflicts.

1.11 VULNERABILITY REDUCTION IN SUSTAINABLE AND RESILIENT COMMUNITIES

The resilience building of vulnerable sections by engaging with other stakeholder groups is essential by understanding the socio-economic and demographic profile of the communities so that the weaker sections can be identified. Communities are not homogenous entities, and there are large variations in caste, class, gender and other parameters. There can also be differential vulnerabilities if a woman-headed household has an elderly person who is bedridden or if there are any children who are differently abled or suffering from any terminal illnesses and undergoing treatment. The vulnerable sections in the local communities include the following:

- Elderly people
- Bed-ridden and wheelchair-bound people
- Differently abled people
- People suffering from debilitating diseases
- Palliative care patients
- Pregnant women
- Infants and children

- Unemployed people
- Adolescent girls
- Transgender people
- Refugees and Internally Displaced People (IDPs)
- Minorities and other marginalized and excluded sections
- Women-headed households
- Bonded labour and trafficked child labour
- Victims of conflict and violence
- Poor, deprived and malnourished people, etc.

Large number of civil society organizations are engaged in resilience building of the communities in geographical areas prone to disasters, climate change, extreme events and conflicts. Several corporate sector entities are also providing financial support to such civil society organizations for capacity building and vulnerability reduction of weaker sections through corporate social responsibility funds.

1.12 DISASTER RISK REDUCTION

In 2009, the United Nations International Strategy for Disaster Reduction (UNISDR) published the UNISDR Terminology on Disaster Risk Reduction. The increasing frequency, magnitude and economic impact of disasters, especially climate change–induced hydro-meteorological disasters in recent years, has highlighted the critical imperative of ensuring that disaster risk reduction is mainstreamed in the development planning efforts at the national, provincial and local levels. The revised Terminology for Disaster Risk Reduction was prepared by an Open-ended Intergovernmental Expert Working Group on Indicators and Terminology Relating to Disaster Risk Reduction. In 2015 at Sendai in Japan, the Sendai Framework for Disaster Risk Reduction (SFDRR) 2015–2030 was formulated by the UNDRR and endorsed by several countries, with four priorities and seven targets. The four priorities of the SFDRR are the following:

Priority 1: Understanding disaster risk.
Priority 2: Strengthening disaster risk governance to manage disaster risk.
Priority 3: Investing in disaster risk reduction for resilience.
Priority 4: Enhancing disaster preparedness for effective response and to "Build Back Better" in recovery, rehabilitation and reconstruction.

The seven global targets of SFDRR are the following:

1. Substantially reduce global disaster mortality by 2030, aiming to lower the average per 100,000 global mortality rate in the decade 2020–2030 compared to the period 2005–2015;
2. Substantially reduce the number of affected people globally by 2030, aiming to lower the average global figure per 100,000 in the decade 2020–2030 compared to the period 2005–2015;

3. Reduce direct disaster economic loss in relation to global gross domestic product (GDP) by 2030;
4. Substantially reduce disaster damage to critical infrastructure and disruption of basic services, among them health and educational facilities, including through developing their resilience by 2030;
5. Substantially increase the number of countries with national and local disaster risk reduction strategies by 2020;
6. Substantially enhance international cooperation to developing countries through adequate and sustainable support to complement their national actions for implementation of the present Framework by 2030; and
7. Substantially increase the availability of and access to multi-hazard early warning systems and disaster risk information and assessments to people by 2030.

(UNDRR, 2015)

The member states of the United Nations were expected to submit Annual Reports on their progress in the achievement of the targets. The Global Assessment Reports, which were published by the UNDRR, monitored their progress in the achievement of the targets. The midterm report published by the UNDRR in 2023 observed that

> the average annual disaster-related mortality 2015–2021 is 40,797 people per year. As at March 2022, the average annual number of deaths and missing persons in the event of a disaster per 100,000 people has decreased from 1.77 from the decade 2005–2014 to 0.82 in the decade 2012–2021.
>
> (UNDRR, 2023a)

The fatalities in the global pandemic COVID-19 or SARS CoV-2, which is the mega disaster of our lifetime to date, are not included in the previously cited figures. The pandemic casualty figures have been under-reported by several countries, and the figures compiled by the World Health Organisation (WHO) were contested by a few countries. Accurately registering deaths in disasters needs to be significantly strengthened to ensure that the member states of the United Nations will be able to prepare for, respond to and recover from disasters, extreme events, climate change and conflicts. The Report of the Mid-Term Review of the Implementation of the Sendai Framework for Disaster Risk Reduction 2015–2030 observed that "reiterated commitment and efforts of traditional disaster risk reduction stakeholders, as well as novel collaborations with other stakeholders, are needed to correct course and ensure that the Sendai Framework is fully realized by 2030" (UNDRR, 2023b).

The floods in Greece, Spain, China and Morocco; the wild fires in Canada, Hawaii, California, Arizona and Greece; the earthquakes in Turkiye, Syria, Morocco and Japan; and the flooding in Libya indicate the need for strengthening multi-hazard preparedness by undertaking risk identification, vulnerability assessment, exposure analysis and risk reduction strategies. It is essential that development planning pathways must incorporate disaster risk reduction and climate change adaptation, as the increasing frequency of disasters are resulting in damage to infrastructure and assets, loss of lives, disruption of livelihoods and phenomenal increase in economic damage in developed and developing countries.

1.13 CLIMATE CHANGE ADAPTATION

President Barack Obama posted on Twitter [1040 p.m.: Sept 23, 2014] that "We are the first generation to feel the effect of climate change and the last generation who can do something about it." This quote by President Obama has been attributed to Washington Governor Jay Inslee, who acknowledged Michael Patrick McGinn, Mayor of Seattle, Washington. When the Intergovernmental Panel on Climate Change (IPCC) published their Working Group Report I on the physical science basis for the Sixth Assessment Report, United Nations Secretary General Antonio Guterres said that the IPCC Report is "a code red for humanity."

Global warming, sea level rise, glacier melting, desertification, declining ground water aquifers, extreme events, heatwaves and cold waves, snow avalanches, droughts, wild fires, unprecedented rainfall and cloud bursts, extinction of species and biodiversity shocks are all indications of the climate emergency. Climate change activists have been arguing that climate justice, gender justice and social justice are all closely related and that the vulnerable sections who are suffering because of discrimination and becoming ecological and environmental refugees need support to safeguard them against these climate change–triggered shocks. In the Climate Change Summits COP26 at Glasgow, Scotland, and COP27 at Sharm el-Sheikh, Egypt, the climate change evangelists argued for establishing a Loss and Damage Fund to provide relief to the victims of climate change triggered by the disasters, extreme events, air pollution, emission of greenhouse gases and collapse of sustainable development strategies because of the indiscriminate exploitation of fossil fuels. The climate change advocates from the developing countries in the Global South are critical of climate colonialism and the way the fossil fuel–vested interest groups are aggravating the climate emergency through indiscriminate exploitation of natural resources.

1.14 CLIMATE FINANCE

Several funds have been established for providing support to national governments to initiate projects on climate change adaptation and climate change mitigation. The major climate change adaptation funds are the following:

- Global Environment Facility (GEF)
- Green Climate Fund (GCF)
- Adaptation Fund (AF)
- Special Climate Change Fund (SCCF)
- Least Developed Countries Fund (LDCF)

1.15 CLIMATE CHANGE GLOBAL STOCKTAKE REPORT

The United Nations Framework Convention on Climate Change (UNFCCC) published the synthesis report by the co-facilitators on the technical dialogue of the first global stocktake recently, as agreed by more than 200 countries which endorsed the Paris Agreement on Climate Change in 2015 to initiate efforts to reduce greenhouse gas emissions and global warming. The first global stocktake found that the just transition to new and renewable energy is not happening in most countries as envisaged, and the emissions of greenhouse gases are not getting reduced substantially. The countries which are signatories of the Paris Agreement on Climate Change have to consciously introduce major policy shifts to ensure that the greenhouse gases and carbon emissions will be reduced with active multi-stakeholder engagement. Green mobility, green buildings and energy conservation must be actively promoted.

1.16 NET ZERO TARGETS

In 2015, in the Paris Agreement on Climate Change, the signatories agreed to reduce greenhouse gas emissions to ensure that global warming is kept in check to 1.5 degrees Centigrade above the pre-industrial levels by 2050. This essentially implies that the sources of carbon emissions and the sinks must neutralize each other by bringing it to net zero (Black et al., 2021). Many countries have come up with innovative net zero transition pathways with carbon-offsetting strategies and mechanisms for carbon credits. These pathways are also connected with eco-friendly development strategies and nature-based solutions, exploring alternatives to ecologically degrading approaches like indiscriminate quarrying in coal mines, deforestation, oil drilling, exploitation of fossil fuels, etc.

Countries such as Bhutan are carbon negative. Even to become carbon neutral, countries have to design and implement progressive affirmative action policies which are eco-friendly with multi-stakeholder engagement and active participation. The phasing out of fossil fuels is a demand made by climate change activists, though the fossil fuel lobby will resist any attempt to interfere with their expansion plans. While many countries are developing electric vehicles and automobiles driven with biofuels and even hydrogen, the energy budgets in several developing countries are showing deficits and critical gaps in their access to energy sources.

1.17 JUST TRANSITION TO NEW AND RENEWABLE RESOURCES

"Just Transition" to net zero targets and new and renewable resources is the sustainable development pathway for communities facing the challenges of climate change in a period witnessing global warming, climate extremes and heatwaves. United Nations Secretary General Antonio Guterres said that the world is not facing global warming, but "global boiling." Countries are making efforts to promote power generation by switching to solar energy, wind energy and hydroelectric energy. The efforts to phase out fossil fuels by switching to electric vehicles and sustainable transport through green mobility have received support from governments and other stakeholder groups. The reduction of greenhouse gas emissions and carbon dioxide emissions, simultaneously introducing frugal innovations to strengthen the carbon offsetting, is envisaged to help planet Earth to achieve net zero targets by 2050. Manufacturing processes in industrial units will also have to be gradually shifted in favour of clean energy solutions. Such whole-of-society approaches will be needed to ensure that just transition happens without creating adverse impact on weaker sections and vulnerable communities of the Global South. The demand for honouring the "polluter pays" principle has also received greater consensus among representatives of the civil society organizations, especially among youth and adolescents. There is also increasing demand for climate change activist ombudsmen to monitor greenwashing by vested interest groups.

BIBLIOGRAPHY

Black, R., Cullen, K., Fay, B., Hale, T., Lang, J., Mahmood, S., Smith, S.M. Taking Stock: A Global Assessment of Net Zero Targets. *Energy & Climate Intelligence Unit and Oxford Net Zero*, WCED Our Common Future 1987, 2021.

Carson, Rachel. *Silent Spring*, Houghton Mifflin, Boston, 1962.

ESCAP: *Asia and the Pacific SDG Progress Report Championing Sustainability Despite Adversities 2023*, Bangkok, 2023.

UN: https://press.un.org/en/2021/sgsm20847.doc.htm.

UNDESA: *MDG Gap Task Force Report 2015: Taking Stock of the Global Partnership for Development*, New York, 2015.

UNDRR: *Report of the Mid Term Review of the Implementation of the Sendai Framework for Disaster Risk Reduction 2015–2030*, Geneva, 2023a.

UNDRR: *Report of the Open-Ended Intergovernmental Expert Working Group on Indicators and Terminology Relating to Disaster Risk Reduction*, New York, 2016.

UNDRR: *Report on the Main Findings and Recommendations of the Midterm Review Report on the Implementation of the Sendai Framework for Disaster Risk Reduction 2015–2030*, Geneva, 2023b.

UNDRR: *Sendai Framework for Disaster Risk Reduction 2015–2030*, New York, 2015.

UNDRR: *Terminology on Disaster Risk Reduction*, Geneva, 2019.

UNFCCC: *Synthesis Report by the Co-Facilitators on the Technical Dialogue of the First Global Stocktake*, Geneva, 2023.

UNISDR: *Terminology on Disaster Risk Reduction*, Geneva, 2009.

World Commission on Environment and Development (WCED): Brundtland Commission: Our Common Future, Report of the World Commission on Environment and Development, United Nations, Oxford University Press, 1987.

2 Attainment of Sustainable Development Goals through Responsible Utilization of Resources as Building Materials

A Case Study from Kerala State, South India

Subha Vishnudas and Lekshmi M S

2.1 INTRODUCTION

Global development trends today are unsustainable. The biggest reason for this lies with our society's consumption and production patterns. It has been widely recognized since 1992 at the Rio Earth Summit that human beings need to change the way they produce and consume. The United Nations' 2030 Agenda for Sustainable Development readdressed this issue and included as the 12th Sustainable Development Goal—Responsible Consumption and Production. Every human being living on this planet is committed in radically altering the society's practices of producing and consuming goods and services. A paradigm shift from control of nature to cooperation with nature is inevitable (Qureshi and Nawab, 2013). With growing consumption and production, the entire world is getting densely populated, yet at an unprecedented rate, people are altering the Earth's natural system both locally and worldwide (Cruickshank and Fenner, 2007). This has brought up the crucial issue of striking a balance between meeting the requirements of a population that is growing at an exponential rate and protecting our ecosystems' carrying capacity as well as our biological and cultural diversity. Everyone should be aware of the reality that there are environmental limits and our resources are finite (Qureshi and Nawab, 2013). It is the responsibility of engineers to create products and services with the lowest possible consumption of raw materials, water and energy. One of the means to achieve this is to reduce waste production through effective utilization of resources.

Earth is a versatile and sustainable material, which is often obtained as waste in construction sites, reducing cost and energy for transportation (Gomes et al., 2018).

DOI: 10.1201/9781032686899-3

The potential of mud as a building material has been very much explored in ancient times, and it is still being practiced in many European, Arab and Egyptian countries (Lekshmi et al., 2017). The magnificent buildings carved out of earth, such as Ziggurates of Mesopotamia (4100 BCE–2334 BCE), the Great Mosque of Djene, Mali (13th–14th century) and the Great Wall of China (206 BC), figures out as ideal monuments of sustainable construction practices using mud bricks. Earth has a unique property of breathability, which makes it different from other conventional building materials (Lekshmi et al., 2020). Despite these positive features, people are restrained from using earth as a construction material mainly due to its major drawbacks, such as vulnerability to erosion, termite attack and development of shrinkage cracks. However, these drawbacks can be nullified by enhancing the physical and mechanical properties of raw earth using natural stabilizers and reinforcements.

There is immense potential for natural resources to be utilized as raw materials in building construction. On the other hand, the livelihood of people, especially women working both in the agricultural sector and related industries, are declining to the extent that they strive hard to make both ends meet. A technological approach of incorporating earth and agricultural waste residues as raw materials in building construction can be a feasible solution to address this global challenge besides reducing the unscientific waste disposal and global warming.

2.2 SUSTAINABLE DEVELOPMENT GOAL (SDG) 12

The sustainable development goals (SDGs) adopted by the United Nations in the 2030 agenda of sustainable development manifests a holistic approach to end poverty, protect Earth and ensure a greener and fairer, better world (Sakai et al., 2022). Among the 17 SDGs, the 12th goal ensures responsible consumption and production patterns that focus on "doing better with less and wasting less" (The 17 Goals | Sustainable Development (un.org); https://17globalgoals.com/sustainable-development-goals-and-the-construction-industry).

Eleven targets have been established for attaining this goal. Of these targets, 12.2, 12.5 and 12.6 pertain respectively to effective utilization of natural resources, reduction of waste generation and encouragement of companies in adopting sustainable practices which are closely associated with construction activities (https://unosd.un.org/es/node/126). In the construction scenario, responsible consumption denotes judicious consumption of raw materials from natural resources, reserving them for future generation without depleting them; responsible production denotes any production processes in construction which involve minimum greenhouse gas emissions. It is alarming to note that the construction industry is the major consumer of natural resources, and especially the cement industry is responsible for 5%–7% of all global anthropogenic CO_2 emissions (Krejcirikova et al., 2018). While producing one tonne of cement, an average quantity of 0.87 tonne of CO_2 is released to the atmosphere (Farhan et al., 2019). On the other hand, enormous wastes in the form of agricultural residues, industrial wastes, and construction and demolition wastes are generated globally day by day, the disposal of which is a permanent menace to the stakeholders. The effective utilization of these wastes from locally available resources in the construction industry can propose sustainable solutions to global warming and unscientific waste disposal. Again, the sustainable utilization of wastes in a region imparts overall well-being and prosperity of the people in the locality.

2.3 NATURAL RESOURCES AS RAW MATERIALS

The State of Kerala, popularly known as "God's Own Country," is located in the southern part of India. The major crops cultivated in Kerala are paddy and coconuts, other crops being plantation crops such as arecanuts, cashew nuts, spices and fruits. Apart from these, livestock farming is also a livelihood of a minority population in Kerala. The real challenges faced by agro-based industries and livestock farming in Kerala are detailed in the forthcoming sections.

2.3.1 Challenges Faced by Agro-Based Industries in Kerala

The State of Kerala accommodates several large, medium and small-scale agro-based industries. The coir industry, cashew nut processing industries, rice mills, and coffee and tea industries are a few among these. Kerala is the major coconut-producing state in India, contributing to about 45% of the total production (https://coconutseller.in/coconut-production-in-kerala). Small-scale coir industries flourished near the banks of backwaters in Kerala about a century ago. Coconuts were dehusked, retted in backwaters for decortification and then fibres were extracted by beating the husks in these industries (see Figure 2.1a–Figure 2.1c).

The extracted golden brown fibres are bundled before spinning (see Figure 2.1d).

About 70% of the labourers involved in the industry were women (see Figure 2.1e).

Subsequent rise in the price of coconuts, decline in the price of coir ropes in the market, followed by low wages for labourers led to the gradual disappearance of these industries. Despite being the major producer of coconuts in India, the state of Kerala is now depending on the neighboring state Tamil Nadu for coir fiber. It is estimated that about 80 tonnes of coir fibers can be extracted from 1 million coconuts. Nevertheless, less than 40% of coconut husk is utilized by coir industries, the remaining used as fuel or as waste materials in rural areas. There is huge potential for utilization of 60% of coconut husk, which extracts about 0.34 million tonnes of coir fibers (National Coir Policy and Vision Document, 2025). Kerala has to become self-sufficient in the extraction of coir fibres and utilize the maximum potential of these fibres without wasting them.

The cashew industry in Kerala started as small-scale agro-based industry and flourished to large-scale industry in the due course of time. This industry provided a livelihood to lakhs (hundreds of thousands) of people, the majority being female (see Figure 2.2).

Kerala contributes to about 60% of India's raw cashew nut export and 85%–98% of cashew kernel export (Stevelal, 2018). However, the cashew industry in Kerala suffered a severe setback during the past 20 years due to various reasons, such as reduction in the area under cultivation and production almost to half, decline in imports of cashew nuts etc., creating an imbalance in supply-demand leading to the permanent shutdown of these factories. The ministry of Kerala is striving hard to rejuvenate cashew industries, which could increase the economy of the state and also create more job opportunities.

FIGURE 2.1A Coconuts.
Photograph taken by the author.

The scenario from rice mills in Kerala is quite different. These mills are on the verge of threat in connection with the dumping or rice husk waste. The agricultural economic statistics from Kerala recorded the paddy production (see Figure 2.3a) during 2020–2021 to be 0.63 million tonnes, from which approximately 0.13 million tonnes of rice husk could be produced, which is often burnt to ash for disposal (Final Estimates of Area. Production and yield of Crops 2020–21). This burnt rice husk ash is often dumped into the yard (see Figure 2.3b and Figure 2.3c), which destroys the formation of topsoil and affects soil fertility.

The rice mill owners of the state are seeking expert opinion for the safe disposal of rice husk ash, as well as the possibility of valorizing this agricultural waste residue.

Considering the production of major agricultural products such as coconuts and paddy and cash crops such as cashew nuts over the past decade (2011–2021), the following observations have been made: (1) decline in the production of coconuts from

FIGURE 2.1B Retting of coconut husks.
Photograph taken by the author.

FIGURE 2.1C Beating of coconut husks.
Photograph taken by the author.

FIGURE 2.1D Extracted brown coir fibres before spinning.
Photograph taken by the author.

FIGURE 2.1E Women engaged in coir spinning.
Photograph taken by the author.

FIGURE 2.2 Women engaged in processing of cashew nuts.
Photograph taken by the author.

FIGURE 2.3A Paddy.
Photograph taken by the author.

FIGURE 2.3B Rice husk waste.
Photograph taken by the author.
(Source: Lekshmi et al., 2023a)

5941 million nuts to 4788 million nuts; (2) decrease in the production of rice from 568.9 thousand metric tonnes to 521.31 thousand metric tonnes during 2017–2018 followed by an increase to 626.89 thousand metric tonnes during 2020–2021; and (3) a considerable decline in the production of cashew nuts from 36.74 thousand metric tonnes to 20.91 thousand metric tonnes (Agricultural Production at a Glance, 2020).

Suitable measures should be undertaken for increasing the production of coconuts, paddy and cashew nuts that would boost the economy of the state, which would be reflected in the overall well-being of the society.

2.3.2 Challenges Faced by Livestock Farmers in Kerala

The majority of Kerala's small-scale farmers rely on livestock as their primary form of income. As per the 19th livestock census in 2012, cattle constitutes the major population of livestocks in Kerala, i.e., about 13.3 lakhs (see Figure 2.4a)

FIGURE 2.3C Rice husk ash residue dumped into yards of a rice mill.
Photograph taken by the author.

Livestock makes up a little over 27% of the Gross State Value Added (GSVA) from the agricultural sector, which is somewhat more than that at the all-India level. However, it has slightly decreased from 27.97% in 2016–17 to 27.49% in 2017–18, primarily due to the decrease in the population of cattle (Ashmi, 2019). The primary cattle products in Kerala that assist the rural population in alleviating the adverse effects of rural poverty are milk, meat and leather.

Little consideration has been given to the excreta of cattle, i.e., cow dung (see Figure 2.4b), which when utilized properly can add value to the state economy.

Besides being excellent manure, cow dung is a well-known disinfectant. It was smeared on the walls and floors of ancient buildings for disinfecting purposes (Bahobail, 2012). The effective utilization of cow dung in nurseries as manure and in strengthening mud-based constructions would earn livestock farmers supplementary income other than the income obtained by selling milk and milk products. Compared to milk, cow dung is obtained free as waste. The greater part of the dung can be used as manure for agriculture, and the problem persists with the remaining portion. Stoking of fresh cow dung for prolonged periods generates a stinky smell and can become colony for microorganisms. Fresh dung can be spread under the sun in open areas and dried. Dried cow dung can be powdered and stocked in airtight bags for longer duration and can be marketed as manure or for construction purposes.

To enable small producers in taking advantage of opportunities, overcoming obstacles and countering threats, a supportive atmosphere must be created. The constraints associated with higher livestock production must be adequately identified and overcome.

FIGURE 2.4A Livestock farming in Kerala State, South India.
Photograph taken by the author.

2.3.2.1 Raw Materials Extracted from Natural Resources as Building Materials

The raw materials available in Kerala that can be promising building materials to the construction industry are (1) earth as mortar and plaster, (2) cow dung from cattle as a stabilizer for earth-based mortar and plaster, (3) cashew nut shell liquid extracted from the kernel of cashew nuts as water repellant in earth-based mortar and plaster, (4) coir fibre extracted from coconut husks as reinforcement in mortar and plaster, and (5) rice husk ash generated by burning rice husks (waste from paddy field) as replacement for cement in mortar and plaster.

The *main objective* of the study has been framed as the attainment of responsible consumption and production (SDG 12) through effective utilization of waste from natural resources. The corresponding subobjective is the attainment of no poverty (SDG-1), zero hunger (SDG-2), good health and well-being (SDG-3), quality education (SDG-4) and gender equality (SDG 5).

2.4 BACKGROUND STUDY

Extensive literature review was carried out to explore the effective utilization of these agricultural residues as raw materials in the construction industry, and the main highlights are discussed:

FIGURE 2.4B Fresh cow dung.

Photograph taken by the author.

- Natural and synthetic fibres enhance the tensile strength of cement mortar by bridging the gap between the grains of the cement matrix (Onuaguluchi and Banthia, 2016; Qamar et al., 2018; Gonilho-Pereira et al., 2011).
- Coir fibres are rich in cellulose and lignin, whose bonding and durability properties can be enhanced through alkali treatment (Kiruthika, 2017; Yadav and Tiwari, 2016; Andic-Cakir, 2014; Karthikeyan and Balamurugan, 2012).
- Alkali-treated coir fibre (0.5%–1.5%) enhanced the mechanical properties of conventional mortar when used as reinforcement (Sathiparan et al., 2017; Kesikidou and Stefanidou, 2019).
- The replacement of cement by supplementary cementitious materials (SCM) with amorphous silica content could lower the increase in global CO_2 emissions by 30% (Ecosmart, 2016).
- Replacement of cement by rice husk ash (10%–30%) enhanced the mechanical properties of cement mortar while displaying greater resistance to acid and alkali attack (Rashid et al., 2010; Subhashi et al., 2021; Christopher et al., 2017).
- Cashew nut shell liquid extracted from the kernel of cashew nuts is excellent water repellant and an oxidizing agent (Pillai et al., 1980; Kubo et al., 2006).

- The addition of animal dung imparts plasticity to soils and can be used as waterproof plaster for earth-based masonry walls (Millogo et al., 2016).
- Mud-based constructions can be stabilized with cow dung, which would also check the crack propagation as the dung is fibre rich (Bahobail, 2012).
- Cementitious composites reinforced with coir fibre and replaced with rice husk ash impart low thermal conductivity and greater fatigue strength (Abdullah and Lee, 2017).

Based on the literature review, a detailed experimental research was planned for the effective utilization of treated coir fibre, rice husk ash, cashew nut shell liquid and cow dung as raw materials for masonry mortar in construction industry.

2.5 EXPERIMENTAL STUDY

Experimental studies were carried out in the following three areas and were found to be promising in the utilization of:

1. Agricultural residues in conventional (cement-based) mortar and plaster
2. Agricultural residues and livestock wastes in traditional (earth-based) mortar and plaster
3. Agricultural residue–based binder and mortar in product development for the construction industry

2.5.1 Utilization of Agricultural Residues in Conventional (Cement-Based) Mortar and Plaster

Coir fibres in pristine form (see Figure 2.5) were given alkali treatment for three days, washed thoroughly, dried and cut into required lengths (10 mm–25mm).

The treated coir fibres were used as reinforcements in percentages varying from 0.1% to 0.3% by weight of 43-grade Portland pozzolana cement. Rice husk ash (RHA) obtained from the yards were dried, ground in ball mills, sieved to the size of Portland cement and stored in airtight bags (see Figure 2.6).

Considering the environmental consequences of river sand mining, crushed graded manufactured sand was used for preparation of mortar. The specimens were tested for strength and durability after checking their material properties (see Figure 2.7).

2.5.1.1 Material and Methods

The material properties of treated coir and rice husk were tested as per standard reference tests in the laboratory and were found suitable to be used respectively as reinforcement and partial replacement for cement. The specific gravity of coir fibre was within the range 1.30–1.38, and it had a breaking force within the range 4.2 N–4.3 N. The biological examination of coir fibre indicated the presence of cellulose (40%–45%) and lignin (30%–35%). The specific gravity of rice husk ash was within the range 1.9–2.0. The chemical composition of RHA showed the presence of silicon dioxide greater than 90%, which indicates greater pozzolanicity. Microstructure examination of RHA using X-ray diffraction technique (XRD) indicated the amorphous nature of

FIGURE 2.5 Coir fiber in pristine form.
Photograph taken by the author.

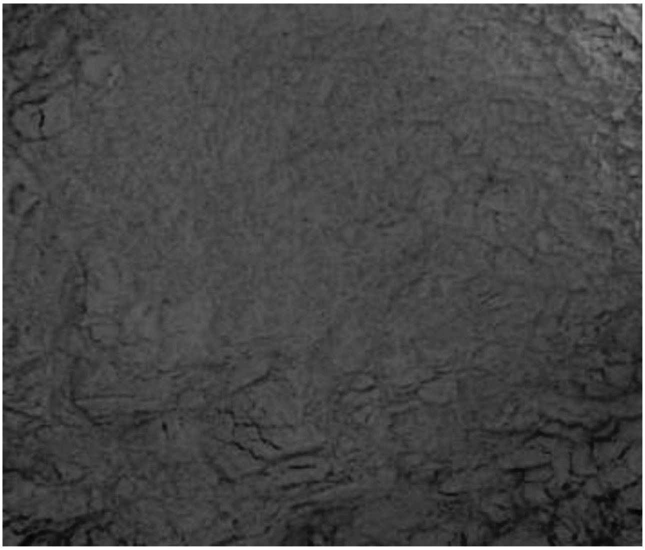

FIGURE 2.6 Rice husk ash ground and sieved.
Photograph taken by the author.
(Source: Lekshmi et al., 2021)

FIGURE 2.7 Agricultural residue-based cement mortar specimens.
Photograph taken by the author.
(Source: Lekshmi et al., 2021)

silica present in it, justifying its pozzolanicity. Ordinary Portland Cement of grade 43 had been used. The crushed graded sand conformed to Zone III of particle size distribution and was used as fine aggregate for mortar.

Coir fibre–reinforced and RHA-replaced binder specimens were prepared for varying lengths (10 mm–25 mm) and percentages (0.1%–0.3%) of coir fibre and varying percentages of RHA (5%–15%) as per standard reference codes for testing compressive strength and water absorption (durability). The results indicated that coir fibre (0.25, 0.5%) of 10 mm length when used as reinforcement gave compressive strength 20% greater than the control binder with desired durability. Partial replacement of RHA (10%) by weight enhanced the compressive strength of control binder, especially for longer duration (Lekshmi et al., 2021). All the binders had compressive strength greater than that of 43-grade OPC (43 N/mm^2) as per IS: 4031 (Part 6)—1988.

2.5.1.2 Application of Agricultural Residue–Based Binders on Mortars and Plasters of Varying Proportions

The experimental results from agricultural residue–based binders were applied to masonry mortars and plasters by varying their proportion from 1:1–1:8. Water-to-cement ratio was fixed to maintain the required flowability as per the standard reference codes. The experimental results indicate that incorporation of coir fibers (0.5%, 10 mm) enhanced the mechanical properties of masonry mortar from strong mixes to weak mixes while maintaining desirable durability parameters. Partial replacement of cement by RHA in required proportion was equally good in maintaining long-term strength parameters of moderate and weak mixes and imparted better resistance to acid and alkali attack (Lekshmi et al., 2023b). All the mortar samples satisfied strength requirements as specified by IS: 1905–1987.

Thus, agricultural residues such as coir fibres and rice husk ash, which would otherwise be dumped as waste, creating environmental pollution and accompanied health hazards, can be effectively utilized as raw materials in the construction sector.

2.5.2 Utilization of Agricultural Residues and Livestock Wastes in Traditional (Earth-Based) Mortar and Plaster

The majority of the world's population dwells in earth-based habitats. According to the renowned architect Laurie Baker, around 58% of buildings in India are made of mud bricks, withstanding over a period of 100 years (Lekshmi et al., 2017). Coming to the Kerala scenario, most of the ancient houses and historical monuments were made of mud/laterite blocks (Gopakumar, 2010). Unlike the conventional plasters, mud possesses a unique property known as breathability, an important factor in any wall system. If the resistance to crack propagation, water penetration and termite attack is properly ensured, then mud is the most suitable and sustainable material for a healthy living. The presence of fibres in cow dung can mitigate crack propagation. The disinfecting property of cow dung can be deployed in resisting termite attack, and the water-repellant property of cashew nut shell liquid can be imparted in resisting water penetration in earth-based constructions.

2.5.2.1 Materials and Methods

Soil samples with less organic content were collected by avoiding top soil, dried, sieved and stored in containers. Powdered and sieved cow dung (see Figure 2.8a) was added in varying percentages (5%–20%) to stabilize the virgin mud mortar (see Figure 2.8b).

The increase in moisture ingress due to the addition of cow dung was regulated by adding varying percentages of cashew nut shell liquid (5%–15%) by weight of soil (see Figure 2.9a–Figure 2.9d).

The material properties of soil, cow dung and cashew nut shell liquid were tested as per standard codes IS: 2720 (Part III/section1)—1980, IS: 2720 (Part 4)—1985, IS 2720 (Part 5)—1985, IS: 2720 (Part 22)—1972, IS: 2720 (Part 26)—1987, and IS: 840–1986 and found adequate to be used as raw materials for mortar. Soil samples were composed of sand (40%–55%), silt (35%–45%) and clay (10%–15%) fractions. The specific gravity of soil varied within the range 2.6–2.8 and that of cow dung within the range 1.2–1.4. The pH of cow dung was between 8.0 and 8.2. Cashew nut shell liquid had viscosity of 105–109 centipoise and specific gravity between 0.92–0.97.

The compressive strength specified by IS: 2250–1981 (i.e., > 2 N/mm^2) was attained by cow dung–stabilized mud mortar that was treated with cashew nut shell

FIGURE 2.8A Powdered cow dung.
Photograph taken by the author.
(Source: Lekshmi et al., 2020)

FIGURE 2.8B Cow dung–stabilized mud mortar specimens.
Photograph taken by the author.

liquid. The stabilization of mud mortar with 10% and 20% cow dung retained the compressive strength of raw mud mortar samples by 88%–98% and 70%–90%, respectively, but there was uptake in moisture ingress compared to raw mud mortar. The addition of 10% cashew nut shell liquid to 10% and 20% cow dung–stabilized mud mortar reduced moisture uptake by 50%–70% and also decreased linear shrinkage by 40%–50% (Lekshmi et al., 2020).

The study explored the potential of livestock waste (cow dung) as a stabilizer for earth-based constructions. The effect of cashew nut shell liquid in mitigating moisture ingress and reducing shrinkage cracks is also proved, thus opening a new platform for the cashew industry.

FIGURE 2.9A Cashew fruit.
Photograph taken by the author.

FIGURE 2.9B Matured nuts before harvesting.
Photograph taken by the author.

2.5.3 Application of Agricultural Residue–Based Binder and Mortar in Product Development for Construction Industry

Three products were developed as promising products to the construction industry as application of the experimental study based on agricultural residues in conventional (cement-based) mortar and plaster:

FIGURE 2.9C Harvested raw nuts.
Photograph taken by the author.

FIGURE 2.9D Cashew nut shell liquid.
Photograph taken by the author.
(Source: Lekshmi et al., 2020)

1. *Coir Fibre-Rice Husk Acoustic Panel (CFRHAP):* Agricultural residue–based binder (10% RHA replaced cement) was used to bond coir fibre and rice husk while fabricating a fibrogranular acoustic panel. The sound absorption tests conducted in low- and high-frequency domains as per ISO 10534–2 (1988) indicate that CFRHAP is capable of absorbing 85%–87% sound within a frequency domain of 500 Hz–5000 Hz and 89%–91% sound in a high-frequency domain (1000 Hz–5000 Hz) (Lekshmi et al., 2023a).

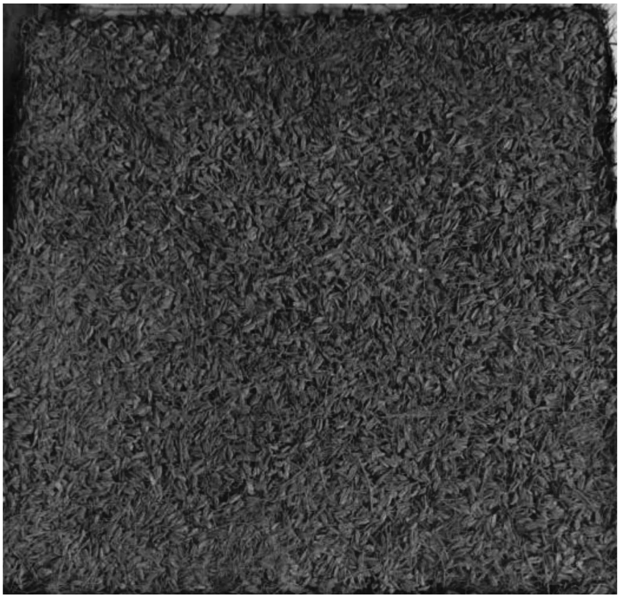

FIGURE 2.10 Coir fibre–rice husk acoustic panel.
Photograph taken by the author.

Existing acoustic panels used for absorbing low-frequency sound are made of synthetic materials and are toxic to nature. The density of CFRHAP is 200 kg/m^3 with dimensions 300 mm × 300 mm × 25 mm (see Figure 2.10).

These panels were rated under a V-1 category of flame resistance, indicating burning is not sustained as per UL-94 and ASTM-D 3801 (2017) standards. Due to their ability to absorb both low- and high-frequency soundwaves (500 Hz–5000 Hz), they have many applications in auditoriums, theatres and other sound insulation applications (UL-94).

2. *Agricultural residue–based cement-sand bricks:* Cement sand bricks were manufactured with moderate and weak mortar proportions reinforced with coir fiber (20–30 mm length), rice husk ash (10–20%) and their combinations, as seen in Figure 2.11.

These cement-sand bricks possessed compressive strength and water absorption conforming to that of first-class bricks (7–14 N/mm^2) as per ASTM-C 67 (2021) and can be used as an alternative for fired clay bricks.

3. *Agricultural residue–based crack-free plaster mortar:* Agricultural residue–based plaster mortar developed in the study can be made available in packets of 25 kg or 50 kg in ready-to-mix form in construction sites that can be used for masonry mortar and plaster (Lekshmi et al., 2023b).

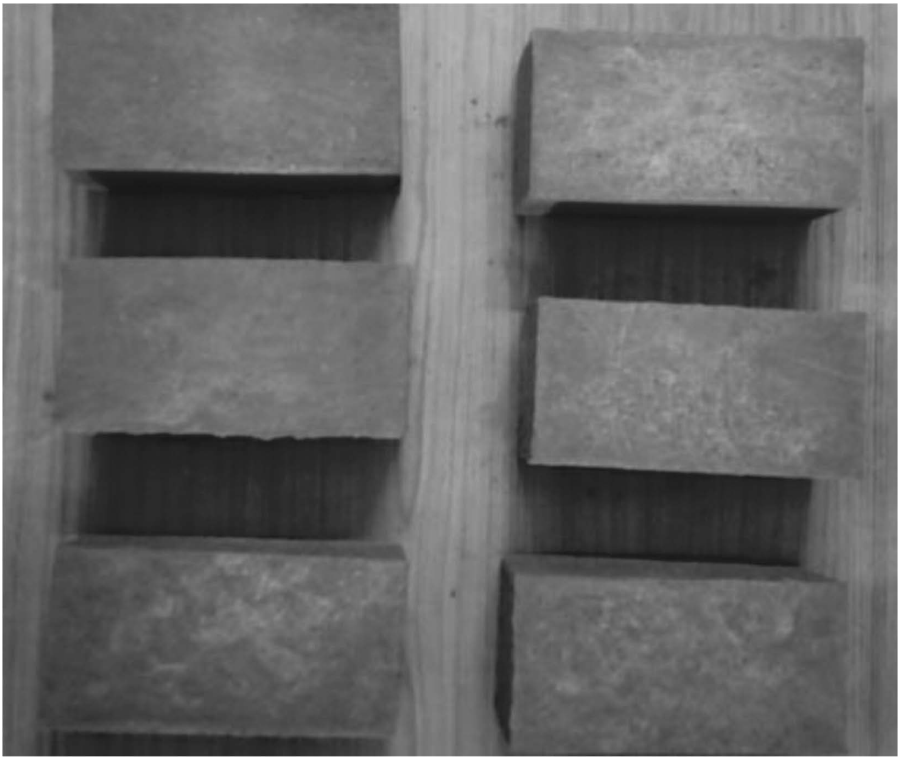

FIGURE 2.11 Agricultural residue–based cement sand bricks.
Photograph taken by the author.

2.6 CONCLUSION

This chapter focused on sustainable development goals through the effective utilization of wastes from natural resources at a regional level with respect to the case study conducted in Kerala State, South India. The methodology adopted in this study may be applied elsewhere in the world with wastes from natural resources having similar material properties and by using appropriate methods.

This study had attempted to attain SDGs pertaining to no poverty (SDG 1), zero hunger (SDG 2), good health and well-being (SDG 3), quality education (SDG 4) and gender equality (SDG 5) through the attainment of SDG 12.

2.6.1 Attainment of SDG 12 (Responsible Consumption and Production)

The main objective of the study was the attainment of responsible consumption and production (SDG 12), which focuses on 'doing better with less' and 'wasting less' by attaining specific targets 12.2, 12.5 and 12.6 (SDG's and Targets Overview Resource (updated as of 6 August, 2020)). Accordingly, the study examined the utilization of coir fiber (wastes from coir industry), rice husk ash (waste from rice mills), cashew nut shell liquid (waste extract from cashew nut industry), earth (natural resource) and cow dung (livestock waste) as effective raw materials for the construction industry. The following applications are recorded for the effective utilization of natural resources in the construction industry specific to the materials selected for the study:

Target 12.2—Achievement of sustainable management and efficient use of natural resources

Attainment—Utilization of products of agricultural crops such as paddy, coconuts, cashew nuts and earth for construction, which are locally available natural resources in Kerala.

Target 12.5—Substantially reduce waste generation through prevention, reduction, recycling and reuse

Attainment—

(i) Effective utilization of agricultural waste residues such as coir fibre, rice husk ash, cashew nut shell liquid and livestock wastes such as cow dung as raw materials in construction, reducing waste disposal.

(ii) Utilization of earth as building material permits reuse after demolition.

Target 12.6—Encourage companies, especially large and transnational companies, to adopt sustainable practices and to integrate sustainability information into their reporting cycle

Attainment—

(i) Cement industries can take necessary steps to launch ready-to-mix plaster cement by adding coir fibres and rice husk ash at the packing stage of cement production to propagate the use of low CO_2 emission cements.

(ii) Industries can take up mass production of agricultural residue-based cement-sand bricks and fibro granular coir fibre rice husk acoustic panels as promising products for construction industries adopting sustainable practices.

The outcome of the study also reflects the attainment of other sustainable development goals as follows:

Attainment of SDG1 (No Poverty) and SDG 2 (Zero Hunger)

- The demand for coir fibers, rice husk ash and cashew nut shell liquid in construction industries would open greater employment opportunities in these industries.
- Labour will have to be employed for supervising alkali treatment of coir fibres, cutting of coir fibres to required length, and for grinding and sieving of rice husk ash.
- Cashew nut shell liquid finds immense application in the chemical and polymer industries.

The findings of this study shall open a new market for cashew nut shell liquid in the construction sector, demanding greater production leading to the full-fledged functioning of cashew industries.

- The rejuvenation of the coir industry and cashew nut industry would secure employment, particularly for women labourers who are unable to seek employment elsewhere like male labourers.
- The demand for cow dung in earth-based construction shall encourage livestock farmers to foster native breeds of cows that provide good-quality dungs.
- Processing of powdered cow dung from fresh dung requires labor.
- The mass production of agricultural residue–based cement-sand bricks and fibrogranular acoustic panels would initiate processing units that require skilled labor.

The requirement for labourers would create jobs for men and women of that locality, gradually eradicating poverty from these families, thus attaining SDG 1 and SDG 2.

Attainment of SDG 3 (Good Health and Well-Being)

- The effective utilization of agricultural wastes as raw materials for the construction industry would minimize unscientific waste disposal, which is the root cause for airborne and waterborne diseases.
- Encouraging earth-based construction techniques would avoid the application of toxic paints in the building. The breathable earth walls would impart health and positive energy to the inhabitants.
- The installation of fibrogranular non-toxic acoustic panels would absorb low-frequency soundwaves that are responsible for hearing loss and associated health hazards to the citizens and the surrounding environment.

Thus SDG 3 is attainment by ensuring good health and well-being of people in that locality.

Attainment of SDG 4 (Quality Education) & SDG 5 (Gender Equality)

- Attainment of SDG 1 and SDG enhances the capabilities, procedures, emotions, skills and resources that communities and enterprises require to survive, change and flourish in a world that is changing swiftly.
- Improvement in the financial status of the community would equip parents to provide quality education to their children.
- Men and women in a family would work together for a better future of their children without gender discrimination, which thus ensures gender equality.

The effective utilization of wastes from natural resources in a locality would thus transform the lives of people in that locality by reforming the society, which in the long run would transform the world into a sustainable place to live in.

2.7 ACKNOWLEDGEMENT

The authors express their sincere gratitude to the National Coir Research and Management Institute (NCRMI), Thiruvananthapuram, Kerala, for extending financial assistance in carrying out the experimental research work (Project ID: NCRMI/project/3295/2017). The authors thankfully acknowledge the authorities of the Naval Physical and Oceanographic Laboratory (NPOL), Kochi, Kerala, for granting permission to conduct the sound absorption test for coir fibre–rice husk acoustic panels at low- and high-frequency ranges.

REFERENCES

The 17 Goals | Sustainable Development (un.org), Department of Economic and Social Affairs, United Nations, accessed on 8 June 2022.

Abdullah, A.C. and Lee, C.C. (2017). Effect of treatments on properties of cement-fiber bricks utilizing rice husk, corncob and coconut coir. *International High-Performance Built Environment Conference—A Sustainable Built Environment Conference 2016 Series (SBE16), iHBE 2016. Procedia Engineering*, *180*, 1266–1273.

Agricultural Production at a Glance. (2020). Directorate of Economics and Statistics, CMIE, RBI.

Andic-Cakir, O., Sarikanat, M., Tufekci, H.M., Demicri, C. and Erdogan, U.H. (2014). Physical and mechanical properties of randomly oriented coir fiber cementitious composites. *Composites: Part B*, *61*, 49–54.

Ashmi, V.G. (2019). Livestock sector development and implications for rural poverty alleviation in Kerala. *International Journal for Recent Scientific Research*, *10* (8), 34484–34487.

ASTM C67/C67M-21. (2021). Standard test methods for sampling and testing brick and structural clay tile. *ASTM International*, West Conshohocken, PA.

ASTM D 3801. (2017). Standard test method for comparative burning characteristics of soild plastics in a vertical position. *ASTM International*, West Conshohocken, PA. www.astm.org.

Bahobail, M.A. (2012). The mud additives and their effect on thermal conductivity of adobe bricks. *Journal of Engineering Sciences, Assiut University*, *40* (1), 21–34.

Christopher, F., Bolatito, A. and Ahmed, S. (2017). Structure and properties of mortar and concrete with rice husk ash as partial replacement of ordinary Portland cement—A review. *International Journal of Sustainable Built Environment*, *6*, 675–692.

Coconut Production in Kerala, Available online June 21, 2021, https://coconutseller.in/coconut-production-in-kerala, accessed on 26 June 2023.

Cruickshank, H.J. and Fenner, R.A. (2007). The evolving role of engineers: Towards sustainable development of the built environment. *Journal of International Development*, *19* (1), 111–121.

Ecosmart, Environmental Impact—Cement |Production and the CO_2 Challenge. (2008), Available online, www.ecosmartconcrete.com/enviro_cement.cfm, assessed on 14 April 2016.

Farhan, J., Fasihi, M. and Breyer, C. (2019). Trends in the global cement industry and oppurtunities for long-term sustainable CCU potential for Power-to-X. *Journal of Cleaner Production*, *217*, 821–835.

Final Estimates of Area. Production and yield of Crops 2020–21, Department of Economics and Statics, Government of Kerala, Available online February 15, 2022, accessed on 18 May 2023. https://ecostat.kerala.gov.in/publication-detail/final-estimates-of-areaproduction-and-yield-of-crops-2020-21.

Gomes, I., Faria, P. and Gonçalves, T.D. (2018). Earth-based mortars for repair and protection of rammed earth walls. Stabilization with mineral binders and fibers. *Journal of Cleaner Production*, *172*, 2401–2414.

Gonilho-Pereira, C., Faria, P., Fangueir, R., Vinagre, P. and Martins, A. (2011). Cement based fibre-reinforced mortar: The fiber influence on mortar performance. *CLME' 4510R.*

https://comum.rcaap.pt/bitstream/10400.26/6551/1/CLME_CEMENT%20BASED%20FIBER-REINFORCED%20MORTAR%20THE%20FIBER%20INFLUENCE%20ON%20THE%20MORTAR%20PERFORMANCE.pdf.

Gopakumar, R. (2010). Blending tradition with modernity—back to earthly homes. *Deccan Herald*, 7 March 2010, Special Features, Available online, www.deccanherald.com, accessed on 27 July 2015.

IS: 4031 (Part 6): 1988. (2019). (First revision) Reaffirmed–2019. Methods of physical tests for hydraulic cement–Determination of compressive strength of hydraulic cement other than masonry cement. *Bureau of Indian Standards*, Manak Bhavan, New Delhi.

IS: 840–1986, Indian Standard Specifications for cashew nut shell liquid (CNSL). (2002). Second Revision (Reaffirmed 2002). *Bureau of Indian Standards*, Manak Bhavan, 9 Bahadur Shah Zafar Marg, New Delhi.

IS: 1905–1987. (1989). Code of practice for structural use of unreinforced masonry. *Bureau of Indian Standards*, Third Revision, New Delhi.

IS: 2250–1981. (1981). Code of practice for preparation and use of masonry mortar, First Revision, New Delhi, India. *Bureau of Indian Standards*, Manak Bhavan, 9 Bahadur Shah Zafar Marg, New Delhi.

IS: 2720 (Part III/Sec 1)–1980. (2002). Indian standard methods of test for soils, part III-determination of specific gravity section I-fine grained soils. First Revision (Reaffirmed in 2002). *Bureau of Indian Standards*, Manak Bhavan, New Delhi.

IS: 2720 (Part 22)–1972. (2010). Indian standard methods of test for soils, part 22-determination of organic matter first revision. Third Reprint (Reaffirmed 2010). *Bureau of Indian Standards*, Manak Bhavan, New Delhi.

IS: 2720 (Part 26)–1987. (2002). Indian standard methods of test for soils, part 26—determination of pH value. Second Revision (Reaffirmed 2002). *Bureau of Indian Standards*, Manak Bhavan, New Delhi.

IS: 4031 (Part 4)–1988. (1988). Indian standard methods of physical test for hydraulic cements, determination of consistency of standard cement paste. *Bureau of Indian Standards*, New Delhi.

IS: 4031 (Part 5)–1988. (1988). Indian standard methods of physical test for hydraulic cements, Determination of initial and final setting times. *Bureau of Indian Standards*, New Delhi.

ISO 10534–2:1998. (1998). Acoustics—Determination of sound absorption coefficient and impedance in impedance tubes—Part 2: Transfer-function method. *Technical Committee ISO/TC 43/SC 2*, Edition 1. https://www.iso.org/standard/22851.html.

Karthikeyan, A. and Balamurugan, K. (2012). Effect of alkali treatment and fiber length on impact behaviour of coir fiber reinforced epoxy composites. *Journal of Scientific & Industrial Research*, *71*, 627–631.

Kesikidou, F. and Stefanidou, M. (2019). Natural fibre-reinforced mortar. *Journal of Building Engineering*, *25*, 100786.

Kiruthika, A.V. (2017). A review on physico-mechanical properties of bast fiber reinforced polymer composites. *Journal of Building Engineering*, *9*, 91–99.

Krejcirikova, B., Kolarik, J. and Wargocki, P. (2018). The effects of cement based and cement-ash-based mortar slabs on indoor air quality. *Building and Environment*, *135*, 213–223. USGS—Minerals Information: Cement [WWW Document].

Kubo, I., Masuoka, N., Ha, T.J. and Tsujimoto, K. (2006). Antioxidant activity of anacardic acids. *Food Chemistry*, *99*, 555–562.

Lekshmi, M.S., Subha, V. and Anil, K.R. (2021). Lignocellulosic materials as reinforcement and replacement for binder in masonry mortar. *Construction and Building Materials*, *282*, 122607.

Lekshmi, M.S., Subha, V. and Anil, K.R. (2023b). Effect of coir fiber reinforcement on flexural and compressive strengths of masonry mortar. *Journal of Materials in Civil Engineering, Forth Coming.* https://doi.org/10.1061/JMCEE7/MTENG-16177.

Lekshmi, M.S., Vishnudas, S. and Anil, K.R. (2023a). Experimental investigation on acoustic performance of coir fibre rice husk acoustic panels. *Applied Acoustics*, *204*, 109244.

Lekshmi, M.S., Vishnudas, S. and Nair, D.G. (2017). An investigation on the potential of mud as sustainable building material in the context of Kerala. *International Journal for Energy Technology and Policy*, *13* (1/2), 107–122.

Lekshmi, M.S., Vishnudas, S. and Nair, D.G. (2020). Strength, sorptivity and shrinkage characteristics of cow dung stabilized mud mortar. *Materials Today: Proceedings*, *32*, 782–787.

Millogo, Y., Aubert, J.E., Séré, A.D., Fabbri, A. and More, J.C. (2016). Earth blocks stabilized by cow-dung. *Materials and Structures*, *49* (11), 4583–4594.

National Coir Policy and Vision Document 2025. (2015). *Ministry of Micro, Small and Medium Enterprises*, Government of India, Coir Board.

Onuaguluchi, O. and Banthia, N. (2016). Plant based natural fiber reinforced cement composites – A review. *Cement and Concrete Composites*, *68*, 96–108.

Pillai, C.K.S., Prasad, S.V. and Rohtagi, P.K. (1980). To evaluate the polymerisation characteristics of cashew nut shell liquid obtained from the expeller. *Report RRL/M/27/29; Materials Division*, Regional Research Laboratory: Trivandrum, India.

Qamar, F., Thomas, T., and Ali, M. (2018). Use of natural fibrous plaster for improving the out of plane lateral resistance of mortar-less interlocked masonry walling. *Construction and Building Materials*, *174*, 320–329.

Qureshi, A.S. and Nawab, A. (2013). The role of engineers in sustainable development. In *Proceedings of the Symposium on Role of Engineers in Economic Development and Policy Formulation*, Lahore, Pakistan, 105–114.

Rashid, B.H., Ali, K., Tarif, M.C. and Ahmed, U. (2010). Long term effect of rice husk ash on strength of mortar. *World Academy of Science, Engineering and Technology, International Journal of Civil, Environmental, Structural. Construction and Architectural Engineering*, *4* (7), 180–183.

Sakai, K., Mohd Hassan, A., Vairappan, C.S. and Shirai, Y. (2022). Promotion of a green economy with the palm oil industry for biodiversity conservation: A touchstone toward a sustainable bio industry. *Journal of Bioscience and Bioengineering*, *5*, 414–424.

Sathiparan, N., Rupasinghe, M.N. and Pavithra, B.H.M. (2017). Performance of coconut coir reinforced hydraulic cement mortar for surface plastering application. *Construction and Building Materials*, *142*, 23–30.

SDG's and Targets Overview Resource (updated as of 6 August, 2020), 4th Sustainable Development Goals Youth Summer Camp, 10–21, Available online, https://unosd.un.org/es/node/1261, accessed on 22 June 2023.

Stevelal. (2018). Issues and challenges of cashew industry in Kerala, *Research Report submitted to Kerala State Planning Board.* https://spb.kerala.gov.in/sites/default/files/inline-files/14.%20CashewInd.pdf.

Subhashi De Silva, G.H.M.J., Vishvalingam, S. and Etampawala, T. (2021). Effect of waste rice husk ash from rice husk fuelled brick kilns on strength, durability and thermal performances of mortar. *Construction and Building Materials*, *268*, 121794.

Sustainable development goals and construction industry, Available online, October 19, 2020, https://17globalgoals.com/sustainable-development-goals-and-the-construction-industry, accessed on 9 June 2022.

UL-94. Test for flammability of plastic materials for parts in device and appliances. *Underwriters Laboratories Inc. (UL)*, 333 Pfingsten Road, Northbrook, IL.

Yadav, J.S. and Tiwari, S.K. (2016). Behaviour of cement stabilized treated coir fibre-reinforced clay-pond ash mixtures. *Journal of Building Engineering*, *8*, 131–140.

3 Sustainable Construction Technologies
A Way Forward

Keerthana Kirupakaran

3.1 INTRODUCTION

According to the World Green Building Council [1], about 40% of annual global carbon emissions can be traced back to the construction sector. With the current surge in urbanization across different parts of the world, the carbon emission from the construction industry is expected to double in the next two decades if substantial measures are not taken [2]. To meet the climate goal, it is critical for builders, manufacturers, and policymakers to incorporate sustainability into every facet of the construction industry.

Sustainability in construction is viewed in three verticals, namely: economic, environmental, and social sustainability [3]. Economic sustainability concerns profitability in the construction processes, efficient use of resources such as water, energy, natural or human-made materials, and labour. Environmental sustainability involves undertaking eco-friendly construction practices. A few ways to achieve environmental sustainability include diligent use of resources, minimizing waste, and employing construction materials and techniques that consume less energy and emit less carbon dioxide. Social sustainability deals with addressing the needs of people in all stages of the construction process, starting from commissioning to demolition of a building/structure. It evaluates the company's engagement with its employees, suppliers, customers, clients, and the local community.

Social sustainability encapsulates human rights, wellness and safety, diversity, and societal impact [4]. The existing and emerging construction technologies should cater to these three verticals to promote sustainable development in the construction industry. Earlier challenges in the construction industry were focused only on three factors: cost, quality, and time. Now sustainability being the prime motto, a new paradigm is proposed by Huovila and Kokela [5], as illustrated in Figure 3.1. This new paradigm modifies the existing construction practices by considering the minimization of resource depletion, reduction in harmful emissions, and preservation of biodiversity. In a global context, the new paradigm aims to achieve a healthy economy, environmental quality, social equity, and cultural heritage. While this task seems intimidating, it is achievable when we break it down into smaller goals.

DOI: 10.1201/9781032686899-4

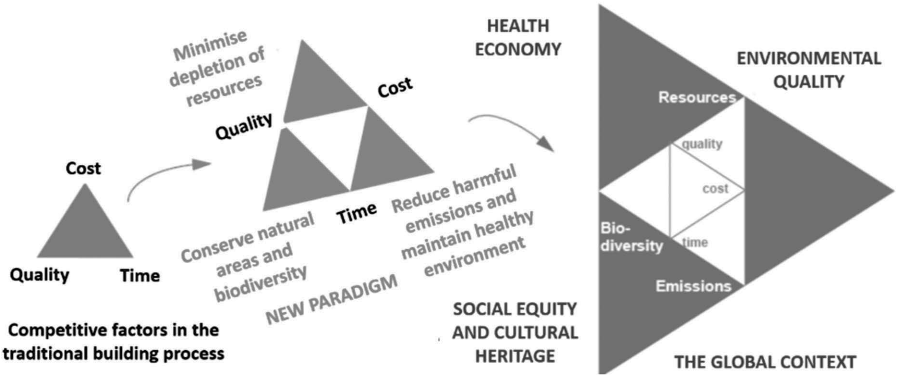

FIGURE 3.1 New paradigm for sustainable construction according to Huovila and Kokela [5].

To achieve environmental sustainability in the construction sector, research efforts are focused on developing various construction materials and technologies that can mitigate net carbon emissions. Some of the approaches and inventions include (1) supplementary cementitious material (SCMs), which are used as a partial replacement for Portland cement either during manufacturing or during concrete mixing; SCMs are widely explored, as they can reduce CO_2 emissions by up to 30–40% without compromising much on the performance of concrete [6]; (2) fibre-reinforced concrete (FRC) and textile-reinforced concrete (TRC) have high ductility and load-bearing capacity, which enables the production of thin and light structural components; (3) concrete 3D-printing technology is the digital fabrication of cementitious components by eliminating formwork; (4) use of construction and demolition (C&D) waste in the new construction; and (5) use of artificial intelligence (AI), robotics, and automation in construction enables better planning in addition to promoting time and cost-effective construction. The sustainability potential of emerging technologies can be truly realized only when we perform a life-cycle assessment to quantify embodied and operational carbon emissions. Further, real change can happen only when there is a drive for the implementation of sustainable technologies through policies and standards. This chapter gives an overview of various research and implementation efforts for achieving environmental sustainability in the construction industry. First, the importance of embodied and operational carbon and life-cycle assessment in the context of the construction industry is elaborated, followed by the discussions on various sustainable construction materials and technologies mentioned previously. The chapter concludes with the significance of policies and standards in the large-scale adoption of sustainable principles and technologies in the construction sector and as a way forward to attain sustainability in construction.

3.2 EMBODIED AND OPERATIONAL CARBON

3.2.1 Embodied Carbon

The total energy consumed or carbon emitted from the manufacturing stage to the point where the product is ready to be used is referred to as embodied carbon or energy. With respect to the construction sector, embodied carbon constitutes carbon emitted during the manufacturing material, including raw material extraction and their processing, the transport of manufactured material to the construction site, and the energy consumed while using the construction equipment and type of construction practices adopted [7]. In other words, embodied carbon refers to the carbon emission in the entire construction process, starting from the manufacture of raw materials for the construction of the building to the point where the people are ready to occupy the building [8, 9].

3.2.2 Operational Carbon

The operational carbon or energy refers to carbon or energy consumed for the operation of the building throughout its service life. It includes energy consumed for maintaining the indoor environment through processes such as heating, ventilation, cooling, lighting, and the operation of appliances [10, 11]. Operational carbon currently accounts for 28% of global greenhouse gas emissions. If the total operational energy demand of the building is met by renewable energy sources such as solar and wind, then a building is said to have 'net zero carbon emissions'. To envisage environmental sustainability in the construction sector, it is essential to promote large-scale implementation of renewable energy sources.

To measure the environmental sustainability potential of a building, it is important to assess and quantify embodied and operational carbon in the entire life cycle. The proportionate share of embodied and operational carbon to the total life cycle carbon of a building depends primarily on the type and function of the building [12], and secondary factors include climate, fuel type used, building orientation, location, and building occupancy [13]. The life-cycle assessment of a building is discussed in the following section.

3.3 LIFE-CYCLE ASSESSMENT

Life-cycle assessment (LCA) is a technique to systematically evaluate the environmental impact of a product or service during its entire life cycle. For instance, during the life cycle of a product, natural resources such as energy, water, and material are consumed and, as a result, waste material, undesirable emissions, and by-products are generated. LCA provides a framework to analyze and quantify one or more undesirable environmental impact parameters, such as embodied carbon, embodied energy, acidification, eutrophication, ozone depletion, and smog formation at each stage of the product's life cycle. This information helps in taking informed decisions on the sustainability potential of a product or service. The life-cycle assessment consists of four stages [11]:

- *Stage 1—Definition of goal and scope*: LCA is performed by defining a system boundary and considering all the input/output of the process within that boundary. Typically, three system boundaries are defined in LCA, which are (1) from cradle to grave—encapsulates all the inputs/outputs of the processes that participate throughout its life cycle including extraction of raw material, processing of materials, manufacture of components, use of the product, and recycling or final disposal; (2) from cradle to gate—considers inputs/outputs from the extraction of raw materials until the product is placed on the market; and (c) from gate to gate—considers only the inputs/outputs of the manufacturing process of the product. The system boundary and embodied carbon emissions at different phases in the LCA of a building [14] are shown in Figure 3.2.

- *Stage 2—Life cycle inventory analysis*: In this stage, input and output data of the processes of the product system is collected and curated.
- *Stage 3—Life cycle impact assessment*: In the third stage, the curated data from the previous stage is translated into indicators of potential environmental impacts.
- *Stage 4—Life cycle interpretation*: In the fourth stage, based on the defined goal and scope, the results are interpreted and the conclusions are drawn.

The execution of these four stages of LCA is a comprehensive process that can be both expensive and time-consuming. Nevertheless, LCA is a powerful tool to evaluate and reduce the environmental impact of the product.

Several research efforts globally are focused on investigating the strategies to decrease the embodied carbon in a building [8, 10, 15, 16]. The commonly used strategies are: (1) use low-carbon materials in construction; (2) minimize waste, reuse and recycle materials; (3) minimize transit of materials/products for long distances and promote local sourcing; and (4) implement construction optimization strategies. In this context, the following sections focus on low-carbon construction materials and technologies that promote environmental sustainability in the construction industry.

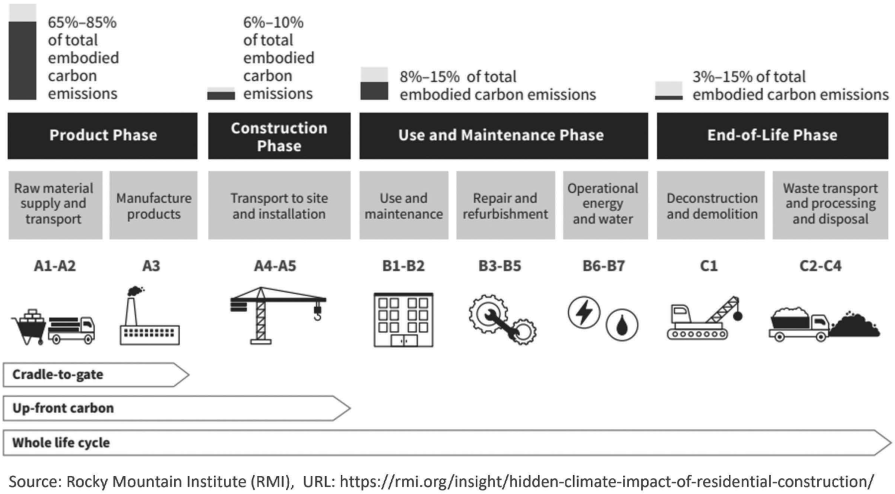

FIGURE 3.2 Schematic of system boundary in the life-cycle assessment of a building [14].

3.4 SUPPLEMENTARY CEMENTITIOUS MATERIALS (SCMs)

Cement production constitutes about 6–8% of the anthropogenic CO_2 emission [17]. Cement production has starkly increased from 2.5 billion tons in 2005 to 4.1 billion in 2022 and it is projected to increase up to 5.8 billion tons by 2050 [18]. The high demand and popularity of cement are due to its low cost, and it is by far the most widely used binder to make concrete. In cement manufacturing, 60% of CO_2 is produced during the clinkering process, and the remaining 40% is produced from electricity and fuel sources used for heating and milling [19]. One way to reduce carbon emissions due to cement production is by reducing cement consumption by exploring alternative sources of binder for making concrete. In this light, supplementary cementitious materials (SCMs) have been the focus of research for the past few decades.

SCMs are used as a partial replacement of Portland cement either during manufacturing or the concrete mixing process. In addition to the reduction of CO_2 emission, some SCMs also improve the strength and durability performance of concrete, leading to further reduction in cost arising from repair and rehabilitation [19, 20]. According to the ASTM 2015 standard [21], SCM is defined as an inorganic material that contributes to the properties of a cementitious mixture through either hydraulic or pozzolanic activity, or both. A pozzolan is either siliceous or both siliceous and aluminous material that possesses almost no cementitious value in its pristine form, but in the finely powdered form, they form compounds having cementitious properties by chemically reacting with calcium hydroxide. Fly ash and ground granulated blast furnace slag (GGBFS) with high calcium contents are the most widely used SCMs [22], and other examples of SCMs include silica fume, calcined clay shale, and volcanic ash.

Fly ash is a byproduct of burning pulverized coal in a power plant, and it displays both pozzolanic and hydraulic behaviour [22]. On the other hand, GGBFS [23] is a byproduct of iron production in the blast furnace. The benefits of using GGBFS in concrete include better workability, durability, low risk of thermal cracking, and low risk of reinforcement corrosion as it restricts chloride ingress and offers high resistance against sulphate attack. Research efforts are ongoing to utilize cement kiln dust (CKD), which is a byproduct of the clinker manufacturing process. CKD are typically composed of alkali, sulfate, and chlorides, and they are used in conjunction with other industrial byproducts to develop an alternative binding material for sustainable concrete [24–26]. A large portion of CKD with lower alkali, sulfate, and chloride contents are recycled as raw material in the cement kiln.

The use of different SCMs imparts different properties to concrete depending upon their mineralogical and chemical compositions [27]. The use of SCMs in the form of blended cement contributes significantly to the refinement of concrete pore structure, which enhances the concrete strength and durability properties [28, 29].

Currently, several research efforts are focused on finding new sources of SCMs, as flyash and GGBFS resources are depleting gradually. Annual production of fly ash is 1 billion tons and GGBFS is 360 million tons, while cement production is projected to be a whopping 5.8 billion tons by 2050 [30, 18]. Due to environmental concerns, several coal power stations are shutting down. In the United States, 40% of coal-fired power plants have been shut down in the past five years, and there are plans to shut all the coal-fired power plants in the UK and Netherlands by 2025 and

2030, respectively [31, 32]. These developments will significantly reduce the fly ash and GGBFS production. Consequently, new sources of SCMs such as natural SCM, calcined natural SCM, and limestone calcined clay cement (LC3) materials [33] are being explored. Further agricultural waste such as rice husk ash, palm oil fuel ash (POFA), bagasse ash (BA) [34, 29], bamboo leaf ash (BLA), wood waste ash, and corn cob ash (CCA) are also being researched for their potential use as SCMs [35, 36]. Some of the challenges faced with the introduction of new SCMs are developing methods to characterize them appropriately and finding the limitations of existing test methods [37]. While the use of SCMs is one way to reduce the carbon footprint in concrete, developing thin and lightweight structures that consume less material is another way to reduce the carbon footprint in concrete.

The following section elaborates on the fibre- and textile-reinforced concrete that facilitates the construction of thin and lightweight concrete structures in contrast to conventional steel-reinforced concrete construction.

3.5 FIBRE- AND TEXTILE-REINFORCED CONCRETE

3.5.1 Fibre-Reinforced Concrete (FRC)

Fibre-reinforced concrete (FRC) is a composite material consisting of discontinuous fibre uniformly dispersed in the concrete matrix. The primary role of fibres in the cementitious matrix is to control crack width opening and crack propagation. Compared to plain concrete, which is quasi-brittle in nature, FRC has improved post-peak behaviour, tensile strength, ductility, and fracture toughness. These properties of FRC are very important for structures located in high seismic regions [38, 39]. Further, its enhanced crack control property restricts the penetration of water and other contaminants into the concrete, thereby increasing the corrosion resistance and service life of the structure [40]. FRC is an ideal material for applications where cracking is a concern, such as bridge decks and industrial flooring.

FRC with its improved durability and strength performance can help in reducing the size of concrete structural members, which leads to less consumption of cement. These advantages of FRC over conventional concrete increase its sustainability potential. FRC research over the past three decades worldwide has resulted in the development of structural design guidelines and codes [41–45]. FRC has been used in several applications, including airport runways, ports, precast concrete, industrial floors, tunnel segments, highways, roads, and bridges. About 100 million cubic meters of FRC are produced annually, of which 60% is used for slab construction [46], 25% is used in the manufacture of precast components, and other applications constitute the remaining 15% [46]. FRC is frequently used to retrofit damaged concrete structures and is a popular option for industrial flooring applications [47, 48]. Owing to the better crack width control property of FRC, permeability in concrete can be substantially reduced, which is highly desirable for coastal structures as they are vulnerable to reinforcement corrosion [49]. FRC also shows better performance under fatigue loading. An experimental study by Stephie et al. [50] revealed that the incorporation of even a low dosage of fibres significantly improves the fatigue performance of concrete due to crack bridging and mitigation of fracture propagation.

In recent years, FRC research is further being explored to employ recycled steel fibres and natural fibres to promote sustainable construction practices.

While there are several advantages of FRC from a strength, durability, and sustainability perspective, one major limitation of FRC is the lack of confidence in ensuring uniform distribution of fibres. During the FRC production stage, the balling effect of fibres is encountered due to improper mixing methods. Proper care should be taken while mixing and placing FRC to ensure uniform fibre distribution. ACI Committee 544 [51] has put forward a few guidelines to ensure the uniform distribution of fibres. However, there is always an uncertainty associated with the fibre distribution, and uniform fibre distribution is critical for its performance and is the primary assumption in FRC structural design. The uncertainty in the fibre distribution can be overcome by using continuous fibre reinforcement in the form of textile fabric, which is discussed in the following section.

3.5.2 Textile-Reinforced Concrete (TRC)

Textile-reinforced concrete (TRC) is a new-generation fibre-cement composite material that contains a multi-axial textile fabric embedded in a fine-grained concrete matrix. The textile fabrics used in TRC are generally made of glass or carbon or basalt fibres. The schematic of multilayer TRC is depicted in Figure 3.3. Unlike conventional steel-reinforced concrete, TRC is non-corrosive, and this feature makes

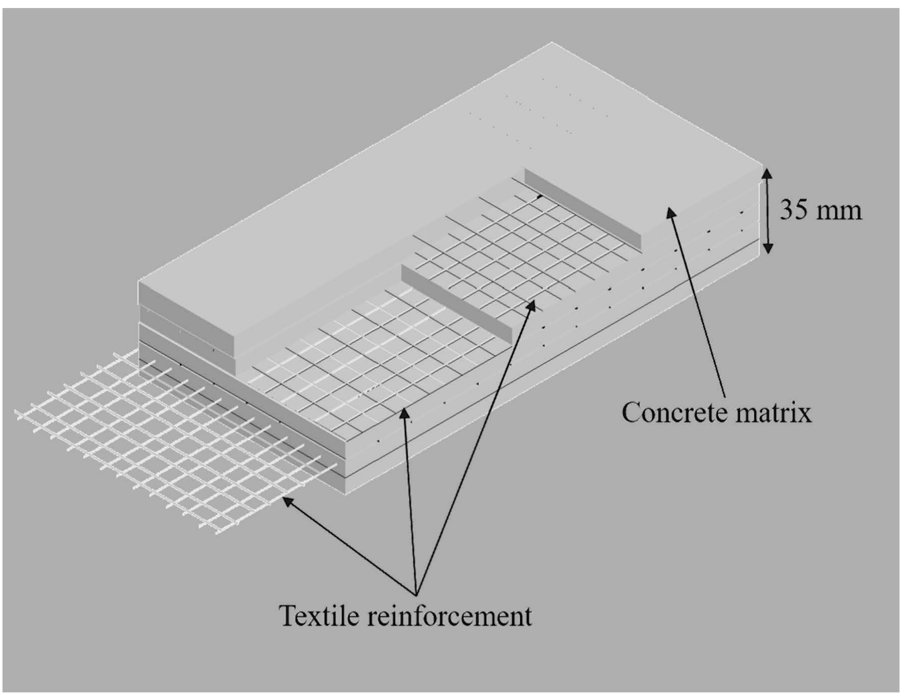

FIGURE 3.3 Schematic of TRC with multilayer textile reinforcement.

it an attractive material from a durability perspective. TRC has excellent bearing capacity and ductility, which enable us to produce thin and lightweight structural components [52]. TRC enhances durability as well as helps in minimizing the use of concrete. Consequently, it is argued to be more environmentally sustainable than traditional steel-reinforced concrete due to less consumption of cement [52, 53].

Currently, the application of TRC is in the form of strengthening existing concrete structures, facades, and structures that carry minor vertical loads.

A few examples of TRC applications are depicted in Figure 3.4. The type of fibre used in the textile reinforcement plays a critical role in influencing TRC properties, and it is chosen depending upon application, with desired material properties such as anti-corrosive, temperature resistance, and bond quality. In addition to these material properties, the cost and environmental impact also play a significant role in the choice of fibre for TRC [54, 55]. Tomoscheit et al. [56] found that concrete consumption can be reduced up to 85% in TRC applications that use carbon or alkali-resistant (AR) glass textiles as reinforcement. The LCA based on a cradle-to-gate system boundary showed that reduced concrete material consumption in TRC considerably decreases the cumulative energy demand and environmental impact compared to the conventional reinforced concrete element [55]. While research on TRC has revealed many promising attributes from a sustainability point of view, its usage is limited due to the lack of design tools, standards, and understanding of its long-term behaviour. Research efforts spanning experimental, analytical, and numerical investigations on TRC are ongoing to efficiently design the TRC components.

The behaviour of TRC depends primarily on the strength of the concrete matrix, the strength of the textile fabric, and the bond between the textile and concrete matrix [59]. Several researchers have studied the direct tensile behaviour of TRC by using different setups [60]. Under uniaxial tension, the TRC exhibits trilinear behaviour, which can be characterized into three zones. Zone I corresponds to the elastic stage dominated by the matrix, zone II corresponds to the multiple-cracking stage, and zone III corresponds to the post-multiple-cracking stage, which is dominated by the properties of textiles [61]. The typical behaviour of TRC under flexural loading is categorized into two zones by Zargaran et al. [62]. The first zone is dominated by the role of concrete where the concrete matrix breaks, and a sudden drop occurs. Following the drop, the concrete cracks begin to widen, and depending on the volume fraction of the textile reinforcement shows either deflection hardening or under-reinforced response. Unlike conventional concrete, two types of bonds must be considered while understanding the bonding behaviour of TRC: (1) the bond between filaments and concrete, and (2) the bonds between the filaments themselves [61, 63, 64].

Smitha et al. [65] reported that stretching or prestressing the textile fabric while preparing TRC can substantially improve the mechanical performance of TRC components. While most researchers used expensive AR-glass textiles, Paul et al. [66] explored the use of E-glass textiles for TRC, with suitable coating and matrix modification. A few research outcomes of the Building Technology and Construction Management (BTCM) group of IIT Madras [67] on TRC are shown in Figure 3.5a–d. The TRC water tanks shown in Figure 3.5d are lighter and more durable than conventional steel tanks, as they do not corrode. Further, TRC tanks are easier to fabricate as less effort is

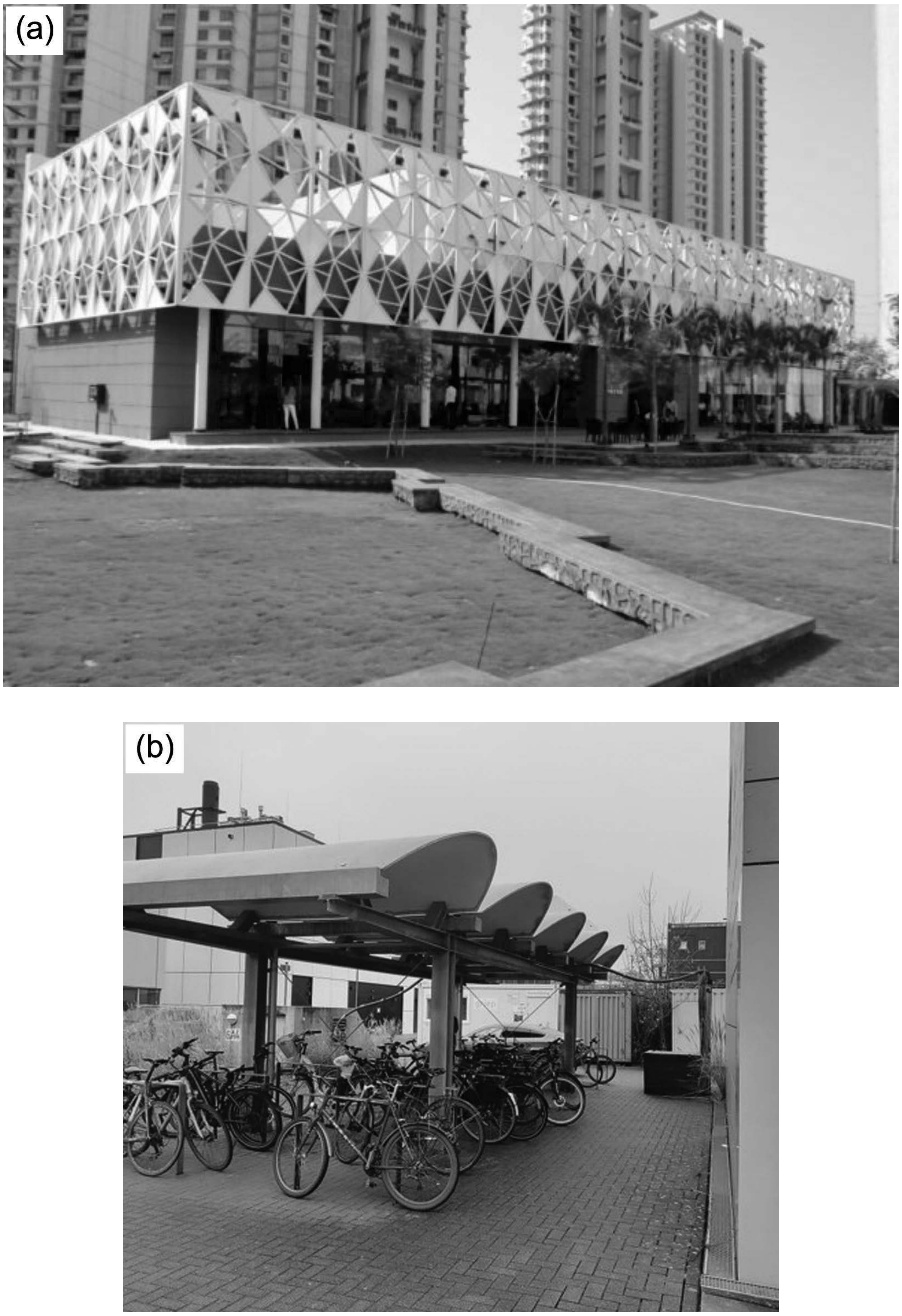

FIGURE 3.4 Application of TRC: (a) TRC facade construction in Mumbai, India, by Raina Industries [57]; (b) cycle shed made of TRC shell elements at Institute of Textile Technology at RWTH Aachen University, Germany [58].

Photo by Keerthana Kirupakaran.

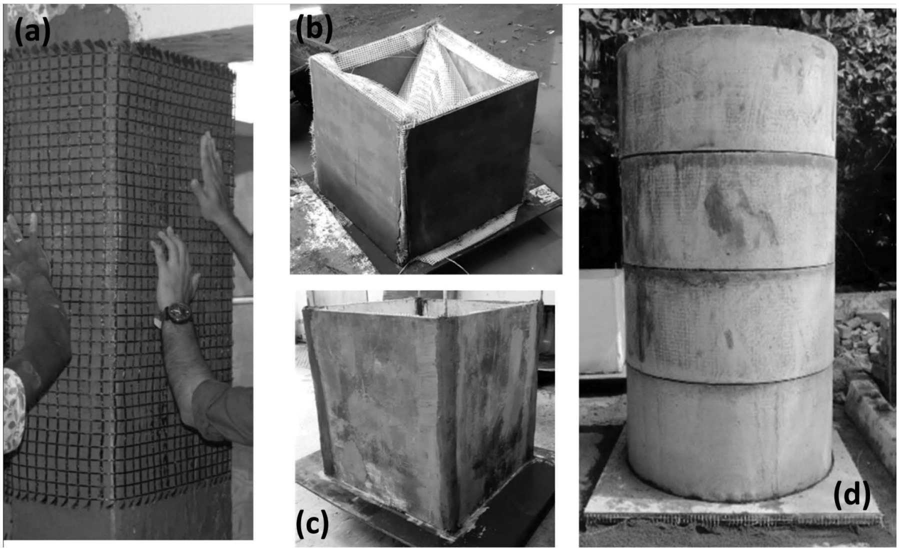

FIGURE 3.5 TRC research at IIT Madras [67]: (a) use of textile mesh to retrofit a concrete structural column; (b) and (c) a boxed form structure by folding planar TRC components; (d) modular TRC sewage water tank.

required to bend the textile fabric, unlike steel rebars. With ongoing research efforts and emerging applications of TRC, large-scale implementation of TRC is envisaged. While utilizing high-performance, low carbon-intensive materials like FRC and TRC is one way towards achieving sustainability goals in construction, minimizing construction waste and reusing them again in new construction is very important for sustainable construction.

3.6 CONSTRUCTION AND DEMOLITION WASTE

Any waste arising from the construction, repair, remodelling, and demolition of a civil structure is referred to as construction and demolition (C&D) waste. C&D waste is composed of non-degradable and inert materials such as concrete, tiles, brick aggregates, rock particles, glass, plastic, metals, wood, and excavated soil. Urbanization and modern infrastructure have significantly increased the demand for natural resources and material consumption. The construction industry utilizes about 32% of the natural resources [68]. Currently, it is estimated that about 75% of C&D waste has a residual value that is neither reused nor recycled [69]. In 2014, China was leading in C&D waste generation worldwide with 1.13 billion tons. C&D waste generated annually in India is estimated to be 10 to 12 million tons, which on a per capita basis is around 8.29 to 3.95 kg/year. According to Ram et al. [70], these projected figures of C&D waste in India are a serious underestimation compared to other countries with C&D waste of 110–842 kg capita per year.

The construction sector is the second largest sector in India in terms of material consumption [71, 72]. The increase in construction activity has led to high demands on construction materials, particularly on river sand [73, 74].

High construction material consumption results in high construction waste. Figure 3.6 shows typical C&D waste composition in India [75]. In the current scenario, C&D waste management is critical owing to its impact on the environment and public health [76, 77].

Several measures are being taken worldwide to mitigate C&D waste reuse through the imposition of strict policies for C&D waste management. Some initiatives by the Indian government to mitigate C&D waste include: (1) The Technology Information, Forecasting and Assessment Council (TIFAC) [78] published guidelines for managing construction waste, which outlines selling reusable materials obtained after construction or demolition at a discounted rate in the market, and utilizing only non-reusable materials for landfill; (2) the Bureau of Indian Standard IS: 383–2016 [79] permitted the use of manufactured sand obtained from C&D wastes and other industrial wastes as partial replacement of coarse and fine aggregate from natural sources; and (3) the National Building Code (NBC) of India (2000) [75] included the provision to use recycled concrete aggregate (RCA) for bank protection, bulk filling cement, sidewalks, drainage system bases etc. It is further stated that 30% of natural aggregate could be replaced by RCA, and this percentage can be increased up to 50% for pavements and other areas under pure compression. With respect to the reuse of C&D materials, RCA has received a lot of attention. However, RCA shows reduced strength when used in concrete due to the old mortar particles sticking on its surface. In order to remove this mortar, thermo-mechanical treatment is necessary, which is

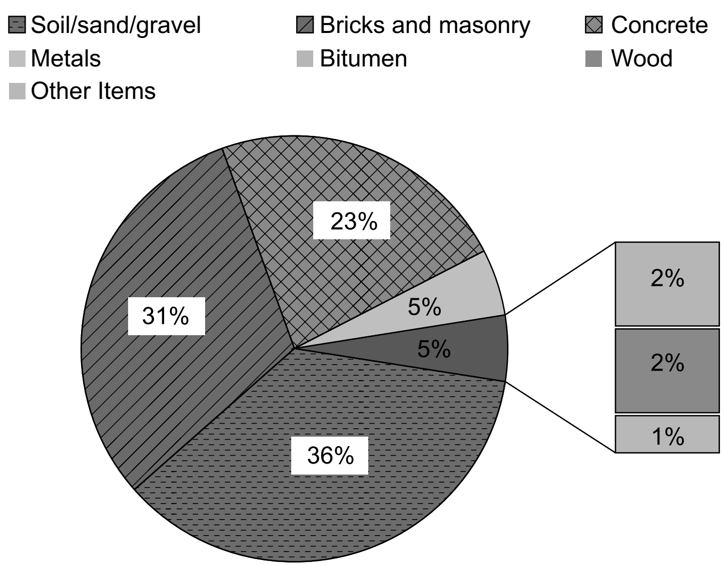

FIGURE 3.6 Typical C&D waste composition in India,

again energy intensive. Rohit et al. [80] used solar power for this purpose and generated RCA of different sizes.

While research efforts and implementation measures are in place, the Indian construction industry cannot profit adequately from cost savings due to several reasons. The following are some of the reasons reported by Wildermuth [81]:

- Lack of awareness of the waste management measures and protocols among local contractors, architects, and construction is a major barrier to the utilization of C&D waste in the industry.
- Lack of interest from the customers/clients to adopt waste minimization and management measures in the project.
- Lack of adequate training and knowledge on the economic benefits and social implications of C&D waste management among customers and contractors. To overcome this situation, more technical institutes should adopt these subjects in the academic curriculum.
- Lack of skilled labour in the construction sector with respect to recycling and reuse of C&D waste in the new construction.
- Lack of market competition between contractors due to the challenges mentioned earlier. If one of the contractors shows profit by implementing C&D waste management and implementation strategies in their project, that will inspire others to implement the same. When more contractors see the value, market competition will grow, thus facilitating effective utilization of C&D waste.
- Lack of enforcement of policies and legislation on C&D waste management measures by government bodies.
- Lack of interest from architects to use C&D waste in the new construction or minimize waste during the design stage.

Given the growth of the construction sector in India, it is imperative that the production of C&D waste must increase manyfold. If proper C&D waste management measures are not adopted, it could pose a serious threat to environmental sustainability and public health. Government intervention in C&D waste management through strict rules and regulations is critical to achieve quantifiable results.

While C&D waste management measures are ongoing, a new construction technology such as concrete 3D printing is gaining a lot of attention. This technology is discussed in the following section.

3.7 CONCRETE 3D PRINTING TECHNOLOGY

Concrete 3D printing (C3DP) is an upcoming technology that involves the digital fabrication of concrete structures by eliminating formwork. In conventional reinforced concrete construction, formwork constitutes about 40% of the total budget of concrete. However, in C3DP technology, the formwork cost, associated labour charges, and time required for setting up formwork are eliminated [82]. While this technology facilitates the construction of highly customized buildings with complex designs, there are several challenges concerning scaling, material, and structural performance and its suitability to severe environmental conditions [83].

Concrete 3D printers are controlled by a machine language called g-codes that directs the printer until the desired shape is printed. To implement C3DP on-site, the construction area is initially levelled, and the printer with nozzle and robotic arms are set up [84]. A hose is connected to the nozzle, through which concrete is extruded to form layers. In 2018, the first concrete 3D-printed fully functional house (Figure 3.7) was built at IIT Madras, in Chennai, India, by a startup called Tvasta [85]. This house was printed using a custom-made 3D printer and took just five days to complete. It showcased the potential of 3D printing technology for affordable housing solutions.

One of the challenging aspects of 3D-printable concrete is to maintain specific properties in its fresh state, such as reduced slump and fast hardening. Since there is no external formwork, the previously printed concrete layers support the subsequent layers, thus it is important for the deposited concrete layers to harden faster while still being extrudable through the nozzle [86]. With the increase in popularity of 3D printing technology, large-scale printing setups are being designed to build large

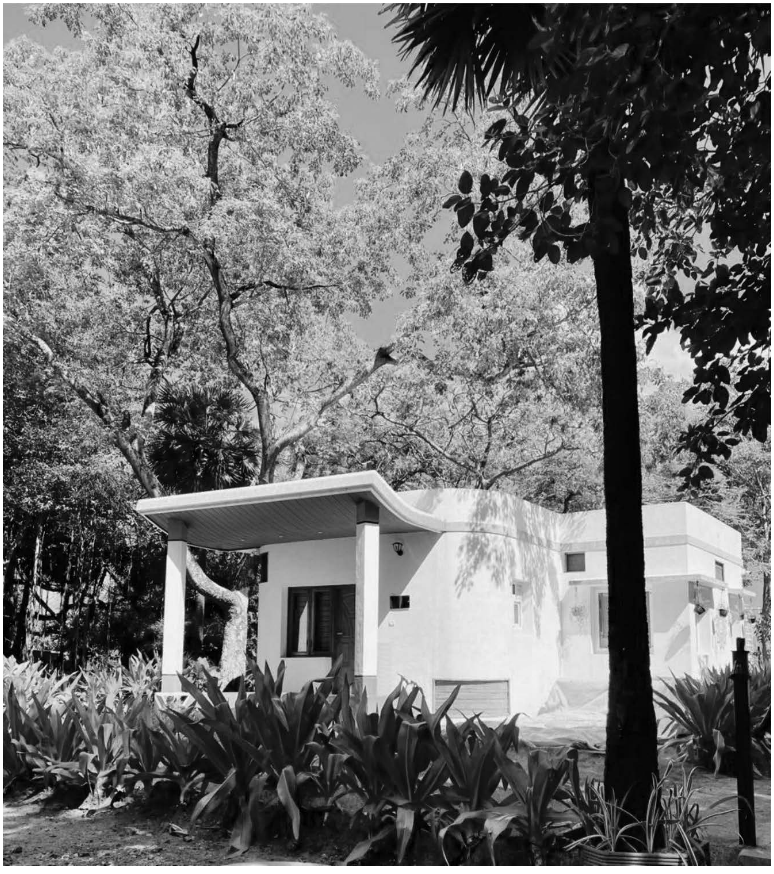

FIGURE 3.7 3D-printed concrete house at IIT Madras.

Photo by Roshini Ramanathan, IIT Madras.

concrete structures. However, the major challenge in upscaling this technology lies in the precise design of concrete mix that can maintain the required workability and buildability properties till the large component is printed [87]. Viktor et al. [88] developed the CONPrint3D concept for on-site monolithic 3D printing driven by the demands and boundary conditions of construction practice. The robotic arm 3D printer developed by Keating et al. [89] uses a multi-axis robotic arm that helps in navigating the printing nozzle.

Currently, several efforts are underway to upgrade the C3DP technology to produce reinforced concrete structures [87]. Cohen and Carlson [90] used the pointillistic time-based deposition (PTBD) method [91], contrary to using a conventional linear layering approach for printing. The steel or micro-cables are also being explored as reinforcement in 3D-printed elements. The reinforcement entrainment device is used to embed the steel cables into the concrete layers (RED) [92]. Hack and Lauer [93] proposed a digital fabrication method of building reinforced meshes and formwork simultaneously with printing.

Hambach et al. [94] added glass, basalt, or carbon fibres to concrete 3DP to increase the flexural strength to 30 MPa, and Gebhard et al. [95] explored the entrainment of fibres in the concrete 3DP process. They emphasized that, unlike conventional FRC mix design, fibres in 3D printable concrete need to be re-engineered with short fibres to ensure pumpability.

While different reinforcement systems are being explored on the one hand, research on less-carbon-intensive alternate material systems is being explored on the other hand. Geopolymer and alkali-activated materials are being widely explored as mixes for use in concrete 3DP. Shantanu et al. [83] reported that the rapid hardening nature of geopolymer mixes can improve buildability properties without the chemical accelerators. Further, the conventional SEMs and limestone-calcined clay cement (LC3) are also being explored to develop a mix suitable for C3DP [83, 96]. Shanthanu et al. [83] showed another way to reduce the binder content by using coarse aggregates in the printable concrete mix. While there are several challenges in terms of workability, extrudability, and buildability associated with the use of coarse aggregate, its economic feasibility and low CO_2 footprint can be beneficial for large-scale 3D printing, particularly from a sustainability viewpoint.

A detailed cradle-to-gate life-cycle assessment (LCA) performed by Mohamed et al. [97] revealed that concrete 3D printing technology significantly reduces environmental effects in terms of global warming potential, eutrophication potential, acidification potential, smog formation potential, and fossil fuel depletion, as compared to conventional construction methods. While C3DP technology looks promising, further research is required to evaluate its long-term performance, and only a whole LCA from cradle-to-grave or cradle-to-cradle can help in evaluating its true sustainability potential. Nevertheless, C3DP is a perfect example of where the modern world of digitization integrates with the construction industry. However, with the dawn of the 21st century, new technologies like machine learning, automation, and robotics have engulfed various facets of the construction industry, which are discussed in the following section.

3.8 ROLE OF ARTIFICIAL INTELLIGENCE, ROBOTICS, AND AUTOMATION IN THE CONSTRUCTION INDUSTRY

Currently, we are in the fourth generation of the Industrial Revolution, commonly termed as Industry 4.0. The industrial sector is revolutionizing with the integration of new technologies such as the Internet of Things, cloud computing, artificial intelligence (AI), and machine learning. The construction industry is also gradually adopting these technologies in construction practices. This revolution in the construction sector is commonly termed as construction 4.0.

The construction industry often experiences cost inefficiencies, delays in projects, poor performance in terms of health, productivity, and safety, uninformed decision-making, and poor-quality performance [98]. Further, the rate of growth in the construction industry is highly hindered because of the amount of work, labour, safety, quality, quantity, and specifications required in construction processes [98]. Most of these processes can be digitized and automated, leading to substantial savings in time and cost. Construction 4.0 is an amalgamation of trends and technologies that transform the way built environment assets are designed, constructed, and operated. There are three primary opportunities where digitization and automation can be used in construction industries [99]:

- Automation of traditional on-site tasks which are physical: this includes usage of robots for laying bricks, paving roads using machines, etc.
- Automation of modular construction which includes production in industries such as 3D printing of components for construction-like facades.
- Automation and digitalization of planning, design, and management procedures.

One question that pops up about the usage of AI, automation, and robots in the construction industry is "Will AI replace humans?". The construction industry is the kind of industry where even a small change in any information/specification provided will lead to a significant impact on the task. So, there is always a need for human supervision to ensure everything goes on track. With the amount of work that lies in hand and the difficulties faced in each one of them, we can make maximum utilization of AI tools with minimum human supervision. The sophisticated collaboration of machines and human labour in automated construction creates a more intricate scenario than conventional construction [100]. Robotics and automation technology can be highly beneficial in repetitive work such as bricklaying. The main advantage is that the task can be done with a lot more precision, accuracy, and safety. Quantifying and controlling productivity are essential for efficiently managing time and cost in construction [101]. For example, the tunnel boring machine (TBM) avoids problems with accuracy and tedious calibration processes by using the conventional laser station [99, 102]. This can also be extended to construction quality control, interference management, and data exchange in construction, development of new tools, schemes, and components in construction [103]. Hence, to answer the question, AI and other tools can be very beneficial to the construction sector provided one knows how to use these technologies properly and effectively.

In recent times, robots have been used successfully in various construction activities such as 3D printing and contour crafting, demolition robots, bricklaying robots, drones, welding robots, forklift robots, robots for roadwork, and humanoid robots [104]. Research efforts are underway across the globe to integrate AI tools with various construction processes. A computer vision (CV)-based textural analysis method is being researched where the images from a 2D camera are processed to quantify the textural variations on the surface of concrete 3D-printed layers [105]. Several machine learning tools are being explored for monitoring the structural stability in an automated construction through sensor measurements taken from the structure [106]. Small robots are being developed to perform repetitive and time-consuming work at construction sites, which can lead to savings in labour cost and time [107]. Further, investigations are underway to automate the work-sampling process for evaluating labour productivity [101], and automated progress monitoring using a photogrammetric point cloud is being explored to track the construction activity [108].

While using AI tools, automation, and robotics in the construction sector is largely beneficial, it also comes with a few challenges, which include explainable AI, cyber security issues, talent shortage among labourers, and high initial costs. The successful implementation of AI and automation tools in construction will require efforts from the following three sectors [99]:

- The public sector should take steps to revamp the old education system to include current trends and emerging technologies.
- The private sector should focus on the skill development of labourers and workers in the construction industry.
- Industry partners should conduct boot camps and hackathons to help their employees transition from the conventional methods and train them to work with construction 4.0 technologies.

As new technologies related to construction 4.0 are emerging rapidly, it is very important to assess their sustainability aspects in terms of social, economic, and environmental viewpoints [109, 110]. Construction 4.0 technologies are at the early stage, and there is a need to further study and examine these technologies to understand their true impact on the society and environment, and for sustainable development.

While several emerging construction materials and technologies show promising attributes towards sustainable development in the construction sector, real change can happen only when these technologies are assessed properly on their impact on the social, environmental, and economic sustainability front. The technologies with positive impacts are then implemented at large scale. In this light, standards and policies imposed by the government have a significant role to play, which is discussed in the following section.

3.9 SIGNIFICANCE OF STANDARDS AND POLICIES IN SUSTAINABLE CONSTRUCTION

Sustainability in construction can be truly achieved only when the technologies or ideas that cater to sustainable development are implemented on a large scale. While there are many sustainable technologies coming up in the construction sector, they are relatively low compared to other industries. The people adopting sustainable technologies are classified into three major categories [111]: (1) government—federal, state, and local governments and related organizations, semi-government organizations, and political leaders; (2) for-profit and non-profit organizations—large business houses, multi-national corporations, community groups, media, trade organizations, etc.; and (3) individuals—general contractors, engineers, architects, owners, developers, sustainable building consultants, etc. However, the adoption of sustainability principles and technologies by these three categories is particularly limited in the construction market. The major obstacles that limit sustainable construction are lack of interest from the investors, lack of training and knowledge on sustainable development and construction, conservatism in the education of architects and civil engineers, inadequate funding for research in this area, financial problems, and lack of a well-defined set of norms, standards, and sustainable construction practices that can be used in projects [112–115]. The government being the major player can bring transformational changes to enable sustainable construction by imposing standards and policies. Sustainable construction requires a holistic approach—starting from the design, construction, operation, and demolition to recycling and reuse of materials, and significant changes in the overall organization of construction, both at the market and company level [112]. The government's role in this aspect is critical as it develops and imposes policies that can influence the construction industry directly or indirectly. Not just at the industry level, government intervention can also play a dominant role in factors affecting energy efficiency, waste management, and climate change as well.

With respect to India, recognizing the importance of sustainable building in addressing environmental issues and fostering long-term sustainability, the government has established certain rules and procedures to help achieve these goals.

These laws include encouraging green building certifications, upholding energy-efficient construction codes, providing financial incentives and subsidies, boosting research and development, and enhancing skill development. Some of the organizations within India related to policies are:

(1) The National Institution for Transforming India (NITI) Aayog is a policy think tank of the Indian government that provides inputs regarding the different programs and policies of the government. Some of their key functions include policy formulation, monitoring, and evaluation, and sustainable development goals. A few NITI Aayog policies are: (a) Atal Innovation Mission (AIM), which is an initiative to create and promote a culture of innovation and entrepreneurship in India; (b) Atal Bhujal Yojana for sustainable groundwater management; and (c) sustainable infrastructure development.
(2) The Ministry of Electronics and Information Technology (MEITY) is responsible for formulating and implementing policies related to information technology, electronics, and the internet. They support work related to artificial intelligence (AI), augmented reality (AR) vs. virtual reality (VR), the internet of things, blockchain, robotics, computer vision, drones, etc.

(3) The Indian Renewable Energy Development Agency (IREDA) facilitates the development and deployment of renewable energy technologies. This organization provides various financial assistance mechanisms such as loans, project financing, and consultancy services to renewable energy projects across different sectors, including wind energy, solar energy, bioenergy, small hydropower, and energy efficiency.
(4) The Bureau of Energy Efficiency (BEE) is established under the Ministry of Power with an objective to promote energy efficiency and conservation across various sectors of the economy. BEE plays a crucial role in formulating and implementing policies, programs, and initiatives to enhance India's energy efficiency standards and practices. Under BEE, the Energy Conservation Building Code (ECBC) sets minimum energy standards for new residential buildings. The ECBC does not cover small residential buildings, whereas these buildings constitute a major part of the residential building sector in the country [10, 11].
(5) The Indian Green Building Council (IGBC) functions as a separate platform for the promotion of green buildings. Its rating system, called the green building rating system, assesses the buildings across different parameters such as energy efficiency, pollution and waste reduction measures, use of non-toxic materials, indoor air quality, etc.

These government bodies are essential and play an important role in sustainable construction in India. Further, the Ministry of Environment, Forest and Climate Change (MoEF&CC) of the Indian government formulated C&D waste management rules [75] in 2016, and the Ministry of Housing and Urban Affairs published a "Strategy for promoting processing of construction and demolition waste and utilisation of recycled products" in 2018 [116].

Strategies and policies play a major role in ensuring that the innovations entering the market are truly sustainable. They provide a structured framework and guidelines to make sure that all the requirements are met. They pave the way for the widespread adoption and deployment of these technologies. They provide benchmarks for various aspects of sustainable construction, allowing various organizations to ensure that the requirements are met. The incentives provided by these policies will help more organizations move towards sustainability and create a healthy living environment, as market demand moves towards sustainable construction, and they lead to the development of new technologies that meet sustainable requirements. Standards and policies are the foundation of India's journey towards sustainable construction. Policies also create quality control standards, ensuring that building projects adhere to necessary requirements. They make sure that the resources are conserved by the use of sustainable materials. By establishing rules for the procurement and tendering processes, they encourage fair competition. Finally, policies reduce risk on the legal and financial fronts by establishing a framework for agreements and dispute settlement.

In order to enable the adoption of sustainable construction-related technology, standards and policies are crucial, and their importance cannot be overestimated. Standards and policies promote innovation, cooperation, and ongoing development in sustainable construction practices by establishing a favourable environment. In the end, they play a critical role in developing a more resilient and sustainable built environment for future generations.

3.10 SUMMARY AND CONCLUSION

Sustainable construction technologies play a pivotal role in addressing environmental concerns, reducing resource consumption, and promoting the long-term viability of the construction industry. This chapter gives an overview of research, innovation, application, and implementation efforts that are being carried out in different facets of the construction sector to achieve sustainability. Several construction materials and technologies are emerging to promote sustainability in construction. However, the sustainability potential of any component or technology can be established only by performing a life-cycle assessment (LCA). With respect to the construction industry, quantifying embodied and operational carbon in the different stages of the building life cycle is essential. With respect to sustainable construction materials, the use of supplementary cementitious materials (SCMs) is one of the focus areas, as the production of Portland cement is a major contributor to CO_2 emissions in the environment. Some of the widely used SCMs include fly ash, ground granulated blast furnace slag, and limestone calcined clay cement (LC3). Another way to reduce carbon-intensive cement is by constructing thin and lightweight structures that consume less material. Fibre-reinforced concrete and textile-reinforced concrete are high-performance materials that enable the construction of thin and lightweight structures. Further, the construction industry generates large amounts of waste during C&D of structures. It is estimated that about 75% of C&D waste which goes into landfill has residual value. Several research efforts are in place to utilize C&D in new construction, and guidelines and standards are coming up to promote C&D utilization. For sustainable construction, waste minimization, recycling, and reuse are very important. Currently, the construction industry is revolutionizing with digitization, artificial intelligence, automation, and robotics technologies, all of which are commonly termed as construction 4.0. Several technologies are emerging with automated systems leading to less human intervention such as 3D printing technology, brick-laying robots, surface finish robots, and drones. While these technologies are largely beneficial, they come with the challenges of cyber security issues, explainable AI, talent shortage among labourers, and high initial cost. Further, it is important to perform the LCA of construction 4.0 technologies to truly understand their sustainability potential and the long-term effects on society. In spite of the promising developments, real change can happen only when these technologies are assessed properly on their social, environmental, and economical sustainability and subsequent implementation of the ones with a positive impact at a large scale. In light of this, standards and policies imposed by the government play a significant role. Standards and policies provide a comprehensive roadmap for incorporating sustainable practices into the building industry. They help establish a unified approach by defining common guidelines, procedures, and benchmarks for sustainable construction. They also encourage consistency and dependability in the use of sustainable technology, ensuring that projects achieve their social and environmental goals.

Thus, a holistic approach of combining research, innovation, and policies is the way forward towards achieving sustainable construction.

3.11 ACKNOWLEDGEMENT

The author thanks the research scholars and professors of the Building Technology and Construction Materials and Management (BTCM) group, Department of Civil Engineering, IIT Madras, Chennai, India. The help of students Roshini Ramanathan (BTech, IIT Madras), Hariharan N (BTech, NIT Trichy), Anusha R (BTech, NIT Trichy), Valliappan R M (BTech, NIT Trichy), and S Cyril John (BTech, NIT Trichy) are highly appreciated. The support from the Institute of Eminence Research Initiative Grant on Technologies for Low Carbon and Lean Construction (TLC2) from IIT Madras is acknowledged.

REFERENCES

[1] G. A. for Buildings, I. E. A. Construction, the United Nations Environment Programme, *2019 global status report for buildings and construction: Towards a zero-emission, efficient and resilient buildings and construction sector* (2019). https://www.unep.org/resources/publication/2019-global-status-report-buildings-and-construction-sector

[2] U. N. E. Programme, *Buildings and climate change: Summary for decision makers* (2009). https://wedocs.unep.org/20.500.11822/32152

[3] J. M. Hussin, I. A. Rahman, A. H. Memon, The way forward in sustainable construction: Issues and challenges, *International Journal of Advances in Applied Sciences* 2 (1) (2013) 15–24.

[4] G.DataReportCode:GDTMT-TR-S348,*Environmental,social,andgovernance(esg)framework thematic research* (2022). www.globaldata.com/store/report/esg-frameworktheme-analysis/

[5] P. Huovila, L. Koskela, Contribution of the principles of lean construction to meet the challenges of sustainable development, in: *Proceedings IGLC*, vol. 98 (1998). https://iglc.net/papers/Conference/8

[6] J. Skibsted, R. Snellings, Reactivity of supplementary cementitious materials (scms) in cement blends, *Cement and Concrete Research* 124 (2019) 105799.

[7] Embodied carbon. www.holcimfoundation.org/embodiedcarbon

[8] M. K. Dixit, J. L. Fernández-Solís, S. Lavy, C. H. Culp, Need for an embodied energy measurement protocol for buildings: A review paper, *Renewable and Sustainable Energy Reviews* 16 (6) (2012) 3730–3743.

[9] B. Sizirici, Y. Fseha, C.-S. Cho, I. Yildiz, Y.-J. Byon, A review of carbon footprint reduction in construction industry, from design to operation, *Materials* 14 (20) (2021) 6094.

[10] T. Ibn-Mohammed, R. Greenough, S. Taylor, L. Ozawa-Meida, A. Acquaye, Operational vs. embodied emissions in buildings a review of current trends, *Energy and Buildings* 66 (2013) 232–245.

[11] T. Ramesh, R. Prakash, K. Shukla, Life cycle energy analysis of buildings: An overview, *Energy and Buildings* 42 (10) (2010) 1592–1600.

[12] E. C. W. Group, et al., Methodology to calculate embodied carbon of materials, *Information Paper* 32 (2012) 2012.

[13] B. Nebel, A. Alcorn, B. Wittstock, *Life cycle assessment: adopting and adapting overseas LCA data and methodologies for building materials in New Zealand*. ISBN: 978-0-478-37560-2 (online). https://www.mpi.govt.nz/dmsdocument/6280/direct

[14] C. Magwood, T. Huynh, V. Olgyay, *The hidden climate impact of residential construction—zeroing in on embodied carbon emissions for low-rise residential buildings in the united states* (2023). https://rmi.org/insight/hidden-climate-impact-ofresidential-construction/

[15] B. V. Reddy, K. Jagadish, Embodied energy of common and alternative building materials and technologies, *Energy and Buildings* 35 (2) (2003) 129–137.

[16] G. P. Hammond, C. I. Jones, Embodied energy and carbon in construction materials, *Proceedings of the Institution of Civil Engineers-Energy* 161 (2) (2008) 87–98.

[17] J. G. Olivier, K. Schure, J. Peters, et al., Trends in global co2 and total greenhouse gas emissions, *PBL Netherlands Environmental Assessment Agency* 5 (2017) 1–11.

[18] K. Scrivener, Issues in sustainability in cements and concrete, *American Ceramics Society Bulletin* 91 (2012) 47–50.

[19] J. Skibsted, R. Snellings, Reactivity of supplementary cementitious materials (scms) in cement blends, *Cement and Concrete Research* 124 (2019) 105799.

[20] M. C. Juenger, R. Siddique, Recent advances in understanding the role of supplementary cementitious materials in concrete, *Cement and Concrete Research* 78 (2015) 71–80.

[21] A. Standard, *C618–15 standard specification for coal fly ash and raw or calcined natural pozzolan for use in concrete*, ASTM International, West Conshohocken, PA.

[22] M. Thomas, Optimizing the use of fly ash in concrete, Vol. 5420, Portland Cement Association Skokie, IL, USA, 2007.

[23] D. Suresh, K. Nagaraju, Ground granulated blast slag (ggbs) in concrete—a review, *IOSR Journal of Mechanical and Civil Engineering* 12 (4) (2015) 76–82.

[24] P. Chaunsali, *Interaction of cement kiln dust (CKD) with fly ash and ground granulated blast furnace slag: A microstructural investigation*, Ph.D. thesis, Department of Civil and Environmental Engineering, Clarkson University, Potsdam, NY, 2010. doi: 10.13140/RG.2.1.3797.0083

[25] P. Chaunsali, S. Peethamparan, Influence of the composition of cement kiln dust on its interaction with fly ash and slag, *Cement and Concrete Research* 54 (2013) 106–113.

[26] P. Chaunsali, S. Peethamparan, Novel cementitious binder incorporating cement kiln dust: Strength and durability, *ACI Materials Journal* 110 (3) (2013) 297–304.

[27] M. M. Johari, J. Brooks, S. Kabir, P. Rivard, Influence of supplementary cementitious materials on engineering properties of high strength concrete, *Construction and Building Materials* 25 (5) (2011) 2639–2648.

[28] P. Dinakar, K. Babu, M. Santhanam, Durability properties of high volume fly ash self compacting concretes, *Cement and Concrete Composites* 30 (10) (2008) 880–886.

[29] A. Bahurudeen, D. Kanraj, V. G. Dev, M. Santhanam, Performance evaluation of sugarcane bagasse ash blended cement in concrete, *Cement and Concrete Composites* 59 (2015) 77–88.

[30] S. Reynolds, *The future of ferrous slag, market forecasts to 2020*, Pira International Ltd., Cleeve Road, Leatherhead, UK.

[31] M. McCarthy, T. Robl, L. Csetenyi, Recovery, processing, and usage of wet-stored fly ash, in: *Coal combustion products (CCP's)*, Woodhead Publishing, 2017, pp. 343–367. https://doi.org/10.1016/B978-0-08-100945-1.00014-9

[32] M. C. Juenger, R. Snellings, S. A. Bernal, Supplementary cementitious materials: New sources, characterization, and performance insights, *Cement and Concrete Research* 122 (2019) 257–273.

[33] Y. Dhandapani, T. Sakthivel, M. Santhanam, R. Gettu, R. G. Pillai, Mechanical properties and durability performance of concretes with limestone calcined clay cement (lc3), *Cement and Concrete Research* 107 (2018) 136–151.

[34] A. Bahurudeen, M. Santhanam, Influence of different processing methods on the pozzolanic performance of sugarcane bagasse ash, *Cement and Concrete Composites* 56 (2015) 32–45.

[35] G. Xu, X. Shi, Characteristics and applications of fly ash as a sustainable construction material: A state-of-the-art review, *Resources, Conservation and Recycling* 136 (2018) 95–109.

[36] E. Aprianti, P. Shafigh, S. Bahri, J. N. Farahani, Supplementary cementitious materials origin from agricultural wastes—a review, *Construction and Building Materials* 74 (2015) 176–187.

[37] M. Juenger, J. L. Provis, J. Elsen, W. Matthes, R. D. Hooton, J. Duchesne, L. Courard, H. He, F. Michel, R. Snellings, et al., Supplementary cementitious materials for concrete: Characterization needs, *MRS Online Proceedings Library (OPL)* 1488 (2012) 8–22.

[38] C. M. Helepciuc, A. A. Serbanoiu, B. V. Serbanoiu, et al., Fibre reinforced concrete-a sustainable material in the context of building industry and environmental challenges, *Advances in Environmental Sciences* 10 (1) (2018) 1–6.

[39] O. Kayali, Sustainability of fibre composite concrete construction, in: Sustainability of construction materials, *Elsevier* (2016) 539–566.

[40] M. Saidani, D. Saraireh, M. Gerges, Behaviour of different types of fibre reinforced concrete without admixture, *Engineering Structures* 113 (2016) 328–334.

[41] British Standards Institution, BS EN 14651:2005+A1:2007, *Test method for metallic fibre concrete: Measuring the flexural tensile strength (limit of proportionality (LOP), residual).* BSI (British Standard Institution), 2008. ISBN 978 0 580 61052 3. https://www.en-standard.eu/bs-en-14651-2005-a1-2007-test-method-for-metallic-fibre-concrete-measuring-the-flexural-tensile-strength-limit-of-proportionality-lop-residual/

[42] F. Bulletins, Bulletins 55–56: Model code 2010—first complete draft. (2010) asquapro technical booklet en 14651: Test method for metallic fibre concrete, Measuring the flexural.

[43] A. C. 544, *Report on design and construction of fiber reinforced precast concrete tunnel segments*, American Concrete Institute (ACI), Farmington Hills, MI, 2016.

[44] L. Vandewalle, D. Nemegeer, L. Balazs, B. Barr, J. Barros, P. Bartos, N. Banthia, M. Criswell, E. Denarie, M. Di Prisco, et al., Rilem tc 162tdf: Test and design methods for steel fibre reinforced concrete'-sigmaepsilon-design method-final recommendation, *Materials and Structures* 36 (262) (2003) 560–567.

[45] B. of Indian Standards, *Flexural strength and toughness parameters of fibre reinforced concrete method of test*, BIS-CED2, New Delhi, 2020.

[46] S. Mindess, Fibrous concrete reinforcement, *Developments in the Formulation and Reinforcement of Concrete* (2008) 154–166.

[47] F. Farhat, D. Nicolaides, A. Kanellopoulos, B. L. Karihaloo, High performance fibre-reinforced cementitious composite (cardifrc)—performance and application to retrofitting, *Engineering Fracture Mechanics* 74 (1–2) (2007) 151–167.

[48] S. S. Pendhari, T. Kant, Y. M. Desai, Application of polymer composites in civil construction: A general review, *Composite Structures* 84 (2) (2008) 114–124.

[49] J. S. Lawler, D. Zampini, S. P. Shah, Permeability of cracked hybrid fiber-reinforced mortar under load, *Materials Journal* 99 (4) (2002) 379–385.

[50] S. J. Stephen, R. Gettu, Fatigue fracture of fibre reinforced concrete in flexure, *Materials and Structures* 53 (3) (2020) 56.

[51] ACI 544.3R-08 *Guide for specifying, proportioning, and production of fiber reinforced concrete*, American Concrete Institute, 2008. https://www.concrete.org/Portals/0/Files/PDF/Previews/544.3R-08web.pdf

[52] T. Gries, A. Roye, P. Offermann, A. Peled, *Textile reinforced concrete-state-of-the-art report of RILEM TC 201-TRC*, Report, Aachen, France, Autumn (2006), Pages 292. ISBN: 2-912143-99-3, e-ISBN: 2351580001. https://www.rilem.net/publication/publication/100

[53] K. P. Mehta, Reducing the environmental impact of concrete, *Concrete International* 23 (10) (2001) 61–66.
[54] P. Domone, J. Illston (Eds.), *Construction materials: Their nature and behaviour* (4th ed.), CRC Press, 2010. https://doi.org/10.1201/9781315272436
[55] N. Williams Portal, *Sustainability and flexural behaviour of textile reinforced concrete*. Degree for Licentiate of Engineering, Licentiate thesis, Civil and Environmental Engineering, Chalmers University of Technology, 2013, p. 53.
[56] S. Tomoscheit, U. Gohil, T. Gries, Textile reinforced concrete-providing sustainability for flexible urban concepts, in: *10th international symposium on ferrocement and thin reinforced cement composites*, 2012. Imprint La Habana, Cuba: Palcograf, Scope 49–58, ISBN: 978-959-247-098-9. https://publications.rwth-aachen.de/record/101034
[57] R. Mohit, *Raina industries private limited*, company website. www.raina-industries.com/#down
[58] RWTH Aachen University. www.ita.rwth-aachen.de/go/id/jezh/?lidx=1
[59] B. Mobasher, *Mechanics of fiber and textile reinforced cement composites* (1st ed.), CRC Press, Boca Raton, 2012. https://doi.org/10.1201/b11181
[60] D. J. Kim, et al., A review paper on direct tensile behavior and test methods of textile reinforced cementitious composites, *Composite Structures* 263 (2021) 113661.
[61] J. Hartig, U. Häußler-Combe, K. Schicktanz, Influence of bond properties on the tensile behaviour of textile reinforced concrete, *Cement and Concrete Composites* 30 (10) (2008) 898–906.
[62] M. Zargaran, N. K. Attari, S. Alizadeh, P. Teymouri, Minimum reinforcement ratio in trc panels for deflection hardening flexural performance, *Construction and Building Materials* 137 (2017) 459–469.
[63] J. Hartig, F. Jesse, K. Schicktanz, U. Häußler-Combe, Influence of experimental setups on the apparent uniaxial tensile load-bearing capacity of textile reinforced concrete specimens, *Materials and Structures* 45 (2012) 433–446.
[64] N. W. Portal, I. F. Perez, L. N. Thrane, K. Lundgren, Pull-out of textile reinforcement in concrete, *Construction and Building Materials* 71 (2014) 63–71.
[65] S. Gopinath, R. Gettu, N. R. Iyer, Influence of prestressing the textile on the tensile behaviour of textile reinforced concrete, *Materials and Structures* 51 (2018) 1–12.
[66] S. Paul, R. Gettu, D. N. Arnepalli, R. Samanthula, *Experimental studies on the durability of glass textile reinforced concrete*. Available at SSRN: https://ssrn.com/abstract=4451291 or http://dx.doi.org/10.2139/ssrn.4451291
[67] S. Paul, K. Murugan, R. Samanthula, A. S. Basavaraj, S. J. Stephen, R. Gettu, R. Zerbino, Development of structural forms using textile reinforced concrete, *Indian Concrete Journal (ICJ)* 97 (8) (2023) 43–54.
[68] M. Yeheyis, K. Hewage, M. S. Alam, C. Eskicioglu, R. Sadiq, An overview of construction and demolition waste management in Canada: A lifecycle analysis approach to sustainability, *Clean Technologies and Environmental Policy* 15 (2013) 81–91.
[69] C. K. Purchase, D. M. Al Zulayq, B. T. OBrien, M. J. Kowalewski, A. Berenjian, A. H. Tarighaleslami, M. Seifan, Circular economy of construction and demolition waste: A literature review on lessons, challenges, and benefits, *Materials* 15 (1) (2021) 76.
[70] V. Ram, S. N. Kalidindi, Estimation of construction and demolition waste using waste generation rates in Chennai, India, *Waste Management & Research* 35 (6) (2017) 610–617.
[71] J.-L. Gálvez-Martos, D. Styles, H. Schoenberger, B. Zeschmar-Lahl, Construction and demolition waste best management practice in Europe, *Resources, Conservation and Recycling* 136 (2018) 166–178.
[72] P. Bhada-Tata, D. Hoornweg, *What a waste?: A global review of solid waste management*, World Bank Group. Retrieved from https://policycommons.net/artifacts/1513146/what-a-waste/2185670/ on 09 Jun 2024. CID: 20.500.12592/dk0mgg

[73] R. Islam, T. H. Nazifa, A. Yuniarto, A. S. Uddin, S. Salmiati, S. Shahid, An empirical study of construction and demolition waste generation and implication of recycling, *Waste Management* 95 (2019) 10–21.

[74] M. Sourabh, S. F. Zia, B. Sandra, T. R. Deep, Sustainable development: A critical review of construction and demolition waste management rules 2016, *Environmental Pollution Control Journal* 20 (1) (2016) 6–21.

[75] C. P. C. BOARD, *Guidelines on environmental management of construction & demolition (c & d) wastes* (2017). https://cpcb.nic.in/openpdffile.php?id=TGF0ZXN0RmlsZS8xNTlfMTQ5NTQ0NjM5N19tZWRpYXBob3RvMTkyLnBkZg

[76] CSTEP, *Construction and demolition waste utilisation for recycled products in bengaluru: Challenges and prospects* (2016). www.cstep.in/publications-details.php?id=167

[77] W. Lu, H. Yuan, A framework for understanding waste management studies in construction, *Waste Management* 31 (6) (2011) 1252–1260.

[78] F. Technology Information, *A. Council*. https://tifac.org.in/

[79] B. of Indian Standards, *Corase and fine aggregate-specification*, BIS-CED02, New Delhi, 2016.

[80] R. Prajapati, R. Gettu, S. Singh, B. J. Rathod, A novel beneficiation process for producing high-quality recycled concrete aggregates using concentrated solar energy, *Materials and Structures* 55 (9) (2022) 233.

[81] B. Wildermuth, India-a building industry in transition, *Construct* 6 (2008) 21–28.

[82] I. Kothman, N. Faber, How 3d printing technology changes the rules of the game: Insights from the construction sector, *Journal of Manufacturing Technology Management* 27 (7) (2016) 932–943.

[83] S. Bhattacherjee, A. S. Basavaraj, A. Rahul, M. Santhanam, R. Gettu, B. Panda, E. Schlangen, Y. Chen, O. Copuroglu, G. Ma, et al., Sustainable materials for 3d concrete printing, *Cement and Concrete Composites* 122 (2021) 104156.

[84] R. Manju, R. Deepika, T. Gokulakrishnan, K. Srinithi, M. Mohamed, A research on 3D printing concrete, *International Journal of Recent Technology and Engineering* 8 (2019) 1691–1693.

[85] Tvasta construction. https://tvasta.construction/home

[86] F. Bos, R. Wolfs, Z. Ahmed, T. Salet, Additive manufacturing of concrete in construction: Potentials and challenges of 3d concrete printing, *Virtual and Physical Prototyping* 11 (3) (2016) 209–225.

[87] B. Raphael, S. Senthilnathan, A. Patel, S. Bhat, A review of concrete 3d printed structural members, *Frontiers in Built Environment* 8 (2023) 291.

[88] V. Mechtcherine, V. N. Nerella, F. Will, M. Nather, J. Otto, M. Krause, Large-scale digital concrete construction—conprint3d concept for on-site, monolithic 3d-printing, *Automation in Construction* 107 (2019) 102933.

[89] S. J. Keating, J. C. Leland, L. Cai, N. Oxman, Toward site-specific and self-sufficient robotic fabrication on architectural scales, *Science Robotics* 2 (5) (2017) eaam8986.

[90] Z. Cohen, N. Carlson, Piling and pressing: Towards a method of 3d printing reinforced concrete columns, *Construction Robotics* 4 (1–2) (2020) 61–73.

[91] Z. Cohen, Hold up: Machine delay in architectural design, in: J. Willmann, P. Block, M. Hutter, K. Byrne, T. Schork (Eds.), *Robotic fabrication in architecture, art and design 2018. ROBARCH 2018*, Springer, Cham, 2019. https://doi.org/10.1007/978-3-319-92294-2_10. ISBN: 978-3-319-92293-5.

[92] F. P. Bos, Z. Y. Ahmed, E. R. Jutinov, T. A. Salet, Experimental exploration of metal cable as reinforcement in 3d printed concrete, *Materials* 10 (11) (2017) 1314.

[93] N. Hack, W. V. Lauer, Mesh-mould: Robotically fabricated spatial meshes as reinforced concrete formwork, *Architectural Design* 84 (3) (2014) 44–53.

[94] M. Hambach, M. Rutzen, D. Volkmer, Chapter 5: Properties of 3d-printed fiber reinforced portland cement paste, in: *3D concrete printing technology*, Butterworth-Heinemann, Elsevier, 2019, pp. 73–113. ISBN 9780128154816, https://doi.org/10.1016/B978-0-12-815481-6.00005-1. https://www.sciencedirect.com/science/article/pii/B9780128154816000051
[95] Gebhard, L., Mata-Falcón, J., Anton, A., Burger, J., Lloret-Fritschi, E., Reiter, L., Kaufmann, W. Aligned interlayer fibre reinforcement and post-tensioning as a reinforcement strategy for digital fabrication, in: F. Bos, S. Lucas, R. Wolfs, T. Salet (Eds.), *Second RILEM international conference on concrete and digital fabrication*. DC 2020. RILEM Bookseries, vol. 28, Springer. https://doi.org/10.1007/978-3-030-49916-7_63
[96] T. T. Le, S. A. Austin, S. Lim, R. A. Buswell, A. G. Gibb, T. Thorpe, Mix design and fresh properties for high-performance printing concrete, *Materials and Structures* 45 (2012) 1221–1232.
[97] M. Mohammad, E. Masad, S. G. Al-Ghamdi, 3d concrete printing sustainability: A comparative life cycle assessment of four construction method scenarios, *Buildings* 10 (12) (2020) 245.
[98] S. O. Abioye, L. O. Oyedele, L. Akanbi, A. Ajayi, J. M. D. Delgado, M. Bilal, O. O. Akinade, A. Ahmed, Artificial intelligence in the construction industry: A review of present status, opportunities and future challenges, *Journal of Building Engineering* 44 (2021) 103299.
[99] M. Chui, J. Mischke, The impact and opportunities of automation in construction, *Voices: Global Infrastructure Initiative* (2019) 5.
[100] A. Harichandran, B. Raphael, A. Mukherjee, Determination of automated construction operations from sensor data using machine learning, in: *Proceedings of the 4th international conference on civil and building engineering informatics*, 2019. https://www.researchgate.net/profile/Aparna_Harichandran/publication/337388054_Determination_of_Automated_Construction_Operations_from_Sensor_Data_Using_Machine_Learning/links/5dd4ee58299bf11ec8629bc4/Determination-of-Automated-Construction-Operations-from-Sensor-Data-Using-Machine-Learning.pdf
[101] L. Joshua, K. Varghese, Accelerometer-based activity recognition in construction, *Journal of Computing in Civil Engineering* 25 (5) (2011) 370–379.
[102] S. Mao, X. Shen, M. Lu, Virtual laser target board for alignment control and machine guidance in tunnel-boring operations, *Journal of Intelligent & Robotic Systems* 79 (2015) 385–400.
[103] M. J. Kim, H.-L. Chi, X. Wang, L. Ding, Automation and robotics in construction and civil engineering, *Journal of Intelligent and Robotic Systems* 79 (3–4) (2015) 347.
[104] St. Laurent, C. Logan, A. N. Ruggiero, S. D. Salvo, *Robotics in construction*, Worcester Polytechnic Institute, 2016. https://digitalcommons.wpi.edu/iqp-all/2749
[105] S. Senthilnathan, B. Raphael, Using computer vision for monitoring the quality of 3d-printed concrete structures, *Sustainability* 14 (23) (2022) 15682.
[106] A. Harichandran, B. Raphael, A. Mukherjee, A hierarchical machine learning framework for the identification of automated construction operations. *Journal of Information Technology in Construction* 26 (2021).
[107] B. Raphael, K. S. C. Rao, K. Varghese, Automation of modular assembly of structural frames for buildings, in: *2016 Proceedings of the 33rd the international symposium on automation and robotics in construction (ISARC)*, Auburn, USA, 2016, pp. 412–420. ISBN 978-1-5108-2992-3, ISSN 2413-5844. https://doi.org/10.22260/ISARC2016/0050
[108] A. Pushkar, M. Senthilvel, K. Varghese, Automated progress monitoring of masonry activity using photogrammetric point cloud, in: *ISARC. Proceedings of the international symposium on automation and robotics in construction*, vol. 35, IAARC

Publications, July 20–25, 2018, pp. 1–7. ISBN 978-3-00-060855-1. https://www.iaarc.org/wp-content/uploads/2021/10/ISARC-2018-Proceedings.pdf

[109] S. Balasubramanian, V. Shukla, N. Islam, S. Manghat, Construction industry 4.0 and sustainability: An enabling framework, *IEEE Transactions on Engineering Management*, 71 (2024) 1–19. doi: 10.1109/TEM.2021.3110427

[110] K. Wang, F. Guo, Towards sustainable development through the perspective of construction 4.0: Systematic literature review and bibliometric analysis, *Buildings* 12 (10) (2022) 1708.

[111] V. Potbhare, M. Syal, S. Korkmaz, Adoption of green building guidelines in developing countries based on US and India experiences, *Journal of Green Building* 4 (2) (2009) 158–174.

[112] A. Marichova, Role of the government for development of sustainable construction, *Ovidius University Annals of Constanta – Series Civil Engineering*, 22 (1) (2020) 53–62. https://doi.org/10.2478/ouacsce-2020-0006

[113] X. Zhang, L. Shen, Y. Wu, G. Qi, Barriers to implement green strategy in the process of developing real estate projects, *The Open Waste Management Journal* 4 (1).

[114] Q. K. Qian, E. H. Chan, A. G. Khalid, Challenges in delivering green building projects: Unearthing the transaction costs (TCS), *Sustainability* 7 (4) (2015) 3615–3636.

[115] A. P. Chan, A. Darko, E. E. Ameyaw, D.-G. Owusu-Manu, Barriers affecting the adoption of green building technologies, *Journal of Management in Engineering* 33 (3) (2017) 04016057.

[116] R. Prakash, *Strategy for promoting processing of construction and demolition (C&D) waste and, National Institution for Transforming India (NITI Aayog), India* (2018). Retrieved from https://policycommons.net/artifacts/2436636/strategy-for-promoting-processing-of-construction-and-demolition-cd-waste-and/3458228/ on 09 Jun 2024. CID: 20.500.12592/bkzn8d

Section 2

Climate Change

4 Visualization of Ecologically Sensitive Regions at Disaggregated Levels in the Central Western Ghats

T V Ramachandra, Tulika Mondal, Paras Negi and Bharath Setturu

4.1 INTRODUCTION

Ecological resilience refers to the capacity of an ecosystem to withstand disturbances with the potential to alter the inherent nature of natural landscapes. Alterations in the structure of the landscape due to unplanned developmental activities have been affecting the ecosystem process, evident from the presence of barren hilltops, retreat of native forests, and alterations in the hydrologic regime with the conversion of perennial streams to intermittent or seasonal streams (Nilsson and Grelsson, 1995). Mismanagement of ecologically sensitive regions (ESRs) leads to loss of biodiversity, induces water and food insecurity, frequent occurrence of floods and droughts, and decline of ecosystem services, which negatively impacts the livelihood of dependent communities. Mapping of ESRs by considering bio-geo-climatic, ecological parameters with social aspects and assigning weights based on the extent and condition of these factors is essential for development planning (Gadgil et al., 2011; Ramachandra et al., 2018). Utilizing biophysical and socio-economic information for regional planning empowers decision-makers to address challenges to ensure the sustenance of natural resources (Watson et al., 2011a; Asare et al., 2013; Villegas-Palacio et al., 2016). Identification of sensitive regions through the integration of multi-disciplinary information corresponding to biotic and abiotic components of an ecosystem is a widely accepted practice for the conservation of biodiversity (Myers et al., 2000).

Globally, forest ecosystems cover 4.06 billion hectares, representing 31% of the total landscape, with tropical forests covering 45% of the global forests, followed by the boreal, temperate, and subtropical and five countries (Brazil, Canada, China, United States of America, and Russian Federation), consists of 54% of the global forest cover (FAO, 2020). The decline of forests is attributed to the expansion of croplands, pastures, plantations, and urban areas (FAO, 2010) with industrialization

DOI: 10.1201/9781032686899-6

and globalization. Globally, forest ecosystems occupied 2.5 million ha (1999–2000), which has reduced to 1.7 million ha at the rate of 2% per annum (FAO, 2011). India shares only 2.4% of the global land area and is home to 7–8% of the recorded species of the world (Goyal and Arora, 2009). Human-induced processes have a negative effect on forests and ultimately cause the depletion of natural resources, global warming, mass extinction, and biodiversity loss (Shivanna, 2022; Rockström et al., 2009).

The Western Ghats (WG), spanning from the Tapti valley in southern Gujarat to Kanyakumari in Tamil Nadu, for about 1600 km and area coverage of 160,000 km^2 with an exceptional biodiversity, endemism, and diverse ecosystems, constitute one of the eight hottest global biodiversity hotspots and one among 36 global biodiversity hotspots (Ramachandra et al., 2018; Chandran, 1997; Gadgil et al., 2011; Aravind et al., 2008). WG supports the livelihood of 400 million dependent population through provision of food, fodder, water (drinking, commercial, agriculture, and industry), and mitigating global warming through sequestration of carbon, etc. (Molur et al., 2011).

Karnataka federal state in India is endowed with native forests, perennial rivers, water sources, and rich mineral reserves. Forests occupy the second-largest portion of land usage after agriculture, with substantial areas designated as reserve forests in the state. The invaluable water resources encompassing rivers, lakes, and various water bodies are of irreplaceable significance. Forest is defined as an expanse of land covering over 0.5 hectares, characterized by trees higher than 5 meters in height and a canopy coverage exceeding 10%, and it also encompasses trees capable of meeting these criteria in their natural location (FAO, 2020). Forest ecosystems perform pivotal functions in sustaining the ecological cycle, hydrological balance, and mitigating climate change, which are essential to achieve Sustainable Development Goals (SDGs).

The Malnad region of the WG is a geographically diverse landscape, which holds significant potential for driving ecological, biological, economic, and social processes. It is enriched by its abundant natural resources and topographical variation. The region's landscapes are conducive to extensive horticulture activities, with the production of arecanut and coffee. Malnad spans across Belagavi, Shivamogga, Hassan, Chikkamangaluru, Kodagu, and portions of Udupi, Dakshina Kannada, and Uttara Kannada districts in Karnataka. Major commercial hubs such as Sagara, Sirsi, Yellapur, Sringeri, Koppa, Teerthahalli, Siddapura, Sakaleshpura, Moodugere, Balehonnur, Narasihmarajapura, and Aldur contribute to the region's business vitality. Noteworthy towns within the coffee-growing belt include Chikkamangaluru, Madikeri, Sakaleshpura, and Somavarapete. Additionally, the forests of Malnad also play a crucial role in providing various ecosystem services such as regulating the microclimate, recharging groundwater, preventing soil erosion, and conserving habitat for wildlife. Bababudangiri Hills, B.R. Hills, Malemahadeshwara Hills, and Gopalswamy Hills are the major areas in the Malnad range with an abundance of wildlife.

There have been substantial alterations in rainfall distribution due to large-scale land use changes, deforestation, soil degradation, etc. Land use and land cover (LULC) change resulted in alteration in the climate regime has altered the abundance, distribution of species, diversity, and interactions among species (Davison et al., 2021; Oliver and Morecroft, 2014; Lambin et al., 2003), which will ultimately lead to habitat loss and species extinction. Habitat loss is the primary reason for the extinction of several species due to exacerbating anthropogenic activities (Ceballos et al., 2017; Hanski, 2011). Nevertheless, climate change has impaired the dependability and predictability in the region's crucial ecological occurrence of rainfall. Land use change has substantial effects on carbon sources and sinks, drives habitat loss, and serves as the foundation of food production (Ramachandra and Bharath, 2021).

Land use changes during the last six decades has impacted almost one-third (32%) of the world's total land area (Winkler et al., 2021). Prudent management of natural resources is quintessential for addressing global challenges related to sustainability, such as climate change, biodiversity loss, and food security (Mariye et al., 2022; Pacheco et al., 2018; Alam et al., 2020; Tan et al., 2020; Bharath et al., 2013; Aithal et al., 2013; Turner, 1997; Jiyuan et al., 2002; Aithal and Ramachandra, 2016).

Unregulated land use changes within the forest ecosystem, resulting in the fragmentation of contiguous native forests into smaller, isolated patches, is known as forest fragmentation (Riitters et al., 2002; Young and Boyle, 2000; Laurance et al., 2002; Harper et al., 2005; Ramachandra et al., 2016). The process of forest fragmentation has been intensified by the edge effect caused by various development projects such as linear projects, which has led to the loss of connectivity and continuity of the natural forest (Ramachandra et al., 2016; Wade et al., 2003; Ramachandra et al., 2018; Cagnolo et al., 2006). These consequences include disturbances in hydrological patterns, biodiversity loss, modifications in microclimates, increase in vulnerability to fires, increase in instances of human-animal conflict, reduction in carbon sequestration potential, and increased carbon emissions (Riitters et al., 2000; Bharath et al., 2014; Houghton and Nassikas, 2017; Harper et al., 2007; Vinay et al., 2013). The degradation of the forest ecosystem has negatively impacted the ecosystem's goods and services.

Ecosystem services refers to the direct or indirect benefits humans derive from ecosystems for livelihoods and survival (De Groot et al., 2012; Costanza et al., 1997; Gomez-Baggethun and Barton, 2013; Silvestri et al., 2013). These benefits or services include provisioning (food, fodder, fuelwood, timber, etc.), regulating (groundwater recharge, carbon sequestration, biological control, air purification, etc.), and cultural services such as aesthetic, culture, recreational, education, etc. (Shivanna, 2020; Ouyang et al., 2020; Hasan et al., 2020; Liu et al., 2010). The degradation of ecosystems erodes the ecosystem process affecting the function and resilience of ecosystems, which pose a serious threat to the sustenance of ecosystem services (Carpenter et al., 2006; Tolessa et al., 2017). Diverse anthropogenic activities and climate change have had adverse effects on ecosystem services (De Groot et al., 2010; Scott et al., 2017; Ramirez-Gomez et al., 2015; Nunez et al., 2019; Fu et al., 2015; Fu et al., 2017; Li et al., 2007). LULC changes are driven by unplanned developmental activities coupled with the burgeoning resource demand of an increasing population, leading to higher exploitation of natural resources (Tan et al., 2020; Foody, 2003; Amini et al., 2022; Arowolo et al., 2018) with the continuous alteration, degradation, and transformation of ecosystems (Basse et al., 2014; Keshtkar and Voigt, 2016; Bharath et al., 2013; Tilman and Lehman, 2001).

Integration of spatiotemporal, biophysical, socio-cultural, etc. considerations in the decision-making criteria would enhance efficacy (Lombardi et al., 2017). Multiple criteria decision analysis (MCDA) systematically supports decisions by accounting diverse factors, their value judgments, and relative importance for the local sustainable transitions (Moghadam et al., 2018). Decision-making in addressing semi-structured spatial decision challenges and landscape visualization (Armstrong and Densham, 1992; Wan, 2009; Karnatak et al., 2007) could be achieved through a web-based spatial decision support system (SDSS). Geoinformatics (geographic information system) facilitate structured data organization, spatial database management, spatial analyses, analytical modelling, and visualization, coupled with the domain expertise (Ramachandra et al., 2017; Moghadam et al., 2019) would aid in decision-making to ensure sustainable development with the conservation of ecologically fragile regions while supporting the livelihood of people (Jankowski, 2009).

4.1.1 Objectives

Objectives of the current endeavour to visualize ecologically sensitive regions at disaggregated levels are as follows:

1. Quantification of land use land cover (LULC) dynamics using temporal remote sensing data with the machine learning approach
2. Assessment of spatial patterns of forest degradation through computation of forest fragmentation metrics
3. Predication of likely land uses using the CA-Markov method
4. Prioritization of eco-sensitive regions (ESRs) at disaggregated levels based on landscape dynamics, ecological, geo-climatic, hydrological, renewable energy, and social characteristics
5. Visualization of ESRs at disaggregated levels (villages) through the spatial decision support system (SDSS).

4.2 MATERIALS AND METHOD

4.2.1 Study Area

The Hassan district, with a spatial extent of 6826.15 km^2, is situated between 12°13′N and 13°33′N and 75°33′E and 76°38′E across three physiographic regions (Figure 4.1) from east to west: Malnad, Semi Malnad, and Maidan in the southern part of Karnataka (Hassan District Disaster Management Plan, 2011–12). The district spreads across 116 kilometres east and west, and 129 kilometres north to south and has Tumakuru district in the east, Mysuru district in the south, Chikamagaluru district in the north, and in the west, the Western Ghats forms a boundary with the district of Dakshin Kannada. The district has 8 Taluks with 38 hoblies, 2369 inhabited villages, and 183 uninhabited villages: Alur Taluk (432 km^2), Holenarasipura Taluk (602 km^2), Arakalagud Taluk (675 km^2), Belur Taluk (845 km^2), Hassan Taluk (942 km^2), Sakaleshapura Taluk (1034 km^2), Channarayapatna Taluk (1044 km^2), and Arasikere Taluk (1271 km^2).

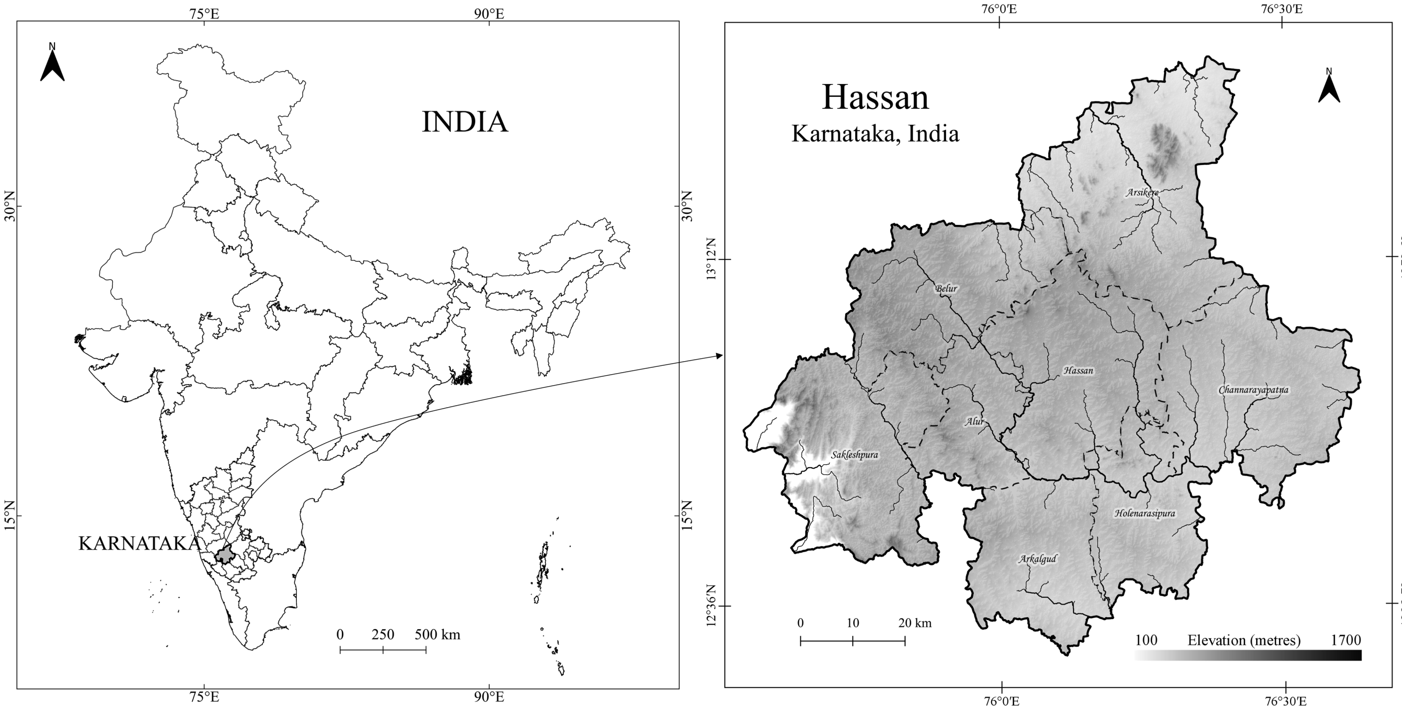

FIGURE 4.1 Study area.

The western part of this district is the 'Malnad' area, which is an undulating forested hilly area of the Western Ghats. The important peaks in this region are Pushpagiri or Subramanya (1715m), Devarabetta (1282m), Murukanagudda (1300m), and Jenukal-betta (138m). The eastern part of the district is the 'Maidan' area, which denotes the plain region.

There are two main rivers in the district named Hemavathi and Yagachi. Other rivers like the Gundiya, Kaveri, Vateholé, Ethinaholé, Ganadaholé, and Kempuholé keep flowing throughout the year. The notable dams in this district are Gorur Dam (Gorur Hassan Taluk), Yagachi Dam (Belur Taluk), Vateholé Dam (Belur Taluk), and Sri Ramadevara Katte (Holenarasipura Taluk).

The district is a part of the Precambrian terrain. The major lithological units are granitic gneiss, granulites, granites, Dharwarian schists, and dyke rocks. The most important rock formation of the district is the Nuggehalli and Holenarasipura Schist Belt. These two schist belts host several mineral deposits like chromite, titaniferous magnetite, chalcopyrite, kaolin, asbestos, quartz, etc.

Soils in the district are very fertile, and the main soil types are red soil, red sandy soil, mixed soil, and silty clay soil. The soils in the western taluks are derived from granites, laterites, and schists. These soils are shallow to medium in depth, and the colour changes with depth from red at the surface and red and yellow mottles at depth. The soils are suitable for horticulture crops. In parts of the Arsikere taluk, black soils are also seen locally. There are four agroclimatic zones in the Hassan district, which are hilly zone, central dry zone, southern dry zone, and southern transition zone.

The average annual rainfall of the district is 1031 mm. The rainfall during the southwest monsoon season (from June to September) constitutes 59% of the annual rainfall. February and March are the driest months of the year, when the relative humidity in the afternoon is less than 35%. Temperature ranges from 11.68°C to 39.07°C in the district.

The western part of the district is a part of Western Ghats that is covered in evergreen forest. The major portion of the forest is located in the Sakleshpura taluk. The Kabbinale State Forest in the taluk ranks among the biggest forest plantations in the State. There are four types of forest, namely evergreen, moist deciduous, dry deciduous, and scrub.

As per the 2011 Census, the population of the Hassan district is 1,776,421. The male-female ratio is 1000:1010. The population density of the district is 251 persons per sq. km. Hassan taluk has the highest population density (385 persons per sq. km). The rural population is 1,399,658 (78.79%) and the urban population is 376,763 (21.209%). The decadal growth rate is 18.86%. The literacy rate in the district is 76.07. The SC and ST populations of the district are 345031 and 32329 respectively.

The total district GDP was 6612 crore Rs (2.2% contribution) in 2014–2015. The agricultural sector contributes 4.3% and industries contribute 1.7% of the GDP in the district. In the year 2012–2013, the per capita annual income of the district was Rs. 53,000.

The district has two important ghat roads, which connect the eastern plains with the places beyond the Western Ghats. The district has a total road length of 8,897 km. (National Highway 168 km and State Highway 813 km). The district has a total rail length of 246 km. Arsikere and Hassan are the important railway junctions of the district.

4.2.2 Method

Figure 4.2 outlines the protocol adopted for visualizing ESRs at disaggregated levels in the Hassan district, Central Western Ghats. Temporal Landsat data from 1973 to 2021 were used to identify landcover dynamics through the spatial extent of vegetation cover, which was calculated using the Normalised Difference Vegetation Index (NDVI) (Equation 1).

$$NDVI = \frac{(NIR - Red)}{(NIR + Red)} \quad (1)$$

The different land use types were identified using the French Institute Forest map of South India (Pascal, 1993), the Survey of India toposheet (1:50000), high-resolution spatial data (Google Earth), published literature, and reports of the study area. The

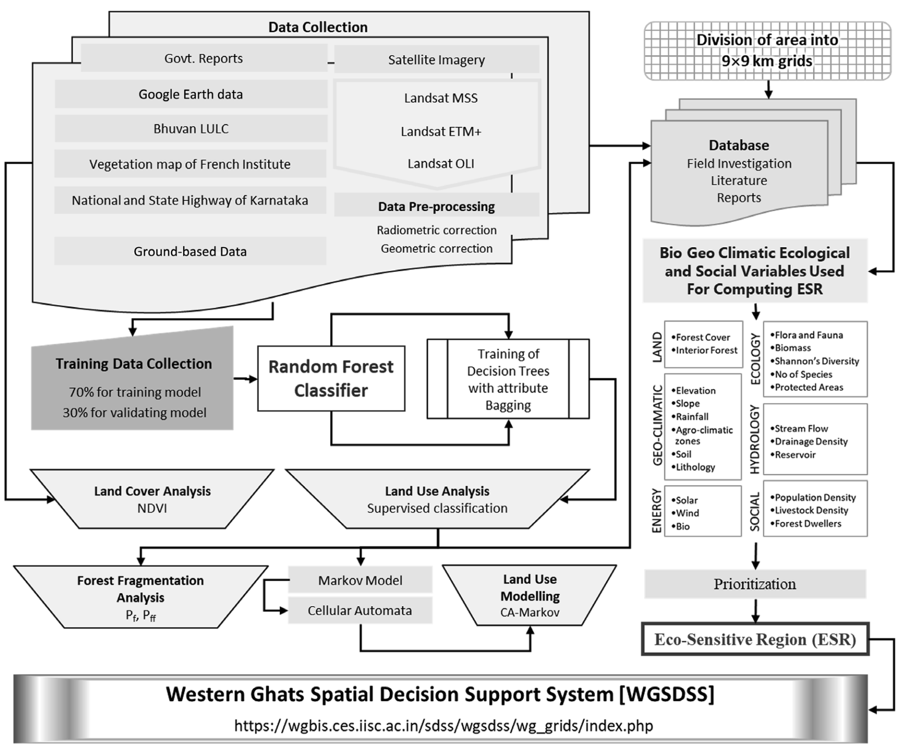

FIGURE 4.2 Protocol for delineating ESR at disaggregated levels.

land use analysis was performed using Landsat MSS (1973), Landsat TM (1998), Landsat ETM+ (2005), and Landsat OLI (2013 and 2021) spatial data integrated with field data. The remote sensing data was pre-processed with geometrical and radiometric rectifications and projected to UTM43N/WGS84 projection (Kennedy et al., 2009). Landsat ETM+ bands of 2005 were corrected using image enhancement techniques to resolve SLC line error, followed by nearest-neighbour interpolation.

The land use analyses were carried out using a supervised machine learning classifier—Random Forest (RF) (Breiman 1996) in the Google Earth Engine Platform (earthengine.google.com), considering several decision trees on various subsets of the given dataset and average value to improve the predictive accuracy of that dataset. The random forest algorithm is designed to take the prediction from each tree, and based on the majority votes of predictions, for the prediction of the final output. RF uses bagging or bootstrap aggregation, which chooses a random sample from the dataset to generate individual models from the samples (bootstrap samples) provided by the original data with a replacement. Bagging enhances classification accuracy, offering improved estimations of the combined ensemble's generalization error from multiple trees. Additionally, it measures the individual strength of each tree and assesses the correlation among the diverse trees.

The analyses are done in the following method: (a) identification of heterogenous patches in the landscape through false colour composite (FCC) using spatial data of green, red, and NIR wavelengths; (2) digitization of training polygons corresponding to the select heterogeneous patches, covering 15% of the study area and are uniformly distributed over the entire study area); (3) collection of the attribute data (land use types) for these polygons from the field (Figure 4.3) using a handheld pre-calibrated global positioning system (GPS), online virtual spatial data portals, and published reports; and (4) 70% of the training data has been used for supervised classifier based on RF algorithm, and the remaining 30% of training data is used for validation or accuracy assessment.

Condition of the forest was quantified through fragmentation metrics such as patch, transitional, edge, perforated, and interior (Riitters et al., 2000) through computation of P_f (the proportion of forest pixels in the window) and P_{ff} (the proportion of all adjacent or cardinal pixel pairs that include at least one forest pixel, for which both are forest pixels), considering 3×3 kernel. A pixel is categorized based on the type of fragmentation, and the result of the kernel is stored at the location of the centre pixel (in the derived map), which represents fragmentation around the corresponding forest location (Ramachandra et al., 2013). A pixel is categorized as interior (P_f=1), perforated forest (for pixels with $P_f > 0.6$ and $(P_f - P_{ff}) < 0$), edge forest ($P_f > 0.6$ and $(P_f - P_{ff}) > 0$), transition (pixels with P_f<0.6 and P_f>0.4), or patch forest (with pixels $P_f < 0.4$). Non-forest pixels include pixels other than forests with anthropogenic land use areas.

Prediction of likely land uses in the next 20 years has been done using the Integrated CA-Markov model, which can accurately simulate and predict future conditions by its dynamic explicit simulation efficiency (Rimal et al., 2018). The spatial transition probability (equation 2) is obtained based on the Markov process, which determines the likelihood of a pixel changing from an LU category to other

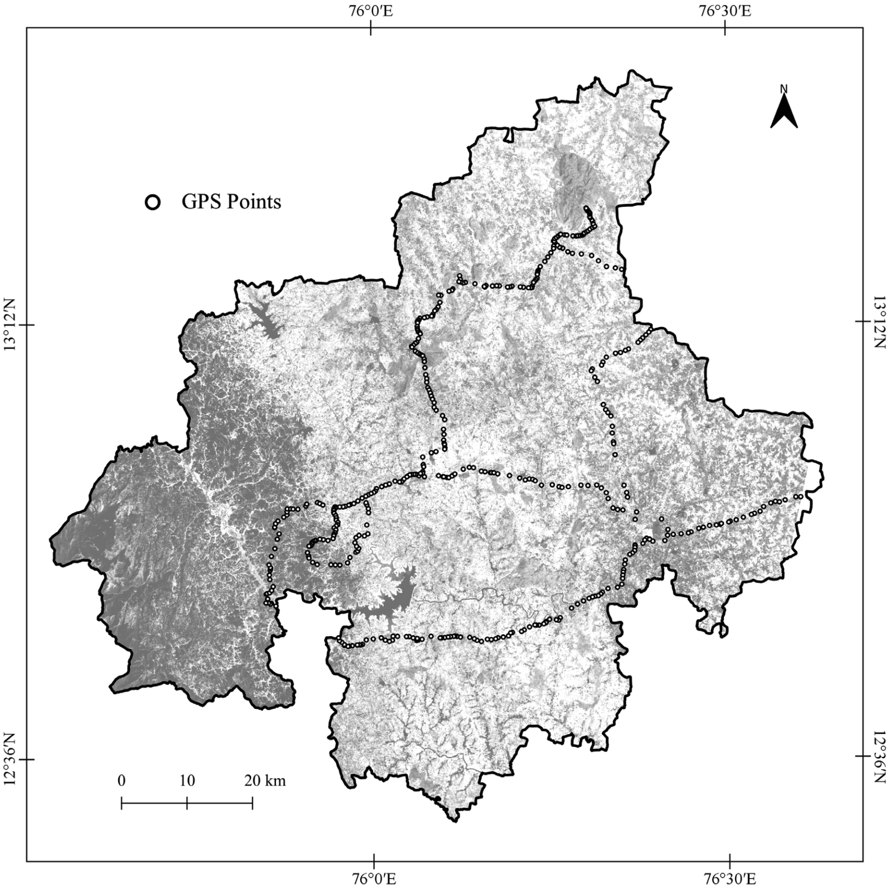

FIGURE 4.3 FCC of Hassan with GPS points collected from the field.

categories during time 1 to 2 from cross-tabulation of the two images adjusted by the proportional error, and is translated into a set of probability images, which records the number of cells or pixels that are expected to change over the next time period.

$$P = \left(P_{ij}\right) = \begin{bmatrix} P_{11} & \dots & P_{1n} \\ \dots & \dots & \dots \\ P_{n1} & \dots & P_{nn} \end{bmatrix} \sum_{j=1}^{n} P_{ij} = 1, i = 1, 2, \dots, \dots, n \quad (2)$$

where P_{ij} = the transition probability of land-use changes from one class to another, and n = land-use type.

Cellular Automata (CA) is used to simulate and predict LU based on transition potential. The CA model consists of state, cell and cell space, neighborhood, rule, and time in case of land use transformation, the cell represents the cells of the LULC class, and the class represents itself as a state. A discrete dynamic function of CA consists of four elements expressed by equation 3:

$$CA = \left(l, \Sigma, \eta, \delta\right) \tag{3}$$

where l = physical environment and discrete lattice, Σ = the set of possible states, η = the neighborhood of a cellular automaton, and δ = local transition rule.

The efficiency of the model depends on the neighborhood size, the state of test pixels, and transition rules. Von Neumann's 5 × 5 filter was used for modelling. Water bodies were taken as a constraint for simulation. Validation was carried out by comparing the simulated land use map against the actual land use map using Kappa Statistics. The model was calibrated by varying the input variables in order to achieve higher accuracy. The calibrated model was used to predict and visualize the land use change pattern for the years 2030 and 2038.

Prioritization of ESRs: Ecologically sensitive areas (ESRs) refer to areas with high sensitivity and fragility based on the environmental and ecological aspects, where anthropogenic activities can cause disturbance in the natural structure of the biological communities and natural habitats. Prioritizing regions at disaggregating levels entails an integrated assessment of environmental and ecological parameters through assignment of a weightage metric score, which requires knowledge of multi-disciplines (Termorshuizen and Opdam, 2009). The study area is divided into 5'×5' grids (9 km × 9 km) equivalent to a grid in the Survey of India topographic maps of 1:50000 scale to calculate the ESRs. Grid-based (disaggregated level) mapping is a standardized approach to spatial data collection that efficiently compiles large datasets, where the output can be consistently and efficiently comprehensible. Each grid was given a value according to its landscape structure (ecosystem extent and condition), ecological, geo-climatic, hydrological, energy availability, and social characteristics. These data were collected from published scientific literature, published datasets (Karnataka Forest Department), administrative reports, and field surveys.

Landscape dynamics essentially involved the assessment of spatial extent of forest cover and interior contiguous forests. Ecology consists of flora, fauna biomass, number of species, Shannon's diversity, protected areas under reserve forests, conservation areas, sacred groves, etc. Geo-climatic parameters refer to the various geological and climatic parameters such as rainfall, elevation, slope, soil, agroclimatic zones, and lithology. Hydrological parameters include drainage density, stream flow, and the presence of a reservoir. The prospect of renewable energy like solar, wind, and bioenergy has also been considered. The social aspects included population density, the presence of forest dwellers, and livestock density. Finally, a weightage matrix based on equation 4 was used to generate weights for each variable, considering the relative significance of various themes:

$$Weightage = \sum_{i=1}^{n} W_i V_i \tag{4}$$

where n is the number of variables, W_i is the weight associated with criterion i, and V_i is the associated value with criterion with that criterion.

An indicator defines each criterion mapped to a value normalized from 10 to 1. The value 10 corresponds to a very high priority for conservation. The values 7, 5, and 3 correspond to high, moderate, and low levels of conservation, respectively. Themes include forests (10: >60% forest cover, 8: 45–60%, 6: 30–45%, 4: 15–30%, and 2: <15%), interior forests (10: >60% interior forest cover, 8: 45–60% interior forest cover, 6: 30–45%, 4: 15–30%, and 2: <15%).

The ecology theme covers biomass, carbon (Gg) (10: > 1200, 8: 900–1200, 6: 600–900, 4: 300–600, and 2 for grids with < 300), Shannon's diversity (10 for grids having Shannon's diversity > 2.5, 8: 2–2.5, 6: 1.5–2, 4: 1–1.5, and 2: <1), number of species of flora and fauna (0: absence of any species, 2: < 50, 4: 50–100, 6: 100–150, 8: 150–200, 10: > 200), 10 for grids with endangered or threatened species, and 8 for endemic species, 10 for grids covering Mysore elephant reserve, and protected areas.

Within the context of the geo-climatic theme, the study has taken into account various factors including altitude (10:>750 m, 8: 500–750, 6: 250–500, 4: 100–250, 2: < 100), slope (10: > 30%, 8: 15–30%, 6:10–15, 4: 5–10, 2: <5%), rainfall (10: >2400 m, 8: 1800–2400, 6: 1200–1800, 4: 600–1200, 2: <600), agroclimatic zones (10: hot moist sub-humid, 8: hot dry sub-humid, 6: hot dry semi-arid, 4: arid, 2: hot dry arid), lithology (10: for grids in deccan trap, 8: Dharwars or granite, 6: Peninsular Gneiss, and 4: Charnokites), and soil type (10: grids with loamy or clayey soil, 8: loamy or clayey skeletal soil, 6: fragmental or rocky outcrops, 4: sandy or sandy skeletal soil types, and 2: coarse loamy soil).

The hydrological theme encompasses considerations of stream flow (10: streams having water all 12 months; 8: 8 months, 6: 6 months, 4: 5 months, and 2: during monsoon), stream density (10: grids having stream density >2.5, 8: 2–2.5, 6: 1.5–2, 4: 1–1.5, and 2: 0.5–1), and reservoir (presence of dam: 10, absence of dam: 0) parameters.

Renewable energy potential is accounted considering solar (grids having solar potential > 6.5 kWh/m^2), bioenergy (10 for grids with potential of > 600 MKcal, 8: 400–600, 6: 200–400, 4: 100–200, 2: < 100), and wind energy (10 for grids with wind speed 4 m/sec, 8: 3.5–4, 6: 2–3.5, 4: 1.5–2, and 2: <1.5m).

Social theme includes population density (10: for grids with a population density > 100 persons/km^2, 8: 100–250, 6: 250–500, 4: 500–1000, and 2: >1000), livestock density (10: < 1m, 8: 1–1.5, 6: 1.5–2.25, 4: 2.25–3.5, and 2: >3.5), and the presence of tribes (10 for grids having tribal population).

Prioritizing ESRs at disaggregated levels through weights (based on the relative significance of chosen parameter) provides an objective and transparent system of combining multiple datasets together as per the framework widely adopted (Beinat, 1997), and application of geoinformatics stands out as the novelty of the approach.

The aggregated weight for each grid is computed, and grids are grouped into four groups based on mean and standard deviation of aggregates, which aided in identifying various levels of fragility. ESR1 represents ecologically highly fragile and requires strict conservation measures. ESR2 is as good as ESR1, requiring stringent measures to minimize degradation. ESR3 represents a moderate conservation region, and ESR4 represents less fragility.

Spatial Decision Support System (SDSS): Visualization of ESRs is done through the web-based SDSS. The database of SDSS consists of the geospatial data and attribute information. Geo-rectified data layers are stored in the PostgreSQL database. The Geo-server with services such as Web Mapping Service (WMS), Web Feature Service (WFS), and Web Coverage Service (WCS) is customized for inclusion of all chosen input layers. Symbology or styles are encapsulated in the Styled Layer Descriptor (SLD) format for each classification of data to ensure visualization and differentiation while allowing for consistent and coherent portrayal. Subsequently, application programming interfaces (APIs) are configured for facilitating data access from Geo-server. In this context, Leaflet, a versatile JavaScript library, is employed as the backend application to harness the Geo-server APIs to access, compile, and effortlessly present data layers alongside dynamic base layers. An interactive webpage is developed by utilization of Leaflet and hosted on an Apache server, which aid as the interface for end users to access and visualize the data. It offers an array of interactive features, including zoom-in, zoom-out, visualization, differentiated layer styles, map manipulation, and the ability to click on vector features for pop-up information. SDSS demonstrates the flawless integration of various technologies, which provide a powerful platform for geospatial data exploration, visualization, and utilization.

4.3 RESULTS

4.3.1 Land Cover

The Hassan district is very rich in agricultural and horticultural resources due to suitable climatic conditions of hot-dry-semi-arid and Sahyadri agroclimatic zones and fertile soil (Basavaraja et al., 2017). The analysis showed that vegetation cover of 2980.37 km^2 (43.69%) in 1973 has increased to 4393.19 km^2 (64.4%) by 2021, and the results listed in Table 4.1 and Figure 4.4 show land cover dynamics. The increasing trend of agricultural cropland and horticultural land resulted in the inclination of vegetation cover of the study area. As the fallow land and open spaces were converted into croplands, horticultural lands, agroforestry, and forest plantation, the area

TABLE 4.1
Land Cover Analysis of Hassan from 1973 to 2022

Land Cover (NDVI)		1973	1998	2005	2013	2021
Non-vegetation	sq. km	3841.57	3187.37	2878.47	2815.65	2428.75
	%	56.31	46.72	42.19	41.27	35.60
Vegetation	sq. km	2980.37	3634.57	3943.48	4006.29	4393.19
	%	43.69	53.28	57.81	58.73	64.40

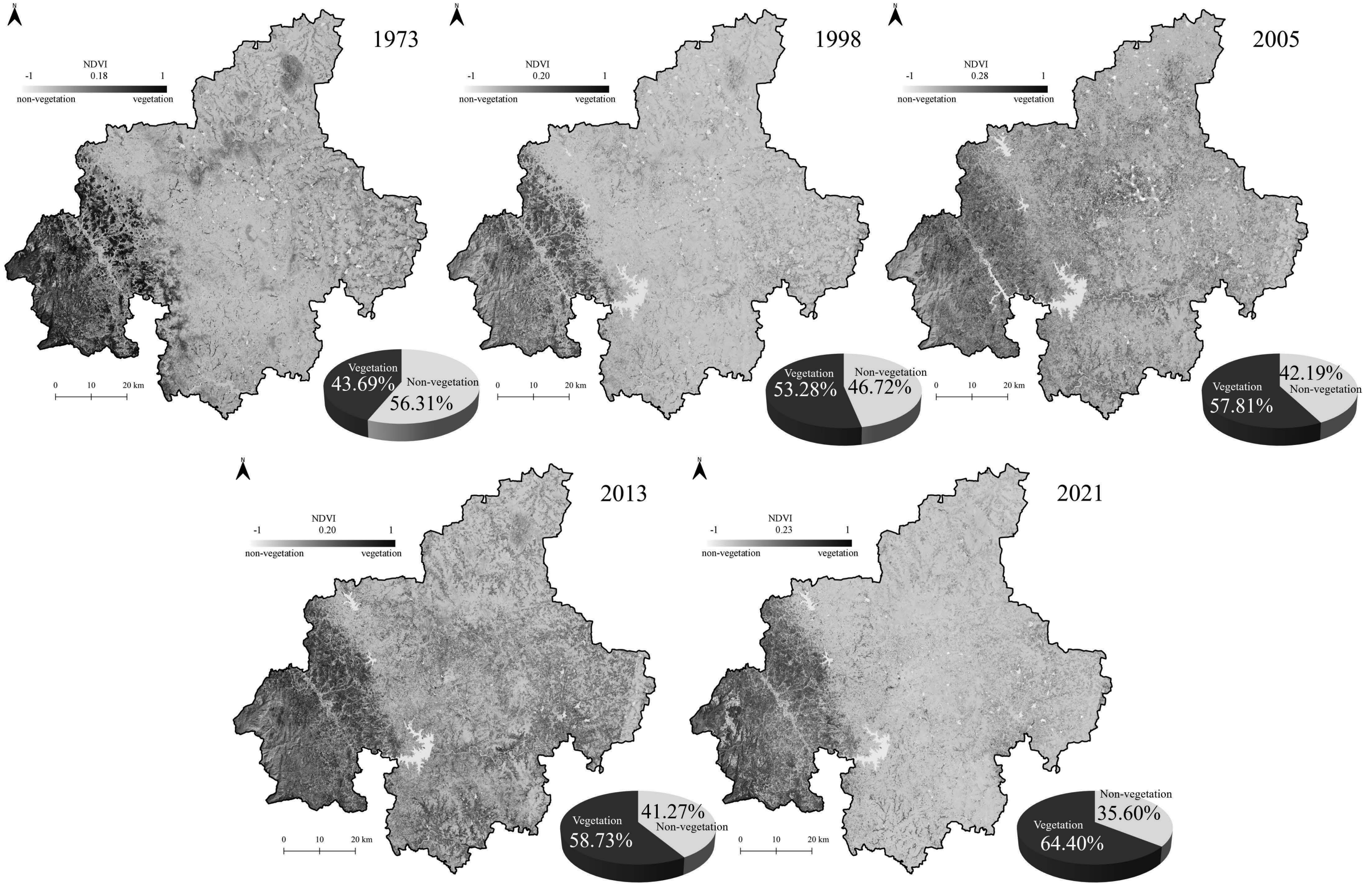

FIGURE 4.4 Land cover analysis of Hassan from 1973 to 2022.

under non-vegetation shows a decline from 56.31% (3841.57 km^2) in 1973 to 35.6% (2428.75 km^2) in 2021.

4.3.2 Land Use

Temporal land use analyses were performed to understand land use transitions from 1973 to 2021, and category-wise land use transitions are provided in Table 4.2 and Figure 4.5, which highlight a decrease in forest cover from 14.79% (in 1973) to 6.44% (in 2021). The district has an evergreen forest cover with shola forest on its eastern side, and some part of the district is covered by dry deciduous and scrub forest (Dudani et al., 2010). Temporal land use analyses revealed the degradation of evergreen forests from 10.97% (748.47 km^2 in 1973) to 3.72% (254.08 km^2 in 2021). Besides evergreen forest, shola forest cover decreased from 0.65% (44.42 km^2) in 1973 to 0.45% (30.97 km^2) in 2021. Similarly, the deciduous forest also degraded from 2.1% (143.42 km^2) in 1973 to 1.38% (94 km^2) in 2021. Also, the area under scrub forest was 1.07% (73.28 km^2) in 1973 and decreased to 0.89% (60.62 km^2) in 2022.

TABLE 4.2
Land Use Analysis of Hassan from 1973 to 2021

Land Use		1973	1998	2005	2013	2021
Evergreen	sq. km	748.47	446.12	348.29	300.57	201.73
	%	10.97	6.54	5.11	4.41	2.96
Shola	sq. km	44.42	32.68	42.74	46.33	30.97
	%	0.65	0.48	0.63	0.68	0.45
Deciduous	sq. km	143.42	117.41	112.03	107.84	93.96
	%	2.1	1.72	1.64	1.58	1.38
Scrub	sq. km	73.28	47.47	48.36	46.66	59.29
	%	1.07	0.7	0.71	0.68	0.87
Water	sq. km	118.19	171.64	218.19	126.21	131.29
	%	1.73	2.52	3.2	1.85	1.92
Agriculture	sq. km	3551.53	2759.7	2465.37	2636.93	2124.72
	%	52.06	40.45	36.14	38.65	31.14
Horticulture (plains)	sq. km	1635.33	2284.7	2400.45	2324.96	2373.18
	%	23.97	33.49	35.18	34.08	34.78
Horticulture (hills)	sq. km	235.85	610.94	826.41	842.65	1276.98
	%	3.46	8.95	12.11	12.35	18.72
Built-up	sq. km	36.41	109.04	113.77	137.11	247.61
	%	0.53	1.6	1.67	2.01	3.63
Open	sq. km	199.65	174.44	173.46	164.92	187.92
	%	2.93	2.56	2.54	2.41	2.75
Plantation	sq. km	35.98	68.38	73.37	88.27	94.9
	%	0.53	1	1.08	1.29	1.39

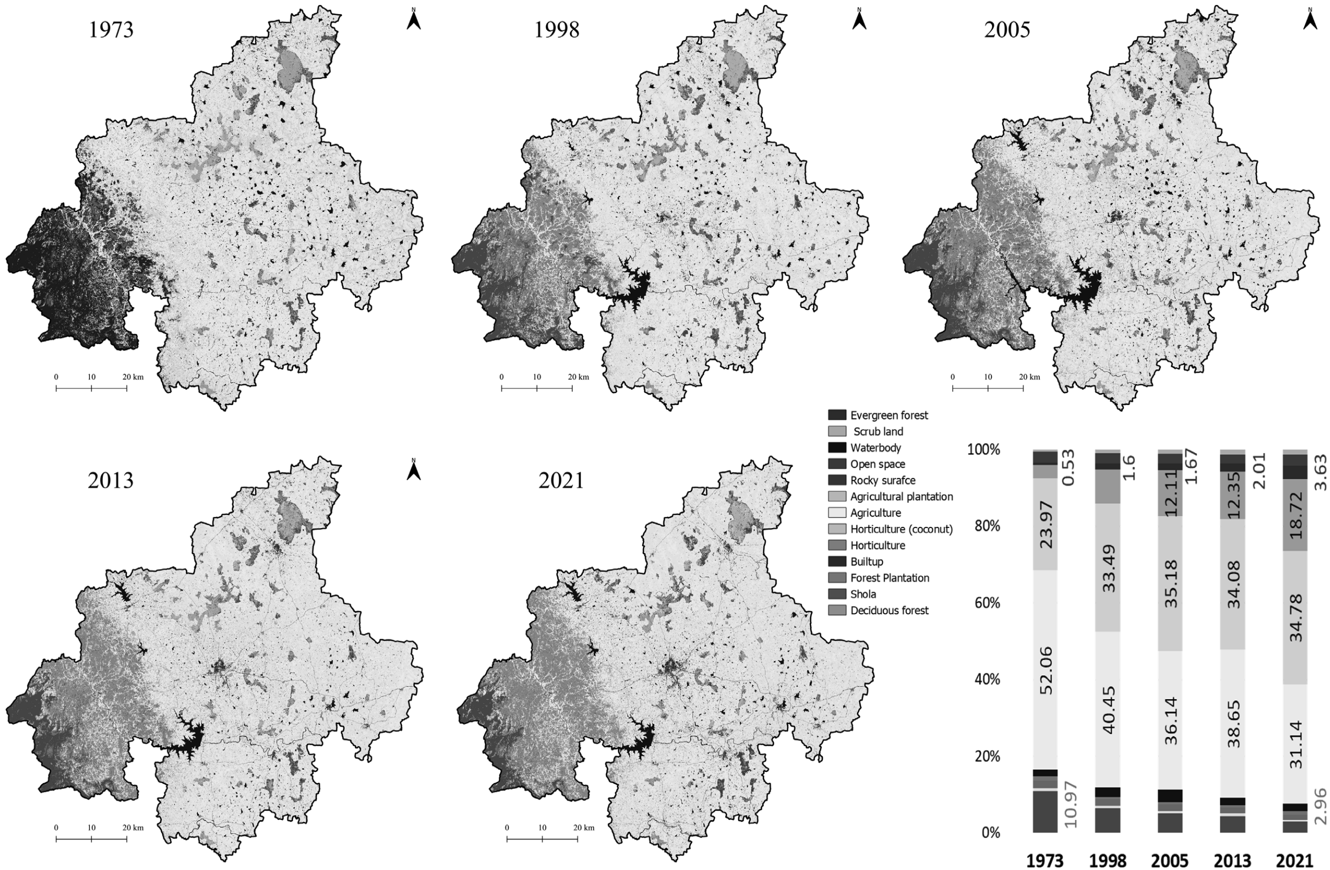

FIGURE 4.5 Land use analysis of Hassan from 1973 to 2021.

Forest plantations of acacia, eucalyptus, teak, and other monoculture plantations have increased from 0.53% (3.98 km^2) in 1973 to 94.91% (439.66 km^2) in 2021.

Approximately 1.73% (118.19 km^2) of the district was covered by water bodies like the Hemavati and Kaveri Rivers in 1973. In the 1990s, reservoirs such as the Hemavathi Dam, Yetihole Dam, and Yagachi Reservoir were built, which increased water availability in the district. The water bodies comprised 2.52% (171.64 km^2) in 1998, 3.2% (218.19 km^2) in 2005, 1.85% (126.21 km^2) in 2013, and 2% (136.36 km^2) in 2021.

The economy of the Hassan district is based on its agricultural and horticultural activities, evident from the fact that 52.06% (3551.53 km^2) of the district was under agricultural lands in 1973. Then, due to increased water availability, conversion of agricultural lands to horticulture was practiced predominantly in the region. The total area under agriculture was 40.45% (2759.7 km^2) in 1998 to 34.24% (2335.9 km^2) in 2021. The area under horticulture of coconut, arecanut, and different fruits and vegetables increased from 23.97% (1635.33 km^2) in 1973 to 38.53% (2628.82 km^2) in 2021. Horticulture of coffee, black pepper, and other cash crops has also increased, which covered 3.46% (235.85 km^2) in 1973, 8.95% (610.94 km^2) in 1998, 12.11% (826.41 km^2) in 2005, 12.35% (842.65 km^2) in 2013, and 12.39% (845.44 km^2) in 2021.

The district has experienced continuous urban growth, which led to an increase in built-up area from 0.53% (36.41 km^2) in 1973 to 1.6% (109.04 km^2) in 1998, 1.67% (113.77 km^2) in 2005, 2.01% (137.11 km^2) in 2013, and 2.11% (144.21 km^2) in 2021. The open spaces in the district covered 2.93% (199.65 km^2) in 1973, 2.56% (174.44 km^2) in 1998, 2.54% (173.46 km^2) in 2005, 2.41% (164.92 km^2) in 2013, and 2.89% (197.23 km^2) in 2021.

4.3.3 Forest Fragmentation

The structure of the forest in the Hassan district from 1973 to 2021 was assessed using temporal land uses through fragmentation metrics, which provided the spatial extent of the interior of contiguous forest patches in the diverse categories of forests, which include evergreen, shola, deciduous, and scrub forest areas, and this excludes forest plantations (acacia, teak, eucalyptus, and others). The forest fragmentation analyses presented in Table 4.3 and Figure 4.6 illustrate that the interior forest had declined from 8.93% (609.27 km^2) in 1973 to 4.91% (335.1 km^2) in 1998, 4.24% (288.99 km^2) in 2005, 3.7% (252.73 km^2) in 2013, and 3.58% (244.39 km^2) in 2022.

4.3.4 Prediction of Likely Land Uses—Integrated CA-Markov Modelling

The land use analyses provided insights into the transition of land use categories from 1973 to 2019. Simulation of the land use has been carried out to understand the impact of the current rate of land use transitions in the next two decades, with the help of Markov and Cellular Automata techniques. The model was validated by comparing the actual land use classification of 2021 with the simulated land use of 2021. The validation value was K_{no} = 0.8569, $K_{location}$ = 0.8394, $K_{locationStrata}$ = 0.8394,

TABLE 4.3
Forest Fragmentation Analysis of Hassan from 1973 to 2021

Forest Fragmentation		1973	1998	2005	2013	2021
Non-Forest	sq. km	5694.75	6007.2	6052.84	6194.84	6300.23
	%	83.47	88.05	88.72	90.8	92.34
Patch	sq. km	23.84	78.27	58.03	66.92	53.28
	%	0.35	1.15	0.85	0.98	0.78
Transitional	sq. km	92.04	77.38	65.71	62.96	22.86
	%	1.35	1.13	0.96	0.92	0.34
Edge	sq. km	72.61	12.7	14.29	10.5	9.38
	%	1.06	0.19	0.21	0.15	0.14
Perforated	sq. km	211.83	140.23	124.41	108.29	56.04
	%	3.1	2.06	1.82	1.59	0.82
Interior	sq. km	609.27	335.1	288.99	252.73	244.39
	%	8.93	4.91	4.24	3.7	3.58
Water	sq. km	118.19	171.64	218.19	126.21	136.36
	%	1.73	2.52	3.2	1.85	2

and $K_{standard}$ = 0.8113, suggesting the model's high efficiency. The simulated land use showed an underestimation of horticultural land and an overestimation of agricultural land in 2021.

Predicted land uses for 2030 and 2038 are depicted in Figure 4.7, and categorized land use details are listed in Table 4.4, which highlights further degradation of the evergreen forest to 2.62% (179.06 km^2) in 2030 and 2.18% (148.84 km^2) in 2038. Deciduous forests would also decrease to 1.09% (74.43 km^2) in 2030 and 0.85% (58.06 km^2) in 2038. Similarly, scrub forest would decrease by 0.88% (60.18 km^2) in 2030 and 0.74% (50.76 km^2) in 2038. The area under plantation is likely to increase to 1.9% (129.55 km^2) in 2030 and 1.89% (128.87 km^2) in 2038. The built-up area is expected to increase to 4.62% (315.1 km^2) in 2030 and 5.49% (374.36 km^2) in 2038 in the business-as-usual scenario.

4.3.5 Ecologically Sensitive Regions

Prioritization of ESRs in the Hassan district has been done through grid-based analysis to get a detailed picture of ecological fragility at village levels, considering eco-geo-climatic-socio variables for implementing conservation measures.

The district has evergreen forests in the west of the Western Ghats area, and there are deciduous and scrub forests in the hillocks of the district (Figure 4.8). Major forest cover has been identified in Arsikere Hill and the Western Ghats area. The interior forest density is highest in the Western Ghats section of Sakleshpura taluk.

The ecology of the Hassan district was evaluated by assessing biodiversity variables such as endemic flora, fauna, the biomass of forests, number of species, Shannon's diversity, the spatial extent of conservation reserves, etc. Figure 4.9 and

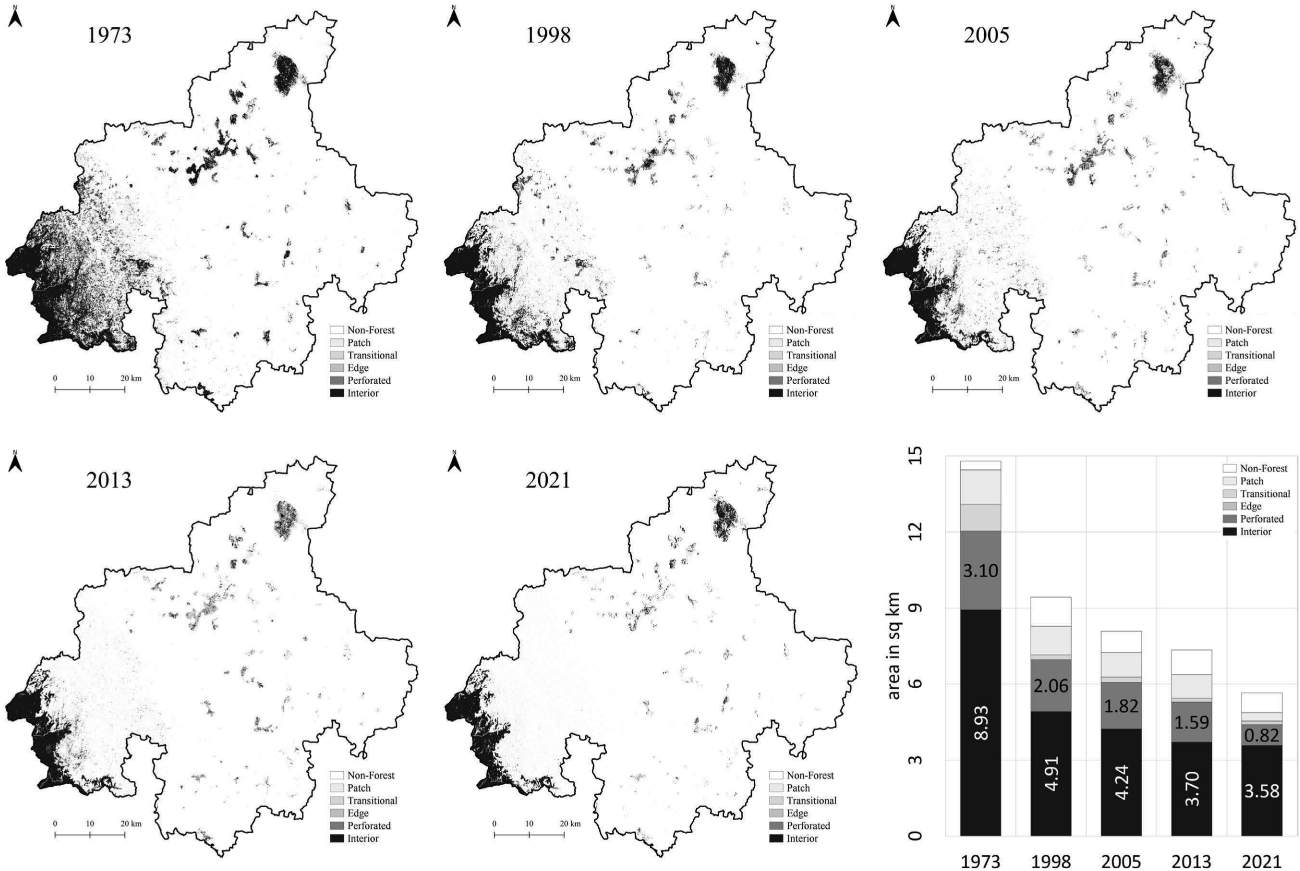

FIGURE 4.6 Forest fragmentation analysis of Hassan from 1973 to 2021.

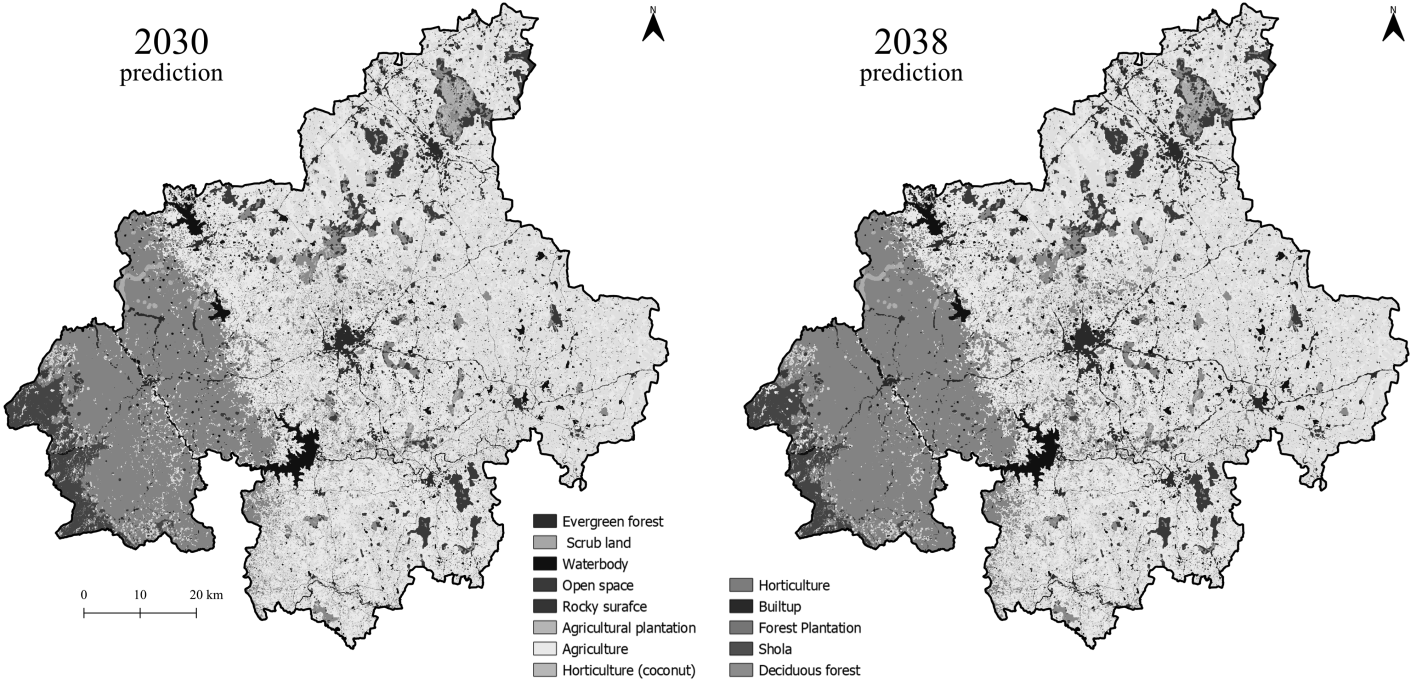

FIGURE 4.7 Simulation of land use of 2030 and 2038 in Hassan district.

TABLE 4.4
Simulation of Land Use of 2030 and 2038 in Hassan District

	2030 Simulation		2038 Simulation	
Land Use Simulation	**sq. km**	**%**	**sq. km**	**%**
Evergreen	179.06	2.62	148.84	2.18
Deciduous	74.43	1.09	58.06	0.85
Scrub/Grass	60.18	0.88	50.76	0.74
Water	154.33	2.26	158.6	2.32
Agriculture	1973.97	28.93	1879.05	27.54
Horticulture (plains)	2359.02	34.58	2312.93	33.9
Horticulture (hills)	1317.24	19.31	1449.86	21.25
Built-up	315.1	4.62	374.36	5.49
Open	259.65	3.81	261.2	3.83
Plantation	129.55	1.9	128.87	1.89

Figure 4.10 give the spatial distribution of endemic and non-endemic flora and fauna. The density of species and Shannon's diversity are higher in the forest areas. The evergreen forest area has >1200 Gg total carbon, and the deciduous forest has 300–900 Gg total carbon. The biomass concentration is higher in the evergreen forest region. The district shares its boundary with the Pushpagiri Wildlife Sanctuary in the southern part of Sakleshpura taluk.

The district has an average elevation >750m and a slope of less than 15%, except for the Western Ghats section, where the elevation is 250–750m and slope <15% (Gundiya River region) (Dudani et al., 2010). The district has a decreasing rainfall pattern from west to east. The Western Ghat section receives >2400 mm of rain, the middle part of the district with forest cover receives 1200–2400 mm of rain, the middle part without forest cover receives 600–1200 mm of rain, and the eastern part receives <600 mm of rain. The western part of the district is under the Sahyadri or Western Ghat agroclimatic zone and the eastern part is under hot-dry-semi-arid. Most of the district is composed of Peninsular Gneiss and the hillocks of the district are of Dharwars or Granite. The entire district has clayey loamy soil.

This district is under the Hemavathi sub-basin and Kaveri basin. Gundiya and Kumaradhara river network are in the Western Ghats. The streams in the forest region have more than 6 months of water and the rivers in the plain region have less than 3 months of water. Similarly, hilly forested areas have >2.5 per sq. km drainage density and the plain area has 1–1.5 per sq. km drainage density. The areas with rivers have stream density 1.5–2 per sq. km, and drainage density in the other parts of the district is 1–1.5 per sq. km (Figure 4.11). This district has two major reservoirs—Gorur Hemavathi Reservoir on the Hemavathi River and Yagachi Reservoir on the Yagachi River.

Figure 4.12 depicts the spatial variability of renewable energy sources in the study region. The whole district has more than 6 kWh/m^2 solar energy potential (Figure 4.12a). Also, the entire district has less than 1.5 m/sec wind speed (Figure

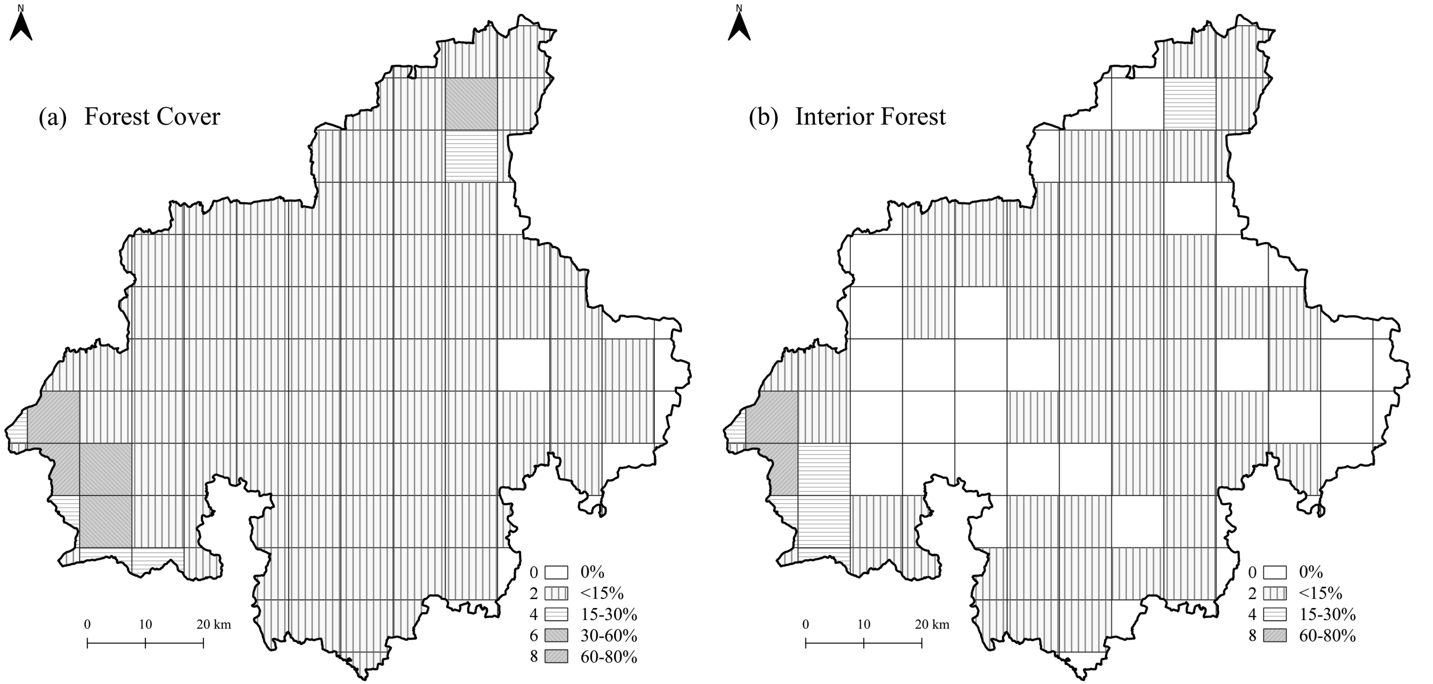

FIGURE 4.8 Forest cover, interior forest cover with their relative weights in Hassan.

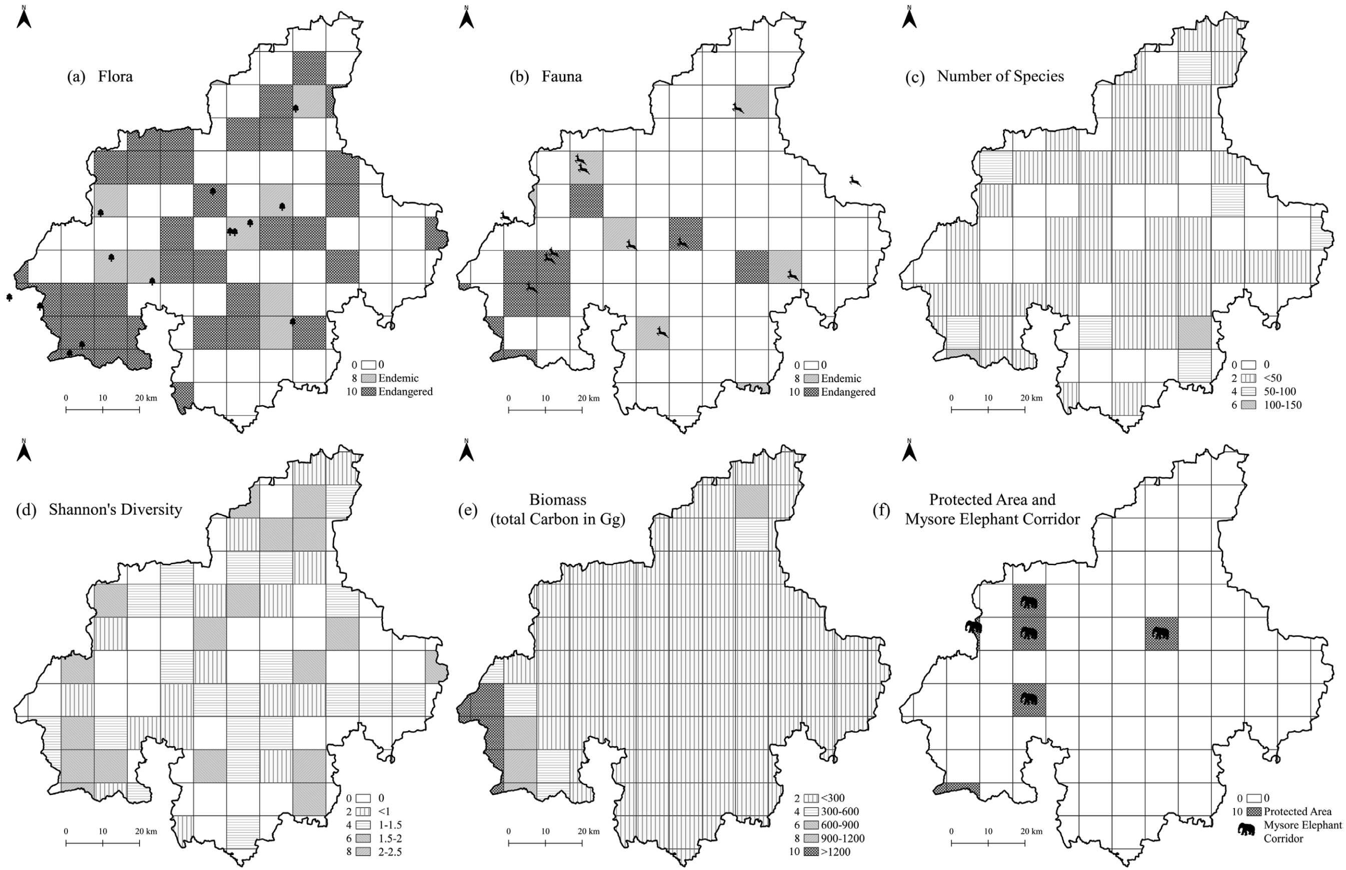

FIGURE 4.9 Ecological variables with their relative weights in Hassan.

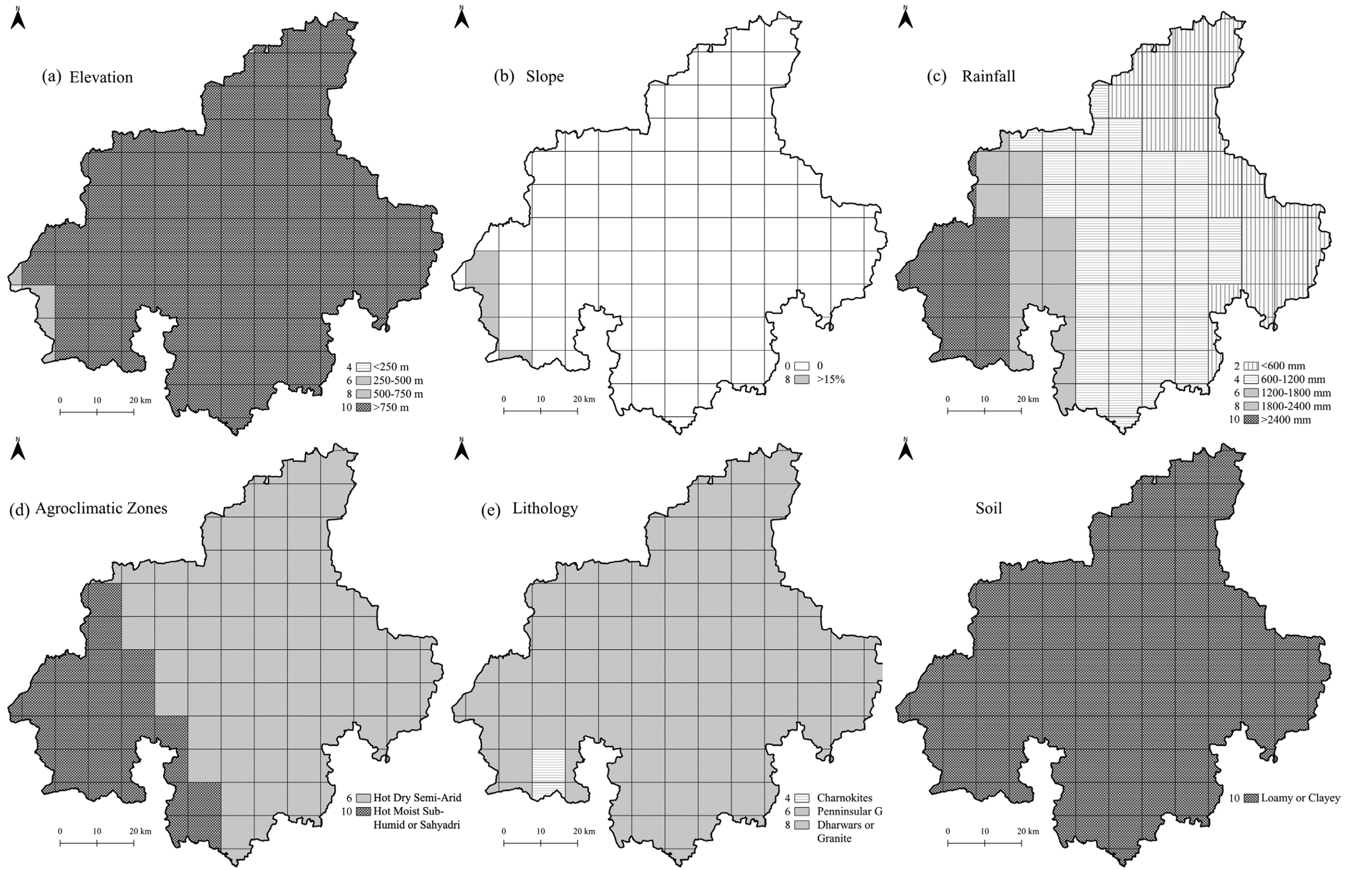

FIGURE 4.10 Geo-climatic variables with their relative weights in Hassan.

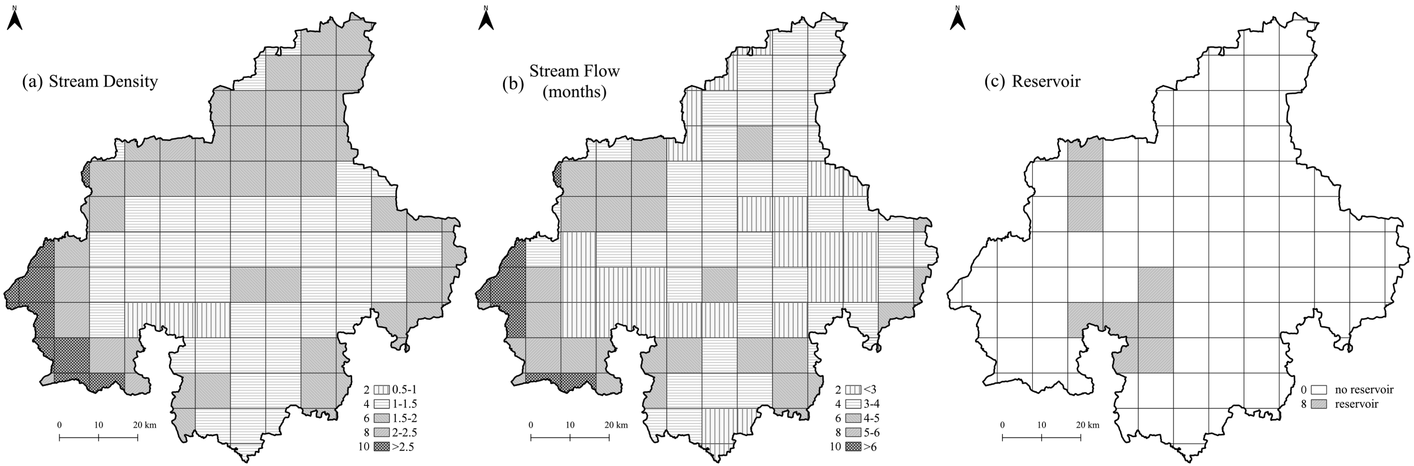

FIGURE 4.11 Hydrological variables with their relative weights in Hassan.

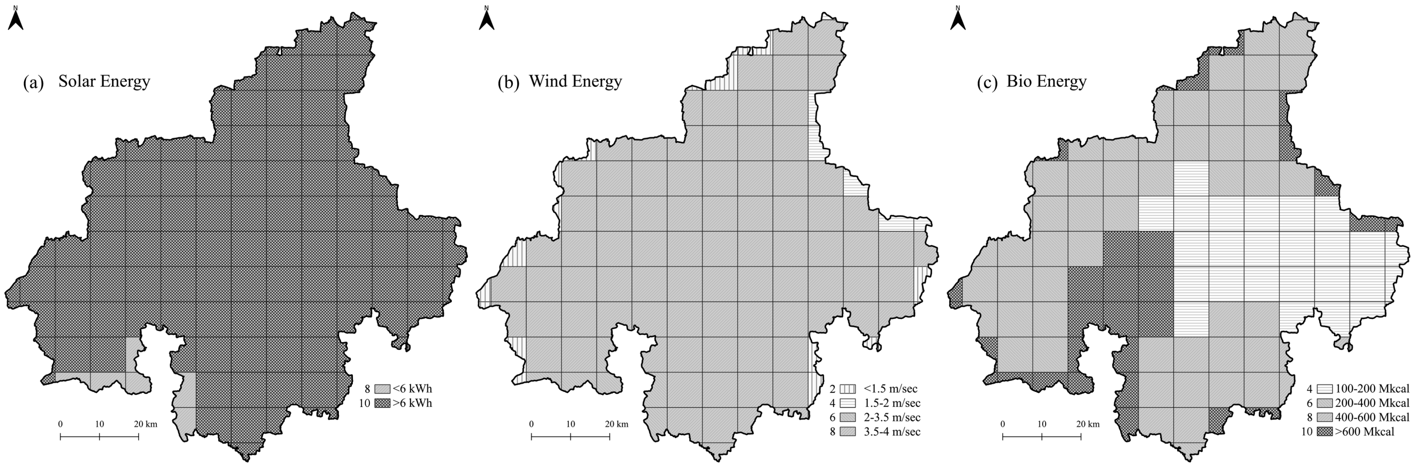

FIGURE 4.12 Renewable energy variables with their relative weights in Hassan.

4.12b) throughout the year. The bio-energy potential is highest in Alur taluk (>600 MKcal), followed by Arkalgud and Holenarasipura (400–600 MKcal), Sakleshpura, Belur, and Arsikere (200–400 MKcal). The lowest is in Hassan (Figure 4.12c) and Channarayapatna (100–200 MKcal).

The population density is 500–250 persons per sq. km in the district, except for Sakleshpura and Belur taluk, where the population density is 250–100 persons per sq. km. Livestock density is 1.5–2.25 animals per ha in Arkalgud, Holenarashipura, and Hassan taluk, whereas Alur taluk has 0.75–7.5 animals per ha, and Sakleshpura and Belur have <0.75 animals per ha livestock density. The presence of forest dwellers is in the Western Ghats in the Sakleshpura taluk and Nagapuri forest areas in Arsikere taluk. Figure 4.13 depicts population density, livestock density, and forests dwellers spatial distribution.

Based on the significance of chosen themes, regions were prioritized using aggregated weights metric scores as ESR1 (regions of highest sensitivity), ESR2 (regions of higher sensitivity), ESR3 (regions of high sensitivity), and ESR4 (regions of moderate sensitivity). Spatially, 20 grids of the district represent ESR1, while 37 represent ESR2, 46 grids represent ESR3, and about 16 grids are in ESR4. Figure 4.14 depicts grid-level analysis of ESRs. ESR1 has the maximum forest cover and rich biodiversity along with less population. ESR2 represents a zone of higher conservation and forms a transition between the highest conservation and moderate conservation regions. ESR3 represents a moderate conservation region; only regulated sustainable development is allowed in these areas. ESR4 represents the least diverse areas, and location-specific developments may be allowed with strict vigilance from regulatory authorities.

4.4 DISCUSSION

Forest ecosystems provide a biodiverse habitat supporting a variety of flora and fauna, which are essential for the survival of organisms that rely on both biotic and abiotic elements within their specific habitats. However, the fragmentation of continuous forest areas into isolated patches has resulted in the degradation of natural resources, soil and water contamination, and reduction in species diversity and abundance (Ramachandra et al., 2019). Additionally, the transformation of climax evergreen vegetation to secondary deciduous forests and scrub due to plantations has affected hydrological services, evident from the diminished water flow in streams and rivers, with potentially adverse effects on the livelihoods of those in the Malnad region and beyond, including the drier Deccan plains (Ramachandra et al., 2020). The Hassan district, being a part of the Malnad region, is endowed with abundant natural resources, and landscapes are conducive to extensive agricultural and horticultural activities, with production of arecanut and coffee (Lakshmidevi and Manjunath, 2019). Coffee cultivation is dominant in the Sakaleshpura and Alur taluks, along with cardamom, oranges, and pepper. Coffee cultivation faces challenges, particularly due to climate change and irregular rainfall patterns. Karnataka contributes approximately 71.03% of India's total coffee production. The disturbances in the animal habitats contribute to a rise in human-animal conflicts, inbreeding, and, ultimately, the extinction of species (Hayward and Kerley, 2009). One of the reasons for

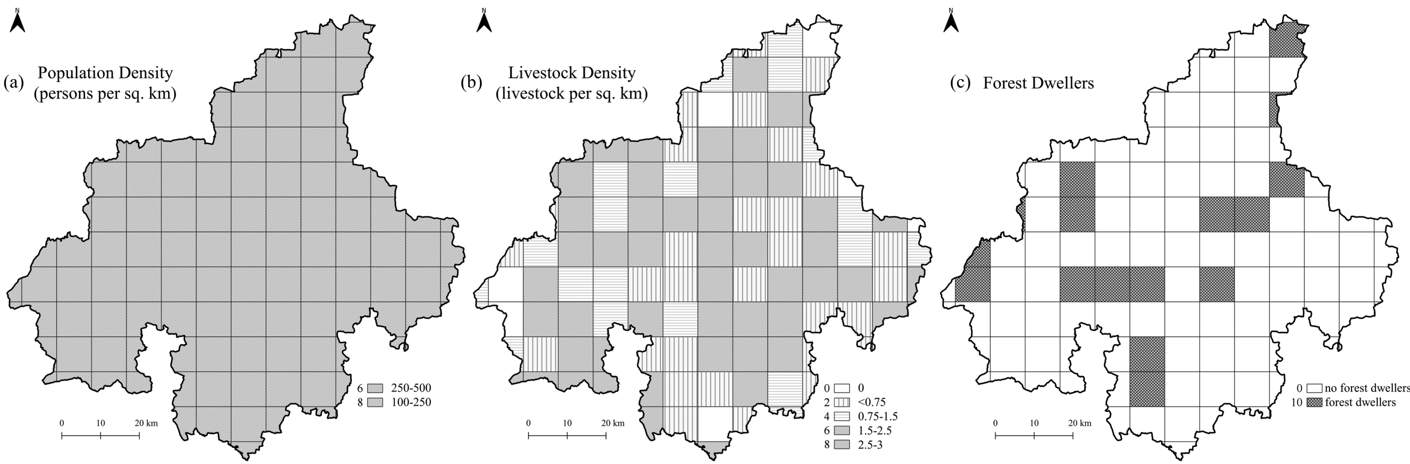

FIGURE 4.13 Social variables with their relative weights in Hassan.

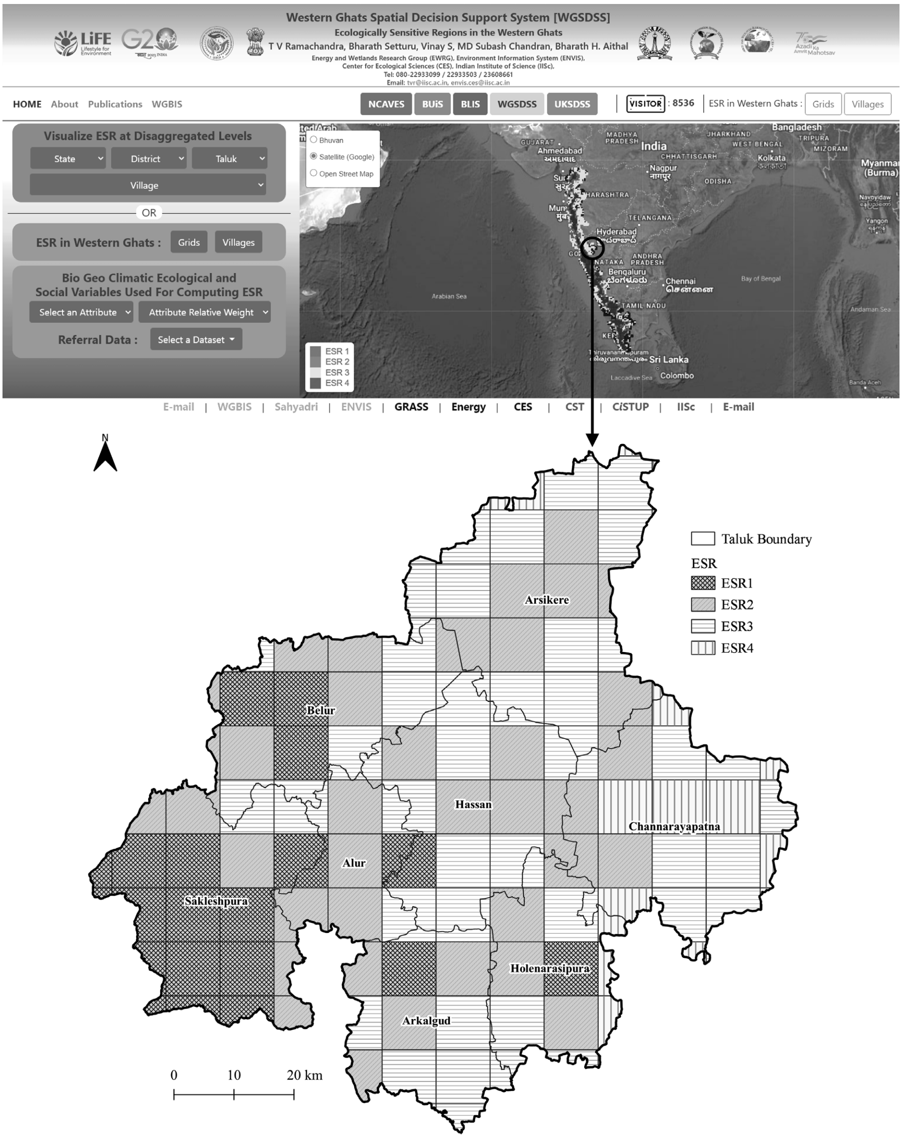

FIGURE 4.14 Visualization of grid-based ESRs of Hassan in Western Ghats Spatial Decision Support System (WGSDSS: https://wgbis.ces.iisc.ac.in/sdss/wgsdss/index.php).

human-animal conflict is the coffee cultivation in the Hassan district. Instances of elephants venturing into human settlements have become common, particularly in Alur and Sakaleshpur regions of the district. Recurring instances of human-animal conflicts necessitate evolving appropriate mitigation strategies through identification and mapping of animal movement paths or animal corridors, while enriching animal habitats with fodder and water. Also, alterations in the ecosystem integrity with fragmentation of native forests and degradation of landscapes have altered the microclimate within and around the degraded patches, evident from an increase in temperatures and heat island effects (Bharath et al., 2013).

The natural landscape in Karnataka is witnessing rapid transitions due to unplanned developmental activities, with spurts in industrial activities to boost the economy. The Hassan district has been witnessing urban growth driven by factors like development of industrial zones, B. Katihalli Industrial Area, Holinarshipura, Thimmanhalli, and Special Economic Zones such as KIADB Pharmaceutical SEZ, KIADB SEZ Hassan—Textiles, KIADB Food Processing SEZ, and Opto Infrastructure Hassan. The agriculture (croplands, horticulture, and livestock) sector has facilitated the growth of the agro and food processing industries. Recently, a 300MT cattle feed plant was established in the center of Hassan city for the growth, maintenance, and milk production and to increase the reproductive efficiency of animals. The district is well-connected by roadways (NH 48 and NH 206) and railways network. The district is midway between Mangalore and Bangalore, making it a location for new industries to establish their operations. Additionally, the nearest international airport and seaport are situated in Mangalore, around 174 kilometers from the district, which acts as a gateway for Karnataka for exports. The Karnataka Industrial Area Development Board (KIADB) has contributed to the growth of real estate, IT industries, road connectivity, infrastructure, and industrial areas. The district is also home to the Master Control Facility of ISRO for spacecraft operations starting from the Launch and Early Orbit Phase (LEOP) of the geosynchronous and IRNSS class of spacecraft.

Spatial decision support systems (SDSS), with geographic information systems (GIS) and multi-criteria decision analysis (MCDA), have aided in the assessment and visualization of information of sustainable scenarios, etc. (Sugumaran and Degroote, 2010; Omidipoor et al., 2019). Query-based visualization through SDSS aids in making well-informed conclusions such as land usage, management of natural resources, and the layout of urban areas. SDSS empowers decision-makers to grasp the complex interconnections within different spatial elements due to integration of diverse data, with the advanced analytical methodologies and visualization utilities (Bui, 2000). Assessment of potential environmental, economic, and societal effects tangled to divergent developmental scenarios facilitates stakeholders to collectively participate in the decision-making process (Lombardi and Ferretti, 2015), which aids in formulating adaptive strategies as per the principles of sustainable development.

4.5 CONCLUSION

Temporal land use and land cover of the Hassan district, Karnataka, was quantified from 1973 to 2021 using the remote sensing data—Landsat dataset. The land cover analyses showed a 20.8% increase in vegetation cover due to an increase in agricultural (cropland and horticultural) activities in the district. Land use analyses indicate that the evergreen and deciduous forest has decreased by 546.74 km^2 and 49.46 km^2, respectively, with an increase in horticultural practices by 1778.98 km^2 in the last five decades. The availability of water has led to prosperity in horticultural crops like coffee, cotton, etc. Also, main city centres like Hassan, Arsikere, Holenarsipura, and Channarayapatna showed an increasing trend in build-up due to urbanization and industrialization, along with establishment of the special economic zones (SEZs) in the district. Forest fragmentation analyses show a decline in interior or contiguous forest from 609.27 km^2 (1973) to 244.39 km^2 (2021). Per visualization of likely land uses, the forest cover is expected to decrease further. ESRs have been delineated at disaggregated levels for prudent management of natural resources by conserving ESRs (ESR1 and ESR2) and identifying the regions suitable for development to benefit the local population (ESR4). Prioritization of ESRs has been done by dividing the study regions into 5'×5' grids and assessment of eco-geo-climatic-social aspects. Spatially, 20 grids indicating maximum forest cover and rich biodiversity in the district represent ESR1, and about 16 grids are in ESR4, indicating the least diverse areas in this region. The development may be allowed in ESR4 with strict vigilance from regulatory authorities. The landscape extent and condition assessment with visualization of likely scenarios would help in decision-making to sustain natural resources. The Western Ghats Spatial Decision Support System (WGSDSS) is designed and implemented at https://wgbis.ces.iisc.ac.in/sdss/wgsdss/index.php, which would help in visualization of current and future scenarios and aid in monitoring, ensuring that decisions remain responsive to evolving challenges and opportunities. Thus, the WGSDSS empowers decision-making with the insights of complex spatial challenges to promote a balanced and sustainable future.

Author Contributions: Conceptualization, development of methods, soft computing, field investigation, validation, writing, formatting, and reviewing were carried out by all authors. All authors have read and agreed to the published version of the manuscript.

Funding: Field research is funded by the EIACP (ENVIS) division, the Ministry of Environment, Forests and Climate Change, Government of India, and infrastructure support is provided by the Indian Institute of Science.

Data Availability Statement: Data are archived at our data portal: https://wgbis.ces.iisc.ac.in.

Conflicts of Interest: The authors declare no conflicts of interest.

4.6 ACKNOWLEDGEMENT

We are grateful to the EIACP (ENVIS) Division, the Ministry of Environment, Forests and Climate Change, Government of India (grant: SP/DEOO-22–001).

REFERENCES

Aithal, B. H., & Ramachandra, T. V. (2016). Visualization of urban growth pattern in Chennai using geoinformatics and spatial metrics. *Journal of the Indian Society of Remote Sensing*, 44, 617–633.

Aithal, B. H., Vinay, S., Durgappa, S., & Ramachandra, T. V. (2013, November). Modeling and simulation of urbanisation in greater Bangalore, India. In *Proc. of National Spatial Data Infrastructure 2013 Conference*. IIT, Bombay, pp. 34–50.

Alam, A., Bhat, M. S., & Maheen, M. (2020). Using Landsat satellite data for assessing the land use and land cover change in Kashmir Valley. *GeoJournal*, 85, 1529–1543.

Amini, S., Saber, M., Rabiei-Dastjerdi, H., & Homayouni, S. (2022). Urban land use and land cover change analysis using random forest classification of landsat time series. *Remote Sensing*, 14(11), 2654.

Aravind, N. A., Patil, R. K., & Madhyastha, N. A. (2008). Micromolluscs of the Western Ghats, India: Diversity, distribution and threats. *Zoosymposia*, 1, 281–294.

Armstrong, M. P., & Densham, P. J. (1992). Domain decomposition for parallel processing of spatial problems. *Computers, Environment and Urban Systems*, 16(6), 497–513.

Arowolo, A. O., Deng, X., Olatunji, O. A., & Obayelu, A. E. (2018). Assessing changes in the value of ecosystem services in response to land-use/land-cover dynamics in Nigeria. *Science of the Total Environment*, 636, 597–609.

Asare, R. A., Kyei, A., & Mason, J. J. (2013). The community resource management area mechanism: A strategy to manage African forest resources for REDD+. *Philosophical Transactions of the Royal Society B: Biological Sciences*, 368(1625), 20120311.

Basavaraja, R., Przygrodzka, E., Pawlinski, B., Gajewski, Z., Kaczmarek, M. M., & Meidan, R. (2017). Interferon-tau promotes luteal endothelial cell survival and inhibits specific luteolytic genes in bovine corpus luteum. *Reproduction*, 154(5), 559–568.

Basse, R. M., Omrani, H., Charif, O., Gerber, P., & Bódis, K. (2014). Land use changes modelling using advanced methods: Cellular automata and artificial neural networks. The spatial and explicit representation of land cover dynamics at the cross-border region scale. *Applied Geography*, 53, 160–171.

Beinat, E. (1997). Value functions for environmental management. In *Environment & Management*, vol. 7. Springer, Dordrecht.

Bharath, S., Rajan, K. S., & Ramachandra, T. V. (2013). Land surface temperature responses to land use land cover dynamics. *Geoinfor Geostat: An Overview*, 54, 50–78.

Bharath, S., Rajan, K. S., & Ramachandra, T. V. (2014). Visualization of forest changes in Uttara Kannada, Volume 8. *Paper presented in Seminar on Lake 2014 National, in Sirsi, November 13 to 15, 2014*. Sirsi, India.

Bui, T. X. (2000). Decision support systems for sustainable development: An overview. In *Decision Support Systems for Sustainable Development: A Resource Book of Methods and Applications*, pp. 1–10.

Cagnolo, L., Cabido, M., & Valladares, G. (2006). Plant species richness in the Chaco Serrano Woodland from central Argentina: Ecological traits and habitat fragmentation effects. *Biological Conservation*, 132(4), 510–519.

Carpenter, S. R., DeFries, R., Dietz, T., Mooney, H. A., Polasky, S., Reid, W. V., & Scholes, R. J. (2006). Millennium ecosystem assessment: Research needs. *Science*, 314(5797), 257–258.

Ceballos, G., Ehrlich, P. R., & Dirzo, R. (2017). Biological annihilation via the ongoing sixth mass extinction signaled by vertebrate population losses and declines. *Proceedings of the National Academy of Sciences*, 114(30), E6089–E6096.

Chandran, M. S. (1997). On the ecological history of the Western Ghats. *Current Science*, 146–155.

Costanza, R., d'Arge, R., De Groot, R., Farber, S., Grasso, M., Hannon, B., . . . & Van Den Belt, M. (1997). The value of the world's ecosystem services and natural capital. *Nature*, 387(6630), 253–260.

Davison, C. W., Rahbek, C., & Morueta-Holme, N. (2021). Land-use change and biodiversity: Challenges for assembling evidence on the greatest threat to nature. *Global Change Biology*, 27(21), 5414–5429.

De Groot, R. S., Alkemade, R., Braat, L., Hein, L., & Willemen, L. (2010). Challenges in integrating the concept of ecosystem services and values in landscape planning, management and decision making. *Ecological Complexity*, 7(3), 260–272.

De Groot, R. S., Brander, L., Ploeg, S., Costanza, R., Bernard, F., Braat, L., . . . & van Beukering, P. (2012). Global estimates of the value of ecosystems and their services in monetary units. *Ecosystem Services*, 1, 50–61.

Dudani, S., Chandran, M. S., Rao, G. R., Mukri, V., Bhat, H., & Ramachandra, T. V. (2010). Biodiversity, ecology and socio-economic aspects of gundia river basin. *Economical Survey of Karnataka*, 2021–2022.

FAO. (2010). *Global Forest Resources Assessment 2010. Forestry Paper 163*. FAO, Rome. ISBN 978-92-5-106654-6. https://www.fao.org/4/i1757e/i1757e.pdf

FAO. (2011). *State of the World's Forest 2011. FAO Report*. FAO, Rome. ISBN 978-92-5-106750-5. https://www.fao.org/4/i2000e/i2000e.pdf

FAO. (2020). *Global Forest Resources Assessment 2020: Main Report*. FAO, Rome. https://doi.org/10.4060/ca9825en

Foody, G. M. (2003). Remote sensing of tropical forest environments: Towards the monitoring of environmental resources for sustainable development. *International Journal of Remote Sensing*, 24(20), 4035–4046.

Fu, B., Zhang, L., Xu, Z., Zhao, Y., Wei, Y., & Skinner, D. (2015). Ecosystem services in changing land use. *Journal of Soils and Sediments*, 15, 833–843.

Fu, Q., Li, B., Hou, Y., Bi, X., & Zhang, X. (2017). Effects of land use and climate change on ecosystem services in central Asia's arid regions: A case study in Altay Prefecture, China. *Science of the Total Environment*, 607, 633–646.

Gadgil, M., Daniels, R. R., Ganeshaiah, K. N., Prasad, S. N., Murthy, M. S. R., Jha, C. S., . . . & Subramanian, K. A. (2011). Mapping ecologically sensitive, significant and salient areas of Western Ghats: Proposed protocols and methodology. *Current Science*, 175–182.

Gómez-Baggethun, E., & Barton, D. N. (2013). Classifying and valuing ecosystem services for urban planning. *Ecological Economics*, 86, 235–245.9

Goyal, A. K., & Arora, S. (2009). *India's Fourth National Report to the Convention on Biological Diversity*. Ministry of Environment and Forests, Government of India, New Delhi, 75, 143.

Hanski, I. (2011). Habitat loss, the dynamics of biodiversity, and a perspective on conservation. *Ambio*, 40(3), 248–255.

Harper, G. J., Steininger, M. K., Tucker, C. J., Juhn, D., & Hawkins, F. (2007). Fifty years of deforestation and forest fragmentation in Madagascar. *Environmental Conservation*, 34(4), 325–333.

Harper, K. A., Macdonald, S. E., Burton, P. J., Chen, J., Brosofske, K. D., Saunders, S. C., . . . & Esseen, P. A. (2005). Edge influence on forest structure and composition in fragmented landscapes. *Conservation Biology*, 19(3), 768–782.

Hasan, S. S., Zhen, L., Miah, M. G., Ahamed, T., & Samie, A. (2020). Impact of land use change on ecosystem services: A review. *Environmental Development*, 34, 100527.

Hassan District Disaster Management Plan, 2011–12. Hassan.nic.in—DC Office Hassan.

Hayward, M. W., & Kerley, G. I. (2009). Fencing for conservation: Restriction of evolutionary potential or a riposte to threatening processes? *Biological Conservation*, 142(1), 1–13.

Houghton, R. A., & Nassikas, A. A. (2017). Global and regional fluxes of carbon from land use and land cover change 1850–2015. *Global Biogeochem Cycles*, 31(3), 456–472.

Jankowski, P. (2009). Towards participatory geographic information systems for community-based environmental decision making. *Journal of Environmental Management*, 90(6), 1966–1971.

Jiyuan, L., Mingliang, L., Xiangzheng, D., Dafang, Z., Zengxiang, Z., & Di, L. (2002). The land use and land cover change database and its relative studies in China. *Journal of Geographical Sciences*, 12, 275–282.

Karnatak, H. C., Saran, S., Bhatia, K., & Roy, P. S. (2007). Multicriteria spatial decision analysis in web GIS environment. *Geoinformatica*, 11, 407–429.

Kennedy, R. E., Townsend, P. A., Gross, J. E., Cohen, W. B., Bolstad, P., Wang, Y. Q., & Adams, P. (2009). Remote sensing change detection tools for natural resource managers: Understanding concepts and tradeoffs in the design of landscape monitoring projects. *Remote Sensing of Environment*, 113(7), 1382–1396.

Keshtkar, H., & Voigt, W. (2016). A spatiotemporal analysis of landscape change using an integrated Markov chain and cellular automata models. *Modeling Earth Systems and Environment,* 2(1). doi:10.1007/s40808-015-0068-4

Lakshmidevi, B. V., & Manjunath, K. R. (2019). Women Entrepreneurship—problems and prospects in Malnad Region. *International Journal of Emerging Technologies and Innovative Research*, 6(1), 572–584, ISSN:2349–5162.

Lambin, E. F., Geist, H. J., & Lepers, E. (2003). Dynamics of land-use and land-cover change in tropical regions. *Annual Review of Environment and Resources*, 28(1), 205–241.

Laurance, W. F., Lovejoy, T. E., Vasconcelos, H. L., Bruna, E. M., Didham, R. K., Stouffer, P. C., . . . & Sampaio, E. (2002). Ecosystem decay of Amazonian forest fragments: A 22-year investigation. *Conservation Biology*, 16, 605–618.

Li, R. Q., Dong, M., Cui, J. Y., Zhang, L. L., Cui, Q. G., & He, W. M. (2007). Quantification of the impact of land-use changes on ecosystem services: A case study in Pingbian County, China. *Environmental Monitoring and Assessment*, 128, 503–510.

Liu, S., Costanza, R., Farber, S., & Troy, A. (2010). Valuing ecosystem services: Theory, practice, and the need for a transdisciplinary synthesis. *Annals of the New York Academy of Sciences*, 1185(1), 54–78.

Lombardi, P., Abastante, F., Torabi Moghadam, S., & Toniolo, J. (2017). Multicriteria spatial decision support systems for future urban energy retrofitting scenarios. *Sustainability*, 9(7), 1252.

Lombardi, P., & Ferretti, V. (2015). New spatial decision support systems for sustainable urban and regional development. *Smart and Sustainable Built Environment*, 4(1), 45–66. https://doi.org/10.1108/SASBE-07-2014-0039

Mariye, M., Jianhua, L., & Maryo, M. (2022). Land use and land cover change, and analysis of its drivers in Ojoje Watershed, Southern Ethiopia. *Heliyon*, 8(4), e09267.

Moghadam, S. T., Coccolo, S., Mutani, G., Lombardi, P., Scartezzini, J. L., & Mauree, D. (2019). A new clustering and visualization method to evaluate urban heat energy planning scenarios. *Cities*, 88, 19–36.

Moghadam, S. T., Toniolo, J., Mutani, G., & Lombardi, P. (2018). A GIS-statistical approach for assessing built environment energy use at urban scale. *Sustainable Cities and Society*, 37, 70–84.

Molur, S., Smith, K. G., Daniel, B. A., & Darwall, W. R. T. (2011). *The Status and Distribution of Freshwater Biodiversity in the Western Ghats, India*. IUCN, and Coimbatore India, Zoo Outreach Organisation, Cambridge, UK and Gland, Switzerland.

Myers, N., Mittermeier, R. A., Mittermeier, C. G., Da Fonseca, G. A., & Kent, J. (2000). Biodiversity hotspots for conservation priorities. *Nature*, 403(6772), 853–858.

Nilsson, C., & Grelsson, G. (1995). The fragility of ecosystems: A review. *Journal of Applied Ecology*, 32, 677–692.

Nunez, S., Arets, E., Alkemade, R., Verwer, C., & Leemans, R. (2019). Assessing the impacts of climate change on biodiversity: Is below 2° C enough?. *Climatic Change*, 154, 351–365.

Oliver, T. H., & Morecroft, M. D. (2014). Interactions between climate change and land use change on biodiversity: Attribution problems, risks, and opportunities. *Wiley Interdisciplinary Reviews: Climate Change*, 5(3), 317–335.

Omidipoor, M., Jelokhani-Niaraki, M., Moeinmehr, A., Sadeghi-Niaraki, A., & Choi, S. M. (2019). A GIS-based decision support system for facilitating participatory urban renewal process. *Land Use Policy*, 88, 104150.

Ouyang, Z., Song, C., Zheng, H., Polasky, S., Xiao, Y., Bateman, I. J., . . . & Daily, G. C. (2020). Using gross ecosystem product (GEP) to value nature in decision making. *Proceedings of the National Academy of Sciences*, 117(25), 14593–14601.

Pacheco, F. A. L., Fernandes, L. F. S., Junior, R. F. V., Valera, C. A., & Pissarra, T. C. T. (2018). Land degradation: Multiple environmental consequences and routes to neutrality. *Current Opinion in Environmental Science & Health*, 5, 79–86.

Pascal, J. P. (1993). Management oriented forest map of South India: Thematic derivations. *Vegetatio*, 109(1), 47–61.

Ramachandra, T. V., & Bharath, S. (2021). Carbon footprint of Karnataka: Accounting of sources and sinks. In *Carbon Footprint Case Studies*. Springer, Singapore, pp. 53–92

Ramachandra, T. V., Bharath, S., & Bharath, A. H. (2020). Insights of forest dynamics for the regional ecological fragility assessment. *Journal of the Indian Society of Remote Sensing*, 48(8), 1169–1189.

Ramachandra, T. V., Bharath, S., & Chandran, M. D. S. (2016). Geospatial analysis of forest fragmentation in Uttara Kannada District, India. *Forest Ecosystems*, 3(1), 10.

Ramachandra, T. V., Bharath, S., Chandran, M. D. S., & Joshi, N. V. (2018). Salient ecological sensitive regions of central Western Ghats, India. *Earth Systems and Environment*, 2(1), 15–34.

Ramachandra, T. V., Bharath, S., & Vinay, S. (2019). Visualisation of impacts due to the proposed developmental projects in the ecologically fragile regions-Kodagu district, Karnataka. *Progress in Disaster Science*, 3, 100038.

Ramachandra, T. V., Subash Chandran, M. D., Joshi, N. V., & Bharath, S. (2013). Fragmentation of Uttara Kannada forests, Sahyadri Conservation Series 29, ENVIS Technical Report 57, ENVIS, Centre for Ecological Sciences, Indian Institute of Science, Bangalore. https://wgbis.ces.iisc.ac.in/energy/water/paper/ETR57/sec3.html

Ramachandra, T. V., Tara, N. M., & Bharath, S. (2017). Web based spatial decision support system for sustenance of western ghats biodiversity, ecology and hydrology. In Sharma, A., & Rajeswaran, J. (eds) *Creativity and Congition in Art and Design*, pp. 58–70.

Ramirez-Gomez, S. O., Torres-Vitolas, C. A., Schreckenberg, K., Honzák, M., Cruz-Garcia, G. S., Willcock, S., . . . & Poppy, G. M. (2015). Analysis of ecosystem services provision in the Colombian Amazon using participatory research and mapping techniques. *Ecosystem Services*, 13, 93–107.

Riitters, K. H., Wickham, J. D., O'Neill, R. V., Jones, B. B., & Smith, E. R. (2000). Global-scale patterns of forest fragmentation. *Conservation Ecology*, 4(2).

Riitters, K. H., Wickham, J. D., O'Neill, R. V., Jones, K. B., Smith, E. R., Coulston, J. W., Wade, T. G., & Smith, J. H. (2002). Fragmentation of continental United States forests. *Ecosystems*, 5(8), 815–822.

Rimal, B., Zhang, L., Keshtkar, H., Haack, B. N., Rijal, S., & Zhang, P. (2018). Land use/land cover dynamics and modeling of urban land expansion by the integration of cellular automata and markov chain. *ISPRS International Journal of Geo-Information*, 7(4), 154.

Rockström, J., Steffen, W., Noone, K., Persson, Å., Chapin III, F. S., Lambin, E., . . . & Foley, J. (2009). Planetary boundaries: Exploring the safe operating space for humanity. *Ecology and Society*, 14(2).

Scott, G. J., England, M. R., Starms, W. A., Marcum, R. A., & Davis, C. H. (2017). Training deep convolutional neural networks for land—cover classification of high-resolution imagery. *IEEE Geoscience and Remote Sensing Letters*, 14(4), 549–553.

Shivanna, K. R. (2020). The sixth mass extinction crisis and its impact on biodiversity and human welfare. *Resonance*, 25(1), 93–109.

Shivanna, K. R. (2022). Climate change and its impact on biodiversity and human welfare. *Proceedings of the Indian National Science Academy*, 88(2), 160–171.

Silvestri, S., Zaibet, L., Said, M. Y., & Kifugo, S. C. (2013). Valuing ecosystem services for conservation and development purposes: A case study from Kenya. *Environmental Science & Policy*, 31, 23–33.

Sugumaran, R., & Degroote, J. (2010). *Spatial Decision Support Systems: Principles and Practices*. CRC Press/Taylor & Francis Group, Boca Raton, FL.

Tan, J., Yu, D., Li, Q., Tan, X., & Zhou, W. (2020). Spatial relationship between land-use/land-cover changes and land surface temperature in the Dongting Lake Area, China. *Scientific Reports*, 10(1), 1–9.

Termorshuizen, J. W., Opdam, P. (2009). Landscape services as a bridge between landscape ecology and sustainable development. *Landscape Ecology*, 24(8), 1037–1052. doi: 10.1007/s10980-008-9314-8

Tilman, D., & Lehman, C. (2001). Human-caused environmental change: Impacts on plant diversity and evolution. *Proceedings of the National Academy of Sciences*, 98(10), 5433–5440.

Tolessa, T., Senbeta, F., & Kidane, M. (2017). The impact of land use/land cover change on ecosystem services in the central highlands of Ethiopia. *Ecosystem Services*, 23, 47–54.

Turner, B. L. (1997). The sustainability principle in global agendas: Implications for understanding land-use/cover change. *Geographical Journal*, 133–140.

Villegas-Palacio, C., Berrouet, L., López, C., Ruiz, A., & Upegui, A. (2016). Lessons from the integrated valuation of ecosystem services in a developing country: Three case studies on ecological, socio-cultural and economic valuation. *Ecosystem Services*, 22, 297–308.

Vinay, S., Bharath, S., Bharath, H. A., & Ramachandra, T. V. (2013). Hydrologic model with landscape dynamics for drought monitoring. *Paper presented in Seminar on Joint International Workshop of ISPRS WG VIII/1 and WG IV/4 on Geospatial Data for Disaster and Risk Reduction*. Hyderabad, India, November 21 to 22.

Wade, T. G., Riitters, K. H., Wickham, J. D., & Jones, K. B. (2003). Distribution and causes of global forest fragmentation. *Conservation Ecology*, 7(2).

Wan, S. (2009). A spatial decision support system for extracting the core factors and thresholds for landslide susceptibility map. *Engineering Geology*, 108(3–4), 237–251.

Watson, J. E. M., Grantham, H., Wilson, K. A., & Possingham, H. P. (2011a). Systematic conservation planning: Past, present and future. In Whittaker, R., & Ladle, R. (eds) *Conservation Biogeograph*. WileyBlackwell, Oxford, pp. 136–160.

Winkler, K., Fuchs, R., Rounsevell, M., & Herold, M. (2021). Global land use changes are four times greater than previously estimated. *Nature Communications*, 12(1), 2501.

Young, A. G., & Boyle, T. J. (2000). Forest fragmentation. In *Forest Conservation Genetics: Principles and Practice*. CSIRO Publishing and CAB International, Wallingford, UK, pp. 123–134.

5 Hydrological Alterations under Climate Change

Global-Scale Challenges and Opportunities for Adaptation and Sustainable Development

Rajib Maity

5.1 INTRODUCTION

Both climatic and non-climatic determinants exert influence upon the dynamics of the hydrological cycle. The intricate interplay among greenhouse gas concentrations, aerosol particles, and surface albedo perturbs the radiative equilibrium, consequently modulating evaporation and precipitation processes across both global and regional domains. Concomitant with atmospheric warming, discernible trends manifest in augmented global and regional mean precipitation, alongside intensified precipitation events. Regional precipitation responses, in tandem with alterations in atmospheric circulation, exhibit variability. The geographical distribution of aerosols, influencing atmospheric circulation patterns, imparts noteworthy repercussions upon precipitation regimes, notably exemplified in the context of the Asian monsoon (Douville et al., 2021; Srivastava et al., 2022a). Elevated levels of atmospheric CO_2 generally lead to decreased plant transpiration, influencing various aspects of the hydrological cycle, such as surface temperature, soil moisture, runoff, stream flows, and moisture recycling. However, in some regions, the reduction in transpiration may be offset to some extent by an increase in leaf area due to factors like rising CO_2 levels, land use changes, nitrogen deposition, and the effects of climate change. Additionally, increased ozone levels can negatively impact a plant's transpiration capacity (Ganguly et al., 2012; IPCC, 2022).

Concerning the impact of anthropogenic activities on the planetary hydrological cycle, human agency manifests through deliberate interventions, such as the regulation of streamflow through dam construction, extensive trans-basin water transfers, and the extraction of surface and groundwater for purposes encompassing potable water supply, agriculture, and diverse freshwater applications (Rane et al., 2023). A multifaceted array of sociological and economic factors, encompassing shifts in land utilization and urban expansion, can exert discernible repercussions on these

DOI: 10.1201/9781032686899-7

direct human interventions, thereby influencing the global and regional hydrological cycle and the equilibrium of water resources (Chinnasamy & Srivastava, 2021; Dhanuka et al., 2023; Shumilova et al., 2018). Through abstraction, irrigation may decrease river flows and groundwater levels while increasing local precipitation. It can also influence precipitation remotely through moisture advection and alter the timing of monsoons through differences in land and sea temperatures. Land cover changes impact evapotranspiration (ET), precipitation, precipitation intercepted by plant canopies, infiltration, and runoff. Human water consumption has comparable effects on the hydrological cycle as land cover. Moreover, urbanization engenders a diminishment in ground surface permeability, thereby heightening the susceptibility to flooding and rapid runoff. Simultaneously, this phenomenon diminishes the capacity for local moisture replenishment of the atmosphere, thus impacting local precipitation dynamics. However, urbanization can also lead to an increase in the sensible heat flow or more severe precipitation (Bosmans et al., 2017; Douville et al., 2021; IPCC, 2022).

In addition to natural and human-induced influences that alter hydrological processes, it is imperative to evaluate the magnitude of influence exerted by these factors on the pivotal dimension of water security, concerning its role in both adaptation to and mitigation of climate change. According to the IPCC (2022), an estimated global population of around 4 billion individuals is anticipated to face pronounced susceptibility to severe water scarcity during specific periods of the year. This susceptibility arises from the intricate interplay of both climatic and non-climatic determinants. Depending on regional climate change patterns and socioeconomic scenarios, it is estimated that between 0.9 and 3.9 billion people may experience heightened vulnerability to water stress under a global warming level of approximately 2°C (Koutroulis et al., 2019). In the agriculture sector, the peril to food production looms prominently within basins constituting the top decile in global water stress, accounting for 35% of the world's output in irrigated calories, as elucidated by Srivastava et al. (2022a). Concurrently, as of 2017, approximately 4.2 billion individuals encountered insufficiencies in access to adequate sanitation, while around 2.2 billion people lacked access to potable drinking water. From 1971 to 2000, surface-water deficits were identified in various cities worldwide, ranging from 16% to 39% (Flörke et al., 2018). Since 2014, a mere 20% of recorded case studies on adaptation responses have measured their outcomes, making it challenging to assess the relationship between positive outcomes and the reduction of climate risks. Henceforth, the efficacious mitigation of climate change–induced perils pertaining to the hydrological cycle and water security necessitates implementing a holistic systems approach. This approach must encompass a contemplation of not only the immediate ramifications of adaptation strategies on water resources but also their indirect consequences stemming from efforts towards mitigating climate change (IPCC, 2022).

The study thus evaluates and reviews the hydrological alterations under climate change in view of global-scale challenges and opportunities for adaptation and sustainable development. The study also examined research from India to advance understanding of the precipitation characteristics under observed and projected climate as a case study. This is a critical aspect of the study since India is highly vulnerable to the impacts of climate change, particularly in the water sector. With the objective of examining the subject comprehensively, this study endeavors to evaluate and analyze three main aspects. Firstly, it aims to assess and review the documented alterations in the hydrological cycle, including precipitation, evapotranspiration, soil moisture, floods, and droughts, attributable to climate change. Secondly, it seeks to explore the projected changes in the aforementioned hydrological variables. Finally, this research endeavors to scrutinize the benefits and effectiveness of water-centric adaptations, in conjunction with an examination of the seven foundational principles that facilitate the achievement of water security and the promotion of sustainable, climate-resilient development within transformative systemic frameworks. The present investigation is essential, given that there is a need to balance the competing demands for water resources while ensuring its sustainability. Hence, the findings from this study can help decision-makers in the water sector to develop effective regional adaptation strategies

5.2 OBSERVED GLOBAL-SCALE ALTERATIONS IN HYDROLOGICAL CYCLE DUE TO CLIMATE CHANGE

According to the IPCC (2022), it has been scientifically demonstrated that the presence of increased greenhouse gas (GHG) concentrations in the atmosphere, resulting from human activities, has heightened the probability of various extreme hydrometeorological events. These events include heavy precipitation, flooding, drought, and wildfires, which have caused loss of life, substantial economic damage, and far-reaching ecological consequences. The human-induced modification of the global water cycle significantly affects ecosystems and populations worldwide. On these lines, this section examines alterations to the hydrological cycle from the perspective of social effects.

5.2.1 Observed Changes in Precipitation

Worldwide, annual mean precipitation (P) is rising in several areas but falling in smaller areas, especially in the tropics. Presently, in excess of 160 million inhabitants occupy geographies characterized by historical aridity, with nearly 500 million individuals residing in regions that have traditionally exhibited elevated precipitation levels. Notably, the intensity of torrential rainfall has exhibited conspicuous escalation in various locales, encompassing substantial portions of North America, Europe, the Indian subcontinent, segments of Asia, South America, southern Africa, and Australia. In contrast, select regions, exemplified by eastern Australia, northeastern South America, and western Africa, have witnessed a decline in intense precipitation events (Dunn et al., 2020). There has been a notable increase in the duration of dry periods, as indicated by a rise in the average number of consecutive dry days (CDD) throughout various regions. This trend is particularly evident in southeast Asia, eastern and southwestern South America, as well as western and southern Africa. In certain areas where yearly precipitation shows no trend, precipitation extremes have altered. Specific geographic zones, including segments of southern South America and southern Africa, are currently undergoing a notable augmentation in intense rainfall events, concomitant with prolonged periods of aridity. This phenomenon is conspicuously evident in densely populated regions, such as the Indian subcontinent, southeast Asia, Europe, and select areas across North and South America, as well as southern Africa. Notably, an estimated 709 million individuals inhabit territories where the annual maximum one-day precipitation has experienced intensification, while approximately 86 million dwell in regions where it has declined. However, it is worth noting that longer dry spells are more prevalent than shorter ones, with 711 million people inhabiting regions where the annual average of CDD has lengthened compared to the 1950s, in contrast to 404 million people in areas with shorter CDD (Douville et al., 2021; IPCC, 2022).

The observed shifts in precipitation patterns are primarily ascribed to the escalation in anthropogenic GHG concentrations. According to the findings of the IPCC (2022), heightened GHG levels have engendered conspicuous disparities in precipitation regimes between wet and dry seasons, thereby introducing alterations in meteorological patterns across tropical terrestrial domains. Particularly noteworthy is the significant increase in precipitation across northern high latitudes. Additionally, GHG-induced forcing has contributed to the emergence of dry summer conditions in various regions, including the Mediterranean, southwestern Australia, southwestern South America, south Africa, and western North America. The IPCC's 2022 assessment report also underscores that well-monitored inland areas exhibit a heightened likelihood of experiencing an elevated frequency and severity of intense precipitation events on a global scale. This trend is particularly evident in North America, Europe, and Asia when considered on a continental scale.

5.2.2 Observed and Reconstructed Changes in Evapotranspiration

According to recent studies, global evapotranspiration (ET) increased between the early 1980s to 2009 and 2013 (Figure 5.1). Based on rigorous calculations using observational data, it has been observed that a majority of global regions have witnessed an increase in ET. These increases have been statistically significant in significant portions of North America and northern Eurasia ($p<0.05$), reaching up to 10 mm yr-2. Moreover, several other regions, such as northeast Brazil, western central Africa, southern Africa, southern India, southern China, and northern Australia, have experienced even larger increases in ET. However, it should be noted that certain areas, like western Amazonia and central Africa, have shown decreases in ET of approximately 10 mm yr-2, although these patterns may not be consistent across all datasets (Bosmans et al., 2017; Douville et al., 2021; Elbeltagi et al., 2022; IPCC, 2022).

According to the assessment by the IPCC (2022), a robust scientific consensus exists affirming the substantial contribution of human activities to the discernible augmentation in global terrestrial annual ET since the inception of the 1980s. This upswing can be ascribed to a multifaceted interplay of factors, encompassing heightened atmospheric water vapor demand and enhanced vegetation vitality driven by elevated atmospheric carbon dioxide (CO_2) concentrations. Furthermore, changes in temperature, land surface properties, and ecosystem characteristics influence regional

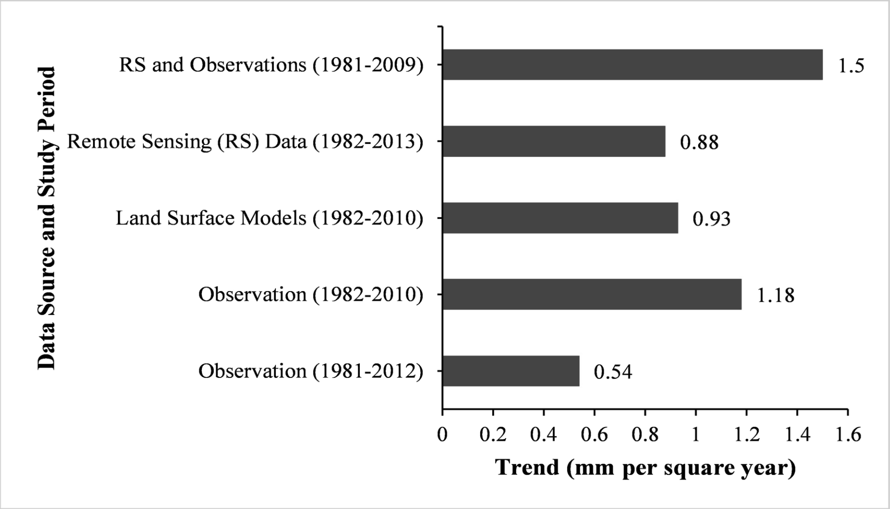

FIGURE 5.1 Temporal variations in global evapotranspiration during distinct intervals spanning from 1981 to 1982 and 2009 to 2013.

(Source: IPCC, 2022)

variations in ET. The latter react to modifications in the environment and structure of the atmosphere. For instance, whereas seasonal rainfall totals alter the quantity of soil moisture available for evaporation, a warmer climate increases evaporative demand. Fluctuations in vegetation exert a significant influence on the overarching fluctuations in ET, given that transpiration constitutes a substantial component of the water exchange occurring between terrestrial surfaces and the atmosphere. The phenomenon of reduced stomatal conductance, denoted as the 'physiological effect,' diminishes transpiration rates and augments leaf-level water use efficiency (WUE). This effect, to a certain degree, serves as a counterbalancing mechanism to mitigate the escalation in evaporative demand associated with rising atmospheric CO_2 concentrations, although it is notably contingent on the species under consideration. Increased CO_2 additionally accelerates photosynthesis, albeit this effect might not last over the long term, especially in environments with temperatures higher than the thermal maximum for photosynthesis. Higher photosynthesis raises the Leaf Area Index (LAI), which has a 'structural effect' on transpiration and is responsible for 55 ± 25% of documented increases in ET between 1980 and 2011. Based on satellite observations spanning from 1982 to 2012, it has been projected that the increase in ET resulting from the rise in LAI is estimated to be around 0.32 ± 0.07 mm month-1 per decade. This increase in ET corresponds to a climatic forcing of approximately 0.31 Wm-2 per decade. These findings indicate a quantifiable impact of rising LAI on the Earth's energy balance and the water cycle, highlighting the important role of vegetation dynamics in shaping climate patterns over the studied period (Zeng et al., 2017).

5.2.3 Observed and Estimated Past Changes in Soil Moisture and Aridity

The widely acknowledged 'Wet Grow Wetter, Dry Get Drier' (WGWDGD) paradigm may prove insufficient in characterizing spatial differentials in soil moisture trends, as discerned from an analysis encompassing changes in P-ET estimations spanning from 1948 to 2005. Scrutiny of soil moisture datasets derived from the European Space Agency Climate Change Initiative Soil Moisture (ESA CCI SM v03.2) over the period of 1979 to 2013 unveils that merely 15% of terrestrial regions conform to the anticipated correlation between soil moisture dynamics and prevailing precipitation and temperature conditions, as postulated by the widely embraced WGWDGD paradigm. Remote sensing data corroborates this observation (Figure 5.2), presented in the study conducted by Feng and Zhang (2015).

Across all types of regions, including arid, humid, and transitional areas, there exists a prevailing pattern characterized by a decrease in soil moisture rather than an increase when categorized based on precipitation and temperature regimes. Increased soil moisture trends in the ESA CCI product are primarily observed in wet or transitional zones and are uncommon in arid ones. Changes in the balance between precipitation and evapotranspiration (ET) are responsible for variations in soil moisture and land surface aridity. Irrigation practices also influence the moisture level of the soil. Examination of satellite remote sensing data spanning from the late 1970s to the late 2010s unveils discernible regional trends, characterized by

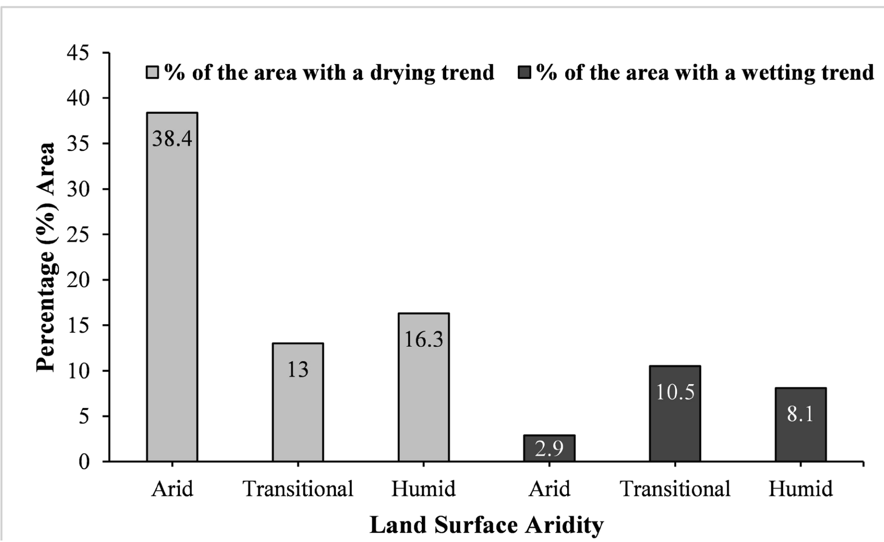

FIGURE 5.2 Examination of remote sensing data spanning from 1979 to 2013, elucidating the delineation of arid, transitional, and humid regions, while concurrently elucidating trends in both desiccation and humidification concerning surface soil moisture.

Information Source: IPCC (2022)

alterations in annual surface soil moisture exceeding 20% in select locales. Through the integration of data derived from ESA CCI SM v03.2 products, it becomes evident that approximately 2.1 billion individuals inhabit territories witnessing an augmentation in surface soil moisture, while 0.9 billion people dwell in regions experiencing a reduction (Douville et al., 2021; Feng & Zhang, 2015; IPCC, 2022).

In alignment with climate model simulations illustrating the consequences of anthropogenic climate change, assessments grounded in data-driven models and process-based land surface models elucidate a visible augmentation in arid conditions during dry seasons, primarily concentrated within extratropical zones. This pattern is observed in various locations, including Europe, western North America, northern Asia, southern South America, Australia, and eastern Africa. Additionally, increased ET typically results in decreased water availability during the dry season rather than decreased precipitation. Indeed, the IPCC (2022) discerns a global trend in soil moisture, evident in reanalysis data, which arises as a consequence of GHG forcing. Their conclusive determination conveys a high level of probability that human-induced climate change has exerted a discernible influence on these patterns over the course of the 20th century.

5.2.4 Observed Changes in Floods and Droughts

Based on a comprehensive global flood database that incorporates both in-situ measurements and satellite remote sensing, floods have increased significantly from 1985 to 2015. Specifically, floods have experienced a fourfold rise in tropical regions and a 2.5-fold increase in the northern mid-latitudes. Estimates of flood exposure based on high-resolution population data and satellite-derived inundation indicate a 20–24% rise between 2000 and 2018 (Tellman et al., 2021). Examination of on-site streamflow measurements unveiled fluctuations in the frequency of river floods across Europe and the USA during the period spanning from 1960 to 2010. In tandem, a general upsurge was observed in China, Brazil, and Australia, juxtaposed with a reduction in specific zones within the Mediterranean and southern Australia. Depending on the locale, warming over the past 40–60 years has caused spring floods to occur 1–10 days sooner every decade (the most frequent being 2–4 days per decade). Floods were responsible for 31% of all economic losses and 44% of all disasters between 1970 and 2019 (IPCC, 2022). Recent increases in observed flood hazards are frequently the result of human influences, such as population expansion and growing urbanization, rather than only climate change. Flood vulnerability has been attributed to be influenced by regional and national disparities in GDP, hazard intensity and characteristics, as well as political and social factors. In many areas, economic growth has reduced flood susceptibility, while in some, increasing exposure has increased danger. Considering the climate conditions observed between 1976 and 2005, the predicted damage, based on current flood protection standards, amounts to approximately USD 54 million per year on a global scale. Similar estimates made using several models indicate that flood exposure has increased in the past (Tanoue et al., 2016; IPCC, 2022).

Drinking water shortages and severe economic harm can be caused by hydrologic drought. Aridity in the agricultural sector negatively impacts food production by reducing yields, destroying crops, and having an adverse effect on the economy.

For instance, it was reported that the 2014 drought in India caused losses of up to USD 30 billion. Wildfire dangers are increased by ecological drought. The consequences of droughts can have cascading effects, which may involve the displacement of human communities, the breakdown of social connections, loss of cultural identity, and health issues arising from inadequate sanitation. Although drought-induced calamities comprised merely 7% of all catastrophic occurrences from 1970 to 2019, they have disproportionately accounted for 34% of fatalities linked to such disasters, with a pronounced impact on Africa. A holistic examination of risk, vulnerability, and exposure reveals that regions characterized by lower population densities, such as tundra and tropical forests, exhibit reduced susceptibility to drought risk. Conversely, areas marked by intensive agricultural practices, encompassing central Europe, southern and central Asia, southeast South America, and the southeast United States, are confronted with elevated drought risk (WMO, 2021; IPCC, 2022).

In summary, discernible geographical disparities have manifested in both the frequency and magnitude of river floods over the past few decades. Anthropogenic climate change has resulted in an increased risk of severe precipitation events, leading to more frequent and severe river floods. There exists a high level of confidence in the assertion that the observed warming spanning the past four to six decades has played a contributory role in altering the incidence and intensity of snowmelt-related floods, as well as influencing the patterns of ice-jam floods. Furthermore, a discernible trend has emerged, indicating that spring floods are transpiring up to 10 days earlier per decade. Concomitantly, both agricultural and ecological drought conditions have demonstrated an elevated prevalence and heightened severity across numerous global regions, although there are exceptions where such conditions have exhibited reduced frequency and intensity. While the disparity has narrowed since the 1980s, lower-income nations continue to experience a significantly higher proportion of their GDP being affected by drought-related economic losses compared to higher-income nations. Additionally, the global trend of economic susceptibility to drought is declining.

5.3 PROJECTED ALTERATIONS IN HYDROLOGICAL CYCLE

According to the IPCC (2022), it is expected that there will be an amplification of the terrestrial hydrological cycle, leading to increased water exchange between the land surface and the atmosphere. This is attributed to the projected increase in near-surface atmospheric water capacity due to ongoing warming, which will impact atmospheric circulation patterns, intensify convective processes, and result in higher subsurface temperatures. Persistent warming and additional physical determinants are poised to exert an impact on the depletion of snow cover, glaciers, and permafrost. This segment seeks to elucidate the projected reactions of these hydrological systems and associated processes, recognizing their inherent variability and the attendant uncertainties that prevail across diverse locales, seasons, and spatiotemporal scales.

5.3.1 Projected Changes in Precipitation

The anticipated changes in annual mean precipitation within the CMIP6 multi-model ensemble exhibit significant variations worldwide, as observed in previous model ensembles. Furthermore, there remains considerable uncertainty regarding the magnitude and direction of future changes in most geographical locations. Under a global warming scenario of 1.5°C, certain regions such as the central and eastern Sahel, south-central Asia, portions of Greenland and Antarctica, and the far northern areas of North America and Asia show agreement among models for increased precipitation, with projections ranging from a 20% to 30% increase. However, there is no unanimous consensus across all land areas regarding decreased precipitation, although a stronger agreement is observed in South America, southern Africa, and the Mediterranean. Importantly, the multi-model median change in precipitation at 1.5°C of global warming is generally less than 10% over the majority of the world's land surface. With the exception of extremely dry regions, where percentage changes in precipitation might be significantly greater due to extremely low baseline values, the median anticipated changes with 4°C global warming are larger, ranging from a 20% decline to a 40% rise in precipitation (Douville et al., 2021; IPCC, 2022). The agreement regarding heavy precipitation changes is stronger than mean precipitation, both within specific ensembles like CMIP6 and across different ensembles. For global warming of 4°C, the 50th percentile estimate for worldwide land indicates an increase in annual maximum one-day precipitation, with median increases exceeding 20% for a significant portion of the land. In most mid-latitude regions, the 95th percentile rise ranges from 20% to 40%, while in the tropics and subtropics, it is at least 40% to 70%. Significantly, in regions encompassing western Amazonia, central Africa, and the majority of the Indian subcontinent, the augmentation surpasses an impressive 80%. The prospect of diminished heavy precipitation in these zones, as indicated by the 5th percentile, stands at a probability of less than 5%. Nevertheless, albeit less likely, there persists a potential for reductions, notably in specific areas, such as northern South America and northern and western Africa. These patterns of transformation are expected to exhibit comparable trends on a global scale under both 2°C and 1.5°C global warming scenarios, albeit with reduced magnitudes at the 50th and 95th percentiles (Douville et al., 2021; IPCC, 2022).

In the absence of substantial reductions in GHG emissions, the IPCC (2022) prognosticates substantial modifications to the global and regional water cycle. It duly acknowledges the presence of marked uncertainties within various assessments rendered by regional climate models pertaining to the water cycle. Across the majority of global domains and under diverse emission scenarios, a rapid rise in the variability and intensity of water cycle phenomena is anticipated to outpace mean alterations. Furthermore, the IPCC underscores that heavy precipitation events are poised to exhibit increased frequency and severity as global warming continues. In summary, it is predicted that with 4°C of global warming, the annual mean precipitation range will either rise or decrease by up to 40% or more over numerous terrestrial regions. At lower rates of global warming, the expected ranges of precipitation changes are narrower. Most regions might witness either a rise or a drop, but there is strong confidence among models that the far north will witness an increase. Across most geographical domains, there exists a more pronounced convergence of modeling consensus that associates global warming with an augmentation of heavy precipitation. Diverse projections exist regarding alterations in the duration of arid intervals, yet in regions where an upsurge in dry spells is envisaged, the magnitude of this escalation appears more substantial in the context of elevated global warming levels.

5.3.2 Projected Changes in Evapotranspiration

Studies indicate that it is quite unknown how regional ET may alter in the future. The multi-model CMIP6 ensemble predicts changes in ET that differ across ensemble members in terms of magnitude and sign. The ensemble median projection suggests that ET is anticipated to experience an approximate 25% increase in mid to high-latitude territories, while conversely, a reduction of up to 10% is expected across the bulk of tropical South America, southern Africa, and Australia under conditions of 4°C global warming. Notably, with the exception of central Africa and southeast Asia, the ET alterations projected by the CMIP6 ensemble closely align with those derived from the CMIP5 ensemble. At lower magnitudes of global warming, the envisaged impacts exhibit proportionately lesser changes, although the spatial patterns of alteration persist (Berg & Sheffield, 2019; IPCC, 2022).

In the preponderance of models within the CMIP5 and CMIP6 frameworks, anticipated alterations in ET are intricately intertwined with soil moisture dynamics, meteorological conditions, and the physiological responses of vegetation to elevated CO_2 levels. These multifaceted interactions subsequently exert influence on both meteorological parameters and soil moisture content via surface fluxes. Elevated CO_2 concentration induces stomatal closure, resulting in a reduction in ET. However, it also triggers an increase in the LAI, which in turn elevates ET. It is worth noting that these two effects do not consistently offset each other. In regions characterized by already elevated LAI values, further LAI augmentation may not occur due to the fact that increased LAI intensifies transpiration, leading to reduced soil moisture levels, albeit offering more shade and decreasing soil evaporation. The anticipated reductions in ET are pervasive, with the most substantial declines occurring exclusively as a result of physiological factors within tropical forests. Nonetheless, it is pertinent to note that the ensemble projections encompass a wide spectrum of outcomes, encompassing both anticipated ET increases and reductions across various geographic domains. Within these scenarios, mid-latitude ET elevations may peak at approximately 50%, while reductions in ET within southern Africa may reach levels of around 30% (Lemordant & Gentine, 2019; IPCC, 2022).

5.3.3 Projected Changes in Soil Moisture

The expected changes in surface soil moisture due to global warming exhibit varying degrees of agreement among the Earth System Models (ESMs) in the CMIP6 multi-model ensemble. Similar to CMIP5, there are significant uncertainties associated with regional precipitation projections. In most regions, the ensemble predicts both increases and decreases in precipitation. The anticipated alterations in soil moisture levels following a 4°C global warming scenario span a wide spectrum. Projections encompass a decline ranging from 20% to 30% to an increase spanning 30% to 40% in the far northern reaches of North America and Asia. Conversely, eastern North America exhibits projected changes, whether increases or decreases, that are comparatively modest, staying below 10%. In contrast, western Europe and the Mediterranean regions demonstrate a more unanimous consensus in forecasting reduced soil moisture levels, with reductions reaching up to 25%. Meanwhile, projections for the northern mid-latitude regions encompass a range from a 10% to

20% decrease to a 20% to 30% increase. Furthermore, there is greater agreement across South America, southern Africa, and Asia, indicating reduced soil moisture of up to 40% or more in certain areas (Cheng et al., 2017). Most CMIP6 models incorporate the direct effects of CO_2 on plant transpiration, which has been shown to impact predictions of future changes in soil moisture significantly. Greater losses in soil moisture availability are predicted by methods that ignore this process than by climate models. Therefore, despite a majority of the research predicting a rise in global aridity and the spread of drylands, these studies may overestimate future dryness. However, land surface models still predict decreased soil moisture in many areas, including vegetation responses to CO_2 (Douville et al., 2021; Grillakis, 2019; IPCC, 2022).

In summary, it is anticipated that changes in soil moisture will intensify with higher levels of global warming, although the specifics of regional alterations remain a subject of ongoing discourse. Within the multi-model ensemble of CMIP6, a consensus emerges regarding the diminished soil moisture, reaching a maximum decline of up to 40% in regions encompassing Amazonia, southern Africa, and western Europe under conditions of 4°C global warming. Nonetheless, there is divergence among model projections concerning the direction of soil moisture changes in other geographic zones, spanning from a 30% reduction to a 40% increase in response to 4°C global warming. At lower levels of global warming, the envisioned impacts are less pronounced and display analogous regional transformational patterns.

5.3.4 Projected Changes in Floods and Droughts

Empirical scientific investigations have revealed that alterations in the occurrence and intensity of river floods will exhibit global variability (IPCC, 2022). Looking ahead to the period beyond 2050, projections indicate a diminishing frequency of river floods in geographical regions encompassing northern North America, southern South America, the Mediterranean, and eastern Europe. In contrast, expectations point towards an amplified incidence of river floods in various territories, including Asia, central Africa, western Europe, Central and South America, as well as eastern North America. There is a high level of confidence that these regions will experience larger and more frequent floods in the future, while the opposite trend is expected in northern North America, southern South America, the Mediterranean, and eastern Europe, where flood sizes and frequencies are likely to decrease (Arnell et al., 2016). There is a high probability that the combination of projected socioeconomic development and climate change will result in increased exposure to flood-prone areas, leading to a substantial escalation in direct flood damages across all levels of global warming (refer to Figure 5.3). It is anticipated that tens of millions of people in each affected country will be impacted by river floods annually, with the greatest numbers concentrated in southern, eastern, and southeastern Asia (IPCC, 2022). The escalation in flood occurrences is foreseen to present escalating risks, culminating in economic losses amounting to 1.2–1.8 times and 4–5 times higher under global warming scenarios of 2°C and 4°C, respectively, when juxtaposed with a warming of 1.5°C. In the absence of adaptation measures, the envisioned upsurge in flood events is anticipated to result in global GDP deficits that range from 1.4 to 2.5 times and 2.5

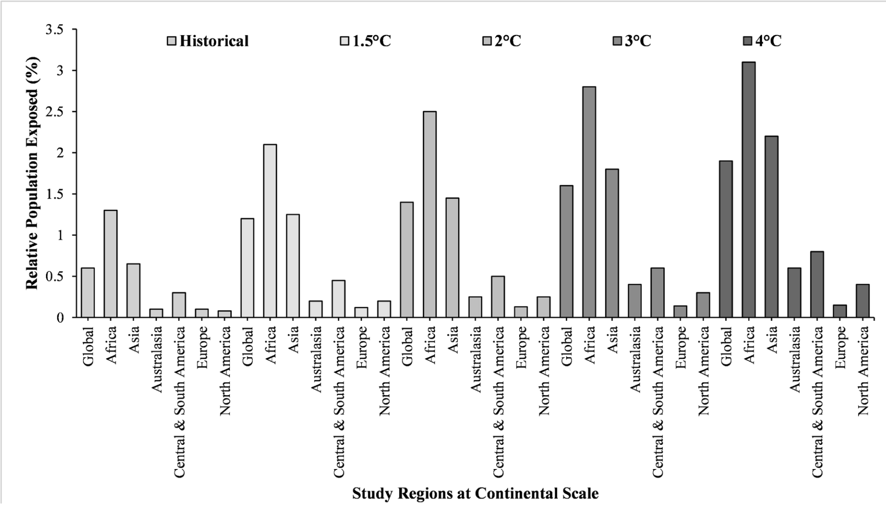

FIGURE 5.3 The prospective vulnerability to flooding, quantified as a percentage of the aggregate population impacted, exhibits spatial and temporal variations on a global or regional scale within distinct global warming levels (historical, 1.5°C, 2°C, 3°C, and 4°C). This assessment takes into account the population scenario of Shared Socioeconomic Pathway 5 (SSP5) and utilizes climate projections derived from the Coupled Model Intercomparison Project Phase 6 (CMIP6).

Information Source: IPCC (2022)

to 3.9 times greater at warming levels of 2°C and 3°C in contrast to a 1.5°C scenario, respectively. It is worth noting that regional disparities in flood hazards persist, primarily due to the substantial influence of socioeconomic factors and the inherent high degree of uncertainty in flood hazard predictions. There is moderate confidence that anticipated heavy rainfall increases would lead to locally caused floods in minor river basins and urban areas. Under RCP8.5, there is an expectation of a decline in snowmelt floods, with these events projected to transpire 25–30 days earlier in the annual calendar by the conclusion of the 21st century (IPCC, 2022).

The projected changes in drought conditions are influenced by various factors, such as the definition of drought and the magnitude of change. In the CMIP6 forecasts, it is observed that soil moisture and runoff drying are more persistent, widespread, and severe compared to changes in precipitation. As a result, agricultural droughts are anticipated to occur more frequently and over larger areas than are meteorological droughts. For instance, extreme agricultural droughts, characterized by soil moisture deficits, are expected to become more likely in several regions. These regions encompass northern South America, the Mediterranean, western China, and high latitudes within North America and Eurasia. Under a 1.5°C global warming scenario, the likelihood of experiencing extreme agricultural drought is poised to double (100%), with this probability foreseen to escalate from 150% to 200% at 2°C global warming, accompanied by an expanded geographical extent of impact. In the context of a 4°C global warming scenario, the probability of encountering extreme agricultural drought is estimated to surge by more than 200%. Similarly, regions such as Australia, southern Asia, southwest Africa, and southwestern North America are anticipated to witness a heightened probability of agricultural drought ranging from 100% to 250% under 4°C global warming. However, certain areas, such as western and eastern Asia, central North America, the Sahel, the Horn of Africa, and the eastern Indian subcontinent, are projected to experience a reduction in the likelihood of extreme drought. These projections are supported by studies conducted by Cook et al. (2020) and the IPCC (2022). Even with significant climate change mitigation, the chance of drought is predicted to rise in many locations throughout the course of the 21st century, and it will worsen in the absence of this mitigation. The anticipated expansion of agricultural drought is poised to encompass larger geographical extents than meteorological drought. However, different types of drought generally exhibit comparable patterns of anticipated change in many places. Therefore, a clear definition of drought is crucial for influencing decisions.

5.3.5 Climate Change Implication on Precipitation Pattern in India

This section attempts to explore how precipitation patterns are changing in India, which is essential for identifying potential impacts and planning adaptation measures (discussed in Sect. 6.4). The findings can inform decision-makers in the water sector to develop effective adaptation strategies that are tailored to the local context, ultimately contributing to sustainable development.

The probable maximum precipitation (PMP), regarded as a crucial design criterion, is anticipated to vary over time due to climate change effects and the intensification of the global hydrological cycle. Hence, it is of utmost importance to reconstruct the PMP map and examine its temporal evolution within the context of climate change. To investigate the temporal changes in India, Sarkar and Maity (2020) generated a one-day PMP map for five consecutive time periods using three general circulation models (GCMs) (Figure 5.4). The time periods include two historical periods (1901–1970 and 1971–2010) and three future periods (2010–2039, 2040–2069, and 2070–2100). The results reveal a clear and significant increase in PMP over a large portion of India. Approximately 84% of the Indian mainland exhibits an upward trend in PMP, with an average rise of approximately 35% from the pre-1970 (1901–1970) to the post-1970 period (1971–2100). Specifically, when considering the recent past (1971–2010) and the far future (2071–2100) under the RCP 8.5 scenario, a rise in PMP is observed in 70–80% of India's area, with an estimated average increase of 20%–35%. These findings underscore the considerable and concerning increase in PMP due to climate change, emphasizing the need for water resources engineers to account for these changes when revising planning and design strategies.

As a result of an increase in severe short-term precipitation, climate change has been reported to be manifested by an intensification of the hydrologic cycle. The intensity-duration-frequency (IDF) relationship may thus vary, which might affect other hydrological processes. To ensure the effective design of water infrastructure,

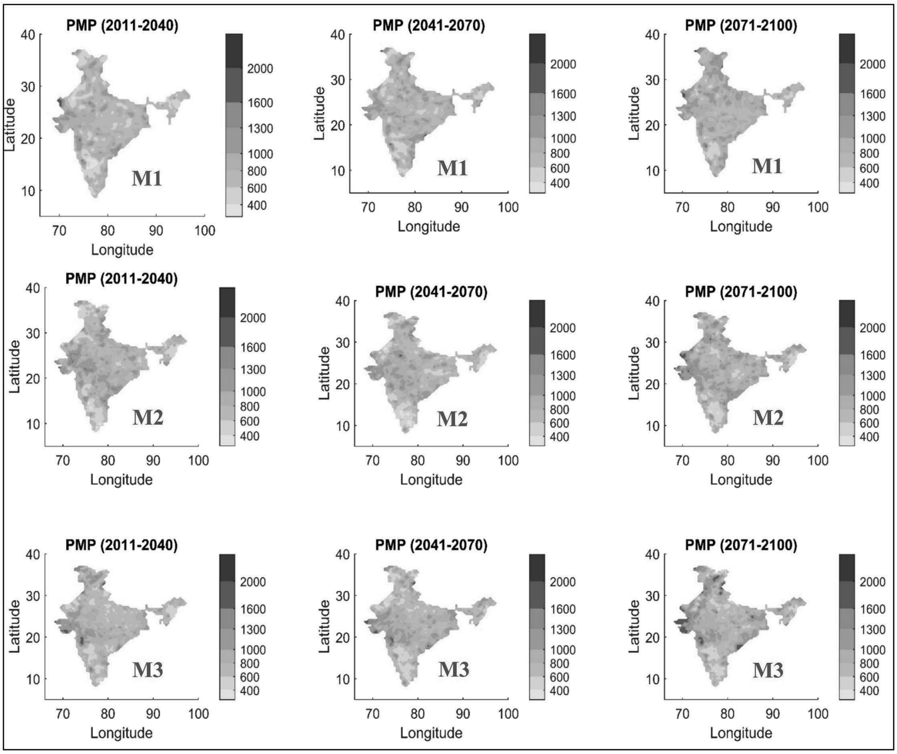

FIGURE 5.4 Projected maximum precipitation (PMP) maps for India delineated across three distinct future timeframes and predicated upon three different global climate models (GCMs)—denoted as M1, M2, and M3—employed within the current investigation under the Representative Concentration Pathway 8.5 (RCP 8.5) scenario.

Adapted from Sarkar and Maity (2020)

it is crucial to consider IDF curves as a fundamental source of information. In line with this, Maity and Maity (2022) conducted a study to examine the impact of climate change on IDF curves for precipitation in India (Figure 5.5). The study utilized two reanalysis datasets that portray historical conditions, alongside future precipitation simulations derived from three CMIP6 models. The future timeframe was segmented into three distinct periods: the immediate future (2015–2039), the near future (2040–2059), and the far future (2060–2100), all relative to the historical reference period spanning from 1979 to 2014. Comparing the two sets of reanalysis data, the study revealed that under the SSP245 scenario, precipitation intensity is projected to increase by approximately 17% to 21%, while under the SSP585 scenario, the increase is expected to be in the range of 40% to 48%. The augmentation in precipitation intensity is conspicuously pronounced within the central zones of India, spanning the coastal regions of Gujarat, the mountainous terrain of Himachal Pradesh and Uttarakhand, as well as the Terai region and northeast

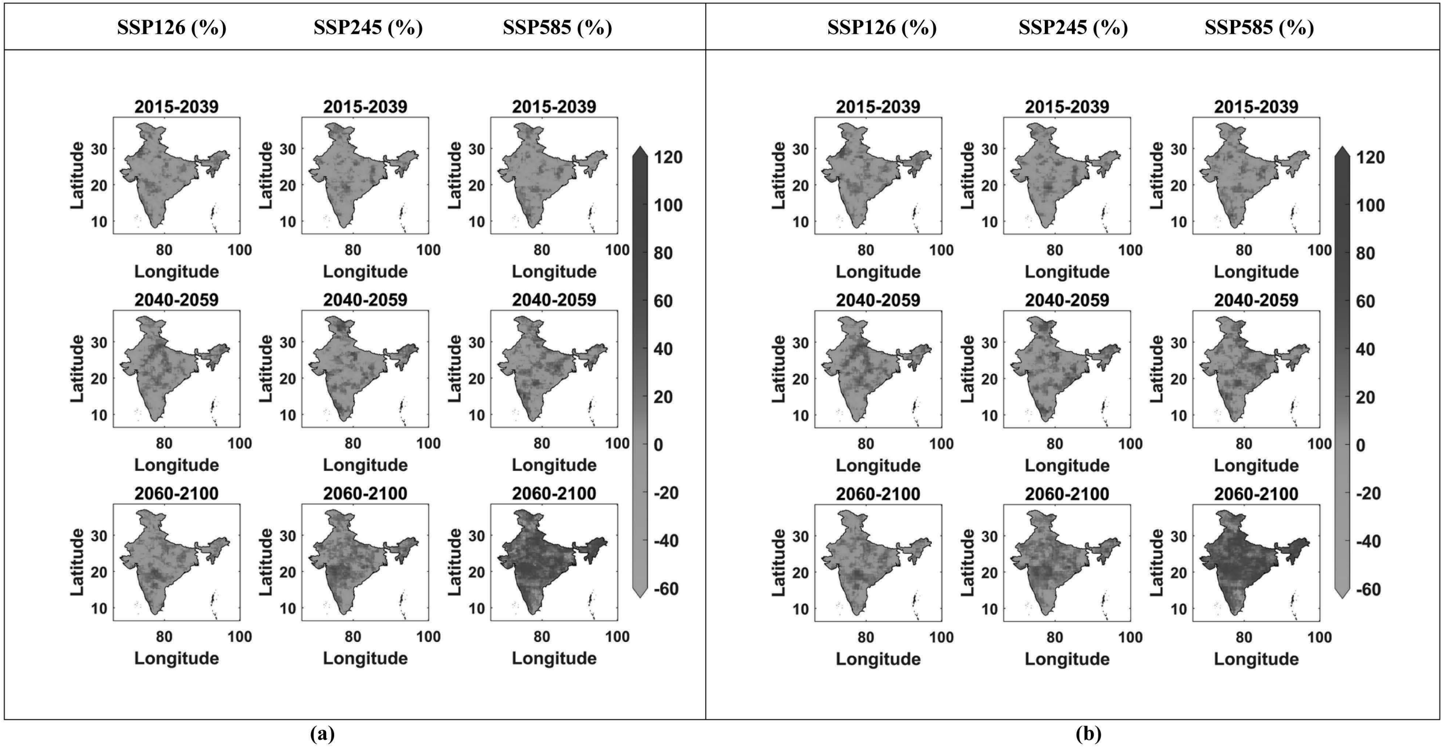

FIGURE 5.5 (**A**) Percentage change in precipitation intensity for a 1-hour duration and a 100-year return period between future periods (2015–2039, 2040–2059, 2060–2100) and the historical period (1979–2014) under three climate change scenarios. The precipitation data has been bias-corrected using the Indian Monsoon Data Assimilation and Analysis (IMDAA) as a reference. (b) The same analysis but with bias correction based on the Fifth Generation of the European Centre for Medium-Range Weather Forecasts (ECMWF) Reanalysis (ERA5) dataset.

Adapted from Maity and Maity (2022)

India. It is noteworthy, however, that the research also prognosticated a marginal uptick in precipitation intensity across geographical areas encompassing the desert terrain, the southern peninsula, and the expansive northern plains. The results underscore the imperative of accounting for climate-induced shifts in IDF curves when formulating water infrastructure strategies in India. As opposed to the other two scenarios, SSP126, which expects sustainable growth in the future, predicts a negligible rise. With these alterations, their study concluded that India would see a considerable rise in hourly precipitation intensity in the future if the pattern of rapid growth and unrestrained usage of fossil fuels continues. As a result of climate change, India's environmentally delicate Himalayan regions would face more frequent floods than the rest of the country. The most populous metro areas would also suffer severely as a result of an increase in the frequency of extremely intense precipitation in the near future.

To gain insights into the repercussions of climate variability on precipitation dynamics, Sarkar and Maity (2022) conducted a comprehensive evaluation of diverse facets of precipitation extremes, encompassing total precipitation, frequency, and intensity (refer to Figure 5.6). The analysis harnessed data derived from a composite ensemble mean, comprising data from 14 GCMs sourced from the CMIP6 initiative. The investigation zeroed in on two distinct temporal epochs: the near-future span, from 2021 to 2060, and the far-future period, from 2061 to 2100. Their study concluded that the changes in precipitation's intensity and frequency together determine how much precipitation occurs overall over a given extreme threshold. The frequency variations, however, are what contribute most. Indeed, the alterations in intensity play a discernible role. Over the time span since 1980, a substantial upswing in precipitation extremes, primarily driven by changes in frequency, has been evident across a substantial portion of the Indian subcontinent. Projections suggest that this trend is poised to persist in the ensuing decades, maintaining a comparable or potentially even more pronounced trajectory. Both historical and future periods have shown a notable and consistent intensification of both the frequency and intensity of precipitation extremes, leading to an overall increase in the total amount of severe precipitation, despite the infrequent occurrence of such extreme events. Moreover, the anticipated elevations in precipitation extremes during the near-future period exhibit a striking similarity under both the SSP245 and SSP585 scenarios. Nevertheless, in the far-future horizon, SSP585 surpasses SSP245, implying a plausible influence of anthropogenic actions on the observed augmentation in precipitation extremes. Notably, the last decade has witnessed a noteworthy shift within the realm of hydroclimatology research, with a growing emphasis on harnessing the substantial capabilities of artificial intelligence and machine learning methodologies for the modeling of hydrometeorological attributes (Elbeltagi et al., 2023a, 2023b, 2023c; Ibrahim et al., 2022; Khan et al., 2023; Kumar et al., 2023; Lee et al., 2020; Pande et al., 2022). These advancements have allowed researchers to gain a more comprehensive understanding of the alterations occurring in the hydrological cycle, not only in specific regions like India but also on a global scale (Huntingford et al., 2019; Kraft et al., 2022; Mosaffa et al., 2022; Yang et al., 2021).

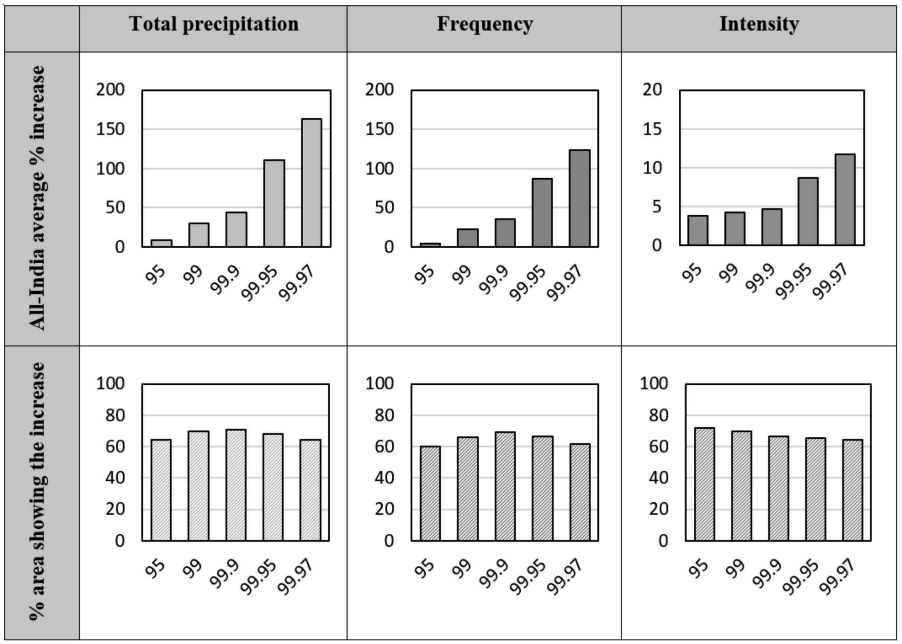

FIGURE 5.6 This diagram delineates the regionally averaged augmentation in overall precipitation, occurrence frequency, and intensity spanning the Indian mainland, with a comparative assessment of the post-1980 era relative to the pre-1980 period. The upper row provides a depiction of the magnitude of this augmentation, while the lower row illustrates the geographical scope of the observed increases. These transformations are subject to comprehensive scrutiny across all five percentiles.

Adapted from Sarkar and Maity (2022)

5.4 ADVANTAGES AND EFFICACY OF WATER-RELATED ADAPTATION STRATEGIES: GUIDING PRINCIPLES FOR ATTAINING SUSTAINABILITY AND CLIMATE RESILIENCE

There is a paucity of research on the efficiency of expected future adaptation in lowering climate hazards. Even yet, the results are not synthesized across different possibilities to provide a comprehensive evaluation of the success of the expected future adaptation. This section evaluates the advantages of present adaptation and the efficacy of anticipated future adaptation in lowering climate risks. Furthermore, it is imperative to highlight at this point that there is a conflicting opinion in the literature regarding how to evaluate how well present adaptation strategies are working to mitigate climate-related consequences. However, a number of approaches, such as feasibility analysis, have been used. Specifically, the IPCC (2022) has focused on examining the outcomes of water-related adaptation efforts across diverse facets, owing to the intricate challenges inherent in delineating and quantifying the efficacy of adaptation measures in mitigating climate-related risks. A comprehensive review was undertaken, encompassing a total of 359 referenced studies that offered compelling substantiation of validated adaptation outcomes, serving as the underpinning for this assessment. Positive results show the advantages of adaptation, whereas negative results might indicate that adaptation was ineffective or maladaptive. The findings have been evaluated and presented in the following subsections.

5.4.1 Present Responses to Water-Related Adaptation, Their Advantages, Synergistic Gains, and Maladaptation

There is a strong likelihood that the agriculture industry is responsible for a sizable portion of water-related adaptations. The livelihoods of populations in low-income countries are largely reliant on agriculture, which contributes to approximately 60–70% of total water withdrawals. The adoption of adaptation measures is primarily observed within the agricultural sector, with a majority of case studies stemming from Asia and Africa. While adaptation efforts in Europe and Australasia are predominantly focused on urban areas, agriculture remains the foremost sector for adaptation across all continents, with the exception of these regions (Schmied et al., 2021).

According to IPCC (2022), the foremost adaptation measures encompass enhancements in crop varieties, advancements in agronomic practices, the implementation of efficient irrigation and water management methodologies, and the adoption of strategies for conserving water and soil. The advantages stemming from these primary responses entail heightened agricultural incomes and yields, enhanced efficiency in water utilization, and their attendant outcomes. Nevertheless, it is crucial to note that these benefits are of an incremental nature, signifying their role in augmenting agricultural productivity and incomes, primarily in the short term. They may not, however, necessarily engender transformative gains or a commensurate reduction in the risks posed by climate change.

Although adaptation measures may yield short-term benefits, it is essential to acknowledge that not all such responses result in risk reduction, and certain adaptations may inadvertently lead to adverse long-term consequences. Maladaptation frequently results from inadequate planning and execution of adaptation actions and from failure to address the underlying reasons for vulnerability. A third of the 319 case studies by IPCC (2022) that examined adaptation response to having some positive effects also discussed the potential for maladaptation. Because migration can make migrants' innate vulnerabilities worse, it frequently has unintended consequences. Moreover, maladaptive consequences may result from adaptation strategies that prioritize increasing incomes through increased output, such as groundwater over-exploitation. Similarly, interventions aiming for carbon neutrality, such as forestry and agroforestry, may also engender maladaptive consequences for land and water resources, particularly when unsuitable species with elevated water demands are cultivated.

5.4.2 Projections Regarding the Future Efficacy of Adaptation Measures

In the present climatic conditions, numerous adaptation strategies have exhibited favorable impacts on outcomes of societal significance, and their continued relevance will be indispensable in accommodating future climate change. Considering IPCC (2022), some of them are discussed as follows:

- The predominant body of research concentrates on the consequences of temperature increases up to 1.5°C and lacks substantiation for scenarios involving more pronounced warming. These conclusions suggest that alterations in crop choices and agricultural systems may prove insufficient in effectively alleviating the envisaged climate-related hazards. In Africa, adaptation efforts at 1.5°C of warming are largely inadequate, carrying the potential for significant maladaptive outcomes. In Asia, effectiveness is primarily insufficient at both 1.5°C of warming, resulting in notable residual effects, and at 4°C of warming, leading to significant residual risks.
- Research assessing the efficacy of irrigation-related measures in forthcoming scenarios encompasses a range of strategies, including enhancements in irrigation efficiency, deficit irrigation practices, the expansion of irrigated zones, transitions from rain-fed to irrigated agriculture, and the adoption of specific irrigation methods. It becomes evident that there is a diminishing effectiveness observed across all geographical contexts as the temperature escalates from 1.5°C to more elevated levels, thereby amplifying the residual risk with sustained warming.
- Mulching, no-tilling, and contour farming are only a few of the water and soil management strategies that have been evaluated for future efficacy. Results highlight the necessity to carefully adapt particular options to a regional environment and the context-specific character of those options, with differences in options resulting in effective results or residual effects within individual studies and across locations and warming levels.
- The most effective agricultural adaptation outcomes are demonstrated by research evaluating combinations of the aforementioned agricultural adaptation alternatives, and these studies often predict moderate to high efficacy with the possibility of co-benefits. Even at greater degrees of warming, residual hazards are minimal, despite the existence of maladaptive effects.
- On a global scale, adaptations linked to agroforestry exhibit a degree of effectiveness ranging from moderate to notably high, particularly within the temperature range of 1.5°C to 2°C. Nonetheless, as temperatures advance to 3°C and 4°C, there is a discernible reduction in efficacy, accompanied by a notable increase in residual risk and unfavorable consequences.
- As global warming increases, the co-benefits of adaptation related to flood risk decrease. The constraints inherent in the appraised alternatives become conspicuous as temperatures reach 3°C and 4°C of warming, ushering in an escalation of lingering risks across the majority of scrutinized scenarios.

Context-specific strategies that are sufficiently flexible to adapt to the constantly shifting conditions on the ground will be necessary for the practice to address the growing climate risk. Although residual impacts are anticipated at this warming level across industries and geographies, adaptation typically works better around 1.5°C. The necessity for contextualized responses is further highlighted by the possibility of further growing maladaptation across industries, locations, and at different warming levels.

5.4.3 Foundational Principles Facilitating the Attainment of Water Security, Sustainable Development, and Climate Resilience Via Systemic Transformations

When considering the Sustainable Development Goals (SDGs), it is evident that water plays a central role in nearly all of them. Specifically, SDG6, which focuses on clean water and sanitation, as well as SDG11, which aims for sustainable communities and cities, explicitly addresses water-related issues. There exists a statistical correlation between SDG1, aimed at poverty eradication, and SDG6, as poverty reduction serves to augment adaptive capacity in accordance with the adaptation objectives delineated in the Paris Agreement. The accomplishment of SDG2, which targets the eradication of hunger, is contingent upon ensuring equitable access to water for agricultural purposes. SDG7, which underscores the importance of affordable and clean energy, relies upon water resources for hydropower generation. Additionally, the realization of SDG3, dedicated to promoting health and well-being, is intrinsically linked to access to fundamental infrastructure, including water and sanitation. The mitigation of water-related disasters assumes paramount importance for the achievement of SDG11. In summation, water assumes a pivotal and irreplaceable role in the pursuit of the SDGs, and its role in implementing the requisite systemic changes for fostering climate-resilient development (Fonseca et al., 2020; Iacobuţă et al., 2022; Srivastava & Chinnasamy, 2023). To this end, the following list of seven enabling concepts, as discussed by IPCC (2022), is essential for attaining water security and the SDGs and system transformations:

- *Appropriate Technologies*: Technology plays a significant role in the water adaptation response, and a variety of social elements, such as institutions, governance structures, and concerns of equality and justice, influence the effects of technology adoption.
- *Adequate and Appropriate Financing*: Funds for public and private adaptation go largely towards water. However, the present COVID-19-related reductions in adaptation funds may make it even more difficult for developing nations to make sufficient investments in water adaptation.
- *Gender, Equity, and Social Justice*: There is a strong likelihood that not all communities will experience the impacts of water insecurity driven by climate change. Women, children, people with disabilities, and Indigenous Peoples are particularly at risk because they have limited access to appropriate water, which varies by race, ethnicity, and caste. Since a changing climate most severely impacts the poorest people and nations in the world, equity and justice are thus essential to both sustainable development and adaptation to climate change.
- *Inclusion of Indigenous Knowledge (IK) and Local Knowledge (LK)*: IKLK possesses adaptability and has demonstrated its ability to evolve over time, employing culturally specific and location-based approaches in response to

climatic and environmental changes. To effectively address water security and other related areas, the collaboration between holders of ILK and technical knowledge through ethical co-production emerges as a crucial facilitating factor for the implementation of adaptation measures and strategies. This cooperative process acknowledges the importance of integrating the wisdom and expertise of ILK holders with scientific and technical knowledge, ensuring a holistic and inclusive approach to addressing challenges in various domains.

- *Participative, Cooperative, and Bottom-Up Engagement*: To uphold the legitimacy and inclusivity of the decision-making process and foster the development of adaptation measures characterized by social justice, it is imperative to actively incorporate and engage marginalized and disproportionately impacted demographics, including women and Indigenous Peoples, in participatory and grassroots decision-making processes. By integrating these communities, which exhibit heightened vulnerability to climate change repercussions, a more comprehensive and equitable approach can be realized. This approach ensures that their voices, requirements, and viewpoints are duly acknowledged and integrated into adaptation strategies.
- *Polycentric Water Governance*: Polycentric governance assumes a pivotal role in facilitating enhanced water management and the successful implementation of climate change adaptation measures. Nevertheless, to secure its effectiveness and prevent the exacerbation of prevailing disparities, it is imperative to encompass and meaningfully engage less influential stakeholders, including women, Indigenous Peoples, and young individuals, in the decision-making procedures. Their meaningful participation and representation are key to achieving more equitable outcomes in water management and climate adaptation initiatives. By including diverse perspectives and addressing power imbalances, polycentric governance can contribute to more inclusive and socially just outcomes, aligning with the principles of scientific rigor and promoting equitable and effective climate change adaptation.
- *Strong Political Support*: Insufficient institutional capacity poses a significant barrier to adaptation efforts in the water sector. Overcoming this obstacle, along with gaining strong political support, is crucial to achieving the goal of limiting global warming to 1.5°C. Inadequate institutional support can impede the implementation of effective water management strategies and hinder adaptation initiatives in response to climate change. Addressing this lack of institutional capacity is essential to enable successful adaptation measures in the water sector, ensuring scientific rigor in the pursuit of climate change mitigation and adaptation goals.

5.5 CONCLUSIONS

This study has contributed significant insights into the hydrological modifications resulting from climate change and their consequences for water resources. The investigation delves into the observed and anticipated shifts in precipitation, evapotranspiration, soil moisture, river floods, drought occurrences, and various hydrological indicators, consequently underscoring the susceptibility of the water sector to the ramifications of climate change. The findings have established a clear association between acute water scarcity and the impacts on water resources. These include a heightened frequency and intensity of heavy precipitation, accelerated glacier melt, alterations in the occurrence, magnitude, and timing of floods, increased incidence and severity of droughts in specific regions, and degradation of water quality due to extreme events. In a comprehensive assessment, it can be concluded that the cumulative outcomes of these anthropogenic activities have affected all major sectors—agriculture, energy and industry, water supply for health and sanitation, urban and municipal water provision, and freshwater ecosystems—by subjecting them to the influences of climate change and extreme weather events on water resources. The study thus emphasized the need for effective water-related adaptations to ensure water security and sustainable development. The seven enabling principles were identified in this study as a roadmap for policymakers and stakeholders to develop effective regional adaptation strategies. To summarize, the study has the following focused conclusions to make:

- Human-induced climate change has led to significant alterations in the global water cycle, resulting in shifts in precipitation patterns and increased variability in extreme weather events. The impacts of these changes are far-reaching, affecting millions of people living in areas with shifting precipitation extremes. Projections for changes in precipitation vary across regions, but models suggest that heavy precipitation events will become more frequent and severe. Without significant reductions in GHG emissions, the water cycle will continue to be significantly altered, and dry periods may increase in areas where they are already expected to rise. It is imperative to act to mitigate the effects of climate change and protect vulnerable populations and ecosystems.
- Recent studies have shown a significant increase in global ET, which can be attributed to human activities and natural factors. Changes in vegetation play a significant role in the increase in ET, with transpiration contributing to a large portion of the water exchange between land and the atmosphere. The CMIP6 ensemble predicts varying changes in ET across different regions under 4°C global warming, with some regions experiencing a decrease in ET. The projected ET changes are influenced by various factors, including soil moisture, weather, and plant physiological responses to increasing CO_2, and the impact of elevated CO_2 on ET is dependent on factors such as LAI and transpiration.
- The 'Wet Grow Wetter, Dry Get Drier' paradigm inadequately explains observed soil moisture trends, especially in arid regions, where changing precipitation-ET balance causes soil moisture declines. Human-induced climate change will amplify these trends. Monitoring and managing soil moisture is crucial for climate adaptation. CMIP6 models vary in projecting soil moisture changes due to global warming. Ignoring CO_2's direct

impact on plant transpiration leads to aridity overestimation. Projections suggest escalating global warming will intensify soil moisture changes, potentially reducing levels by up to 40% in specific regions under a 4°C global warming scenario.

- The analysis of precipitation patterns in India reveals significant changes due to climate change. The PMP has shown a notable increase, particularly after the 1970s, and is projected to rise further in the future. The IDF relationship of precipitation is also expected to change, with an increase in intensity, especially in the central parts of India. These changes indicate a rise in severe short-term precipitation and the likelihood of more frequent floods in environmentally vulnerable regions. The frequency of precipitation extremes has been predominantly increasing, with both intensity and frequency contributing to the overall increase. However, the anthropogenic influence on precipitation extremes is more pronounced in the far-future scenario.
- Human-induced climate change has had significant impacts on the occurrence and intensity of floods and droughts globally. Floods have become more frequent and severe in the tropics and northern mid-latitudes, while droughts continue to cause harm to society. Regional and national disparities influence the vulnerability and exposure to these events. However, global trends suggest that the economic susceptibility to droughts is declining. While the projected scenarios are subject to uncertainty and socioeconomic factors, adaptation measures are necessary to mitigate the adverse effects of floods and droughts. Urgent action is needed to address climate change and its impacts.
- Water-related adaptations are crucial to address the impact of climate change, especially in the agriculture sector. While short-term benefits can be achieved through these adaptations, it is important to ensure that they lead to transformational benefits in the long run and avoid unintended consequences and maladaptive outcomes. Achieving sustainable and resilient development requires enabling principles, such as adequate financing, gender equity, social justice, and strong political support. Equitable and just water governance and management are also crucial to ensuring that vulnerable populations are not left behind in the effort to achieve water security.

5.6 DECLARATION OF INTEREST

Acknowledgment: This work is partially supported by the Ministry of Earth Science, Government of India (Ref No: IIT/SRIC/R/SMT/2021/101) through sponsored projects. The authors further acknowledge the National Supercomputing Mission (NSM) for providing computing resources of 'PARAM Shakti' at IIT Kharagpur, which is implemented by C-DAC and supported by the Ministry of Electronics and Information Technology (MeitY) and Department of Science and Technology (DST), Government of India. Organizers of the International Conference on Interdisciplinary Approaches in Civil Engineering for Sustainable Development (IACESD-2023) are gratefully acknowledged where this work was presented.

Competing Interest: The authors declare that they have no known competing financial interests or personal relationships that could have appeared to influence the work reported in this study.

Funding: No funding was received for conducting this study.

Data availability: The datasets generated during the current study will be made available from the corresponding author upon reasonable request.

REFERENCES

Arnell, N. W., Brown, S., Gosling, S. N., Gottschalk, P., Hinkel, J., Huntingford, C., et al. (2016). The impacts of climate change across the globe: A multi-sectoral assessment. *Climatic Change*, 134, 457–474. https://doi.org/10.1007/s10584-014-1281-2

Berg, A., & Sheffield, J. (2019). Evapotranspiration partitioning in CMIP5 models: Uncertainties and future projections. *Journal of Climate*, 32(10), 2653–2671. https://doi.org/10.1175/JCLI-D-18-0583.1

Bosmans, J. H., van Beek, L. P., Sutanudjaja, E. H., & Bierkens, M. F. (2017). Hydrological impacts of global land cover change and human water use. *Hydrology and Earth System Sciences*, 21(11), 5603–5626. https://doi.org/10.5194/hess-21-5603-2017

Cheng, S., Huang, J., Ji, F., & Lin, L. (2017). Uncertainties of soil moisture in historical simulations and future projections. *Journal of Geophysical Research: Atmospheres*, 122(4), 2239–2253. https://doi.org/10.1002/2016JD025871

Chinnasamy, P., & Srivastava, A. (2021). Revival of traditional cascade tanks for achieving climate resilience in Drylands of South India. *Frontiers in Water*, 3, 639637. https://doi.org/10.3389/frwa.2021.639637

Cook, B. I., Mankin, J. S., Marvel, K., Williams, A. P., Smerdon, J. E., & Anchukaitis, K. J. (2020). Twenty-first century drought projections in the CMIP6 forcing scenarios. *Earth's Future*, 8(6), e2019EF001461. https://doi.org/10.1029/2019EF001461

Dhanuka, A., Srivastava, A., Khadke, L., & Kushwaha, N. L. (2023). Smart geometric design of highways using HTML programming for sustainable and climate resilient cities. In Chatterjee, U., Bandyopadhyay, N., Setiawati, M. D., & Sarkar, S. (eds) *Urban commons, future smart cities and sustainability*. Springer Geography, Cham. https://doi.org/10.1007/978-3-031-24767-5_39

Douville, H., Raghavan, K., Renwick, J., Allan, R. P., Arias, P. A., Barlow, M., et al., (2021). Water cycle changes. In Masson-Delmotte, V., Zhai, P., Pirani, A., Connors, S. L., Péan, C., Berger, S., Caud, N., Chen, Y., Goldfarb, L., Gomis, M. I., Huang, M., Leitzell, K., Lonnoy, E., Matthews, J. B. R., Maycock, T. K., Waterfield, T., Yelekçi, O., Yu, R., & Zhou, B. (eds) *Climate change 2021: The physical science basis. contribution of working group I to the sixth assessment report of the intergovernmental panel on climate change*. Cambridge University Press, Cambridge.

Dunn, R. J., Alexander, L. V., Donat, M. G., Zhang, X., Bador, M., Herold, N., et al. (2020). Development of an updated global land in Situ-Based data set of temperature and precipitation extremes: HadEX3. *Journal of Geophysical Research: Atmospheres*, 125(16), e2019JD032263. https://doi.org/10.1029/2019JD032263

Elbeltagi, A., Raza, A., Hu, Y., Al-Ansari, N., Kushwaha, N. L., et al. (2022). Data intelligence and hybrid metaheuristic algorithms-based estimation of reference evapotranspiration. *Applied Water Science*, 12(7), 152. https://doi.org/10.1007/s13201-022-01667-7

Elbeltagi, A., Srivastava, A., Al-Saeedi, A. H., Raza, A., Abd-Elaty, I., & El-Rawy, M. (2023b). Forecasting long-series daily reference evapotranspiration based on best subset regression and machine learning in Egypt. *Water*, 15(6), 1149. https://doi.org/10.3390/w15061149

Elbeltagi, A., Srivastava, A., Deng, J., Li, Z., Raza, A., Khadke, L., Yu, Z., & El-Rawy, M. (2023c). Forecasting vapor pressure deficit for agricultural water management using machine learning in semi-arid environments. *Agricultural Water Management*, 283, 108302. https://doi.org/10.1016/j.agwat.2023.108302

Elbeltagi, A., Srivastava, A., Kushwaha, N. L., Juhász, C., Tamás, J., & Nagy, A. (2023a). Meteorological data fusion approach for modeling crop water productivity based on ensemble machine learning. *Water*, 15(1), 30. https://doi.org/10.3390/w15010030

Feng, H., & Zhang, M. (2015). Global land moisture trends: Drier in dry and wetter in wet over land. *Scientific Reports*, 5(1), 1–6. https://doi.org/10.1038/srep18018

Flörke, M., Schneider, C., & McDonald, R. I. (2018). Water competition between cities and agriculture driven by climate change and urban growth. *Nature Sustainability*, 1(1), 51–58. https://doi.org/10.1038/s41893-017-0006-8

Fonseca, L. M., Domingues, J. P., & Dima, A. M. (2020). Mapping the sustainable development goals relationships. *Sustainability*, 12(8), 3359. https://doi.org/10.3390/su12083359

Ganguly, D., Rasch, P. J., Wang, H., & Yoon, J. H. (2012). Fast and slow responses of the South Asian monsoon system to anthropogenic aerosols. *Geophysical Research Letters*, 39(18). https://doi.org/10.1029/2012GL053043

Grillakis, M. G. (2019). Increase in severe and extreme soil moisture droughts for Europe under climate change. *Science of the Total Environment*, 660, 1245–1255. https://doi.org/10.1016/j.scitotenv.2019.01.001

Huntingford, C., Jeffers, E. S., Bonsall, M. B., Christensen, H. M., Lees, T., & Yang, H. (2019). Machine learning and artificial intelligence to aid climate change research and preparedness. *Environmental Research Letters*, 14(12), 124007. https://doi.org/10.1088/1748-9326/ab4e55

Iacobuţă, G. I., Brandi, C., Dzebo, A., & Duron, S. D. E. (2022). Aligning climate and sustainable development finance through an SDG lens. The role of development assistance in implementing the Paris agreement. *Global Environmental Change*, 74, 102509. https://doi.org/10.1016/j.gloenvcha.2022.102509

Ibrahim, K. S. M. H., Huang, Y. F., Ahmed, A. N., Koo, C. H., & El-Shafie, A. (2022). A review of the hybrid artificial intelligence and optimization modelling of hydrological streamflow forecasting. *Alexandria Engineering Journal*, 61(1), 279–303. https://doi.org/10.1016/j.aej.2021.04.100

IPCC. (2022). Contribution of working group II to the sixth assessment report of the intergovernmental panel on climate change. In Pörtner, H.-O., Roberts, D. C., Tignor, M., Poloczanska, E. S., Mintenbeck, K., Alegría, A., Craig, M., Langsdorf, S., Löschke, S., Möller, V., Okem, A., & Rama, B. (eds). *Climate change 2022: Impacts, adaptation, and vulnerability* (p 3056). Cambridge University Press, Cambridge and New York. https://doi.org/10.1017/9781009325844

Khan, M. I., Sarkar, S., & Maity, R. (2023). Artificial intelligence/machine learning techniques in hydroclimatology: A demonstration of deep learning for future assessment of stream flow under climate change. In *Visualization techniques for climate change with machine learning and artificial intelligence* (pp. 247–273). Elsevier. https://doi.org/10.1016/B978-0-323-99714-0.00015-7

Koutroulis, A. G., Papadimitriou, L. V., Grillakis, M. G., Tsanis, I. K., Warren, R., & Betts, R. A. (2019). Global water availability under high-end climate change: A vulnerability based assessment. *Global and Planetary Change*, 175, 52–63. https://doi.org/10.1016/j.gloplacha.2019.01.013

Kraft, B., Jung, M., Körner, M., Koirala, S., & Reichstein, M. (2022). Towards hybrid modeling of the global hydrological cycle. *Hydrology and Earth System Sciences*, 26(6), 1579–1614. https://doi.org/10.5194/hess-26-1579-2022

Kumar, S., Srivastava, A., & Maity, R. (2023). Modeling climate change impacts on vector-borne disease using machine learning models: Case study of visceral leishmaniasis (Kala-azar) from Indian State of Bihar. *Expert Systems with Applications*, 121490. https://doi.org/10.1016/j.eswa.2023.121490

Lee, T., Shin, J. Y., Kim, J. S., & Singh, V. P. (2020). Stochastic simulation on reproducing long-term memory of hydroclimatological variables using deep learning model. *Journal of Hydrology*, 582, 124540. https://doi.org/10.1016/j.jhydrol.2019.124540

Lemordant, L., & Gentine, P. (2019). Vegetation response to rising CO_2 impacts extreme temperatures. *Geophysical Research Letters*, 46(3), 1383–1392. https://doi.org/10.1029/2018GL080238

Maity, S. S., & Maity, R. (2022). Changing pattern of intensity—duration—frequency relationship of precipitation due to climate change. *Water Resources Management*, 36(14), 5371–5399. https://doi.org/10.1007/s11269-022-03313-y

Mosaffa, H., Sadeghi, M., Mallakpour, I., Jahromi, M. N., & Pourghasemi, H. R. (2022). Application of machine learning algorithms in hydrology. In *Computers in earth and environmental sciences* (pp. 585–591). Elsevier. https://doi.org/10.1016/B978-0-323-89861-4.00027-0

Müller Schmied, H., Cáceres, D., Eisner, S., Flörke, M., Herbert, C., Niemann, C., . . . & Döll, P. (2021). The global water resources and use model WaterGAP v2. 2d: Model description and evaluation. *Geoscientific Model Development*, 14(2), 1037–1079. https://doi.org/10.5194/gmd-14-1037-2021

Pande, C. B., Al-Ansari, N., Kushwaha, N. L., Srivastava, A., Noor, R., Kumar, M., et al. (2022). Forecasting of SPI and meteorological drought based on the artificial neural network and M5P model tree. *Land*, 11(11), 2040. https://doi.org/10.3390/land11112040

Rane, N. L., Achari, A., Choudhary, S. P., Mallick, S. K., Pande, C. B., et al. (2023). A decision framework for potential dam site selection using GIS, MIF and TOPSIS in Ulhas River Basin, India. *Journal of Cleaner Production*, 138890. https://doi.org/10.1016/j.jclepro.2023.138890

Sarkar, S., & Maity, R. (2020). Increase in probable maximum precipitation in a changing climate over India. *Journal of Hydrology*, 585, 124806. https://doi.org/10.1016/j.jhydrol.2020.124806

Sarkar, S., & Maity, R. (2022). Future characteristics of extreme precipitation indicate the dominance of frequency over intensity: A multi-model assessment from CMIP6 across India. *Journal of Geophysical Research: Atmospheres*, 127(16), e2021JD035539. https://doi.org/10.1029/2021JD035539

Shumilova, O., Tockner, K., Thieme, M., Koska, A., & Zarfl, C. (2018). Global water transfer megaprojects: A potential solution for the water-food-energy nexus? *Frontiers in Environmental Science*, 6, 150. https://doi.org/10.3389/fenvs.2018.00150

Srivastava, A., & Chinnasamy, P. (2023). Watershed development interventions for rural water safety, security, and sustainability in semi-arid region of Western-India. *Environment Development and Sustainability*. https://doi.org/10.1007/s10668-023-03387-7

Srivastava, A., Jain, S., Maity, R., & Desai, V. R. (2022b). Demystifying artificial intelligence amidst sustainable agricultural water management. In Zakwan, M., Wahid, A., Niazkar, M., & Chatterjee, U. (eds) *Water resource modeling and computational technologies*. Current Directions in Water Scarcity Book Series, vol. 7 (pp. 17–35). Elsevier. https://doi.org/10.1016/B978-0-323-91910-4.00002-9

Srivastava, A., Maity, R., & Desai, V. R. (2022a). Assessing global-scale synergy between adaptation, mitigation, and sustainable development for projected climate change. In Chatterjee, U., Akanwa, A. O., Kumar, S., Singh, S. K., & Dutta Roy, A. (eds) *Ecological* *footprints of climate change*. Springer Climate, Cham. https://doi.org/10.1007/978-3-031-15501-7_2

Tanoue, M., Hirabayashi, Y., & Ikeuchi, H. (2016). Global-scale river flood vulnerability in the last 50 years. *Scientific Reports*, 6(1), 36021. https://doi.org/10.1038/srep36021

Tellman, B., Sullivan, J. A., Kuhn, C., Kettner, A. J., Doyle, C. S., Brakenridge, G. R., et al. (2021). Satellite imaging reveals increased proportion of population exposed to floods. *Nature*, 596(7870), 80–86. https://doi.org/10.1038/s41586-021-03695-w

WMO. (2021). *Atlas of mortality and economic losses from weather, climate and water extremes (1970–2019).* WMO, Geneva, Switzerland.

Yang, D., Yang, Y., & Xia, J. (2021). Hydrological cycle and water resources in a changing world: A review. *Geography and Sustainability*, 2(2), 115–122. https://doi.org/10.1016/j.geosus.2021.05.003

Zeng, Z., Piao, S., Li, L. Z., Zhou, L., Ciais, P., Wang, T., et al. (2017). Climate mitigation from vegetation biophysical feedbacks during the past three decades. *Nature Climate Change*, 7(6), 432–436. https://doi.org/10.1038/nclimate3299

6 Sustainable Water Management and Climate-Smart Agriculture for Livelihood and Food Security in India

Manoj P Samuel and U Surendran

6.1 INTRODUCTION

Indian agriculture is swiftly shifting towards sustainability from yield-focused approaches. Climate change threatens productivity, altering practices and water availability. Tech solutions like artificial intelligence (AI), the Internet of Things (IoT), and robotics offer hope for managing constraints, boosting production, and countering climate effects. With population growth, doubling food output faces challenges from land scarcity (Chand 2022). Advanced tech can enhance practices, curb climate impact, optimize resources, and foster sustainable agriculture.

6.2 GAP IN KNOWLEDGE

Our country seeks eco-friendly, sustainable agriculture through advanced tech and resource optimization. The growing information and communications technology (ICT) sector and socio-economic shifts offer precision agriculture opportunities, reducing global disparities. There is a need to integrate nutrient balance, eco-hydrology, climate forecasts, and crop simulation for holistic impact.

6.3 TECHNOLOGY-DRIVEN SMART MANAGEMENT OF AGRICULTURE

Modern farming tech, including AI, analytics, sensors, and IT platforms, boosts yields, water efficiency, and sustainability. Global internet access and mobile use revolutionize communication, aiding service delivery. Successful agricultural connectivity could add $500 billion to the global gross domestic product (GDP) by

DOI: 10.1201/9781032686899-8

2030. Advanced tools transform agriculture worldwide, simplifying processes and enhancing product quality and value. Technology aids smallholder farming in India, addressing traditional challenges. Integration of sensors, global positioning systems (GPS), and data assists rural farmers in production strategies, finance, and market insights. ICT offers vital crop information, weather alerts, and water resource details, enhancing productivity and resilience.

ICT in modern agriculture transforms developed countries farming with IoT, machine learning (ML), cloud computing, and Big Data (Figure 6.1). The United States and Europe employ remote sensing, drones, and data gathering for precision farming. Projects like FATIMA (FArming Tools for external nutrient Inputs and water MAnagement), an EU-funded project under Horizon 2020, involved nine countries. Landsat-8 and Sentinel-2 satellite data tracked traditional crop plots. Over three years, harvest data enhanced crop water forecasts and yield insights (Stamatiadis et al., 2018), and the OpenET platform in the western USA offers satellite-based evapotranspiration (ET) estimates for enhanced water management. Users access ET data

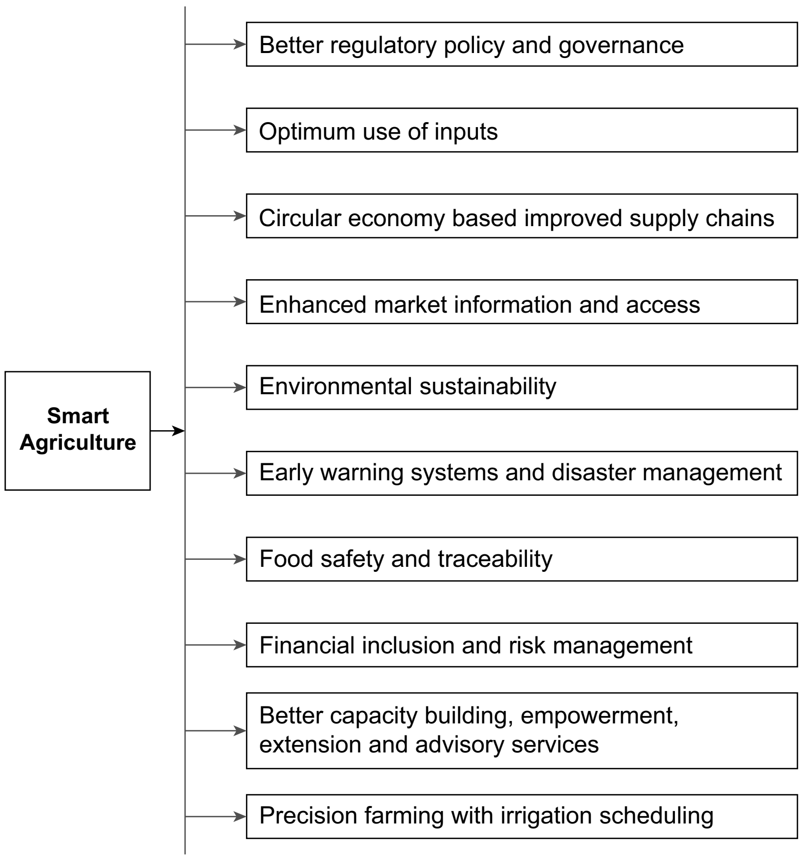

FIGURE 6.1 Facets of smart agriculture.

at field scale on openetdata.org, even at quarter-acre resolution (Melton et al., 2021). They utilize satellite data for water management and crop yield forecasting. User-friendly tools, like DSS and mobile apps, Web-based tool, URL, and GUI, aid farmers in optimizing practices and resources. IoT monitors soil, plant, and supply chain health, while AI-powered agrobots herald self-managed precision farming's future.

6.4 INDIA'S WATER WOES AND OPPORTUNITIES

India's total water resources are 1123 billion cubic meters (BCM), while demand may reach 1200 BCM by 2050, straining supply (Gupta and Deshpande 2004). Agriculture, using 90% of water, faces declining groundwater and inefficient irrigation. Canal network efficiency is 35–50% (Madhok, 2020) with potential for improvement. Rainwater harvesting helps marginally, but demand outpaces supply growth. Enhancing water use efficiency and adopting modern tools are crucial to combat scarcity and sustain ecosystems (Drechsel et al., 2015). Agricultural water productivity is the benefit-to-water ratio in farming. Enhancing it involves minimizing losses during water distribution and application. Adoption of modern tools for optimized water scheduling is vital for improvement (Molden and Oweis, 2007).

6.5 MANAGING LAND AND WATER: NOVEL APPROACHES

Sustaining agriculture relies on conserving vital resources like land and water. Climate change disrupts water availability, requiring efficient management. Low crop productivity due to factors such aslimited irrigation, poor soils, and high costs challenges farmers. Government intervention with modern tools is essential. Water management, especially efficiency enhancement, is critical for sustainable production. New practices, micro-irrigation, and technology adoption are vital. Community-based approaches and innovative technologies can improve yields, quality, and reduce environmental impact. Micro-irrigation eases rainfed areas' reliance on groundwater, boosting yield and reducing greenhouse gas emissions.

6.6 CASE STUDY I: PRECISION AGRICULTURE DEMONSTRATION PLOTS ESTABLISHED UNDER THE DST-FUNDED PROJECT IN KERALA

Precision agriculture for managing water and nutrients in a precise way was carried out in Kerala as a farmer participatory approach in a Department of Science and Technology (DST)-funded project as demonstrations (Figure 6.2). Plots were assessed for soil, water, and power, with drip fertigation systems installed accordingly. The Food and Agriculture Organization (FAO)'s CROPWAT estimated crop water needs, receiving 100% irrigation. Fertigation matched soil and crop test values. The HYDRUS model guided irrigation scheduling, with soil wetting pattern data (Figure 6.3) showcasing effectiveness. Advanced tools for precise water and nutrient application boosted crop yield in demonstrations. Yield increase ranged from 13% to 124% over control. Drip fertigation'sbenefit-cost ratio ranged from 2.05 to 3.50 for chosen crops.

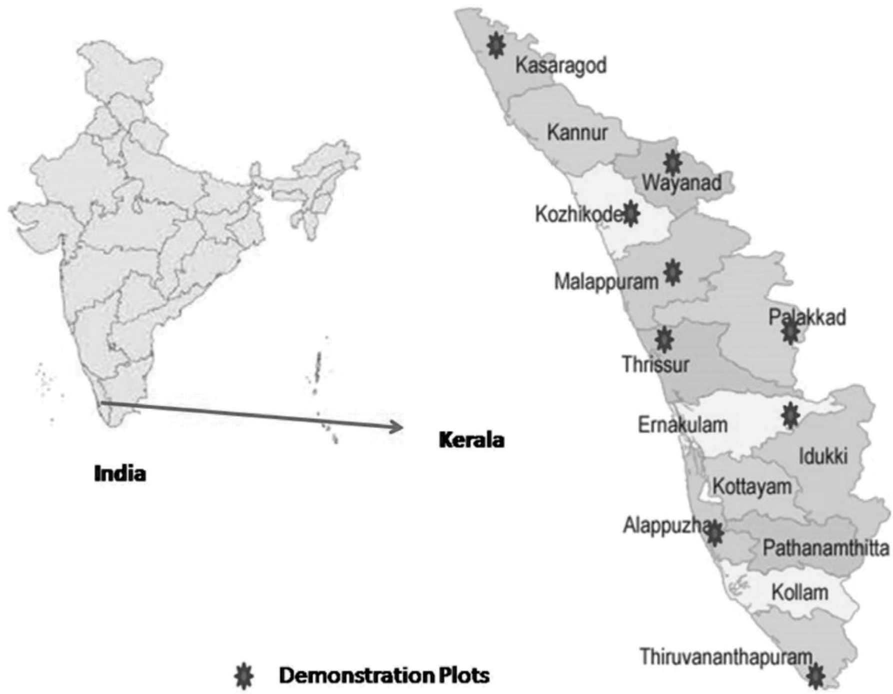

FIGURE 6.2 Selected demonstration plots in Kerala.

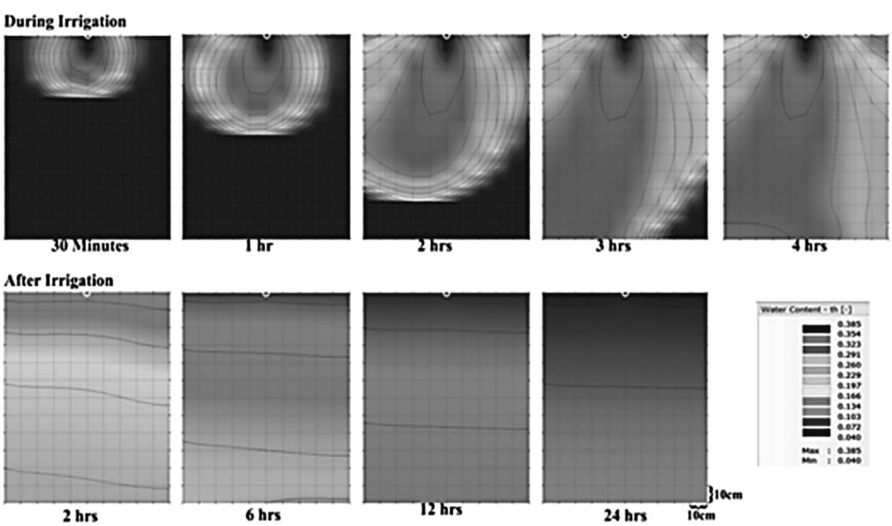

FIGURE 6.3 Simulated soil wetting pattern for coconut plot at Thiruvananthapuram.

6.7 CASE STUDY II: DROUGHT MANAGEMENT USING RS, GIS, AND MODELLING TECHNIQUES AS A TOOL TO SUSTAIN THE CROP PRODUCTIVITY AND WATER MANAGEMENT

Satellite data aids drought management by offering real-time insights using indices like Normalized Difference Vegetation Index (NDVI), Water Stress Index (WSI),

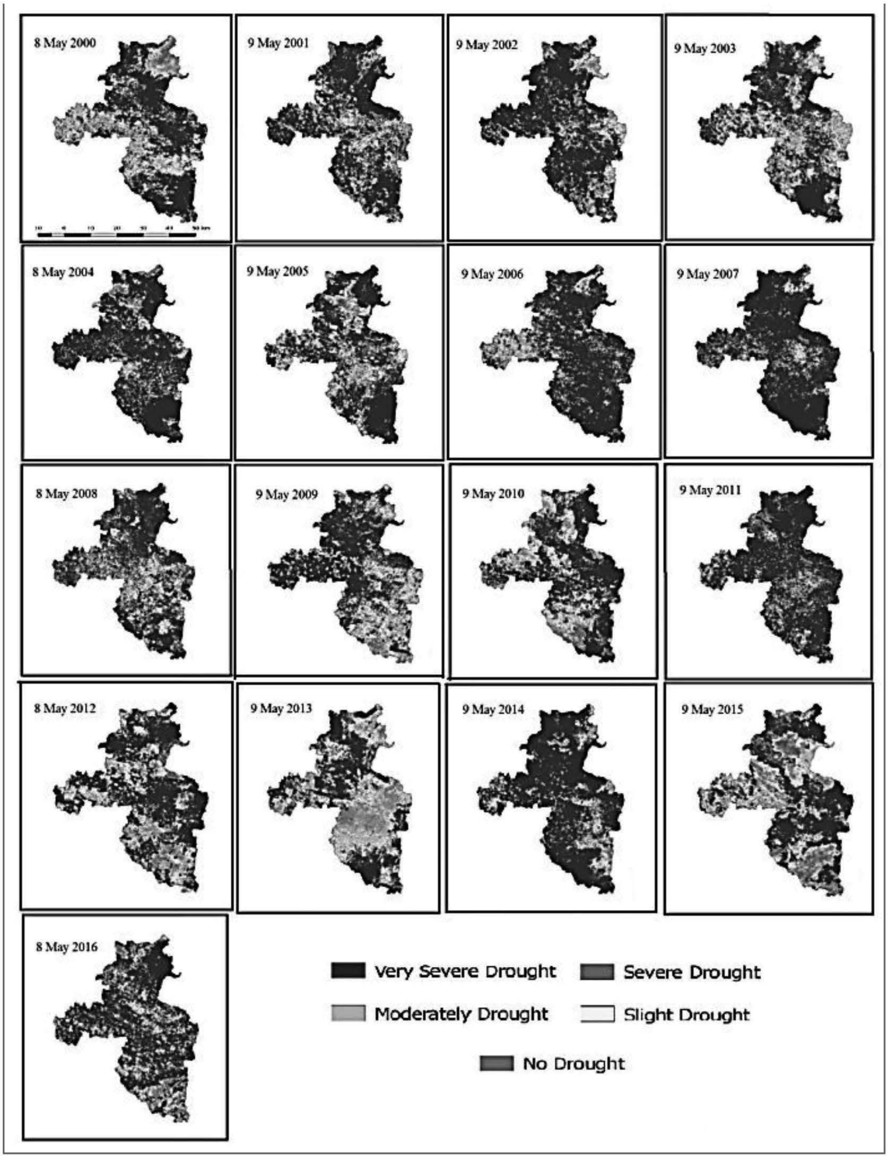

FIGURE 6.4 Anomaly/drought map of Palakkad district for the biweek of 9th May over the period 2000–2016.

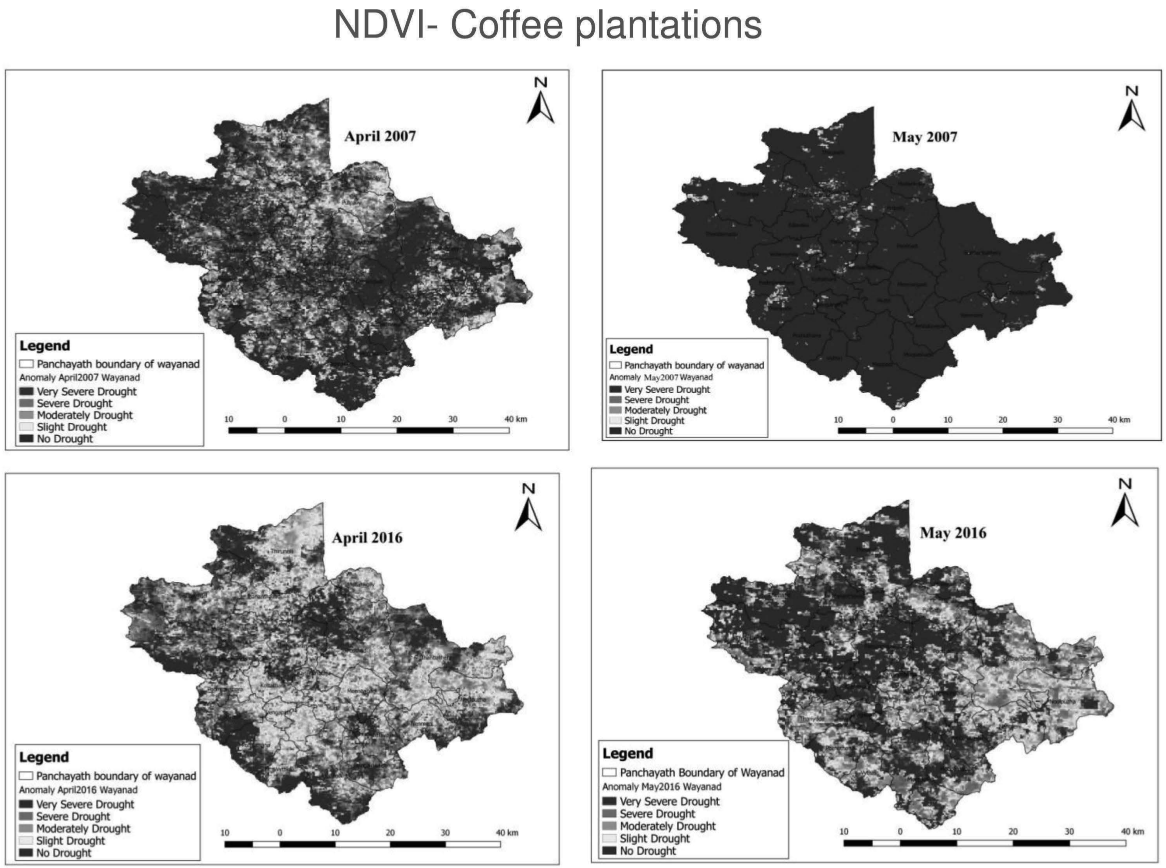

FIGURE 6.5 Spatial representation of NDVI anomaly for Wayanad district.

Temperature Condition Index (TCI), and Vegetation Condition Index (VCI). The NDVI is widely used for vegetation health and drought analysis. Kerala's rainfed farming (80% of land) necessitates drought understanding for effective water management and sustained crop production. An anomaly/drought map (Figure 6.4) of the Palakkad district for the biweek of 9th May over the period of 2000 to 2016 shows severe drought years aligning with actual drought declarations (2000, 2009, 2013, 2016).

In Kerala, NDVI analysis revealed differing climatic scenarios due to strong El Niño (2015–2016) and weak El Niño (2006–2007) conditions. Figure 6.5 shows distinct vegetation index images for these periods, impacting NDVI anomaly and drought predictions. The image showed that in April and May 2007, the vegetation index is much better when compared to 2016 images, and this has a direct impact on the NDVI anomaly or drought prediction map. The Wayanad district exhibited higher drought patches, influencing coffee yield (Figure 6.5). Yield data have confirmed that Arabica coffee declines in strong El Niño years, while Robusta fared better (Figure 6.6), suggesting Robusta's suitability in Wayanad due to climate variations (Jayakumar et al., 2016). Climate adaptation strategies are crucial for sustaining Arabica coffee production.

Figure 6.7 shows the drought risk map of Kozhikode, which will give an understanding for effective water management.

6.8 CONCLUSION

Comprehensive drought risk mapping aids stakeholders, policymakers, and planners in real-time monitoring and severity assessment. It informs effective strategies like

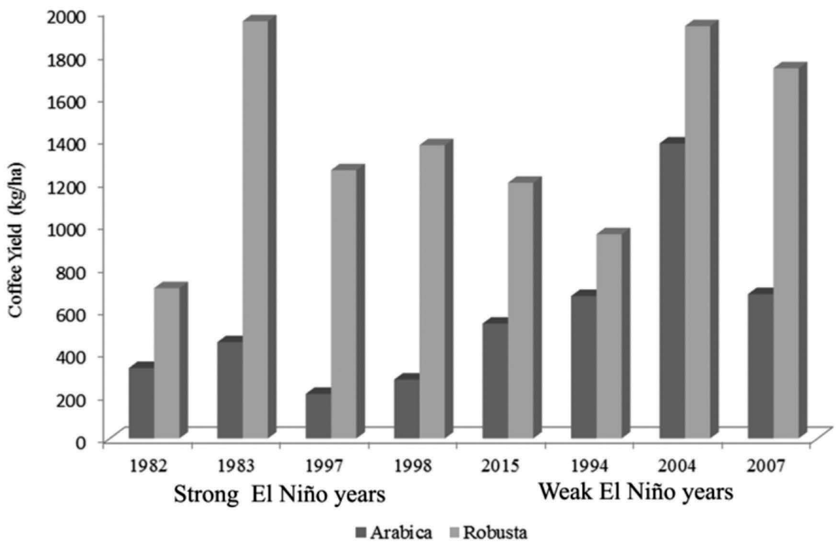

FIGURE 6.6 Impact of El Niño on Arabica and Robusta yield of coffee in Kerala.

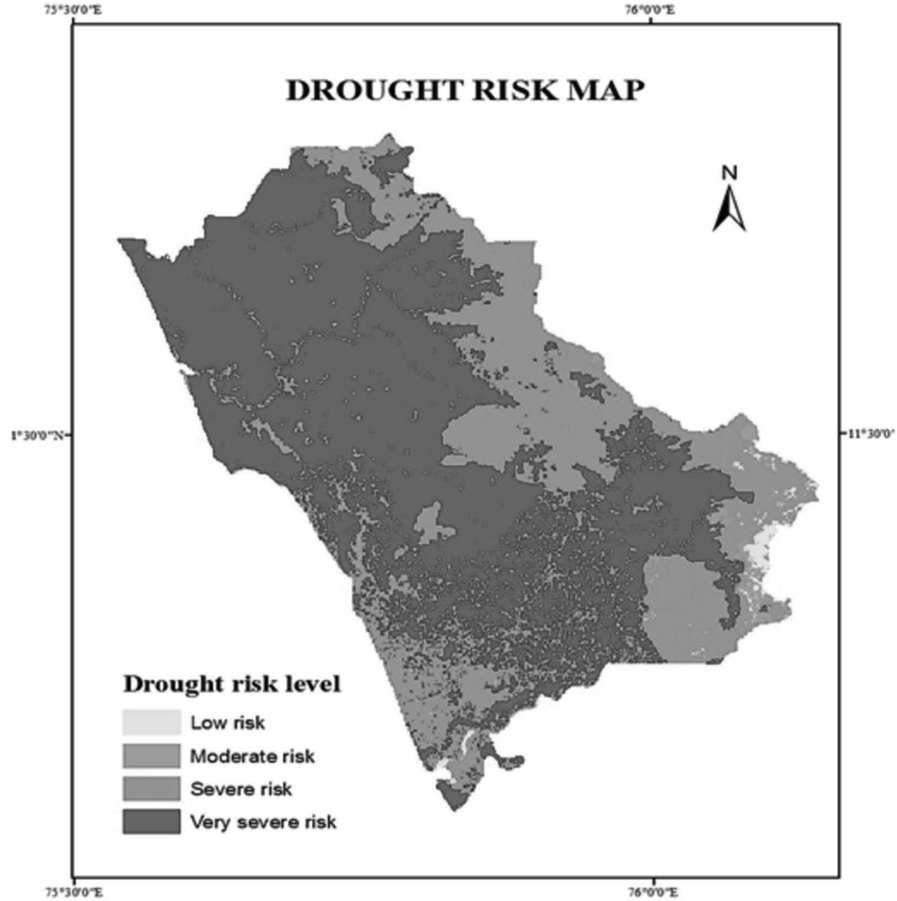

FIGURE 6.7 Drought risk map of Kozhikode.

potash/kaolin spray, mulching, conservation, and irrigation methods for sustained crop production and water supply in vulnerable regions. Policymakers can identify and support drought-prone areas, empowering local bodies to aid rural farmers and agriculture.

REFERENCES

Chand, R. (2022). *Agricultural challenges and policies for the 21st century.* NABARD Research and Policy Series (No. 6). Department of Economic Analysis and Research. National Bank for Agriculture and Rural Development (NABARD), Mumbai.

Drechsel, P., Heffer, P., Magen, H., Mikkelsen, R., & Wichelns, D. (2015). Managing water and fertilizer for sustainable agricultural intensification (No. 613–2016–40784). International Fertilizer Industry Association (IFA), International Water Management Institute (IWMI), International Plant Nutrition Institute (IPNI), & International Potash Institute (IPI).

Goedde, L., Katz, J., Menard, A., & Revellat, J. (2020). *Agriculture's connected future: How technology can yield new growth*. McKinsey Center for Advanced Connectivity and Agriculture Practice, McKinsey Global Publishing. https://cordis.europa.eu/project/id/633945

Gupta, S. K., & Deshpande, R. D. (2004). Water for India in 2050: First-order assessment of available options. *Current Science*, 1216–1224.

Jayakumar, M., Rajavel, M., & Surendran, U. (2016). Climate based statistical regression models for crop yield forecasting of coffee in humid tropical Kerala, India. *International Journal of Biometeorology*, 60, 1943–1952.

Madhok, A. K. (2020). Enhancing water use efficiency. *Roorkee Water Conclave 2020*. Indian Institute of Technology Roorkee and National Institute of Hydrology, Roorkee During February 26–28.

Melton, F. S., Huntington, J., Grimm, R., Herring, J., Hall, M., Rollison, D., Erickson, T., et al. (2021). OpenET: Filling a critical datagap in water management for the Western United States. *Journal of the American Water Resources Association*, 1–24. https://doi.org/10.1111/1752-1688.12956

Molden, D. J., & Oweis, T. (2007). Pathways for increasing agricultural water productivity. In Molden, D. (ed.). *Water for food, water for life. Comprehensive assessment of water management in agriculture*. Earthscan, London and International Water Management Institute, Colombo.

Stamatiadis, S., Schepers, J. S., Evangelou, E., Tsadilas, C., Glampedakis, A., Glampedakis, M., Eskridge, K. (2018). Variable-rate nitrogen fertilization of winter wheat under high spatial resolution. *Precision Agriculture*, 19(3), 570–587. doi:10.1007/s11119-017-9540-7

7 Greenhouse Gas Emissions and Life-Cycle Assessment of Biocomposites from Agro-Residues for Sustainable Infrastructure Development and Climate Change Mitigation

Gaurav Jagtap, Kusum Saini, Vasant Matsagar, Sagnik Dey and Venkatesh Kodur

7.1 INTRODUCTION

India is one of the most populated countries, and according to world population prospects, the population is going to increase further, as per statistics. This will lead to a continuous increase in food demand, agricultural activities, and, consequently, mismanagement of agricultural residues (agro-residues). Wheat and rice crops contribute about 63% of the total agro-residues generated in India, and 69% of the total agro-residues burned is associated with the wheat and rice crop systems (Ravindra et al., 2019). Approximately 3.15 million hectares area of Punjab are under rice cultivation, accounting for 85% of the total cropped area during the kharif season. Punjab contributes about 22.6% of the central pool of rice and produces 10% of the total rice of India (ESO, 2021). Rice straw has a high silica content, making it unsuitable for use as animal fodder, unlike wheat straw, which is largely used for animal feed (Lohan et al., 2018). There are several challenges associated with straw management faced by farmers, i.e., the effective utilization of rice straw residues to clear the field for sowing the next rabi crops and small land holdings for machinery, costly rice straw

DOI: 10.1201/9781032686899-9

management, and an insufficient supply of equipment hiring services. Moreover, the lack of technical knowledge, low demand for ex-situ applications of straw, involvement of lack of private firms, and unattractive economic returns (Bhattacharyya et al., 2021). Therefore, farmers tend to burn the straw residues to clear the field, which results in greenhouse gas (GHG) emissions and air pollution. Every year, stubble burning has become a regular practice in Punjab and Haryana, which causes air pollution (~42 ± 17%) in nearby states of India, especially in the Delhi area, throughout the winter and autumn (Bikkina et al., 2019). Additionally, emitted fine particulate matter (PM2.5) causes major negative effects on human health (Balakrishnan et al., 2019). A total of approximately 44,000–98,000 premature deaths due to PM2.5 exposure were reported annually caused by the burning of agricultural residues, where Punjab, Haryana, and Uttar Pradesh contributed 67–90% of the total (Lan et al., 2022).

Satellite remote sensing is one of the techniques used worldwide for monitoring forest fires, residue burning events, mapping the area burned, and quantifying the residue burned with the emerging space-based imaging technology, processing capacity, and data analytics approaches (Korontzi et al., 2006). The satellite remote sensing data from CREAMS (2020) reported 79,093 fire events that took place in Punjab after the paddy (rice) harvest during the period of October to November 2020. The most burning events occur within 20–25 days from mid-October to mid-November, which reflects the main reason for stubble burning, i.e., the minimal duration available for clearing fields to sow rabi crops. According to Maraseni and Qu (2016), the Indian agriculture sector generates 658,823 Gg CO_2eq. emissions, which is 12.2% of total global GHG emissions from the agricultural sector. As per MoEFCC (2021), the contribution of the Indian agricultural sector to the total GHG emissions of India is 14%, where stubble burning is accountable for 2.2% of emissions.

Severe impacts of stubble burning show a need to develop an alternative to use agro-residues instead of burning and assess its impacts on the environment. Raza et al. (2019) suggested spreading awareness about the adverse impacts of agro-residues burning and providing training to farmers about sustainable agro-residues management practices. The use of agro-residues for biocomposites could be an alternative to stubble burning and can reduce air pollution, relative health problems, and GHG emissions, as illustrated in Figure 7.1. Moreover, the use of these biocomposites can also contribute to reducing GHG emissions in the construction industry due to synthetic materials and promote sustainable infrastructure development.

The rice straw consists of 39–45% cellulose, 19–30% hemicellulose, 5–28% lignin, and 8–17% ashes. The provided ratio of constituents may vary according to crop variety, cultivation method, fertilizers, climate, and environmental conditions (Sharma et al., 2019; Singh and Arya, 2021). Cellulose is a long linear chain of polymer, hemicellulose is a smaller cross-linked polymer, and lignin is a polymeric aromatic structure. A complex 3D structure is formed by all these polymers combined called lignocellulose (Ralph et al., 2004). High silica content, ash content, and wax layer on the surface of rice straw results in a weak bond between the straw and resin and reduces the strength of biocomposites (Li et al., 2010; Zhang and Hu, 2014). An improvement in the adhesive properties of rice straw–based fiberboards is reported due to the removal of ash and wax using mechanical, chemical, physical, or biological pretreatments (Basta et al., 2014). Dong et al. (2019) reported the enhancement in thermal properties and stability of biocomposites due to wheat straw. In addition, enhancement in the dynamic strength of structure with sisal fiber–based biocomposites was observed (Saini and Matsagar, 2023). Thus, natural fibers can be used in various forms, i.e., biocomposites and reinforcement for construction, with some improvement in the properties of natural fibers (Daba et al., 2023).

However, the processing and management of agro-residues are some of the major challenges, which require a large number of heavy vehicles for logistics, storage facilities, and skilled labor (Kurinji and Kumar, 2021). The estimation made in the study showed that transportation of rice straw bales over a 5–15 km distance from a farm to the straw storage center generally costs 1,150–1,350 INR (14–16 US$) per ton of straw. Out of the total cost incurred to deliver straw from the field to the straw bank, approximately 55% is associated with cutting and baling (Kurinji and Kumar, 2021). A similar study by Nguyen et al. (2016) estimated straw collection cost as 1,000–1,500 INR (12–18 US$) per ton of straw and corresponding GHG emissions as 60–165 kg CO_2eq. per ton of straw collected.

As per a study performed by Krasny et al. (2017), a straw bale house has the advantages of half of the energy consumption, smaller peak heating load, negative global warming potential (GWP), and lower cost of construction as compared to conventional concrete houses. Singh and Arya (2021) also showed the environmental and financial advantages of cleaner technologies, such as straw conversion into biohydrogen, biomethane, bio-oil production, biochar, etc.

A life-cycle assessment (LCA) study (Soam et al., 2017) reported 1,213 kg CO_2eq. GHG emissions in the decomposition of straw into the field as fertilizer, 185 kg CO_2eq. in the processing of 1 ton straw to animal fodder, 1,471 kg CO_2eq. in power consumption, and 1,023 kg CO_2eq. in biogas. A net reduction in GWP of 1,343 kg CO_2eq./ton, 1,220 kg CO_2eq./ton, and 1,162 kg CO_2eq./ton of straw is obtained by gasification, incineration, and anaerobic digestion, respectively. However, insignificant corresponding economic benefits of 535 INR/ton, 510 INR/ton, and 168 INR/ton of rice straw were reported, respectively. On the contrary, fermentation and integrated operation of anaerobic digestion resulted in 900–1,525 INR/ton of financial benefit with 152–288 kg CO_2eq./ton of net GWP reduction (Singh and Basak, 2019). Production of biocomposite strawboards offers a higher economic return to farmers and manufacturers than traditional straw management practices. LCA of 1 m^3 rice straw and bamboo biocomposites showed a net carbon flux of −1,198.49 kg CO_2eq. for its production (Pang et al., 2022).

Theng et al. (2017) and Theng et al. (2019) showed that rice straw pretreatment, such as digestion plus defibration, consumes specific energy of 6.176–8.52 kWh/kg dry matter, whereas 0.668–0.946 kWh/kg dry matter specific energy was required for twin screw extrusion of straw fibers. The environmental impacts of the conventional density board were reported to be higher than the straw density board (Deng et al., 2023). Thus, it is observed that the production of biocomposite from

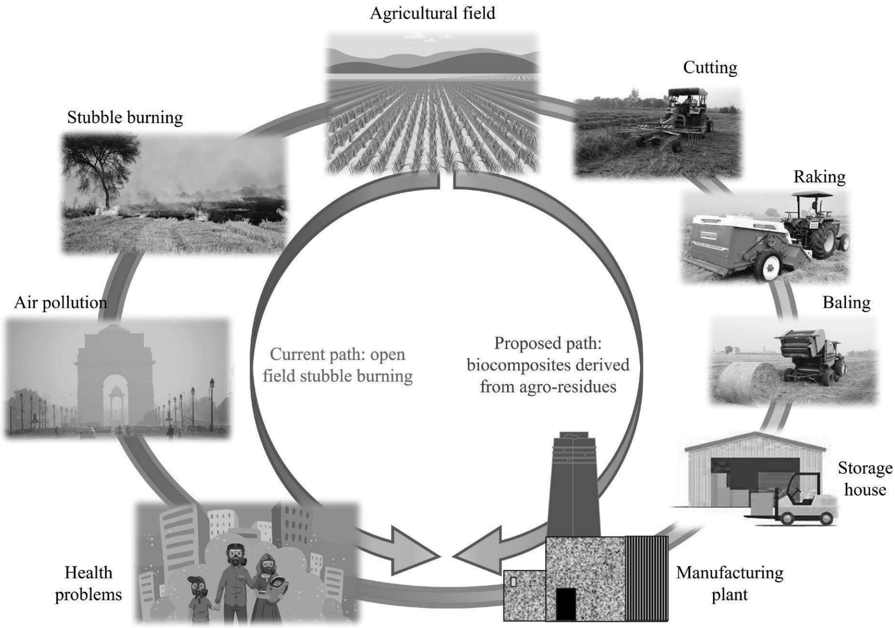

FIGURE 7.1 Comparison between the path of open-field burning and production of biocomposites from agro-residues.

agro-residues is beneficial over stubble burning from environmental, sustainable, and economic aspects.

However, the main challenges in the production of these biocomposites are reported as obtaining comparative material properties, performance, and cost as compared to wooden boards at a larger scale (Li et al., 2010). Therefore, there is a need for a study to improve their mechanical and physical properties and strength. The main objectives of this study are: (a) to compare GHG emissions in the production of biocomposite from agro-residues and in the burning stubble; (b) to estimate GHG emissions from the LCA in the production of rice straw biocomposite fiberboards and particleboards; and (c) to compare the fiberboards and particleboards with industrial bioboards and wooden boards, and present their feasibility for sustainable infrastructure development.

7.2 EMISSIONS IN STUBBLE BURNING

In this study, emissions from stubble burning are estimated considering emission factors of various pollutants, and further, the environmental impacts of the pollutants are assessed. The emission factors in stubble burning are dependent on the climatic zone, type of fire, carbon content of the material, moisture content, and environmental conditions prevailing in a field. The emission for biomass burning is obtained using

Equations 7.1 and 7.2 (Andreae and Merlet, 2001). Some studies (Eggleston et al., 2006; Andreae, 2019; Ravindra et al., 2019; Kanabkaew and Oanh, 2011) obtained the emissions of pollutants from biomass burning, as per Equation 7.1, as listed in Table 7.1.

$$EF_{\mathrm{x}} = \frac{M_{\mathrm{x}}}{M_{\mathrm{bio}}}[C]_{\mathrm{bio}} = \frac{M_{\mathrm{x}}}{M_{\mathrm{c}}}[C]_{\mathrm{bio}}, \tag{7.1}$$

$$EF_{\mathrm{x}} = \frac{[X]}{\left(C_{\mathrm{CO_2}} + C_{\mathrm{CO}} + C_{\mathrm{CH_4}} + \ldots\right)}[C]_{\mathrm{bio}}, \tag{7.2}$$

where EF_{x} is the emission factor for species X, M_{x} is the total mass of considered species, M_{c} is the mass of carbon emitted, $[C]_{\mathrm{bios}}$ is carbon concentration in the biomass burned, $[X]$ is the concentration of species X in the smoke, and C_{Y} is the concentration of various carbon gases and pollutants in the smoke (i.e., Y: CO_2, CO, CH_4, EC: elemental carbon, etc.). There are various uncertainties associated with emission factors of GHG emissions from various types of biomass burning. Therefore, selecting acceptable emission factors as per the prevailing conditions is important for the estimation of GHG emissions.

The statistics for annual crop production and quantity of agro-residues burned in the cities of Punjab and Haryana are presented in Figures 7.2 and 7.3 (CREAMS, 2020). In this study, emission factors (Kanabkaew and Oanh, 2011) are adopted to estimate GHG emissions due to rice (paddy) straw burning. Moreover, GHG emissions are presented in terms of CO_2 equivalent (CO_2eq.) using global warming potential (GWP) (Eggleston et al., 2006). The highest quantity of agro-residues is produced in the Sangrur and Karnal cities of Punjab and Haryana, respectively. Approximately 50% and 15% of produced agro-residues are burned in the

TABLE 7.1
Comparison of Emission Factors (g/kg) of Various Pollutants in the Burning of Agricultural Residue

Pollutant	Eggleston et al. (2006)	Kanabkaew and Oanh (2011)	Andreae (2019)	Ravindra et al. (2019)
CO_2	1,515±177.00	1,177.00	1,430±230.00	1,467.00
CO	92±84.00	93.00	76±55.00	72.85
CH_4	2.70	9.59	5.9±4.80	6.05
N_2O	0.07	-	0.09±0.04	0.62
NOx	2.5±1.00	2.28	2.4±1.20	2.30
NH_3	1.30	4.10	0.99±0.63	2.41
SO_2	0.40	0.18	0.88±0.92	0.27
$PM_{2.5}$	3.90	8.30	8.2±4.40	7.05
EC	0.69±0.13	0.51	0.42±0.28	0.49

post-harvest seasons of Punjab and Haryana, respectively. It is essential to identify the most stubble burning hotspots to propose and investigate alternative in-situ or ex-situ agro-residues or straw management strategies. Ten cities of Punjab, as shown in Figure 7.2, mainly contribute to 75% of the total stubble burning. Therefore, these cities should be prioritized for different agro-residues management policies and strategies.

Accordingly, GHG emission factors for Punjab and Haryana are estimated based on the data of burned agro-residue, as provided in Figures 7.2 and 7.3. The emission of prime GHG in Punjab and Haryana and corresponding estimated emission factors are given in Table 7.2. More than 20.3 million tons CO_2eq. and 2.3 million tons CO_2eq. major GHG emissions are obtained in Punjab and Haryana, respectively, during the period from October to November 2020.

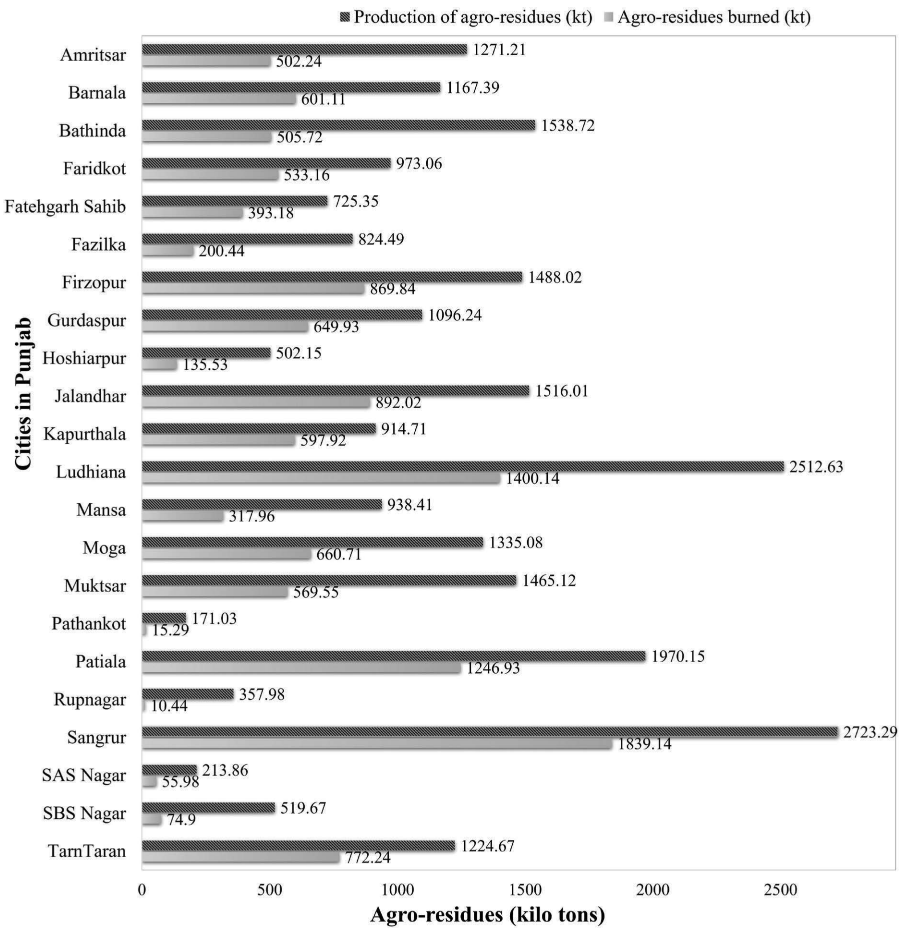

FIGURE 7.2 Production and burning of agro-residues in different cities of Punjab from October to November 2020 in the post-harvest season (CREAMS, 2020).

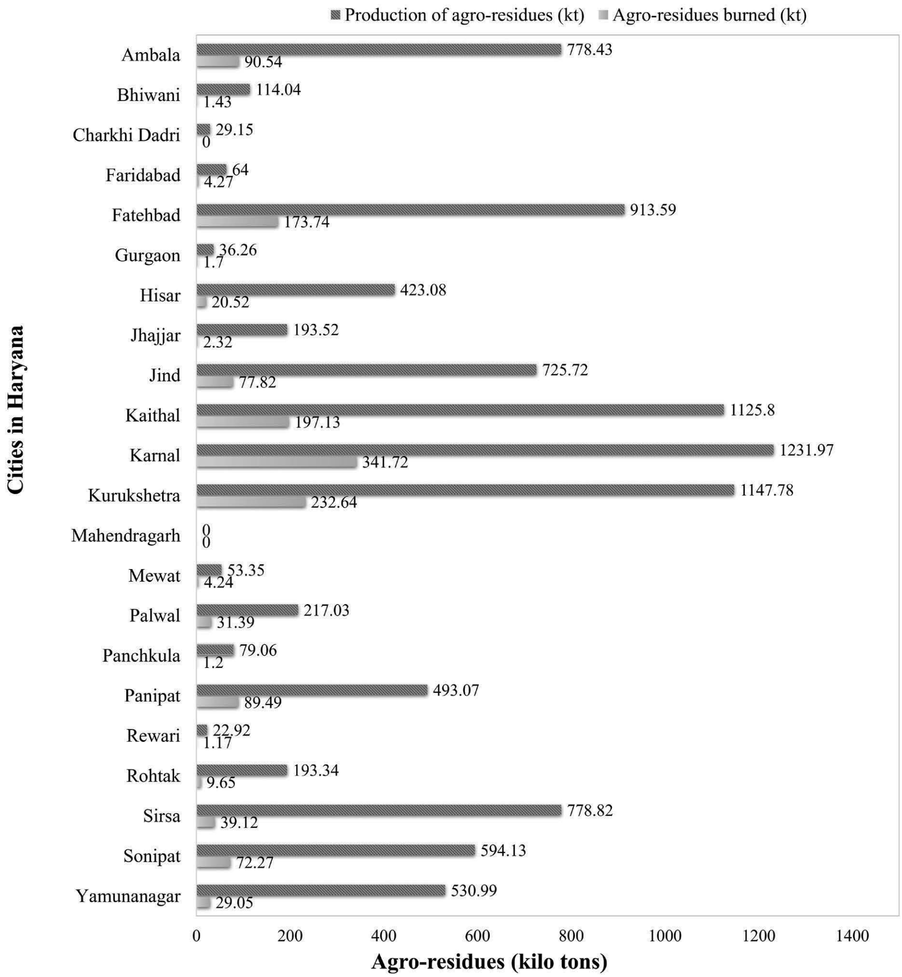

FIGURE 7.3 Production and burning of agro-residues in different cities of Haryana from October to November 2020 in the post-harvest season (CREAMS, 2020).

TABLE 7.2
Estimated Emissions of Various Pollutants from Burning of Rice Straw Residues from October to November 2020 in Punjab and Haryana

Parameter	CO_2	CO	CH_4	N_2O	NO_x	NH_3	SO_2	$PM_{2.5}$	EC
Emission factor (g/kg)	1177.0	93.0	9.6	0.5	2.3	4.1	0.18	8.3	0.5
Emissions in Punjab (Gg)	15117.8	1194.5	123.2	6.2	29.3	52.7	2.3	1066.6	6.5
Emissions in Haryana (Gg)	1673.0	132.2	13.6	0.7	3.2	5.8	0.3	11.8	0.7

7.3 EMISSIONS IN THE PRODUCTION OF BIOCOMPOSITES FROM AGRO-RESIDUES

There are various steps involved in the production of biocomposites from agro-residues, i.e., collection, transportation, processing, and manufacturing, as presented in Figure 7.1.

7.3.1 Collection of Agro-Residues in the Field

The main reasons for stubble burning are the unavailability of space, machinery requirements, and limited time availability for rice straw management to sow the next crop. Kumar et al. (2015) reported that approximately 80% of the rice cultivated area in Punjab is harvested using a mechanical harvester. The disadvantage of this harvester is that it spreads rice residues in the fields while harvesting, which creates difficulty in collecting agro-residues. Therefore, an efficient process of residue collection needs to be implemented.

The collection process with appropriate steps can make the process efficient, i.e., cutting, raking, baling, and loading. The raker is used to collect spread agricultural straw after cutting the crop with a mechanical harvester while keeping some straw as a biodegradable fertilizer for the soil. Afterward, the collected straw is dried and baled. These bales are easy to handle and transport to storage sites. In this collection process, emissions occur due to fuel and power consumption of machinery. The typical emissions of GHG from each collecting process are mentioned in Table 7.3. Here, the energy consumed by manpower is neglected.

Hence, GHG emissions are estimated as:

$$\text{Emission} = Q_{\text{Fuel}} \times EF_{\text{Fuel}}, \quad (3)$$

where EF_{Fuel} is the emission factor of fuel, and Q_{Fuel} is the quantity of fuel consumed per kg straw transported. As per Eggleston et al. (2006), depending upon the provided net calorific value (45.145 MJ/kg), the density of diesel fuel (0.84 kg/l), and the CO_2 emission factor for diesel (74,100 kg CO_2eq./TJ), the emission factor is obtained as 2.81 kg CO_2eq./l. The quantity of fuel consumption depends upon the type of vehicle, distance traveled, and average fuel consumption of the vehicle.

TABLE 7.3
GHG Emissions during the Collection of One Ton Agro-Residues from the Field

Process	Fuel Efficiency (l/acre)	Fuel (l/ton agro-residue)	*EF* (kg CO_2eq./l)	Emissions (kg CO_2eq.)
Cutting	3	1.28	2.81	3.60
Raking	4	1.71	2.81	4.81
Baling	7	2.99	2.81	8.41
Loading	2	0.86	2.81	2.40

Fuel consumption and GHG emissions estimated in individual processes of the collection are given in Table 7.3. It is observed from the data that a total of 6.84 l fuel is consumed for one ton of agro-residues, and corresponding 19.23 kg CO_2eq./ton emissions take place in the collecting process. Some researchers (Jiang et al., 2020; Alengebawy et al., 2022; Bressan et al., 2022) also reported emissions of 27.64 kg CO_2eq., 20 kg CO_2eq., and 23.84 kg CO_2eq. per ton agro-residues in the collection process, respectively. In this study, for the estimation of GHG emissions, the average yield of rice straw is considered as 2.33 tons/acre according to the characteristics of fields in Punjab (Ebrayi et al., 2007; Soam et al., 2016; Singh and Basak, 2019). Accordingly, 109.7 kg CO_2eq. emission is expected per hectare.

7.3.2 Transportation of Straw and Other Materials to the Manufacturing Plant

The collected bales of agro-residues (average density of 150 kg/m^3) are generally transported to some (local) storage facilities from fields with vehicles, such as tractors, trucks, and trolleys. In this study, it is assumed that the storage facility is within a 10 km radius of a field and the manufacturing site is within a 40 km radius of the storage facility. Approximately one ton of agro-residues is transported to a storage facility with an average size tractor of 4.5 km/l efficiency, whereas 10 tons of agro-residues are transported to a manufacturing site with a truck of 5.5 km/l efficiency. Furthermore, to manufacture biocomposites from agro-residues, additional resin for binding, wax for removing a mold, and additional accessories are needed. These materials are considered to be transported from a 300 km distance with a vehicle of 10 tons carrying capacity. This one-way transportation of resin and wax to the manufacturing site results in a 1.83 kg CO_2eq./ton unit. The capacity of commercial vehicles is decided based on their size, height, and weight limit (BEE, 2020). The total fuel consumption per ton of load is calculated as:

$$Q_{\text{Fuel}} = FE \times D, \tag{4}$$

where FE is fuel efficiency (l/km), and D is the distance traveled with load (km/ton). Accordingly, using Equation 7.3, GHG emissions are estimated as 18.35 kg CO_2eq./ton. Soam et al. (2016) reported an emission of 18 kg CO_2eq./ton for the transportation of straw in their study. The GHG emissions resulting from the transportation process can be reduced by using locally available materials in manufacturing.

7.3.3 Manufacturing of Biocomposites from Agro-Residues

Biocomposites are made from resin or matrix reinforced with natural fibers. The resin can be synthetic or natural, which works as a binder for fibers in the composite. Manufacturing biocomposites from agro-residues or straw requires the processing of agro-residues first to obtain a stronger bond between fibers and resin. The processing of agro-residues involves drying to reduce moisture content, chopping to make them easy to handle, dedusting and washing to clean the silica, and surface treatment to remove impurities and improve the bond between fiber and resin. In this section, GHG emissions and energy consumption in various processes involved in the manufacturing of rice straw fiberboards and particleboards are presented. After drying agro-residues, they are chopped to 10–20 mm size with hammer milling (Halvarsson et al., 2010). Subsequently, dust is removed from the ground residues by using an air-density separator and soaked in a defibrator. In the defibrator, a rotation of 1500 rpm with 0.5–0.6 MPa for one minute is applied for defibration. The soaked residues are dried in an oven or with a dryer until the moisture content stays up to 10%. Sometimes, additional alkali, hygrothermal, and acidic treatments are implemented to improve the properties of agro-residues and surfaces for bond. Subsequently, on a rotary drum blender, resin (5%) and wax (1%) are sprayed on fibers. The wax protects the surface of the fibers from water. Further, the sprayed fibers are converted to a sheet in a hot pressing machine at 180°C, and 5 MPa for 80 s up to the required thickness is achieved. The obtained fiberboard from hot pressing is cooled and refined for further packaging and transport.

The emission factors of additional materials used, i.e., NaOH, resin, NH_4Cl, and wax in the manufacturing of biocomposites from agro-residues in fiberboards and particleboards, are illustrated in Table 7.4 and are taken from previous studies (Thannimalay et al., 2013; Franklin Associates, 2022; Pang et al., 2022). Moreover, energy consumption in processes included in the manufacturing of fiberboard and particleboard is shown in Tables 7.5 and 7.6, respectively.

The energy consumption is estimated based on the horsepower rating (kW), load percentage, operating time (hr), and efficiency of an electric motor of equipment for each process. The estimated energy consumption is checked for each process reported in some studies (Adapa et al., 2011; Halvarsson et al., 2010; Wang et al., 2017; Shang et al., 2020; Silva et al., 2020; Pang et al., 2022). The total energy of 313.8 kWh and 277 kWh are consumed in fiberboard and particleboard manufacturing processes, respectively. The emission factors from electricity consumption are taken as 0.81 tons CO_2/MWh (Menghani and Sharma, 2022). Accordingly, total GHG emissions due to materials and energy consumption for the manufacturing of fiberboard results in 145.6 kg CO_2eq. and 254.2 kg CO_2eq. emission, respectively. On the other hand, total GHG emissions due to the energy consumption of particleboard manufacturing are 224.4 kg CO_2eq. emission. It can be observed that the net GHG emissions in the production of particleboard are lesser than those of fiberboard due to less energy consumption in the manufacturing process. Energy consumption

TABLE 7.4
Emission Factors of Materials Used in the Manufacturing of Rice Straw Biocomposite Fiberboard and Particleboard

Material	Emission Factor (kg CO_2eq./kg)	Reference
NaOH	0.6330	Thannimalay et al. (2013)
Methylene diphenyl diisocyanate resin	2.1310	Franklin Associates (2022)
Wax	0.6360	Pang et al. (2022)
Water	0.0012	Pang et al. (2022)

TABLE 7.5
Energy Consumption in Processes during the Manufacturing of Fiberboard from One Ton of Agro-Residues

Manufacturing Process	Electricity Consumption (kWh)	References
Size reduction: chopping, hammer milling, dedusting, and soaking in water	21.84	Wang et al. (2017) and Shang et al. (2020)
Defibration: refining	185.00	Halvarsson et al. (2010)
Oven drying	24.05	Shang et al. (2020)
Resin and wax spraying and chopping	15.47	Adapa et al. (2011) and Pang et al. (2022)
Sheet forming	40.24	Shang et al. (2020) and Silva et al. (2020)
Cooling, conditioning, sanding, and machining	27.20	Shang et al. (2020)

TABLE 7.6
Energy Consumption in Processes during the Manufacturing of Particleboard from One Ton of Agro-Residues

Manufacturing Process	Electricity Consumption (kWh)	References
Size reduction: chopping, hammer milling, dedusting, and soaking in water	21.84	Wang et al. (2017) and Shang et al. (2020)
Oven drying	24.05	Shang et al. (2020)
Resin and wax spraying and hot pressing	195.31	Shang et al. (2020) and Pang et al. (2022)
Cooling, conditioning, sanding, and machining	35.80	Shang et al. (2020) and Silva et al. (2020)

has significant variability with respect to different machines, equipment, techniques, materials, and processes used in manufacturing. Also, the manufacturing of fiberboards requires more energy than that of particleboards due to the additional process of separation of fibers involved.

7.4 LIFE-CYCLE ASSESSMENT OF BIOCOMPOSITES FROM AGRO-RESIDUES

Life-cycle assessment (LCA) is defined as the compilation and evaluation of inputs, outputs, energy consumption, and potential environmental impacts of a product throughout its life cycle (ISO, 14040, 2006). Ead et al. (2021) summarized the LCA steps and their relevance for green composites. LCA is a useful measure for strategic planning, product improvement strategies, and marketing green products. Moreover, LCA also helps analyze each process involved in production to further strategies and steps included for reducing GHG emissions. In this study, LCA of biocomposites from agro-residues is performed to compare GHG emissions from open-field burning of agro-residues and the production of biocomposites. Furthermore, these biocomposites of fiberboards from agro-residues can be used in the construction industry for sustainable infrastructure development (Puettmann and Salazar, 2018).

In this study, the estimation of GHG emissions associated with each process of production is shown for biocomposite fiberboards and particleboards per one ton of agro-residues. The LCA is performed using LCA software with SimaPro 9.0®, and for modeling the life-cycle inventory of biocomposites, Ecoinvent® (see Table 7.7), and agri footprint databases are used. Moreover, the estimated GHG emission values are compared with analytically estimated emission values based on statistics from different reports by the Government of India, databases from industrial documents, and some research studies. The estimation is limited to the process and material included in cradle-to-gate stages. Here, the estimation does not include the environmental impacts of infrastructures for production, maintenance of machinery and infrastructure, and human resources.

The LCA software follows unit processes, detailed databases, and supply networks for estimations (Puettmann et al., 2013). Materials and processes involved in the production of biocomposites are taken considering Indian scenarios. For some materials and processes, that are not available in the inventory database, their respective information is added to the system according to recommendations given in relevant literature. Furthermore, the assembly of strawboards is analyzed using the ReCiPe Midpoint (H) method. The LCA software considered a higher emission factor of 1.25 kg CO_2eq./kWh of medium voltage electricity consumption as compared to the emission factor obtained from the literature (Menghani and Sharma, 2022), which results in higher GHG emissions due to energy consumption. Moreover, the software considers the higher emission factor in resin production as 2.45 kg CO_2eq./kg. The GHG emissions from materials and processes involved in the production of a fiberboard from rice straw using the software are presented in Tables 7.7 and 7.8, respectively. The LCA of production of fiberboard from rice straw results in a total of 548.3 kg CO_2eq./ton straw, which is higher than the estimation made based on formulae from the literature. The maximum contribution to GHG emissions is obtained due to energy consumption (64%) followed by synthetic resins (22.3%) production, as

TABLE 7.7
Life-Cycle Inventory of Materials for Fiberboard and Particleboard from Rice Straw in SimaPro 9.0® LCA Software

Material	Quantity	Total (kg CO_2eq.)
Rice straw	1000 kg	0
NaOH	50 kg	31.65
Methylene diphenyl diisocyanate resin	50 kg	122.24
Wax (paraffin)	10 kg	7.35
Water	850 kg	1.02

TABLE 7.8
Life-Cycle Inventory of Processes Involved in the Manufacturing of Fiberboard and Particleboard from Rice Straw in SimaPro 9.0® LCA Software

Process	Value per Functional Unit	Total (kg CO_2eq.)
Straw cutting	1	3.46
Raking	1	4.61
Baling	1.43	9.53
Bale loading	5	2.17
Transport, tractor, and trailer	10 km	3.56
Transport, truck 10–20 tons capacity	40 km	9.04
Transport, truck 10–20 tons capacity	15 km	1.96
Transport, truck 10–20 tons capacity	3.0 km	0.47
Electricity, medium voltage capacity (fiberboard)	281 kWh	351.25
Electricity, medium voltage capacity (particleboard)	244.2 kWh	305.25

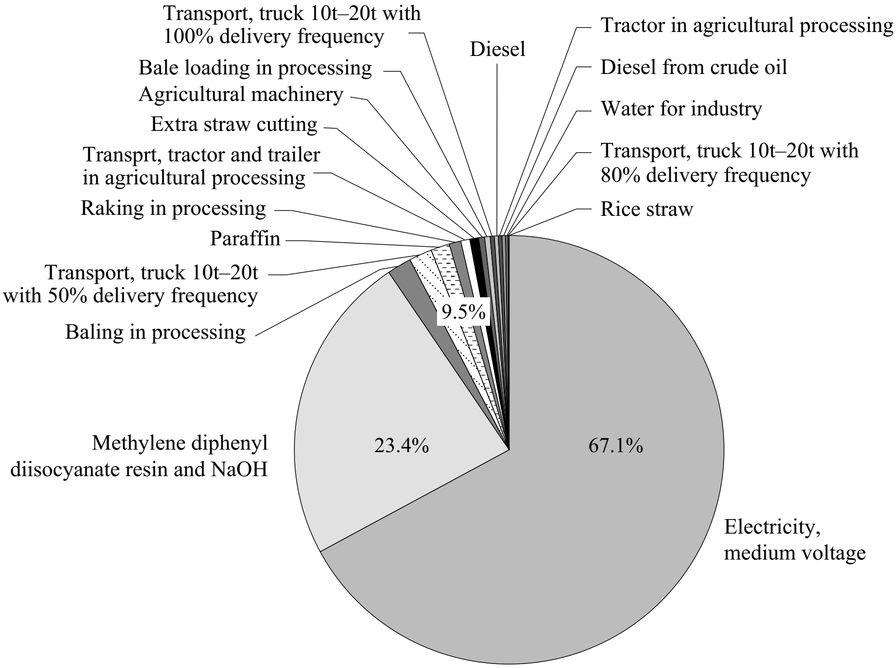

FIGURE 7.4 Greenhouse gas (GHG) emissions in the production of fiberboard from paddy (rice) straw using life-cycle assessment.

depicted in Figure 7.4. On the other hand, 502.3 kg CO_2eq./ton straw is emitted in the production of particleboard from rice straw, which consists of 55.7% contribution by energy consumption. Hence, there is a scope for improvement in reducing emissions from energy consumption and synthetic resin production.

7.5 BIOCOMPOSITE FROM AGRO-RESIDUES FOR SUSTAINABLE INFRASTRUCTURE DEVELOPMENT

Material properties and strength of biocomposites derived from agro-residues are determining parameters to assess the feasibility of their use for sustainable infrastructure. In this study, the materials are selected based on the availability of their properties in the literature (Halvarsson et al., 2010; Li et al., 2010). Moreover, the requirement of minimum strength of the biocomposites fiberboard and particleboard from rice straw in the construction industry is checked with provisions of Indian standards (IS 12406, 2003; IS 3087, 2005). Furthermore, material properties and GHG emissions of the fiberboard and particleboard are compared with available wooden boards to evaluate their applicability for infrastructure.

It is observed from Table 7.9 that fiberboard and particleboard from rice straw considered in this study show comparable mechanical properties with industrial biocomposite boards and wooden boards available in markets. Furthermore, the GHG emissions of various biocomposite boards are compared, as illustrated in Figure 7.5. Also, it is noted that fiberboard has higher strength and stiffness as compared to particleboards due to the higher length of the fiber and better bond with resin. Both fiberboard and particleboard fulfill the minimum limits of Grade I and Grade II physical and mechanical properties as specified in Indian standards (IS 12406, 2003; IS 3087, 2005), respectively. It is observed from Table 7.9 and Figure 7.5 that biocomposite boards from agro-residues have comparable properties with industrial biocomposites and wooden boards and have the least GHG emissions. Therefore, agro-residue-based biocomposites can be used as an alternative to conventional boards for sustainable infrastructure. These biocomposites also provide good thermal and sound insulation to structures. Therefore, such biocomposites are used in walls, flooring, roofing, and formwork. Furthermore, biocomposites are a good choice for lightweight structures and, especially structures in earthquake-prone areas, to reduce inertia forces.

The major contents of agro-residues (natural straw) are cellulose, hemicellulose, lignin, and silica. The removal of hemicellulose, lignin, and silica is necessary to

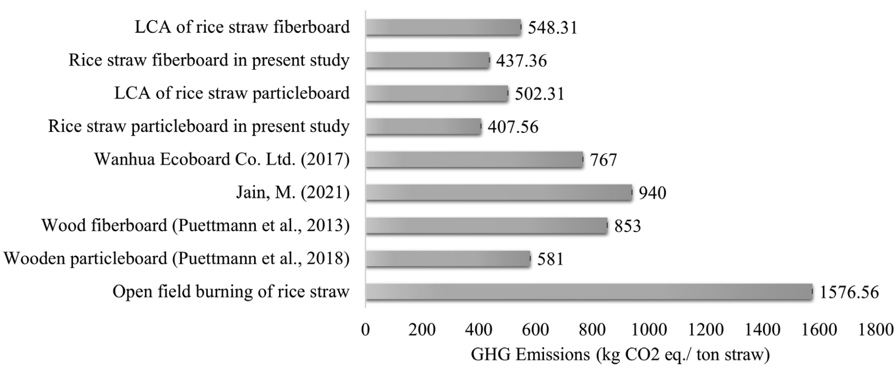

FIGURE 7.5 Greenhouse gas (GHG) emissions comparison of rice strawboards with industrial strawboards, wooden boards, and open field burning of straw.

TABLE 7.9
Comparison of Physical and Mechanical Properties of Rice Straw Boards, Industrial Strawboards, and Wooden Boards

Source	Product Type	Density (kg/m³)	Modulus of Rupture (MPa)	Modulus of Elasticity (MPa)	Water Absorption (%)	Reference
Indian standard requirement	Fiberboard	600–900	28	2,500	30/45	IS 12406 (2003)
	Particleboard	500–900	15/11	2,500/2,000	20/80	IS 3087 (2005)
Industrial bioboards	Agribio panel	733	17.82	1,508	43	Jain (2021)
	Rice straw particleboard	790	17.10	2,846	-	Wanhua Ecoboard Co. Ltd (2017)
	Rice straw fiberboard	720	31	3,103	-	CalPlant (2021)
Industrial wooden board	Wooden particleboard	680	14	2,400	28	ASIS (2023)
	Wooden fiberboard	730	29	2,600	23	ASIS (2023)
Binder-less board	Rice straw binder-less board	800	6	1,500	60	Kurokochi and Sato (2020)
Bioboards in the present study	Rice straw fiberboard	1,060	45	3,000	20–35	Halvarsson et al. (2010)
	Rice straw particleboard	700	13	2,000	40	Li et al. (2010)

improve the bond between fiber and resin in the composite. Therefore, the cleaning and processing of extracted agro-residues is the most important measure for biocomposites. Moreover, some of the major challenges with biocomposites are hydrophilic properties (which result in moisture absorption and, subsequently, swelling and reduction in strength) and vulnerability to termite attack and fire. Therefore, several studies have been conducted to reduce water absorption, prevent termite attacks, and improve the fire resistivity of biocomposites so that they can be used in sustainable infrastructure development. Moreover, the improvement of the mechanical properties, structural performance, and durability of biocomposites from agro-residues have scope for future research.

The use of biocomposites from agro-residues for sustainable infrastructure development has the potential to improve environmental conditions, curtail air pollution problems, and reduce associated human health problems. Also, it contributes to the creation of new employment opportunities in rural areas, sustainable infrastructure development, and economic enhancement of a country as well. Moreover, the production of biocomposites as an alternative to stubble burning is a contributory step towards achieving a net zero carbon emissions target for India, as well as other countries.

7.6 CONCLUSIONS

In the present study, the environmental impact of the production of biocomposites from agro-residues as an alternative to stubble burning is presented in terms of GHG emissions. The GHG emissions in the burning of agro-residues and production of biocomposites using analytical formulations and LCA are estimated and compared. Based on the findings of this study, the following conclusions are drawn:

1. The stubble burning in Punjab and Haryana results in GHG emissions of 1,577 kg CO_2eq./ton of agro-residues burned. In total, more than 20.3 million tons of CO_2eq. and 2.3 million tons CO_2eq. GHG emissions were obtained in 2020 due to stubble burning in Punjab and Haryana, respectively.
2. The production of biocomposite fiberboard and particleboard from agro-residues, which includes processes of collection, transportation, manufacturing, and energy consumption, results in GHG emissions of 437.4 kg CO_2eq./ton of agro-residues and 407.6 kg CO_2eq./ton of agro-residues, respectively.
3. The LCA of fiberboard and particleboard from agro-residues shows GHG emissions of 548.3 kg CO_2eq./ton of agro-residues and 502.3 kg CO_2eq./ton of agro-residues in cradle-to-gate processes, respectively.
4. The prime contributory factors of GHG emissions are the energy consumption of equipment involved and synthetic materials for treatment and binding used in the production of biocomposites.
5. The alternative solution of producing biocomposites from agro-residues to stubble burning reduces GHG emissions by 60–70% and helps in the mitigation of climate change. Moreover, these biocomposites show mechanical properties comparable to industrial biocomposites, which shows their potential for sustainable infrastructure development.

7.7 ACKNOWLEDGMENTS

Financial support received from the United States–India Educational Foundation (USIEF) under the 'Fulbright-Kalam Climate Fellowship for Academic and Professional Excellence' to Vasant Matsagar for a project titled, 'Abatement of Greenhouse Gas Emissions from Stubble Burning by Adapting to New Agriculture Waste Management in Gainfully Making Green Industrial Products' is gratefully acknowledged. Sagnik Dey acknowledges support from IIT Delhi for the Institute Chair Fellowship. Also, the authors gratefully acknowledge the financial support provided under the Science and Engineering Research Board (SERB), Department of Science and Technology (DST), Government of India, under the VAJRA (Visiting Advanced Joint Research) Faculty Scheme. The opinions expressed herein are those of the authors and not necessarily of the funding agencies.

REFERENCES

Adapa, P., Tabil, L., and Schoenau, G. (2011). Grinding performance and physical properties of non-treated and steam exploded barley, canola, oat and wheat straw. *Biomass and Bioenergy*, 35(1), 549–561.

Alengebawy, A., Mohamed, B. A., Ran, Y., Yang, Y., Pezzuolo, A., Samer, M., and Ai, P. (2022). A comparative environmental life-cycle assessment (LCA) of rice straw-based bioenergy projects in China. *Environmental Research*, 212, 113404.

Andreae, M. O. (2019). Emissions of trace gases and aerosols from biomass burning-an updated assessment. *Atmospheric Chemistry and Physics*, 19(13), 8523–8546.

Andreae, M. O., and Merlet, P. (2001). Emission of trace gases and aerosols from biomass burning. *Global Biogeochemical Cycles*, 15(4), 955–966.

ASIS. (2023). Physical and mechanical properties of medium density fibreboard and particleboard. *ASIS International*. https://asisindia.com/wp-content/uploads/2023/04/MDF_tech_specs.pdf; https://asisindia.com/wp-content/uploads/2023/04/Particle_board_tech_specs.pdf (accessed on September 8, 2023).

Balakrishnan, K., Dey, S., Gupta, T., Dhaliwal, R. S., Brauer, M., Cohen, A. J., Stanaway, J. D., Beig, G., Joshi, T. K., Aggarwal, A. N., and Sabde, Y. (2019). The impact of air pollution on deaths, disease burden, and life expectancy across the states of India: The global burden of disease study 2017. *The Lancet Planetary Health*, 3(1), e26–e39.

Basta, A. H., El-Saied, H., and Lofty, V. F. (2014). Performance assessment of deashed and dewaxed rice straw on improving the quality of RS-based composites. *RSC Advances*, 4(42), 21794–21801.

BEE. (2020). *The gazette of India: Extraordinary*. Bureau of Energy Efficiency, Ministry of Power, Government of India, New Delhi. Registration No. D. L.-33004/99. https://beeindia.gov.in/sites/default/files/SO_3215(E).pdf (accessed on September 8, 2023).

Bhattacharyya, P., Bisen, J., Bhaduri, D., Priyadarsini, S., Munda, S., Chakraborti, M., Adak, T., Panneerselvam, P., Mukherjee, A., Swain, S., Dash, P., Padhy, S., Nayak, A., Pathak, H., Kumar, S., and Nimbrayan, P. (2021). Turn the wheel from waste to wealth: Economic and environmental gain of sustainable rice straw management practices over field burning in reference to India. *Science of the Total Environment*, 775, 145896.

Bikkina, S., Andersson, A., Kirillova, E. N., Holmstrand, H., Tiwari, S., Srivastava, A. K., Bisht, D. S., and Gustafsson, O. (2019). Air quality in megacity Delhi affected by countryside biomass burning. *Nature Sustainability*, 2(3), 200–205.

Bressan, M., Campagnoli, E., Ferro, C. G., and Giaretto, V. (2022). Rice straw: A waste with a remarkable green energy potential. *Energies*, 15(4), 1355.

CalPlant. (2021). *Rice straw-based medium density fiberboard*. Northern California. https://arpa-e.energy.gov/sites/default/files/8%20-%20Uhland%20-%20DOE%20CalPlant%20presentation%2018%20March%202021.pdf (accessed on September 8, 2023).

CREAMS. (2020). *Monitoring paddy residue burning in north India using satellite remote sensing during 2020*. Consortium for Research on Agroecosystem Monitoring and Modelling from Space Laboratory, Division of Agricultural Physics, ICAR, New Delhi, India. http://creams.iari.res.in/pdf/bulletin_sp_20/05_RiceResidue_BurnStatistics_2020.pdf (accessed on September 8, 2023).

Daba, E. T., Zelleke, D. H., Matsagar, V. A., and Kodur, V. (2023). Characterization of natural fiber ropes for potential applications as reinforcement in concrete. *The 6th International Conference on Natural Fibers (ICNF) 2023*, Funchal, Madeira, Portugal, June 19–21.

Deng, N., Wang, J., Li, J., and Sun, J. (2023). Straw density board vs. conventional density board: Is straw density board more sustainable? *Science of The Total Environment*, 888, 164020.

Dong, S., Yuan, F., Yang, L., Chi, S., Zhong, J., Lei, J., Bao, L., and Wang, J. (2019). Clean and sustainable biocomposites based on supramolecular interactions induced thermoplasticization of wheat straw powders. *Journal of Cleaner Production*, 233, 590–600.

Ead, A. S., Appel, R., Alex, N., Ayranci, C., and Carey, J. P. (2021). Life-cycle analysis for green composites: A review of literature including considerations for local and global agricultural use. *Journal of Engineered Fibers and Fabrics*, 16. https://doi.org/10.1177/15589250211026940

Ebrayi, K. N., Pathak, H., Kalra, N., Bhatia, A., and Jain N. (2007). Simulation of nitrogen dynamics in soil using infocrop model. *Environmental Monitoring and Assessment*, 131, 451–465.

Eggleston, H. S., Buendia, L., Miwa, K., Ngara, T., and Tanabe, K. (2006). *2006 IPCC guidelines for national greenhouse gas inventories*. The Intergovernmental Panel on Climate Change (IPCC), National Greenhouse Gas Inventories Programme, Institute for Global Environmental Strategies IGES, Japan.

ESO. (2021). *Statistical abstract of Punjab*. Economic and Statistical Organisation, Department of Planning, Government of Punjab, India. https://esopb.gov.in/Static/PDF/Abstract2021.pdf (accessed on September 8, 2023).

Franklin Associates. (2022). *Cradle-to-gate life-cycle analysis of methylene diphenyl diisocyanate (MDI)*. Final Report, Franklin Associates, A Division of Eastern Research Group, Inc. www.americanchemistry.com/content/download/11831/file/Cradle-to-Gate-Life-Cycle-Analysis-of-Methylene-Diphenyl-Diisocyanate-Resin-Precursor.pdf (accessed on September 8, 2023).

Halvarsson, S., Edlund, H., and Norgren, M. (2010). Manufacture of high-performance rice-straw fiberboards. *Industrial and Engineering Chemistry Research*, 49(3), 1428–1435.

IS 3087. (2005). *Particle boards of wood and other lignocellulosic materials (medium density) for general purposes—specification*. Bureau of Indian Standards, New Delhi, India. https://standardsbis.bsbedge.com/ (accessed on September 8, 2023).

IS 12406. (2003). *Medium density fibre boards for general purpose—specification*. Bureau of Indian Standards, New Delhi, India. https://standardsbis.bsbedge.com/ (accessed on September 8, 2023).

ISO 14040. (2006). *Environmental management—life-cycle assessment—principles and framework*. International Organization for Standardization, 2.

Jain, M. (2021). *AgribioPanels™ EPD*. Strawcture Eco Pvt. Ltd. https://strawcture.com/wp-content/uploads/2022/08/LCA_Strawcture.pdf (accessed on September 8, 2023).

Jiang, Z., Dai, Y., and Du, T. (2020). Comparison of the energetic, environmental, and economic performances of three household-based modern bioenergy utilization systems in China. *Journal of Environmental Management*, 264, 110481.

Kanabkaew, T., and Oanh, N. T. K. (2011). Development of spatial and temporal emission inventory for crop-residue field burning. *Environmental Modeling and Assessment*, 16, 453–464.

Korontzi, S., McCarty, J., Loboda, T., Kumar, S., and Justice, C. (2006). Global distribution of agricultural fires in croplands from 3 years of moderate resolution imaging spectroradiometer (MODIS) data. *Global Biogeochemical Cycles*, 20(2).

Krasny, E., Klarić, S., and Korjenić, A. (2017). Analysis and comparison of environmental impacts and cost of bio-based house versus concrete house. *Journal of Cleaner Production*, 161, 968–976.

Kumar, P., Kumar, S., and Joshi, L. (2015). *Socioeconomic and environmental implications of agricultural residue burning: A case study of Punjab, India*. Springer Nature, 144.

Kurinji, L. S., and Kumar, S. (2021). *Is ex-situ crop-residue management a scalable solution to stubble burning*? A Punjab case study. Council on Energy, Environment and Water, New Delhi, India.

Kurokochi, Y., and Sato, M. (2020). Steam treatment to enhance rice straw binder-less board focusing hemicellulose and cellulose decomposition products. *Journal of Wood Science*, 66, 7.

Lan, R., Eastham, S. D., Liu, T., Norford, L. K., and Barrett, S. R. (2022). Air quality impacts of crop-residue burning in India and mitigation alternatives. *Nature Communications*, 13(1), 6537.

Li, X., Cai, Z., Winandy, J. E., and Basta, A. H. (2010). Selected properties of particleboard panels manufactured from rice straws of different geometries. *Bioresource Technology*, 101(12), 4662–4666.

Lohan, S. K., Jat, H. S., Yadav, A. K., Sidhu, H. S., Jat, M. L., Choudhary, M., Peter, J. K., and Sharma, P. C. (2018). Burning issues of paddy residue management in North-West states of India. *Renewable and Sustainable Energy Reviews*, 81, 693–706.

Maraseni, T. N., and Qu, J. (2016). An international comparison of agricultural nitrous oxide emissions. *Journal of Cleaner Production*, 135, 1256–1266.

Menghani, V., and Sharma, K. K. (2022). *CO_2 baseline database for the Indian power sector*. User Guide, 18, Central Electricity Authority, New Delhi, Ministry of Power, Government of India.

MoEFCC. (2021). *Third biennial update report to the united nations framework convention on climate change*. Ministry of Environment, Forest and Climate Change, Government of India.

Nguyen, H. V., Nguyen, C. D., Van Tran, T. V., Hau, H. D., Nguyen, N. T., and Gummert, M. (2016). Energy efficiency, greenhouse gas emissions, and cost of rice straw collection in the Mekong River Delta of Vietnam. *Field Crops Research*, 198, 16–22.

Pang, B., Zhou, T., Cao, X. F., Zhao, B. C., Sun, Z., Liu, X., Chen, Y. Y., and Yuan, T. Q. (2022). Performance and environmental implication assessments of green bio-composite from rice straw and bamboo. *Journal of Cleaner Production*, 375, 134037.

Puettmann, M., Oneil, E., and Wilson, J. (2013). *Cradle-to-gate life-cycle assessment of US medium density fiberboard production*. University of Washington. https://corrim.org/wp-content/uploads/2018/06/MDF-LCA-final-Sept-2013.pdf

Puettmann, M., and Salazar, J. (2018). *Cradle-to-gate life-cycle assessment of North American particleboard production*. University of Washington, Seattle, WA. https://corrim.org/wp-content/uploads/2019/03/LCA-Particleboard.pdf

Ralph, J., Lundquist, K., Brunow, G., Lu, F., Kim, H., Schatz, P. F., Marita, J. M., Hatfield, R. D., Ralph, S. A., Christensen, J. H., and Boerjan, W. (2004). Lignins: Natural polymers from oxidative coupling of 4-hydroxyphenyl-propanoids. *Phytochemistry Reviews*, 3, 29–60.

Ravindra, K., Singh, T., and Mor, S. (2019). Emissions of air pollutants from primary crop-residue burning in India and their mitigation strategies for cleaner emissions. *Journal of Cleaner Production*, 208, 261–273.

Raza, M. H., Abid, M., Yan, T., Naqvi, S. A. A., Akhtar, S., and Faisal, M. (2019). Understanding farmers' intentions to adopt sustainable crop residue management practices: A structural equation modeling approach. *Journal of Cleaner Production*, 227, 613–623.

Saini, K., and Matsagar, V. (2023). *Natural fiber-reinforced foamed concrete panels strengthened with bio-composites for sustainable infrastructures: Restoring traditional Indian construction practices*. Global Indian Young Scientists Research and Innovation Conference, New Delhi, India, May 31 to June 2.

Shang, X., Song, S., and Yang, J. (2020). Comparative environmental evaluation of straw resources by LCA in China. *Advances in Materials Science and Engineering*, 2020, 1–16.

Sharma, M., Sahajpal, I., Bhuyan, A., and Chauhan, A. (2019). *Impact assessment report for crop-residue management project*. Confederation of Indian Industry (CII), New Delhi.

Silva, D. A. L., Firmino, A. S., Ferro, F. S., Christoforo, A. L., Leite, F. R., Lahr, F. A. R., and Kellens, K. (2020). Life-cycle assessment of a hot-pressing machine to manufacture particleboards: Hotspots, environmental indicators, and solutions. *The International Journal of Life-cycle Assessment*, 25, 1059–1077.

Singh, A., and Basak, P. (2019). Economic and environmental evaluation of rice straw processing technologies for energy generation: A case study of Punjab, India. *Journal of Cleaner Production*, 212, 343–352.

Singh, G., and Arya, S. K. (2021). A review on management of rice straw by use of cleaner technologies: Abundant opportunities and expectations for Indian farming. *Journal of Cleaner Production*, 291, 125278.

Soam, S., Borjesson, P., Sharma, P. K., Gupta, R. P., Tuli, D. K., and Kumar, R. (2017). Life-cycle assessment of rice straw utilization practices in India. *Bioresource Technology*, 228, 89–98.

Soam, S., Kapoor, M., Kumar, R., Borjesson, P., Gupta, R. P., and Tuli, D. K. (2016). Global warming potential and energy analysis of second generation ethanol production from rice straw in India. *Applied Energy*, 184, 353–364.

Thannimalay, L., Yusoff, S., and Zawawi, N. Z. (2013). Life cycle assessment of sodium hydroxide. *Australian Journal of Basic and Applied Sciences*, 7(2), 421–431.

Theng, D., Arbat, G., Delgado-Aguilar, M., Ngo, B., Labonne, L., Evon, P., and Mutjé, P. (2017). Comparison between two different pretreatment technologies of rice straw fibers prior to fiberboard manufacturing: Twin-screw extrusion and digestion plus defibration. *Industrial Crops and Products*, 107, 184–197.

Theng, D., Arbat, G., Delgado-Aguilar, M., Ngo, B., Labonne, L., Mutjé, P., and Evon, P. (2019). Production of fiberboard from rice straw thermomechanical extrudates by thermopressing: Influence of fiber morphology, water and lignin content. *European Journal of Wood and Wood Products*, 77, 15–32.

Wang, Z., Lei, T., Yang, M., Li, Z., Qi, T., Xin, X., He, X., Ajayebi, A., and Yan, X. (2017). Life-cycle environmental impacts of cornstalk briquette fuel in China. *Applied Energy*, 192, 83–94.

Wanhua Ecoboard Co. Ltd. (2017). *Wheat/rice straw particleboard sample testing report*. Wood Products Quality Test and Inspection of State Forestry Administration (Nanjing). www.wanhuaboard.com/Home/Index/brand_certification.html (accessed on September 8, 2023).

Zhang, L., and Hu, Y. (2014). Novel lignocellulosic hybrid particleboard composites made from rice straws and coir fibers. *Materials and Design*, 55, 19–26.

Section 3

Critical Infrastructure

8 Assessment of Renewable Energy Strategies to Achieve Net-Zero Energy

A Potential Drive Towards Sustainability in Buildings

J S Sudarsan and Deepak M D

8.1 INTRODUCTION

Energy-efficient buildings have always been a milestone for India to achieve its goal of a green world (Tiwari, 2023). In today's world, development for any country includes active participation towards saving natural resources and using sustainable ways to produce their energy. Energy has always been a point of attraction for developing countries like India for which the government aims to find different ways to produce, save, and utilize energy effectively. Along these lines, energy saving has now become the utmost priority for the construction, real estate, infrastructure, and project (CRIP) market to set a benchmark for the development of any nation (Vecchi et al., 2013). In this regard, identifying proven tried-and-true technologies that combine with each other to support having a green building being an achievable target is essential. Sustainability, in general, means providing needs to the present without compromising the needs of the future generation. In the present world, around 788 crore (tens of millions) people are living on this planet, and still growing, so there will always be a demand for resources (Kumar and Saikia, 2020). The major contributions that drive resource consumption are energy fuels like oil, coal, mineral resources, etc., which are required to make the majority of the products. The major demand and shift are needed to utilize solar panels as a means to provide electricity to buildings, which can contribute to saving energy in large amounts (Mekhilef et al., 2011). All over the globe, solar energy is considered to be one of the main aspects of construction work, whether it is a home, school, office, hospital, skyscraper, or any other kind of building infrastructure. Due to the increase in pollution, global warming is increasing day by day, so to control the environmental aspects, the construction industry can contribute to the environment through wastewater management and

DOI: 10.1201/9781032686899-11

solar energy, which additionally helps in saving our mother earth (Omer, 2008). With the adverse aim to change the trend in urban planning, the green building revolution will result in a better eco-neighborhood model that will change living habits and make them more responsible towards their environment.

India is a country that is endowed with vast solar energy potential and is rapidly developing. Nearly 5000 trillion kWh per year of energy is incident over the land area of India, with most parts receiving 4–7 kWh [per sq. meter] per day (Ummadisingu and Soni, 2011). The industry greatly benefits from this type of renewable source of energy. In this regard, the conversion of solar energy into electricity is carried out from the light and heat of the sun that is captured. Solar energy can be utilized in different ways, and hence this energy from the sun is referred to as solar energy. This technology involves the collection of photovoltaic cells, and through the photovoltaic effect electricity is generated, which can then be used for various purposes like home industry and commercial purposes. Solar power systems are used to generate electricity as there is no emission of hazardous greenhouse gases in the atmosphere. Some benefits of solar energy are regarding the maintenance and energy production of solar energy is actually zero because there is no need for any outside supply of power to work. There is only the initial cost during the manufacturing process and installation of components. Even if there is insufficient space, solar systems can be installed with ease and simplicity. Due to its flexibility and modularity, the solar system can be expanded depending on the needs. In the major places amongst the Indian geographical context, the period of the day between 11.00 am to 4.00 pm is where the energy demand is higher. With the increasing demand in energy, production also reaches its maximum during this period. There is no generation of noise pollution and waste as there is no maintenance, and its lifespan is longer compared to other energy products. In this line, the objectives of the present work are to:

1. Determine the necessity of solar energy as an energy-efficient energy source in buildings.
2. Estimate the cost-benefit analysis of solar panels by taking real-life buildings into consideration and determining the energy consumption among solar energy panels in a residential building.

8.2 LITERATURE REVIEW

8.2.1 Importance of Solar Energy

The importance of solar energy in the commercial sector aims at investigating the solar mission through which the application of utilizing solar energy to free 20 gigawatts of utility-scale grid-linked capability in the Indian growing economy (Millison et al., 2022). This helps in creating an indigenous concentration of solar-strength enterprises and delivery chain systems. Based on this preliminary success, the latest World Bank document argues that India is nicely poised to be the worldwide leader in solar power (Foster and Rana, 2019). The National Solar Mission (NSM) serves as an essential instance of large-scale business renewable power improvement, helping a broader purpose of inclusive financial improvement (Millison et al., 2014). Moreover, Sass et al. (2012) showed that the growing price of fossil fuels, incentives towards government bodies, and the development of public consciousness for the desire to enforce sustainable electricity elements have resulted in a massive growth in solar panel installations throughout the country. Additionally, Ahmad et al. (2018) argued that adding solar panels to a present roof considering the general way elevated masses ought to be borne with the aid of using the construction's structural elements. Based on these implications, the cost-benefit analysis is undertaken to know about the effective use of solar energy. In line with this, Ge et al. (2022) focus on the externalities of funding choices with reference to residential photovoltaic structures that have been converting unexpectedly in recent years. Five case researches have been analyzed to populate the generalized observations of numerous photovoltaic funding conditions. For the ones taking part in both low-energy charges and peak solar hours, the effects of this evaluation no longer aid the setup of a photovoltaic system. Furthermore, Wang and Oliveira (2006) studied solar-powered adsorption air-conditioning systems modified into design aspects of the buildings. The operational average overall performance underneath an ordinary strolling mode in the summer season includes temperature variations of solar collector arrays, warmth storage tanks, and adsorption chillers similar to refrigerating output variations of the system. The solar fraction in the summer season is considered to be 71.73% (Zhai et al., 2006). In addition, the variations of solar-powered air-conditioning systems significantly affect the average overall performance with ambient parameters and strolling parameters.

8.2.2 Integrated Design of Energy-Efficient Buildings

The next step is to understand the dynamics of energy efficiency in buildings with the integration of solar energy. One such study indicated that the use of solar water heating systems shows a 76% reduction in energy consumption as compared to the electric water heater (Abd-ur-Rehman et al., 2018). Moreover, Ufuk Gökçe and Umut Gökçe (2014) proposed a model-driven holistic device structure integrating IT structures at the design, construction, and operation tiers of homes that are offered to optimize the construction operations. The primary intention was to create a holistic environment for tracking systems and structures to grow the performance of the general device improvement method and to make the most of their capacity for discount of constructing electricity consumption. In line with this, Wahju and Nur (2023) advised to assist and solve issues associated with renewable strength initiatives that are concerned with sustainable photovoltaic design.

In the construction sector, Chaudhari et al. (2013) focused on defining the answers for the power green futuristic buildings. The implementation of the latest era in production will cause higher construction with inexperienced rating systems. Green construction has to considerably store water and power as compared to the standard construction process. Some of the green construction process considerations are of excessive thermal insulation, rainwater harvesting, terrace gardening, airflow, and power green appliances (Suribabu et al., 2022). Strategically putting home windows and skylights can reduce the need for electric lights in the course of the day. Lastly, Solmaz et al. (2010) used the approach of synthetic neural networks to estimate the hourly solar radiation of six decided provinces in Turkey. One neuron generating a corresponding output sign of hourly solar radiation becomes applied inside the output layer of the network. The outcomes acquired from each fashion were compared through the usage of distinctive neurons, implying squared error, coefficient of determination, and absolute error. In this observation, the prediction of hourly solar radiation with distinctive fashions is compared.

In designing the solar panels along with its building orientation, Charalambides and Wright (2013) demonstrated that the optimal orientation of a building is significantly affected by the proportions, the latitude, and the climate of the particular location. In contrast, azimuth angles play a much more important role in warmer climates and lower latitudes. Experiments were conducted on rectangular building forms with a predetermined range of U values. Similarly, Iodice et al. (2017) followed the principal concept of the idea that exploitation of solar strength in solar thermal-aided strength-technology plant life may be an extra cost and strength-powerful than the usage of it in solely solar plant life, particularly in medium-temperature systems. For this purpose, the study focuses on biomass-solar mixed configuration with the conversion in performance of solar strength that is appraised to evaluate the exploitation of solar strength in plant life characterized through one-of-a-kind plant configurations. When it comes to bioenergy, the average growth rate is greater than 8%, and this sector accounts for more than two-thirds of the renewable energy mix and 13–14% of overall energy consumption (Srinivasan et al., 2023). In this regard, Ilie et al. (2017) showed the strength used inside the constructed surroundings represents about 40% of the overall strength utilized with the aid of the network, with notably better values in rural communities. Out of this, a sizable proportion is used for heating, cooling, and home warm water manufacturing. In a primary step, renewables—primarily based in totally domestic hot water (DHW) manufacturing—may be taken into consideration due to the fact that it is extraordinarily steady for the duration of the year, and solar-thermal structures constitute top applicants due to the fact there is already an excessive popularity on the network stage for this sort of system. This considers a unique set of techniques for the layout of solar-thermal structures carried out in alternatively small communities, in consideration to the real strength intake for DHW manufacturing in collective households. Furthermore, Atif and Al-Sulaiman (2018) argue about the energy evaluation that turned into the complete incorporated gadgets. The evaluation was performed every whole day in order that the garage gadget operated for 24 hours without the want for any auxiliary warmness supply no matter the internal energy output of the incorporated gadget. It concluded that the best and the lowest energy destruction happened inside the significant receiver gadget and the thermal garage gadget, respectively.

8.3 RESEARCH METHOD AND DATA COLLECTION

The research method adopted in the study (referring to Figure 8.1) involves data collection through a systematic review of the literature and is followed by collecting relevant research articles in the area of the study. Based on these details, a survey was conducted to understand the awareness and mentality of common people about the

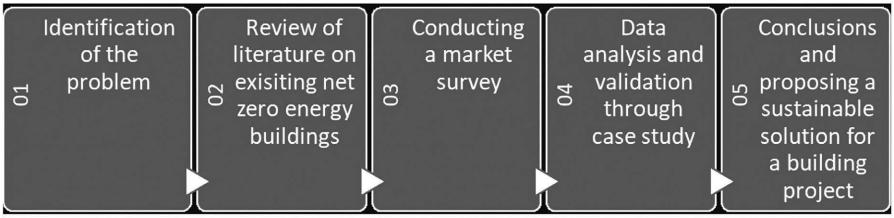

FIGURE 8.1 Research method (authors' own creation).

solar energy aspect in the study area. In order to check the effect of building physics as well as the problems encountered during the adoption and feasibility of solar panels, the case study of a building project is considered to validate the study findings.

8.4 Results and Discussion

For the case study, a building in Nagpur, Maharashtra, India was selected, which has three open sides and one adjacent attached to it. The building is facing towards the west and has a rectangular open slab. Measurements of buildings were taken by conducting a manual survey, and the building plan was prepared using Autodesk Revit Architecture.

8.4.1 Case Study of a Residential Building in Nagpur, Maharashtra

The details of the case study considering the region of Nagpur, Maharashtra, India highlighted with respect to its average solar radiation, ambient temperature, daily solar radiation, and monthly average irradiation. Nagpur in the central region of India experiences various seasonal temperature fluctuations. The prime time for the solar panels to receive appropriate solar radiation is between 11 a.m. to 1 p.m. This region experiences maximum irradiation and minimum variation of daily solar radiation that supports solar panels to receive sun rays in all months, so it is the selection of the case study.

Based on the information obtained from solar panel manufacturers, installers, and solar energy consultants, details were as follows:

One small rectangular panel of size 1m x 2m can produce around 320 to 350 W. Hence, around three such panels constitute 1kW of solar power generation. A 1kW solar panel costs around Rs. 1,50,000 to Rs. 1,80,000. The cost becomes lesser (i.e., increases at a lower ratio) as we go on, increasing the capacity of solar panels. And so, 2–2.5kW panels may cost around 2.5 to 3 lakhs rupees. Further, a 5kW panel will cost around 3.75–4.25 lakhs rupees.

The total cost of the solar system includes (panel cost + structure cost + cable cost + inverter + labor charges + net meter cost + AMC). An inverter is to be installed for converting DC into AC, and one inverter may be sufficient for power generation of 1kW to 5kW. The number of inverters required is equal to the number of meters. Suppose the inverter required for a 1kW solar panel costs 80000 to 90000, then an inverter for a 4–5kW panel will cost 120,000 to 150,000 at maximum.

Maintenance of the solar system includes periodic checking/inspection of solar panels, cables, and structure, periodic cleaning of panels, and checking the condition of the inverter, meter, and all electrical connections. Small windows/openings are provided in big solar panels to reduce the effect of wind pressure on the panels. Also, cleaning of panels is its secondary benefit. A detailed list of different available types of solar cells in India is provided in Table 8.1.

One household where the monthly bill for electricity is around Rs. 400 to 600 would require a 1kW solar panel. Solar panel works on a negative temperature coefficient, i.e., when the panels are less heated, or cooled, they work more efficiently. Hence in summer, though the sunrays/radiations are continuous and intense, the heating of these panels reduces their efficiency up to 70%–80%. But in monsoon season, though the sun's rays may not be available for the entire day, whenever they are present, the excellent panels have increased efficiency in generating power. Hence, the overall efficiency of solar panels, even in monsoon season, is 40% to 60%. The warranty for the complete solar system is around 18 to 20 years, and it increases up to 25 years for solar panels only, whereas the inverter has only about 7 years warranty. Based on the system size and approximate roof space area, the typical annual output of power is determined. For example, for system sizes of 1kW and roof sizes of 8 square meters, the typical annual output is 850kWh.

Two different types of solar panels were studied and compared through their techno-commercial specifications. The details of these panels and their comparison are provided in Table 8.2.

TABLE 8.1
Different Available Types of Solar Cells in India

Solar Cell Type	Efficiency Rate	Advantages	Disadvantages
Monocrystalline Solar Panels (Mono-SI)	20%	High-efficiency rate; optimized for commercial use; high lifetime value	Expensive
Polycrystalline Solar Panels (p-Si)	15%	Lower price	Sensitive to high temperatures; lower lifespan and slightly less space efficiency
Thin-Film: Amorphous Silicon Solar Panels (A-SI)	7–10%	Relatively low costs; easy to produce and flexible	Shorter warranties and lifespan
Concentrated PV Cell (CVP)	41%	Very high performance and efficiency rate	Solar tracker and cooling system needed (to reach high-efficiency rate)

TABLE 8.2
Comparison of Two Types of Solar Panels Commonly Adopted in the Indian Context

Sr. No.	Technical Details	Waaree 350W Monocrystalline Solar Panel	Canadian CS6X-325P 325-Watt Solar Panel
1.	Nominal Maximum Power (Pm) in Watts	350	325
2.	Open Circuit Voltage (Voc) in Volts	46.40	45.5 V
3.	Short Circuit Current (Isc) in Amps	9.80	9.34 A
4.	Maximum System Voltage in Volts	1000	DC 1000 V
5.	Module Efficiency (%)	18.07	16.16%
6.	Length x Width x Thickness (LxWxT) mm	1960 x 990 x 40	1954 x 983 x 40
7.	Weight (kg)	22.50	22
8.	Solar Cells per Module (Unit)/Arrangement	72/(12*6)	72
9.	Frame Material	Anodized Aluminum Alloy	Anodized Aluminum Alloy
10.	Connector (Protection degree/Type)	IP67 rated/MC4 compatible	MC4 or MC4 Comparable
11.	Cable cross-section	4 mm²	4 mm²
12.	Pricing	Buy 2 for Rs.11,936 each, save 8% Buy 6 for Rs.11,723 each, save 9% Buy 10 for Rs.11,404 each, save 12%	Buy 2 for Rs.10,867 each, save 17.88% Buy 6 for Rs.10,787 each, save 18.12% Buy 10 for Rs.10,739 each, save 18.85%.
13.	Warranty	10 Years Materials and Workmanship 25 years linear power output	10 Years Materials and Workmanship 25 years linear power output

8.4.2 Detailed Calculations of Energy Consumption and Its Analysis

The most typical size used for residential installations is 65 inches x 39 inches, while the common size for commercial applications is 77 inches x 39 inches. Additionally, a cost survey is conducted related to the price of solar panels in Pune, Maharashtra.

Different quotations were received and compared with the most suitable market cost vendors, and the price comparison is provided in Table 8.3.

From these data, after comparing all the features and technical details, it was decided that the use of polycrystalline solar panels is proved to be economical with greater technical benefits for residential buildings. After acquiring all these details, it was time to design our solar model in AutoCAD Revit Architecture (refer to Figure 8.2a). We designed the 3D model taking the exact dimensions of the house into consideration. For that, we took a manual measurement survey to take the dimensions of the house (refer to Figure 8.2b).

From Figure 8.2, we can see the 3D model of the residential house we designed for the purpose of installing the solar panels. Four panels were taken into consideration to provide electricity to the house considered for the case study. For the comparison purpose of whether installing these solar panels is actually economical or not, we collected the electricity bill of the house for the year 2022 and approached to calculate total energy consumption. The extraction of units used is determined from the physical bill from the past 12 months and the amount paid as part of energy consumption. Based on the energy consumption, the average consumption of electricity for the period of 2022, the total energy consumption of the building is 2661 units (1 unit = 1kWh; Total kW/h = 2661 KW/h). The calculations of the remaining part of the analysis are as follows:

TABLE 8.3
Comparison of Two Types of Solar Panels Commonly Adopted in the Indian Context

Sr. No.	Technical Details	Silfab SIL-370 HC	Panasonic Solar Module-4
1.	Manufacturer	Silfab	Panasonic
2.	Efficiency %	20.2	21.6
3.	Rated Power W	370	400
4.	Power Tolerance	0 to 10 W	−0/+10 W
5.	Temperature Coefficient	PMax:—0.36 Voc:—0.28	PMax:—0.26 Voc:—0.24
6.	Resiliency	Snow Wind Hail Fire	Snow Wind Hail Fire
7.	Output at End of Warranty Term (%)	82.6	92.0
8.	Cell Colours	Black	Black
9.	Panel Dimensions	1762.0 mm L 1037.0 mm W 35.0 mm D	1821.0 mm L 1016.0 mm W 30.0 mm D
10.	Connector Type	1350 mm, ø 5.7 mm, MC4 from Staubli	Staubli MC4
11.	Manufacturing Location	United States	South Korea

A Model of the residential house.

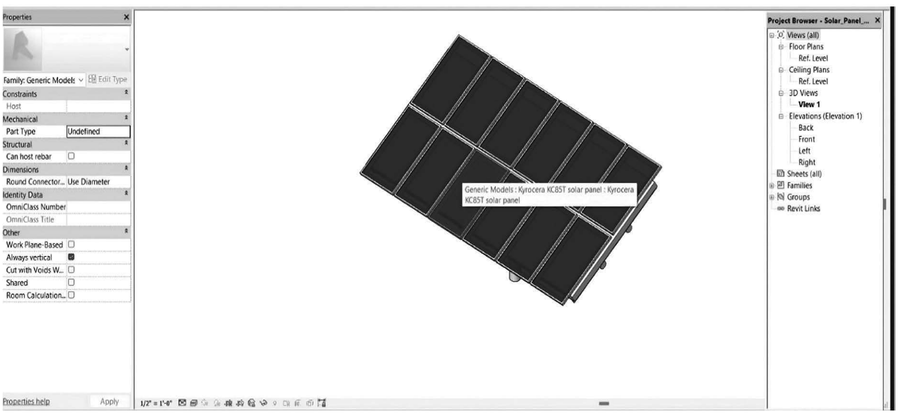

B Placing of solar panels.

FIGURE 8.2 Modelling the building dynamics and placing of the solar panels

The output of the selected solar panel (Silfab SIL-370 HC) is 370 Watts per hour, i.e., 1kW/h for one whole panel. Assuming power loss, it is predicted that the actual output would be approximately 350 Watts per hour. The sun's rays are assumed to be intense and capable of generating electricity only for a period of 6 hours per day. Therefore, the annual output of the above-mentioned solar panel would be = 350 x 6 x 365 = 7,66,500 watts, i.e., 766.5 kW. Based on this, the required number of solar panels for the house would be four as it will produce 766.5kW x 4 = 3066kW. Based on this, the area required for the installation of the solar panels would be four panels of 1762mm x 1037mm x 35mm = 7.30 sq.m.

As per the details provided in Table 8.3, the cost of the selected solar panel (Silfab SIL-370 HC) is Rs.60,000 for a set of one panel. Therefore, the total charges for the installation of four solar panels would be Rs.60000 x 4 = Rs. 2,40,000 (this includes the installation charges). Additionally, the government also provides a 30% subsidy on the installation of solar panels. Therefore, the cost of solar panels would be 2,40,000 x 30% = Rs. 1, 68,000. Now, the total amount paid in the year 2022 is Rs. 26,745. Therefore, taking Rs. 26,745 as the base amount for every year, 1,68,000/26,745 ~ 6.5 years to make installation of solar free (payback period). Overall, the findings of the study indicate that not only cost savings are attained, but also the focus towards environmental sustainability is achieved.

Energy conservation has become a vital area to be concentrated with the increasing demand (Ramana et al., 2015). Cutting down the consumption by a certain percentage is one such key concept to conserve energy for future demand. The outcome of the study was further validated using the Eco Niwas Tool, a platform for clients, contractors, and other environmental specialists to undertake a preliminary evaluation of the effect of project design on energy, environment, and monetary aspects. The analysis was modeled on the platform and is shown in Figure 8.3. The outcome of these figures indicates that the energy savings in the residential building can contribute towards the betterment of society.

Though the cost is found to be huge at present, in the future, the cost of these solar panels will be the same as that of ordinary energy consumption of various tools and appliances and will eventually be the only resource for an enhanced future. The various investment criteria used in the project also indicate that implementing energy conservation methods proves to be beneficial in terms of both energy and cost-savings.

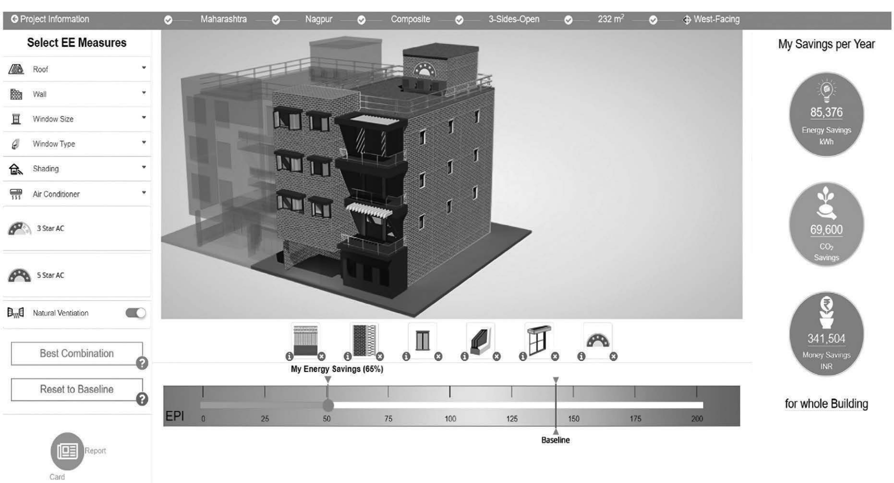

A Eco Niwas Tool.

(Source: www.econiwas.com)

FIGURE 8.3 Analysis and modeling using Eco Niwas Tool.

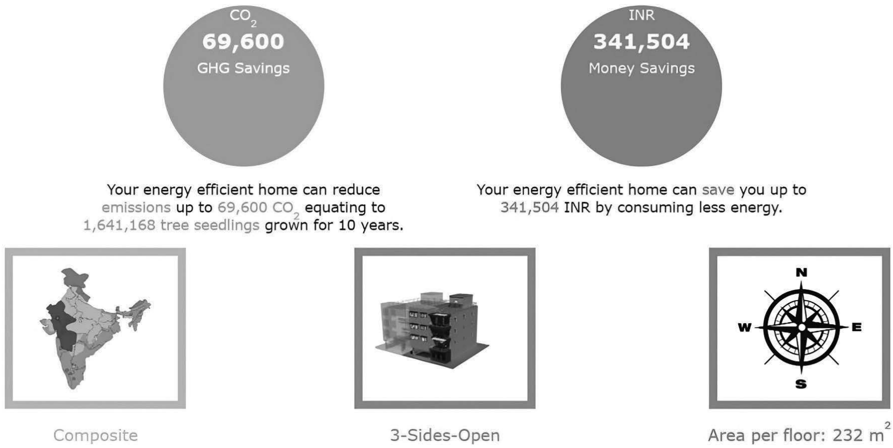

B Comparison of prices between conventional electricity and solar panels.

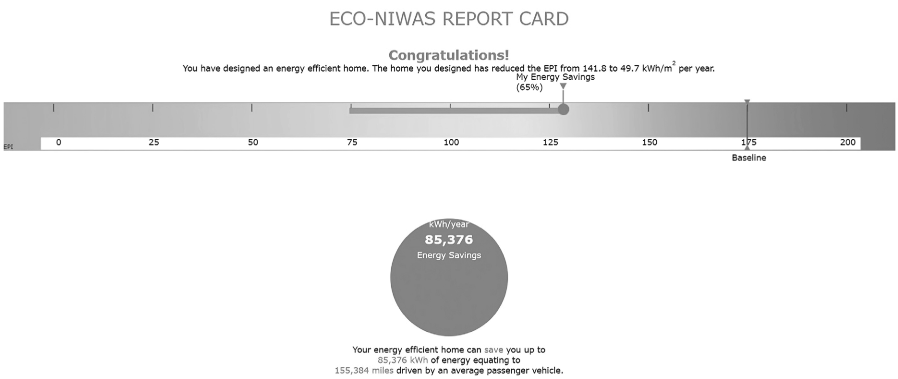

C Report card of the residential building.

FIGURE 8.3 (Continued)

8.5 CONCLUSIONS AND RECOMMENDATIONS

Energy is considered to be one of the most important elements in the present world. With the increase in population, energy demand is also increasing. The energy demand can only be satisfied up to a certain limit, and it is difficult to fulfill the energy demand beyond the reach, especially when energy production is less compared to the demand. Hence there is a necessity to come up with such alternative ideas to fulfill the demand and conserve energy at the same time. One such idea is discussed in this chapter, and the results of the same in the means of its beneficiaries are also discussed. India has a remarkable scope for solar energy in the future because of its geographical location as it has solar radiation all over the year.

In this present time of development, the use of energy plays a vital role in all industry outlooks, but the generation of energy using natural minerals and oils comes with some after-effects. Considering this issue as one of the prime concerns to evaluate, government all over the world is taking the initiative to save our mother earth by using ways to generate energy sustainably. Solar energy is one such energy that is abundant in nature. Over a billion people lack access to electricity, and climate change is serving up droughts, floods, and heatwaves with alarming regularity. Much of the disastrous state of the world is due to the solar power revolution sputtering out. The revolution that spurred around 2020 has created the demand for solar power, which has become the cheapest source of electricity on the planet. From Chile to China, solar farms sprouted more than any other kind of power plant. But today at the midcentury mark, fossil fuels exert a stranglehold on the global economy. Coal and natural gases are burnt to produce the majority of the world's electricity and run its factories. Solar power today is on track to sputter out with urgent investments in innovations from governments around the world. Solar power could actually break through the ceiling that it is currently headed for and achieve its sky-high potential. Every hour, solar beams down more energy than the world uses in an entire year. The major setback is the lack of awareness among individuals and the ability to tap into energy consumption and reusability from these sources. One of the potential ways is considering the application of solar panels that help in taking a significant step towards a sustainable future in our homes. This will not only help our environment but also will save a lot of cost in the future. Based on the study implications, it is recommended to adopt this tool (Eco Niwas Tool) to optimize resource utilization and energy utilization, which will help in achieving sustainability and net-zero energy in the CRIP sector. This initiative must happen at the stage of building approval so that effective implementation can be achieved.

REFERENCES

Abd-ur-Rehman, H. M., Al-Sulaiman, F. A., Mehmood, A., Shakir, S., & Umer, M. (2018). The potential of energy savings and the prospects of cleaner energy production by solar energy integration in the residential buildings of Saudi Arabia. *Journal of Cleaner Production*, 183, 1122–1130.

Ahmad, N. I., Ab-Kadir, M. Z. A., Izadi, M., Azis, N., Radzi, M. A. M., Zaini, N. H., & Nasir, M. S. M. (2018). Lightning protection on photovoltaic systems: A review on current and recommended practices. *Renewable and Sustainable Energy Reviews*, 82, 1611–1619.

Atif, M., & Al-Sulaiman, F. A. (2018). Energy and exergy analyses of recompression brayton cycles integrated with a solar power tower through a two-tank thermal storage system. *Journal of Energy Engineering*, 144(4), 04018036.

Charalambides, J., & Wright, J. (2013). Effect of early solar energy gain according to building size, building openings, aspect ratio, solar azimuth, and latitude. *Journal of Architectural Engineering*, 19(3), 209–216.

Chaudhari, J. R., Tandel, K., & Patel, V. (2013). Energy saving of green building using solar photovoltaic systems. *Energy*, 2(5).

Foster, V., & Rana, A. (2019). *Rethinking power sector reform in the developing world*. World Bank Publications.

Ge, M., Zhao, Y., Li, Y., He, W., Xie, L., & Zhao, Y. (2022). Structural optimization of thermoelectric modules in a concentration photovoltaic—thermoelectric hybrid system. *Energy*, 244, 123202.

Ilie, A. C., Visa, I., & Duta, A. (2017). Solar—thermal systems for domestic hot water production implemented in collective households. *Journal of Energy Engineering*, 143(6), 04017065.

Iodice, P., Langella, G., & Amoresano, A. (2017). A numerical approach to assess air pollution by ship engines in manoeuvring mode and fuel switch conditions. *Energy & Environment*, 28(8), 827–845.

Kumar, R., & Saikia, P. (2020). Forest resources of Jharkhand, Eastern India: Socio-economic and bio-ecological perspectives. In *Socio-economic and eco-biological dimensions in resource use and conservation: Strategies for sustainability* (pp. 61–101). Springer.

Mekhilef, S., Saidur, R., & Safari, A. (2011). A review on solar energy use in industries. *Renewable and Sustainable Energy Reviews*, 15(4), 1777–1790.

Millison, D., George, L., Acharya, J., & Wijayatunga, P. (2022). Enabling policy and regulatory environment for solar power development: Lessons in Asia-Pacific region. *Solar Compass*, 2, 100023.

Millison, D., Purka, D., & George, L. (2014). Power for the people: Early lessons from utility-scale solar power development in India. In *ICSI 2014: Creating infrastructure for a sustainable world* (pp. 337–348). ASCE Proceedings.

Omer, A. M. (2008). Energy, environment and sustainable development. *Renewable and Sustainable Energy Reviews*, 12(9), 2265–2300.

Ramana, P. V., Kumar, B. S., & Maheswar, D. (2015). A comprehensive study on solar power plant at educational institute level. *International Journal of Scientific Research & Engineering Trends*, 2(04), 1063–1071.

Sass, T., Sass, S., & Sass, K. (2012). Solar panel installations on existing structures. In *Advances in hurricane engineering: Learning from our past* (pp. 528–538). ASCE Proceedings.

Solmaz, O., Kahramanli, H., Kahraman, A., & Ozgoren, M. (2010, November). Prediction of daily solar radiation using ANNs for selected provinces in Turkey. In *International scientific conference* (pp. 450–456). Gabrovo, Bulgaria. https://singipedia.singidunum.ac.rs/preuzmi/40331-prediction-of-daily-solar-radiation-using-anns-for-selected-provinces-in-turkey/292

Srinivasan, K., Sudarsan, J. S., & Nithiyanantham, S. (2023). Need of bioenergy—an insight into global perspective. In *Bioenergy* (pp. 7–24). Springer.

Suribabu, C. R., Sudarsan, J. S., & Nithayanntham, S. (2022). Feasibility assessment of low-cost filter to adopt in rooftop rainwater harvesting (RWH). In *Climate change impact on groundwater resources: Human health risk assessment in arid and semi-arid regions* (pp. 421–438). Springer International Publishing.

Tiwari, A. (2023). Advancement of materials to sustainable & green world. *Advanced Materials Letters*, 14(3), 2303–1724.

Ufuk Gökçe, H., & Umut Gökçe, K. (2014). Integrated system platform for energy efficient building operations. *Journal of Computing in Civil Engineering*, 28(6), 05014005.

Ummadisingu, A., & Soni, M. S. (2011). Concentrating solar power—technology, potential and policy in India. *Renewable and Sustainable Energy Reviews*, 15(9), 5169–5175.

Vecchi, V., Hellowell, M., & Gatti, S. (2013). Does the private sector receive an excessive return from investments in health care infrastructure projects? Evidence from the UK. *Health Policy*, 110(2–3), 243–270.

Wahju, M. B., & Nur, T. (2023). Opportunity and challenge for small wind power project in Indonesia. In *AIP conference proceedings* (Vol. 2485, No. 1). AIP Publishing.

Wang, R. Z., & Oliveira, R. G. (2006). Adsorption refrigeration—an efficient way to make good use of waste heat and solar energy. *Progress in Energy and Combustion Science*, 32(4), 424–458.

Zhai, X., Wang, R., Dai, Y., & Wu, J. (2006). *Experimental research and performance analysis of a solar-powered air-conditioning system in a green building*. Green building of Shanghai Institute of Architectural Science, Shanghai, Energy Systems Laboratory, Texas A&M University. https://hdl.handle.net/1969.1/5443

9 Wind and Wave Vulnerability Assessment of Monopile-Supported Offshore Wind Turbine

Thottathil Sarathkumar, Muhamed Safeer Pandikkadavath and K K Akheel

9.1 INTRODUCTION

The increasing demand for clean and renewable energy drives the governments to go for offshore wind turbines (OWTs) (Breton and Moe, 2009). The abundance of higher wind speed, possibility for greater capacity wind turbines and the availability of spacious offshore area further encourages the promoters to invest in OWTs (Jonkman et al., 2008). Among many options, shallow water monopile OWTs are cost effective in terms of design, manufacturing and installation (Markard and Petersen, 2009). Additionally, they are more stable, durable and facilitate lower cost for power transmission to land (Breton and Moe, 2009; Akheel et al., 2021; Markard and Petersen, 2009). Nevertheless, monopile OWTs are vulnerable to extreme wind and wave loads (Jonkman et al., 2009; Wei et al., 2014; Ou et al., 2017; Costoya et al., 2020). Investigations on a 5-MW National Renewable Energy Laboratory (NREL) monopile OWT base model for a given shallow depth showed that vulnerability of flexural demands at monopile mud-level line is significantly large under combined wind and wave effects (Wei et al., 2014; Arany et al., 2015; Pokhrel and Seo, 2019; Zuo et al., 2020). A similar investigation encompassing the wind turbine blade tip deflection reported that there is high exceedance probability (with respect to design limits) of the response under the critical wind speed accounted (Hallowell et al., 2018; Li et al., 2018; Pokhrel and Seo, 2019; Liu et al., 2022). Based on these understandings, many researchers numerically attempted to quantify the safe design loads for OWTs (Wang et al., 2023; Dupuis and Anis, 2013; He and Ye, 2023; Fajuyigbe and Brennan, 2022). Multi-hazard fragility analysis revealed that wind speed is the critical load parameter for tower top deflections, whereas the wave height is the relevant parameter to cause major hike in the mud-line overturning bending moment (OBM) (Hallowell et al., 2018; Li et al., 2018; Pokhrel and Seo, 2019; Wilkie and Galasso, 2020; Mardfekri and Gardoni, 2013). Additionally, the damage to monopile may lead to increased losses compared to the blade failure. Resilience assessment of the OWTs considering the wind and

DOI: 10.1201/9781032686899-12

wave effects reaffirmed the above discussed findings, especially the mudline OBM effects (Pokhrel and Seo, 2019; Wilkie and Galasso, 2021; Seo et al., 2022).

Most of these investigations are carried out for the standard water depth of 20 m (Hallowell et al., 2018; Pokhrel and Seo, 2019; Wilkie and Galasso, 2021; Seo et al., 2022), and hence the current study assesses the vulnerability of mudline OBM of a standard 5-MW NREL monopile OWT for the same benchmark water depth. Initially, standard NREL 5MW monopile reference OWT is selected, and the relevant dimensions and properties are described. The wind speed at different heights, the associated forces and the resultant OBM due to wind are extracted as per DNV guidelines (DNV, 2014). Likewise, to incorporate the wave effect, significant wave height conditioned on wind velocity as well as time period is calculated. It is worth noting that this parameter depends on the water depth as well. Subsequently, wave particle velocity and acceleration over the depth is determined. The resulting wave forces are utilized to get the OBM at mudline due to wave effect. The coupled effect is included by the algebraic sum of peak OBMs due to wind and wave forces (Pokhrel and Seo, 2019). Taking bending strength of the adopted OWT at mudline as the damage state (DS) threshold, and the OBM due to environmental load as the demand (D), fragility curves are also generated and explained (Pokhrel and Seo, 2019; Sarathkumar et al., 2023).

9.2 REFERENCE NREL 5MW OWT

As mentioned in the previous section, NREL 5MW reference OWT supported on monopile is chosen for the demonstration (Jonkman et al., 2008; Hallowell et al., 2018; Li et al., 2018; Pokhrel and Seo, 2019; Liu et al., 2022). The geometric details as well as the material properties of this OWT are readily available, and many researchers used the same model for the benchmark investigations (Hallowell et al., 2018; Li et al., 2018; Pokhrel and Seo, 2019; Liu et al., 2022). The schematic plot of monopile OWT with relevant loading and response is presented in Figure 9.1. The water depth d is taken as 20 m and the depth of pile below mudline is 25m. In fact, the variable d' is the free board, which varies depends on the wave height. Further details are discussed as follows.

There are three blades (each with a length of 63.5 m) at a hub height of 90 m for the OWT. Diameters of rotor, hub, monopile, tower top and tower bottom are 126 m, 3 m, 3.87 m and 6 m, respectively. Tower top, tower bottom and monopile thicknesses are 0.019 m, 0.027 m and 0.06 m; cut in, rated and cutout wind speeds are 3 m/s, 11.4 m/s and 25 m/s, respectively. The density and modulus of elasticity of the OWT material are 8500 kg/m^3 and 210 GPa. Table 9.1 gives the summary of discussed geometric and material properties of the study structure, and further information can be found in literature.

9.3 MUD-LEVEL FLEXURAL DEMAND ESTIMATION

As pointed out earlier, mainly the mud-level flexural demand induced by wave and wind effects are described. The moment at critical level under wave (M_{Wa}) and

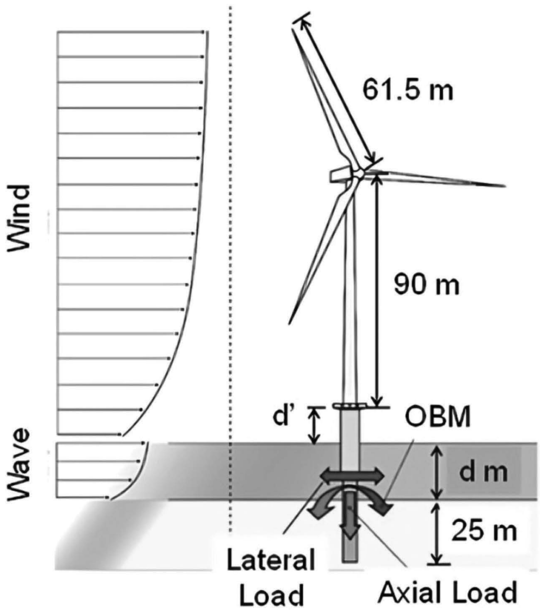

FIGURE 9.1 Schematic plot of the study 5MW OWT with wind and wave loading (Wang et al., 2019).

TABLE 9.1
Benchmark 5 MW Monopile OWT Model Details

Parameter	Value	Parameter	Value
Number of blades	3	Tower density modulus of elasticity	8500 kg/m3
Diameter of rotor	126 m	Cut-in wind speed	210 GPa
Diameter of hub	3 m	Rated wind speed	3 m/s
Height of hub	90 m	Cut-out wind speed	11.4 m/s
Tower base diameter	6 m	Monopile diameter	25 m/s
Tower base thickness	0.027 m	Monopile thickness	6 m
Tower top diameter	3.87 m		0.06 m
Tower top thickness	0.019 m		

wind (M_{Wi}) can be expressed by the following equation (Pokhrel and Seo, 2019; Seo et al., 2022):

$$M_{Wa} = \int z_d \,.\, dF_T \tag{9.1}$$

$$M_{Wi} = \int z. \, dF_W \tag{9.2}$$

where z_d is the variation of water depth, F_T is the total wave force per unit length due to inertia (F_I) and drag (F_D), z is the height above mean sea level and F_W is the total wind force, respectively. The F_T, F_D, F_I and F_W can be obtained by the following formulas:

$$F_T = F_D + F_I \tag{9.3}$$

$$F_D = \left(\frac{1}{2}\right)\rho.D.C_d.u(z_d,t).\left|u(z_d,t)\right| \tag{9.4}$$

$$F_I = C_m.\rho.A_1.\dot{u}(z_d,t) \tag{9.5}$$

$$F_W = C.q.A_2.(sin\,a) \tag{9.6}$$

where $u(z_d, t)$, $\dot{u}(z_d,t)$, C_d, D, ρ, C_m and A_1 are the wave particle velocity, wave particle acceleration, drag co-efficient, outer diameter of monopile, mass density of the sea water, inertia co-efficient and monopile cross-section area, respectively. Likewise, C, q, A_2 and a are the shake co-efficient for the tower, wind pressure, projected area of tower normal to wind and angle between the wind direction and the tower, respectively. Among them q and $u(z_d, t)$ can be obtained from the following equation:

$$q = 0.5\rho_a V_z^2 \tag{9.7}$$

$$u(z_d,t) = \left(\frac{\pi.H_s}{T_p}\right)\left[\frac{Cosh\,k(d+z_d)}{Sinh\,kd}\right]Cos\,\omega t \tag{9.8}$$

where ρ_a, V_z, H_s, T_p, k, ω and t are mass density of air, wind speed at height z (above mean sea level), significant wave height, peak period of wave, wave number, wave angular frequency and time, respectively. The V_z, H_s and T_p can be deduced using the following equations:

$$V_z = V_{10}.\left(\frac{z}{10}\right)^{0.11} \tag{9.9}$$

$$H_s = \frac{0.0016\,C_f V_{10}^2\sqrt{\left(\frac{g.f}{V_{10}^2}\right)}}{g} \tag{9.10}$$

$$T_p = 11.7\sqrt{\left(\frac{H_s}{g}\right)} \tag{9.11}$$

where V_{10}, C_f, g and f are wind speed in m/s at 10 m above mean sea level, depth correction factor as a function of d for wave, acceleration due to gravity and fetch in km, respectively. Finally, the coupled moment (M_T) due to wind and wave can be found algebraically as follows (Pokhrel and Seo, 2019):

$$M_T = M_{Wa} + M_{Wi} \tag{9.12}$$

9.4 FRAGILITY ANALYSIS APPROACH

Initially, the limit state (LS) function needs to be defined. It represents the probability of exceedance of the structural capacity upon the action of external loads. Here, structural capacity can be viewed as the damage threshold, which can be scaled in terms of bending moment capacity of the section at the critical level. Similarly, the bending moment created due to imposed loads can be indicated by engineering demand parameter (EDP). With this background, the LS function can be expressed by the following equation (Hallowell et al., 2018; Li et al., 2018; Pokhrel and Seo, 2019; Wilkie and Galasso, 2020; Mardfekri and Gardoni, 2013; Mo et al., 2021):

$$G(Z_{eb}, X) = R(Z_{eb}, X) - M \tag{9.13}$$

where $G(Z_{eb}, X)$, $R(Z_{eb}, X)$ and M are the LS function, capacity of the section and bending moment created at critical section due to loading, respectively. Taking f_{yb}, γ_{m0} and Z_{eb} as bending yield strength, partial safety factor and bending section modulus at critical section, $R(Z_{eb}, X)$ can be found by the following equation (Pokhrel and Seo, 2019; Seo et al., 2022):

$$R(Z_{eb}, X) = \left({f_{yb}}/{\gamma_{m0}} \right) Z_{eb} \tag{9.14}$$

Thus, the fragility curve due to the load acting on the structure is generated using the probability of exceedance data points by defining the reliability index (β) of the structure. The β value can hint about the chances of exceedance of the defined structural capacity when the structure is subjected to various loading conditions, and it can predict structural safety under various loading scenarios (Pokhrel and Seo, 2019; Seo et al., 2022):

$$\beta = \frac{ln(\mu_R / \mu_M)[1 + V_M^2] / [1 + V_R^2]}{\sqrt{ln[(1 + V_M^2)(1 + V_R^2)]}} \tag{9.15}$$

where μ_R, μ_M, V_R and V_M are the mean and variation co-efficient of structural capacity and induced bending moment, respectively. Using the data points of reliability index and utilizing the standardized normal distribution, the exceedance probability of structural capacity under load can be found. This can be expressed by the following distribution function, Φ (Pokhrel and Seo, 2019; Seo et al., 2022):

$$P_E = \Phi(-\beta) \tag{9.16}$$

9.5 ANALYSIS RESULTS

As discussed in the previous sections, two different loading schemes are accounted. The first one considers the effect due to waves only, whereas the second case takes the effects of the combination of wind and wave events. For each loading scheme, standard water depth scenarios of 20 m are considered. For the wind load with reference wind speed (V_{10}) ranging from 1 m/s to 100 m/s, the significant wave height was found to vary from 0.24 m to 23.53 m. Corresponding to these load cases, the OBM at mud-level and exceedance probability of bending capacity for all the accounted cases are presented as follows.

Figure 9.2 shows the plot of variation of normalized OBM (NOBM) due to wave loading alone and combined wind and wave loading cases. It is worth noting that the OBM is normalized with the bending moment capacity at mud-level. In the wave loading alone case, for a critical wind speed of 50 m/s (Mone et al., 2015), the NOBM value is obtained as 0.83, and the same value for the combined wind and wave load

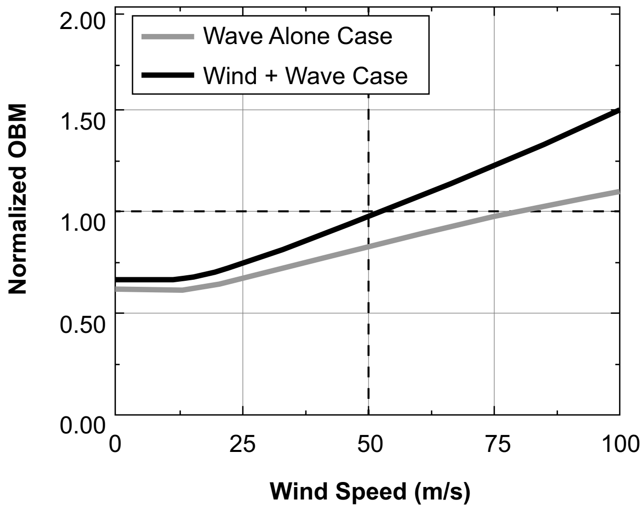

FIGURE 9.2 Variation of normalized OBM at mud-level with wind speed for the wave alone and combined wind and wave loads.

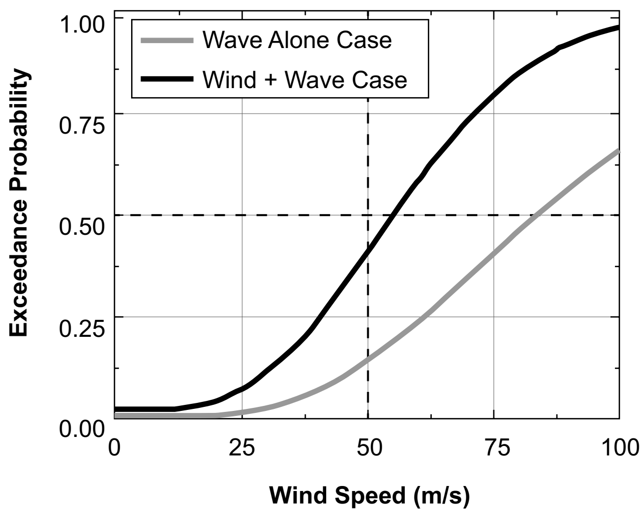

FIGURE 9.3 Exceedance probability of bending capacity at mud-level with wind speed for wave alone and the combined wind and wave loads.

TABLE 9.2
Bending Capacity Exceedance Probability Values for Water Depth of 20 m

		Wave Alone	Wind and Wave
V_{10} *(m/s)*	H_s *(m)*	*d* = 20 (*m*)	
50	11.76	0.14	0.41

action is noted as 0.97. In short, a percentage increase of 17% is observed between the former case and the latter case at the critical wind speed 50 m/s.

Figure 9.3 shows the exceedance probability (P_E) of structural capacity at mud-level with respect to wind speed due to wave load alone and combined wind and wave loads. In the wave loading alone case, for a critical wind speed of 50 m/s (H_s = 11.76 m) (Mone et al., 2015), the P_E value is noted as 0.14, whereas for the combined wind and wave load action, this value is 0.41, for the accounted water depth of 20 m. There is 27% difference in the probability of exceedance of bending capacity between the former case and latter case at the critical wind speed (50 m/s). Similarly, the median values for the fragility are found to be 56 m/s and 84 m/s for wave alone and wind and wave loading cases, respectively. The corresponding H_s values are 12.70 m and 19.76 m, respectively. Table 9.2 summarizes the discussed results in brief.

9.6 CONCLUSIONS

Benchmark 5-MW National Renewable Energy Laboratory (NREL) monopile offshore wind turbine (OWT) in a water depth of 20 m is selected. Two cases of loading scenarios are considered: the first case with wave action alone condition and the second with combined wind and wave loads. Based on the applicable recommendations, the wind and wave loading effects on the OWT structure are calculated. The overturning bending moment (OBM) at mudline is taken as the critical response and the bending capacity at the same location as the damage threshold. With this background, the reliability based on the fragility curves are developed. It is found that the OBM exceedance vulnerability corresponding to a critical wind speed of 50 m/s is more for the second case by a percentage difference value of 27%.

9.6.1 Declaration of Competing Interest

The authors declare that they have no known competing financial interests or personal relationships that could have appeared to influence the work reported in this chapter.

9.6.2 Data Availability Statement

Some or all data used during the study is available in an online repository in accordance with funder data retention policies. Models and codes used to determine the results of this chapter are also provided by the corresponding author upon reasonable request.

9.7 ACKNOWLEDGMENTS

The authors would like to express their thanks and deepest gratitude to the National Institute of Technology Calicut, India, for providing the financial support to complete this study under the Faculty Research Seed Grant Funding Scheme 2022.

REFERENCES

Akheel KK, Pandikkadavath MS, Shashikala AP. Review of free vibration response of spar-supported wind turbine with tuned mass damper. *Sustainable Cities and Resilience: Select Proceedings of VCDRR* 2021;399–405.

Arany L, Bhattacharya S, Macdonald J, Hogan SJ. Simplified critical mudline bending moment spectra of offshore wind turbine support structures. *Wind Energy* 2015;18(12): 2171–2197.

Breton SP, Moe G. Status, plans and technologies for offshore wind turbines in Europe and North America. *Renewable Energy* 2009;34:646–654.

Costoya X, deCastro M, Carvalho D, Gesteira MG. On the suitability of offshore wind energy resource in the United States of America for the 21st century. *Applied Energy* 2020;262:114537.

DNV G. *Design of Offshore Wind Turbine Structures*. Offshore Standard DNV-OS J101. DNV GL AS, Høvik (Norway); 2014.

Dupuis KW, Anis A. Observations and modeling of wind waves in a Shallow Estuary: Galveston bay, Texas. *ASCE Journal of Waterway, Port, Coastal, and Ocean Engineering* 2013;139(4):314–325.

Fajuyigbe A, Brennan F. A simplified formula for calculating the limit load of cracked offshore wind turbine monopile under bending. *Marine Structures* 2022;83:103164.

Hallowell ST, Myers AT, Arwade SR, Pang W, Rawal P, Hines EM, Hajjar JF, Qiao C, Valamanesh V, Wei K, Carswell W, Fontana CM. Hurricane risk assessment of offshore wind turbines. *Renewable Energy* 2018;125:234–249.

He K, Ye J. Dynamics of offshore wind turbine-seabed foundation under hydrodynamic and aerodynamic loads: A coupled numerical way. *Renewable Energy* 2023;202:453–469.

Jonkman J, Butterfield S, Musial W, Scott G. *Definition of a 5-MW reference wind turbine for offshore system development*. National Renewable Energy Limited (NREL) Report No. NREL/TP-500–38060, 2009.

Jonkman J, Butterfield S, Passon P, Larsen T, Camp T, Nichols J, Azcona J, Martinez A. *Offshore code comparison collaboration within IEA wind annex XXIII: Phase II results regarding monopile foundation modeling*. Golden, CO: National Renewable Energy Laboratory (NREL). Report No. NREL/TP-500-42471, 2008.

Li C, Xiao Y, Xu Y, Peng Y, Hu G, Zhu S. Optimization of blade pitch in H-rotor vertical axis wind turbines through computational fluid dynamics simulations. *Applied Energy* 2018;212:1107–1125.

Liu M, Qin J, Lu D-G, Zhang W-H, Zhu J-S, Faber MH. Towards resilience of offshore wind farms: A framework and application to asset integrity management. *Applied Energy* 2022;322:119429.

Mardfekri M, Gardoni P. Probabilistic demand models and fragility estimates for offshore wind turbine support structures. *Engineering Structures* 2013;52:478–487.

Markard J, Petersen R. The offshore trend: Structural changes in the wind power sector. *Energy Policy* 2009;37:3545–3556.

Mo R, Cao R, Liu M, Li M, Huang Y. Seismic fragility analysis of monopile offshore wind turbines considering ground motion directionality. *Ocean Engineering* 2021;235:109414.

Mone C, Smith A, Maples B, Hand M. *2013 cost of wind energy review*. NREL/TP-5000-63267, 2015.

Ou Y, Chatzi EN, Dertimanis VK, Spiridonakos MD. Vibration-based experimental damage detection of a small-scale wind turbine blade. *Structural Health Monitoring* 2017;16(1):79–96.

Pokhrel J, Seo J. Natural hazard vulnerability quantification of offshore wind turbine in shallow water. *Engineering Structures* 2019;192:254–263.

Sarathkumar T, Pandikkadavath MS, Mangalathu S. *Resilience assessment of shallow water offshore wind turbines under combined wind and wave load effects*. SSRN, 2023. https://doi.org/10.2139/ssrn.4518223.

Seo J, Pokhrel J, Hu JW. Multi-hazard fragility analysis of offshore wind turbine portfolios using surrogate models. *Renewable and Sustainable Energy Reviews* 2022;165:112552.

Wang H, Wang T, Ke S, Hu L, Xie J, Cai X, Cao J, Ren Y. Assessing code-based design wind loads for offshore wind turbines in China against typhoons. *Renewable Energy* 2023;212:669–682.

Wang S, Larsen TJ. Permanent accumulated rotation of an offshore monopile wind turbine in sand during a storm. *Ocean Engineering* 2019;188:106340.

Wei K, Arwade SR, Myers AT. Incremental wind-wave analysis of the structural capacity of offshore wind turbine support structures under extreme loading. *Engineering Structures* 2014;79:58–69.

Wilkie D, Galasso C. Gaussian process regression for fatigue reliability analysis of offshore wind turbines. *Structural Safety* 2021;88:102020.

Wilkie D, Galasso C. A probabilistic framework for offshore wind turbine loss assessment. *Renewable Energy* 2020;147:1772–1783.

Wilkie D, Galasso C. Site-specific ultimate limit state fragility of offshore wind turbines on monopile substructures. *Engineering Structures* 2020;204:109903.

Zuo H, Bi K, Hao H, Xin Y, Li J, Li C. Fragility analyses of offshore wind turbines subjected to aerodynamic and sea wave loadings. *Renewable Energy* 2020;160:1269–1282.

10 Identifying the Factors Affecting Users' Safety at Bus Stops

A Step Towards Improving Bus Ridership

G Sethulakshmi and Mithun Mohan

10.1 INTRODUCTION

A tremendous increase in the number of vehicles has been observed in the world over the past decades. Developing countries are hit harder than other countries, and they suffer from traffic congestion, increased fuel consumption, vehicular emission, travel cost, and traffic accidents due to the uncontrolled growth of vehicles. About 1.1 million people in India die prematurely each year from diseases directly related to air pollution, making it the fifth leading cause of death in the country (IHME, 2018). The transportation sector is the major contributor to air pollution through vehicle exhaust emissions in India. India's transportation sector accounts for nearly 18% of the total energy consumption and contributes to 142 million tonnes of CO_2 emission. During the COP21 Summit held in Paris, India committed to reducing its greenhouse gas emissions intensity by 33–35% below 2005 levels by the year 2030 (Bureau of Energy Efficiency, 2020).

Replacement of conventional cars completely with electric vehicles (EVs) results in less level of emissions (Rahman and Mohan, 2023). The study outlined that the emission levels at signalized intersections were reduced by replacing conventional cars in the traffic stream with 25%, 50%, 75%, and 100% of EVs at different levels of traffic volumes. A complete replacement of conventional vehicles can result in a considerable reduction in CO_2 emissions. However, converting all conventional fuel vehicles to electric is not feasible in the present scenario. Therefore, it is essential to find other easy, fast, and economical methods along with the adoption of EVs.

The National Electric Mobility Mission Plan (NEMMP) 2020 was launched in 2013 to achieve national fuel security by promoting hybrid and electric vehicles in the country. As part of the NEMMP 2020, the Ministry of Heavy Industries launched the FAME India Scheme in 2015 to promote the adoption of electric/hybrid vehicles in India. Nevertheless, the primary concerns of the customers regarding the range of EVs, lack of charging facilities, vehicle cost (battery cost), and hesitance to shift

DOI: 10.1201/9781032686899-13

towards new technology are to be resolved to attract more users towards the adoption of EVs (Ministry of Power. Govt of India).

The uncontrolled growth of vehicles has created safety threats to drivers, pedestrians, and other road users. Facilitating sustainable transport modes is necessary to cope with the adverse effects of dangerous growth in vehicle populations on citizens' quality of life and safety. A sustainable transport system will also help bring energy efficiency to transportation and reduce environmental impact. Sustainable transport refers to ways of transportation that are sustainable in terms of their social and environmental impacts. Components for evaluating sustainability include the particular vehicles used, the source of energy, and the infrastructure used to accommodate the transport. One of the most effective measures toward sustainability is to attract more people to public transportation. Shifting private transport to public transport can bring substantial benefits in terms of travel time, travel cost, and safety. Since public transport fails to provide last-mile connectivity, all the travellers using it are forced to become pedestrians at the start or end of their journey. Therefore, improving the quality of the existing public transportation system and its safety standards is vital towards alleviating the aforementioned issues (Sethulakshmi and Mohan, 2023a). Improving the standards of safety should include improving the safety of passengers on board and the safety of passengers at bus stops. Increasing service performance can increase bus ridership to a considerable extent, and among the measures of service performance, safety is most important (Sethulakshmi and Mohan, 2023b).

10.2 LITERATURE REVIEW

Urban sprawl has created uncontrolled vehicle growth, and it has become a challenge to achieve sustainable mobility in road transport, particularly in rapidly developing areas. Bus stops are identified as a critical element of the public transport network because they act as an interface where users interact with transit vehicles (Cheranchery et al., 2019). Studies related to bus stop safety deserve much more attention in the public transport safety domain, as bus stops are associated with significant accident risks derived from the mass movement of passengers (Phillips et al., 2021). Many bus transit stations do not have adequate facilities, such as passenger waiting areas, loading areas, sidewalks, crosswalks, basic amenities, etc. Most of the bus stops are not correctly designated and are used for other purposes, causing road users to experience chaotic situations (Akintayo and Adibeli, 2022). Improper design of bus stops can result in unsafe acts from bus users, operators, and pedestrians, which ultimately lead to accidents (Cheranchery et al., 2019). Providing users with a comfortable and safe environment is also a part of engineering. A limited number of studies focus on pedestrian safety in relation to transit stops or corridors.

Travellers' perception of safety is more important than the actual level of safety (Abenoza et al., 2018). Therefore, it is also necessary to identify unsafe bus stops based on users' judgment of safety criteria instead of crash rates. Even though the research in traffic safety is in its progressive phase, the research on perceived safety is in its infancy, and there are no standard indicators to measure the safety perceived by the users (Sethulakshmi and Mohan, 2023b). Travellers' safety perception has been one of the salient indicators of travel satisfaction. Location, design, and the surrounding environment should be such that they shall meet the users' expectations (Tubis et al., 2021). Therefore, there is a strong demand for perceived safety quantification in areas with high passenger flow rates that will substantially contribute to road safety.

Zhang et al. (2019) carried out a study to derive the public transport passenger satisfaction index using the Partial Least Squares Structural Equation Model (PLS-SEM). They concluded that safety, convenience, reliability, comfort, and operational service significantly affect the passenger satisfaction index. While measuring safety, onboard safety is considered rather than the perceived safety of passengers while using the bus stop facility. Hu et al. (2015) conducted a study to measure the impact of the perception of bus service performance on mode choice using SEM and multinomial logit modelling. The results show that reliability and comfort have greater significance than availability and safety on mode choice.

Improving public transport ridership is an inherent part of sustainable development. Identifying the factors affecting mode choice will help enhance the existing facilities. Therefore, the study will determine the relative importance of factors that affect their mode choice and measure travellers' safety perception while waiting or moving around bus stops. Travel comfort, safety, timeliness of the buses, distance travelled, and travel time are the factors considered to prioritize the travellers' mode choice. Safe conditions at bus stops and their immediate vicinity are essential to avoid catastrophic fatalities and attract more people to public transport. Periodic safety assessment is inevitable in the context of increasing safety issues. A proactive approach to traffic safety evaluation is gaining more attention when reliable and accurate crash data records are not available. Therefore, the study uses online and field surveys to measure the travellers' perceived safety at bus stops. Since it is a proactive approach towards sustainable and safe public transport, the study's findings will be used for planning transit stations, including the travellers' perception.

10.3 METHODOLOGY AND DATA COLLECTION

The study aims to measure the perceived safety of travellers at bus stops. It also tried to identify the relative importance of factors that affect their mode choice and measure travellers' safety perception while waiting or moving around bus stops. Travel comfort, safety, timeliness of the buses, distance travelled, and travel time are the factors considered to prioritize the travellers' mode choice. In the first part of data collection, an online-based questionnaire survey was conducted, and a total of 400 individual responses were collected. Later, the sample was reduced to 337 after data cleaning. In the second part, an opinion survey was administered through face-to-face interviews based on a random sampling of the bus users waiting at 13 selected bus stops in Kerala, India. After the data was cleaned and verified, 384 samples were considered for analysis.

The questionnaire was designed to complete the interview within 6–8 minutes. The questionnaire was provided both in English and the local language for a reliable response. It was framed into four parts to collect information regarding the respondent's socio-demographic characteristics, trip characteristics, accident experiences, and opinions on safety characteristics in and around bus stops. The socio-demographic characteristics included the respondent's age, gender, education, annual income, and vehicle ownership. Trip frequency via buses, frequently used mode of transport, trip purpose, and two-way travel distance were covered under trip characteristics. Trip characteristics also asked the respondents to rank the factors such as travel comfort, safety, timeliness of the buses, distance travelled, and travel time on the basis of their priorities while selecting bus as a mode of transport choice (1 for first priority and 5 for last priority). Under accident experience, information about their previous personal accident experience and accident victimization was recorded.

The last part of the questionnaire collected the travellers' safety perceptions of various factors in and around bus stops on a five-point rating scale from 1 (very unsafe) to 5 (very safe). Twenty questions were asked to collect data regarding their safety perception, which are listed as follows:

- Bus is stopping far away from the bus shelter or improper stopping of bus
- The bus stopped in front of bus stop and maintained wide gap from it
- Hurrying up for departure by bus operators
- Lack of necessary roof shelter and safety barrier at bus
- Lack of safety barrier at bus stop
- Water logging during rainy season at bus stop
- Lack of adequate sitting facility
- Encroachment of bus stop by vendors
- Bus approaching the bus stop at high speed
- Absence of sufficient light at night in the bus stops
- Narrow platform of the bus shelter
- Bus stop is not properly maintained
- Lack of pedestrian crossing facilities like markings or foot over bridges adjacent to bus stop
- Inappropriate sidewalk facilities
- Unruly behavior of other passengers at bus stop
- Bus stop located on curves
- Bus stop located near intersections (road junctions)
- No separate facilities for men and women
- Left-side overtaking by other vehicles at bus stop while passengers are boarding and alighting
- Bus stop located near school

10.4 DATA ANALYSIS AND RESULTS

The analysis starts with the descriptive statistics of the responses. Table 10.1 gives a comparison of the descriptive statistics of field surveys and online surveys. The proportion of male and female respondents is nearly the same in both surveys, while age distribution exhibits a remarkable difference. In the online survey, 46.3% of the respondents are ages 25–34, while in the field, the age groups 18–24 and 45–60 contribute 50% of the respondents. Another considerable variation has been observed in

TABLE 10.1
Descriptive Statistics of Online and Field Surveys

	Description	Online Survey	Field Survey
Number of respondents:		337	384
Gender:	Male	45.99%	44.8%
	Female	54.01%	55.2%
Age:	< 18	1.8%	6.3%
	18–24	37.1%	24.7%
	25–34	46.3%	16.9%
	35–44	7.1%	16.4%
	45–60	6%	24.5%
	> 60	1.7%	11.2%
Education:	Up to Matriculation	1%	31%
	HSE	3.5%	18.7%
	ITI/Diploma	12.8%	12.5%
	Graduate	50%	27.9%
	PG and above	32.7%	9.9%
Frequency of bus trips:	Frequently	37.4%	60.9%
	Once in a week	14.8%	14.6%
	Once in a month	13.3%	10.2%
	Once in 3 months	3.3%	4.4%
	Very rarely	31.2%	9.9%
Accident Experience:	Victim of accident	6.8%	18%
	Witness to accident	38.8%	25.5%
License:	Yes	58.2%	42.7%
	No	41.8%	57.3%
Annual household income:	< 1 Lakh	47.8%	43%
	1–3 Lakh	23.4%	36.2%
	3–5 Lakh	14.5%	14.8%
	5–10 Lakh	11.2%	5.5%
	>10 Lakh	3.1%	0.5%
Two-way travelling distance:	< 20 km	61%	52.6%
	20–40 km	23.4%	23.4%
	40–80 km	11.2%	10.2%
	80–120 km	2.3%	5.7%
	> 120 km	2.1%	8.1%
Frequently used mode of travel:	Bus	19%	58.1%
	Two-Wheeler	38.7%	28.1%
	Car	35.6%	9.4%
	Train	2.8%	1%
	Auto	3.9%	3.4%

the case of the educational qualification of the respondents. Field surveys constituted a significant share of people (31%) with qualifications up to matriculation, while online surveys failed to capture this field reality. The main reason is that specific populations are less likely to have internet access and to respond to online questionnaires.

Drawing samples is more challenging based on email addresses or website visitations. People may not have smartphones, and those needing help reading and understanding the questions will surely be missed during these online surveys. In field surveys, the interviewer can clarify the questions and probe respondents for more complete responses. Even though 400 responses were collected through online surveys, only 337 were complete. Considering the frequency of bus trips, around one-third of the online survey respondents use the bus very rarely. On the other hand, a field survey could capture a better share of bus users, giving a clear picture of the ground reality. Another remarkable difference is in the case of frequently used modes of transport. Most online respondents use two-wheelers or cars as their primary mode of transportation. Therefore, the responses from those people will be based on their limited experience. Ultimately, we can conclude that the demographics of the online respondents differ from those of the field survey, especially the travel characteristics.

Sections 10.4.1 and 10.4.2 describe the analysis of the responses collected through online and field surveys. Firstly, ranking factors like travel comfort, safety, timeliness of the buses, distance travelled, and travel time are analyzed to find the factor which catches prime attention while selecting a bus as a mode of travel. Secondly, the safety responses are analyzed to see the overall perceived safety of the travellers at the bus stop.

10.4.1 Ranking of Factors Affecting Bus Choice

This section analyzes the ranking of factors like travel comfort, safety, timeliness of the buses, distance travelled, and travel time. Table 10.2 and Table 10.3 summarize

TABLE 10.2
Percentage Frequency of Ranking Observations (Online Survey)

Ranking	Comfort	Safety	Timeliness	Travel Time	Distance
1	33.8	18.4	13.4	9.2	24.9
2	21.4	32.0	19.6	18.7	8.6
3	17.5	24.6	36.8	13.6	7.4
4	12.8	13.6	17.5	41.8	14.2
5	14.5	11.3	12.8	16.6	44.8
Weighted Average Score	3.472	3.323	3.036	2.618	2.543

TABLE 10.3
Percentage Frequency of Ranking Observations (Field Survey)

Ranking	Comfort	Safety	Timeliness	Travel Time	Distance
1	12	19	25.5	14.6	14.3
2	11.5	25	16.9	18.2	7.3
3	19	28.4	33.1	14.1	8.1
4	32.8	13.8	13	38.3	25
5	24.7	13.8	11.5	14.8	45.3
Weighted Average Score	2.533	3.216	3.319	2.795	2.203

the percentage frequency of ranking observations. The weighted average scores (the higher the score, the more the priority) reveal that safety has the second most priority and travel distance has the least priority while taking a bus as a mode of travel. Comfort ranked first in online surveys, while timeliness ranked first in field-based surveys.

Even though the priorities differ in online and field surveys, safety plays a significant role in selecting a bus as a mode of travel. Improving safety during bus transport and at transit stations could attract more people to bus transport. Timeliness and travel comfort should be improved for better bus ridership. Providing real-time information about the bus will be more beneficial for the passengers to track the bus.

10.4.2 Analysis of Safety Responses

The responses collected through the online survey were initially analyzed for perceived safety but yielded no significant outcome as the responses were not fit for any analysis. The cross-tabulation analysis of online responses also could not lead to a conclusion. This might be due to fake or randomly selected answers. The chances of just hitting buttons to finish are also high due to impatience. Further, in the case of genuine responses, the respondent marked their responses from a comfortable location, entirely detached from the environment around the bus stops.

The shortcomings of the online survey were rectified through field data collection. The field survey responses were analyzed in three stages. Exploratory factor analysis (EFA) was performed to test whether the items were loaded to the correct factors. Confirmatory factor analysis (CFA) was used to test the first-order measurement model's reliability, convergent validity, and discriminant validity. Second-order CFA was conducted to determine the measurement model's reliability and validity for the overall perceived safety of bus stops (Sethulakshmi and Mohan, 2023a).

The IBM SPSS 25.0 software package was used to group the indicators and conduct EFA on the safety ratings obtained for 20 chosen factors. This study used principal component analysis and varimax rotation to perform EFA. Six items were eliminated due to their low factor loading, including having a separate restroom for men and women (SEPN), water logging at bus stops (WATRLOG), vendor encroachment (VENDOR), location of the bus stop close to the school (SCHOOL), use of a mobile phone while boarding and alighting (MOBILE), and parking other vehicles at bus stops (PARKING). The final analysis of safety perception used 14 indicators with loading >0.5 (Lawson et al., 2013; Sethulakshmi and Mohan, 2023a). Figure 10.1 depicts the path diagram for confirmatory factor analysis.

The first latent construct is the bus stop facility, which includes the bus stop shelter (SHEL), safety barrier at the bus stop (S_BAR), seating facility (SEAT), lighting facility (LIGHT), and platform width (W_PLAT). The second construct is bus operator behaviour (BO_BEH), which covers indicators such as improper

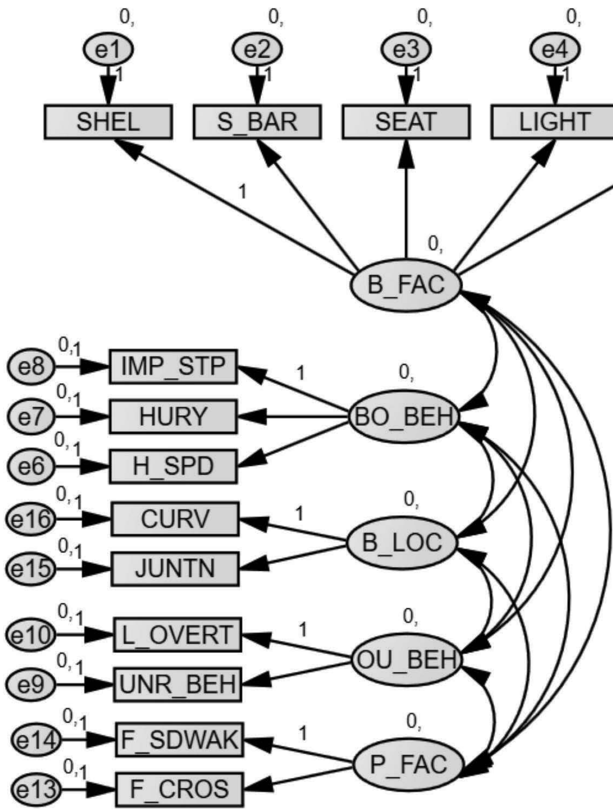

FIGURE 10.1 Confirmatory factor analysis.

stopping of buses at the bus stop (IMP_STP), hurrying up of departure by bus operators (HURY), and buses approaching the bus stop at high speed (H_SPD). The bus stop location is the third construct, which includes positioning the bus stops near the curve (CURV) and junction (JUNTN). The fourth factor, other bus user behaviour (OU_BEH), is measured by left-side overtaking behaviour (L_OVERT) and the unruly behaviour of other passengers waiting at the bus stop (UNR_BEH). The final factor, the pedestrian facility (P_FAC), includes the availability of sidewalk (F_SDWAK) and crossing (F_CROS) facilities for pedestrians near the bus stop (Sethulakshmi and Mohan, 2023a).

CFA was carried out using the IBM-AMOS 22 software on five latent constructs found through EFA. The measurement model provided the following model fit indices: χ^2 = 146.316, χ^2/df = 2.184, RMSEA = 0.056, TLI = 0.956, NFI = 0.942, IFI = 0.968, and CFI = 0.967. All path coefficients have p-values below 0.05, indicating that they are significantly correlated to the safety constructs (Sethulakshmi and Mohan, 2023a). The factor structure produced an acceptable model fit because all the indices are within the allowable range (Table 10.4). Each of the five constructs reported Cronbach's alpha and CR values above the threshold of 0.6 (Jomnonkwao and Ratanavaraha, 2015), denoting good internal consistency and convergent validity of the items in the measurement model (refer to Figure 10.2).

TABLE 10.4
Summary of EFA and CFA (Sethulakshmi and Mohan, 2023a)

	EFA	CFA	
Item	Cronbach's α	CR	AVE
Bus stop facility (B_FAC)	0.861	0.861	0.555
Bus operator behaviour (BO_BEH)	0.860	0.865	0.683
Bus stop location (B_LOC)	0.664	0.669	0.503
Other user behaviour (OU_BEH)	0.871	0.876	0.781
Pedestrian facility (P_FAC)	0.650	0.665	0.500

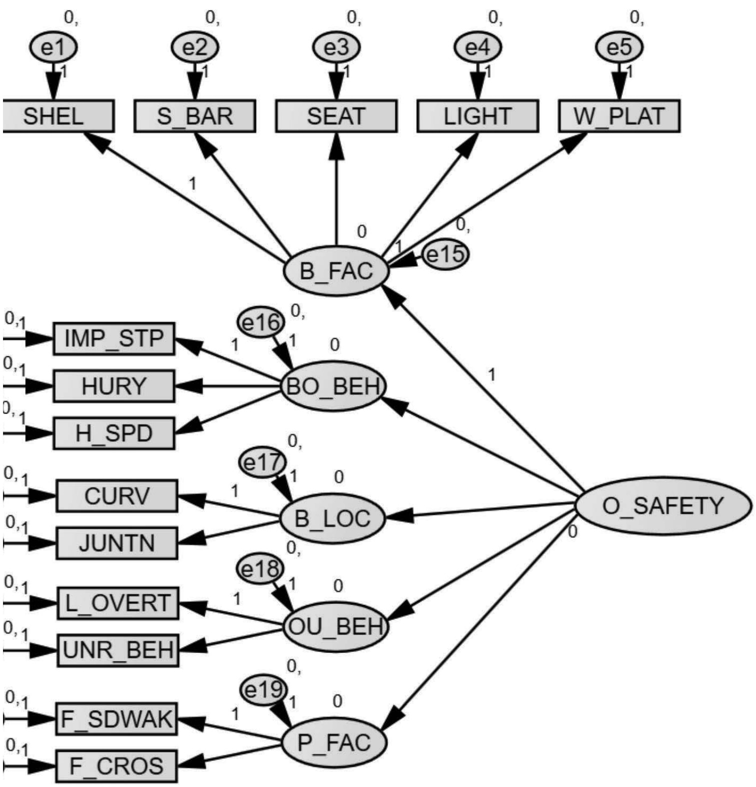

FIGURE 10.2 Measurement model for perceived safety.
(Based on Sethulakshmi and Mohan, 2023a)

Information on prioritizing the safety improvement measures may be found in the loadings generated for the factors based on second-order CFA. For instance, since the bus stop facility obtained the highest CFA score in the second-order model, upgrading its amenities might significantly raise people's perceptions of safety compared to other components. In order to increase the safety provided by the bus stop facility, particular attention should also be paid to the feature with the highest score in the first-order model, namely adequate illumination at the bus stop. Similarly, while improving pedestrian amenities, sidewalks should have come first. Therefore, the factor loadings may be employed efficiently to increase total bus stop safety. Bus operators and other users' behaviour also affect safety perceptions. Improper stopping of the bus at the bus stop greatly impacts perceived safety compared to a bus approaching at high speed and hurrying up of departure by bus operators. Therefore, measures should be taken to ensure proper stopping of buses at the bus stop at the planning stage itself. Providing marked areas for bus stopping and avoiding situations that lead to improper stopping are the best preventive measures.

Similarly, safety from other users' behaviour also significantly contributes to the users' perceived safety. Wrong side (left side in the Indian scenario) overtaking creates more safety impact than the unruly behaviour of waiting and other passengers at bus stops. Other motorists tend to overtake the bus when it is stopped with a wide gap from the bus stop. Therefore, the safety of the boarding and alighting passengers will be affected.

10.5 CONCLUSIONS

Promoting public transport use and improving transit stops' safety and accessibility is a low-cost and efficient measure towards sustainability. Diverse strategies related to public transport planning and the development of better infrastructure could reduce fossil fuel consumption and emissions (Sagaris and Arora, 2016). The safety perception of travellers is an essential constituent to consider when planning transit stations. This study concluded that a field study is more potent than an online survey in gathering reliable and accurate information on travellers' safety perceptions. The safety measured from the five sub-factors, such as bus stop facility, bus stop location, the pedestrian facility near the bus stop, bus operator behaviour, and other bus users' behaviour, contribute to measuring the latent construct, perceived safety. The face-to-face interview survey was conducted at bus stops and concluded that the facilities provided at the bus stop play a significant role in determining their perceived safety at bus stops. Similarly, sidewalks should be given prime importance while improving pedestrian amenities rather than crossing facilities at bus stops. The results also recommend that providing night light facilities, adopting measures to avoid improper stopping of buses and left-side overtaking, and avoiding bus stops on curves and junctions could improve perceived safety. The study findings will benefit transportation planners in developing safer and more reliable bus transit systems, especially bus stops, and designing more effective strategies for increasing passengers' loyalty. Future research could consider the measures towards sustainable transport planning, like integrating different modes of transport with public transit to improve accessibility. Measures to improve public transport's comfort, safety, and timeliness should be considered seriously and could be helpful to make public transport acceptable to all classes of people.

REFERENCES

Abenoza, R. F., Ceccato, V., Susilo, Y. O., and Cats, O. (2018). Individual, travel, and bus stop characteristics influencing travelers' safety perceptions. *Transportation Research Record: Journal of the Transportation Research Board*, 2672(8), 19–28. https://doi.org/10.1177/0361198118758677

Akintayo, F. O., and Adibeli, S. A. (2022). Safety performance of selected bus stops in Ibadan Metropolis, Nigeria. *Journal of Public Transportation*, 24, 100003. https://doi.org/10.1016/j.jpubtr.2022.100003

Bureau of Energy Efficiency. (2020). E-Mobility. *Ministry of Power.* https://beeindia.gov.in/content/e-6mobility

Cheranchery, M. F., Bhattacharyya, K., Salih, M., and Maitra, B. (2019). A proactive approach to assess safety level of urban bus stops. *International Journal of Injury Control and Safety Promotion*, 26(3), 260–270. https://doi.org/10.1080/17457300.2019.1626442

Hu, X., Zhao, L., and Wang, W. (2015). Impact of perceptions of bus service performance on mode choice preference. *Advanced Mechanical Engineering*, 7(3), 168781401557382.

Institute for Health Metrics and Evaluation (IHME). (2018). *Findings from the global burden of disease study 2017.* IHME, Seattle, WA.

Jomnonkwao, S., and Ratanavaraha, V. (2015). Measurement modelling of the perceived service quality of a sightseeing bus service: An application of hierarchical confirmatory factor analysis. *Transport Policy*, 2010, 1–13. https://doi.org/10.1016/j.tranpol.2015.04.001

Lawson, A. R., Pakrashi, V., Ghosh, B., and Szeto, W. Y. (2013). Perception of safety of cyclists in Dublin City. *Accident Analysis & Prevention*, 50, 499–511. https://doi.org/10.1016/j.aap.2012.05.029

Ministry of Power. Govt of India. https://powermin.gov.in/en/content/power-sector-glance-all-india

Phillips, R. O., Hagen, O. H., and Berge, S. H. (2021). Bus stop design and traffic safety: An explorative analysis. *Accident Analysis Prevention*, 153, 105917. https://doi.org/10.1016/j.aap.2020.105917

Rahman, S., and Mohan, M. (2023). Reduction of vehicular emission at urban road junctions through traffic interventions. In Agarwal, A., Velmurugan, S., and Maurya, A.K. (eds) *Recent trends in transportation infrastructure*, Vol. 2. TIPCE 2022. Lecture Notes in Civil Engineering, vol. 347. Springer, Singapore. https://doi.org/10.1007/978-981-99-2556-8_15

Sagaris, L., and Arora, A. (2016). Evaluating how cycle-bus integration could contribute to "sustainable" transport. *Research in Transportation Economics*, 59, 218–227. https://doi.org/10.1016/j.retrec.2016.05.008

Sethulakshmi, G., and Mohan, M. (2023a). Modelling personal safety perceptions at bus stop: employing hierarchical confirmatory factor analysis and structural equation approach. *Advances in Transportation Studies: An International Journal*, Issue LXI (November).

Sethulakshmi, G., and Mohan, M. (2023b). Identification of key determinants of personal safety perception at bus stops using proportional odds logistic regression. *European Transport*, Issue 92, Paper no. 9.

Tubis, A. A., Skupień, E. T., and Rydlewski, M. (2021). Method of assessing bus stops safety based on three groups of criteria. *Sustainability*, 13(15), 8275. https://doi.org/10.3390/su13158275

Zhang, C., Liu, Y., Lu, W., and Xiao, G. (2019). Evaluating passenger satisfaction index based on PLS-SEM model: Evidence from Chinese public transport service. *Transportation Research Part A Policy and Practice*, 120, 149–164.

11 Sustainable Urban Transportation in India
Issue, Challenges, and Adaptations

Jiten Shah and Priyank Trivedi

11.1 INTRODUCTION

Most rising countries' urban transportation systems are far from desirable (OECD, 1996). Traffic congestion is the most obvious and often-criticized transportation issue in a city, and it is widely acknowledged that more vehicle congestion has a noteworthy impact on the gross domestic product (GDP) of any country. Most cities in developing countries lack affordable public transit as well as safe arrangements for non-motorized means of movement like walking and cycling (Steg, 2007). Private autos have progressively expanded in quantity and now monopolize the road. As a consequence, the transportation industry is disproportionately responsible for urban public health issues such as air pollution, noise, greenhouse gas emissions, and traffic accidents (United Nations, 2014). Aligning with these facts, the transport industry in India is extensive and diversified, serving the transportation demands of 1.1 billion individuals. In 2012–2013, the industry generated around 5.2% of the nation's GDP, with the road network accounting for the lion's share (Indian Institute for Human Setttlements, 2015). Economic development requires strong connections in both urban and rural locations.

Since the early 1990s, the developing Indian economy has seen an increase in demand for transportation services and facilities. Reliable and dependable urban transportation networks are critical for India to maintain its rapid economic expansion. The prominence of urban transportation in India originates from its involvement in tumbling poverty through boosting connection to labour markets and consequently raising wages in disadvantaged neighborhoods (Estache, 2007). Logistics and manufacturing sectors are focused around cosmopolitan centres, necessitating the application of effective and reliable transportation systems. But, an absence of integrated transportation planning in India creates issues within the city's social, economic, environmental, and cultural diversity and causes cracks in the community fabric and creates social exclusion. Therefore, political leaders and decision-makers must immediately redirect urban transportation development towards a more sustainable future to return urban spaces back to citizens and establish further livable communities. Developing a sustainable

 DOI: 10.1201/9781032686899-14

urban transport network needs an inclusive and assimilated approach of policymaking and decision-making through the objective of building systems that are affordable, financially feasible, user-centric, and environmentally benign (Steg, 2007).

The following structure is used within the chapter. Section 11.2 delves into India's urban transportation issues in depth. Section 11.3 discusses the concerns and obstacles that make developing sustainable urban transportation in India more challenging. Section 11.4 summarizes the adaptations necessary to accomplish the sustainability targets within the Indian transportation sector, followed by the chapter's conclusion in Section 11.5.

11.2 PROBLEMS FOR URBAN TRANSPORTATION IN INDIA

11.2.1 Unrestrained Motorization

Sustained growth in the economy and rising per capita income have resulted in a significant intensification in motorized vehicles in India. Over the years, the number of automobiles registered has steadily increased. As of March 31, 2020, India has 326 million registered vehicles. The amount of registered automobiles in the nation expanded at a compound annual growth rate (CAGR) of 9.8% between 2010 and 2020 (Ministry of Road Transport and Highways (MoRTH), 2021). The proportion of two-wheelers (74.7%) in the vehicular population in 2020 is followed by automobiles, jeeps, and taxis (13.4%), other vehicles (6.9%), cargo vehicles (4.4%), and buses (0.7%). The composition of vehicles and the pattern of category-wise growth rates of Indian traffic have demonstrated that road users prefer customized modes of transportation (cars and two-wheelers) over public road transportation. Figure 11.1

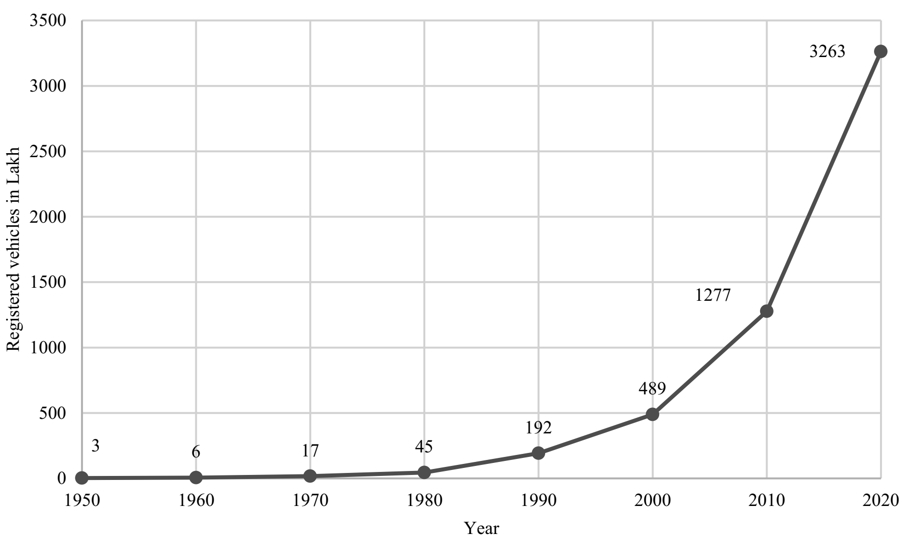

FIGURE 11.1 Decadal trend in numbers of registered vehicles in India.

represents the decadal trends in numbers of registered vehicles in India. The expansion of individualized modes of transportation and the decline in public transportation share have important consequences for traffic congestion and safety. Vehicle density, as measured by the number of vehicles per kilometer of road length, has grown from 28 in 2010 to 47 in 2019. This is symptomatic of the country's increasing road traffic congestion. The problem of congestion disturbs the road space and raises the need for improved traffic flow.

Furthermore, traffic congestion in India is increasing as a result of people's preference for personal vehicles or motorized two-wheelers over public transportation choices (Indian Institute for Human Setttlements, 2015). However, most Indian urban administrative bodies are still following the same personal vehicle transportation–oriented development trends. So, it's clear that road-building policies haven't kept up with the growing need caused by more people driving personal vehicles (Samal et al., 2020). Contrary to popular belief, many cities in advanced economies are presently seeking to rehabilitate from this traditional practice by halting the development of amenities for private automobiles and redeploying road space for public transit and non-motorized mobility (United Nations, 2014). In certain areas, this method has been referred to as a "road diet" or "complete streets".

11.2.2 Urban Air Pollution

Urban air pollution is another significant issue for Indian city administrators. Issues regarding unacceptable air quality in India are rising with intensifying confirmation of the undesirable influences on healthiness (Balakrishnan et al., 2019), agricultural productivity (Ghude et al., 2014), and the budget (Pandey et al., 2021). With the current pace of rise in urban air pollution in India, cities have exceeded the World Health Organization (WHO)-recommended safe limit threshold by 500% (Gurjar, 2021). Rapid urbanization and automation have resulted in some of the world's most toxic air in most major cities. Therefore, the challenge for India in achieving climate mitigation is the decarburization of road transportation sectors. Different research organizations such as Integrated Research and Action for Development (IRADe), Pacific Northwest National Laboratory (PNNL), Council on Energy, Environment, and Water (CEEW), Center for Study of Science, Technology and Policy (CSTEP), The Energy and Resources Institute (TERI) and International Council on Clean Transportation (ICCT) predicted the increasing CO_2 emission trends caused by the road transport sector in India. The range of predicted CO_2 emissions by most of these organizations lies between 800–1900 million tonnes (Paladugula et al., 2018).

High quantities of carbon monoxide and hydrocarbons, among other contaminants, are emitted into the air by the road transportation sector in most Indian cities. Illness caused by air pollution have harmed the economic growth of India by reducing efficiency, labor supply, health spending, and so on (Kanaujia et al., 2022). This economic loss is expected to have a 0.67% to 2.15% influence on the state's GDP. The impact has been particularly severe in states such as Chhattisgarh, Uttar Pradesh, Bihar, Rajasthan, and Madhya Pradesh (Kanaujia et al., 2022). Air pollution has grown in small cities and villages in recent years. It seems to have become a serious problem for municipal managers and policymakers in terms of citizen health. Excessive pollution has prompted the suspension of schools and workplaces in major Indian cities and metropolitan regions, and a portion of the population has been advised to stay indoors (Kanaujia et al., 2022). In most Indian cities, the road transportation sector puts out a lot of carbon monoxide, hydrocarbons, and other pollutants into the air. Controlling air pollution and creating a practical air quality management system requires a complete understanding of its primary contribution (Sharma & Mauzerall, 2022). Projections show greater declines in air quality and a 24% rise in particulate matter (PM) 2.5-related premature deaths by 2050 compared to 2015. This understanding of air pollution and its origins, as well as potential treatments to minimize air pollution, may help lessen the problem in the long run. Air pollutants such as PM1, PM2.5, PM10, NOX, SOx, CO, Ozone, and Pb have a significant influence on degrading air quality in India. These microscopic particles, which are spread in the sky and transported by the wind, concentrate in hotspots and degrade local air quality. The percentage contribution of these pollutants varies according to the source of pollution. However, road traffic emissions are a significant contributor (second largest) to air pollution in India's urban areas (Badami, 2006).

The higher road dust contributes significantly to PM emissions in megacities such as Kolkata (61%), Mumbai (30%), and Delhi (37%). Similarly, in Indore (47%), Surat (42%), Bengaluru (41%), and Chennai (34%), vehicle travel is the biggest contributor to PM 2.5. Furthermore, privately owned two- and four-wheelers account for up to 60% of health-critical PM emissions from passenger cars, whereas diesel-powered buses account for approximately 17% (Badami & Iyer, 2006). Regional and national political leaders need to move quickly to solve this problem.

11.2.3 Increasing Road Accidents

Road accidents are among the list of highest fatality-initiating causes in India (Shah et al., 2022). The relatives of persons involved in road accidents are fronting economic, communal, and psychological health concerns due to after-trauma (Trivedi & Shah, 2022b). Furthermore, as a result of increasing congestion of vehicles, road accidents are more common in Indian cities (Ministry of Road Transport & Highways, 2018). As per Figure 11.2, the cities with million-plus population noted with 15,350 deaths and 58,758 fatalities in year 2021 (Ministry of Road Transport and Highways (MoRTH), 2021). These higher numbers are influenced by many micro-level factors. Generally, these factors are classified as (a) management framework and policy issues, (b) engineering design and standardization challenges, and (c) awareness challenges (Shah et al., 2022). The first category comprises a lack of an organizational strategic framework and proper rule-based administration, a lack of interdepartmental management, a deficiency of inter-ministerial cooperation, financial challenges, and poor data gathering for traffic collisions. The second classification comprises faulty design of urban roads, absence of road infrastructure according to urban needs, and deficiency of consultation with road-safety auditors for safer urban roads. Finally, understanding of road safety rules and guidelines among Indian road users is deficient. In India, for instance, issues with putting public strategies into action include a lack of internal coherence among public policies, as well as a shortage of both materials and human resources, all of which makes

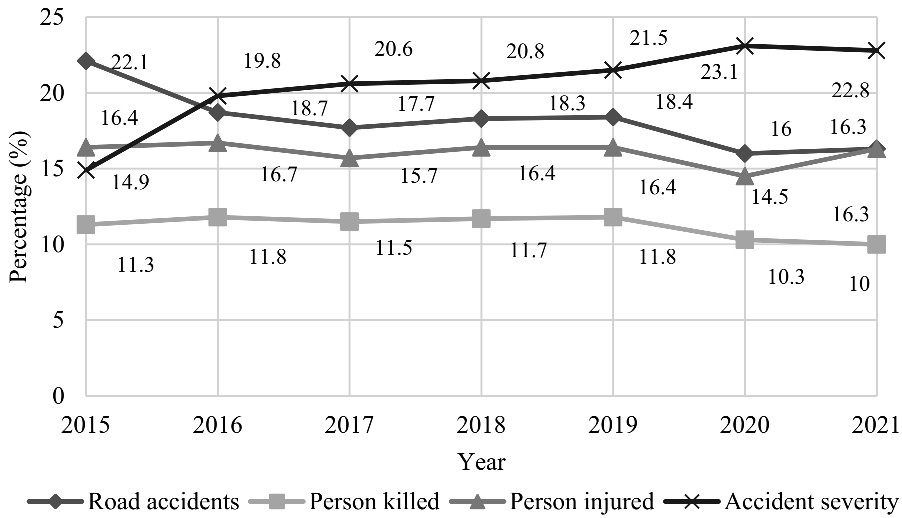

FIGURE 11.2 Percentage share of million-plus populated cities within Indian road accidents and severity trends of year 2015–2021.

it harder to reach the goals that policymakers say they want to reach. In addition, active engagement of stakeholders is needed for undertaking planning, generating standards, establishing indicators, and creating timetables for road safety initiatives in order to effectively execute the road safety map. The conventional severity analysis techniques must be implemented for better decision-making (Trivedi & Shah, 2022a). Many difficulties in road safety need collaborative efforts from different parties in complex urban environments. Good coordination among stakeholders will pave the path for objective achievement, which will be followed by integrated monitoring of operations.

11.2.4 Mobility Within Urban Area

Cities in South Asia, particularly in India, have the highest concentrations of disadvantaged people. Indian cities are situated between the country's enormous population and the world's urban-centric economy. India is home to one-third of the world's impoverished, while Indian cities are home to one-fourth of the world's economically disadvantaged people (Mathur, 2010). This low-income population tries to make a living in Indian cities via swanning, labour work, peddling, moving products, and even scrapping (Joshi, 2014). In their efforts to carve out a place for themselves, the urban poor frequently clash with official major projects, laws, and government rules (Benjamin, 2008). It is imperative that India's urban transportation system be made more sustainable by enhancing its accessibility, affordability, scalability, social equality, productivity, security, comfort, low emissions, and friendliness for both people and the environment. All of this can only be accomplished through a concerted effort to overcome the many obstacles standing in the way.

It's important to recognize the many ways that transportation (or mobility) in cities affects other parts of city life. An integrated approach is required for a holistic solution to describe sustainable urban transportation in a city. In general, sustainable transportation promotes public transportation, bicycles, and walking while discouraging individual motorised modes of transportation (cars and motorcycles). Due to its cheap investment costs, quick timeframe, excellent service quality, and ability to carry huge numbers of people once completed, bus rapid transit (BRT) has gained widespread favour in recent years. Many developing-country megacities are also investing in urban light-rail system development, modernization, and expansion. The initial investment and ongoing upkeep of metro and urban light-rail systems are high, but the long-term economic, social, and environmental advantages may be substantial. According to a number of studies, the public benefits of investing in urban public transportation infrastructure and services far outweigh the investment costs. When commuters can travel from one point in the city to another, urban public transportation systems become more appealing to them and more economically viable for operators. This is possible through network expansion and intermodal connections.

According to rationalists, cities may save a lot of money on energy and fuel by adopting plans where major thoroughfares are easily accessible by public transportation. Mixed-use development is advocated for, and the significance of information and communication technology (ICT) in lowering people's commuting needs is stressed, all of which point to a more tightly integrated approach to land use and transportation planning. This technique may successfully boost accessibility and minimize travel lengths and times by integrating land use and transportation and creating communities such that home, work, and retail sites are adjacent to one another (mixed-use development). Urban development master plans help with this goal. The plan should also highlight initiatives that enhance transportation methods and infrastructure. A more technological strategy is needed to resolve urban transportation issues. It proposes, among other things, raising the bar for fuel quality and vehicle fuel efficiency, formulating emission standards, establishing policies for vehicle inspection and maintenance (I&M), and making the switch to "intelligent transportation systems," which use ICT to optimize transportation networks. Improving freight transportation technologies and logistics is also highlighted.

11.3 ISSUES AND CHALLENGES FOR THE EFFECTIVE DEVELOPMENT OF SUSTAINABLE URBAN TRANSPORTATION IN INDIA

In establishing sustainable urban transportation, Indian cities face comparable concerns and challenges to those in other developing countries. The following are some of the most important challenges that generate or aggravate urban transportation problems within Indian cities.

11.3.1 Rules and Regulations Gaps

Neither the federal government nor any of the individual states has passed any legislation that adequately tackles the problems of urban transportation in India's cities.

The recent system of laws, rules, and management for urban transportation is a holdover from when Indian cities had fewer people and fewer transportation problems. The fragmentation or overlap of laws creates two hurdles to properly managing urban transportation concerns (Indian Institute for Human Setttlements, 2015). First, the numerous varied aims for which laws are made create incoherence in the policy framework. It is also reflected in the scheduling, communication, and handling of a given situation by governments and cities.

No laws exist to facilitate the creation and implementation of mass rapid transportation systems like BRT, light-rail transit (LRT), monorails, and other guided modes. Moreover, there are gaps in the law within the urban transport governance structure due to topics like integrated land use, urban transportation planning, and multimodal integration not being addressed by any act (Verma et al., 2021). This legislative gap results in problems with synchronization and incorporation of urban transportation systems in Indian cities. Similarly, the comparatively lax enforcement of current legislation, along with the lack of severe punishments, contributes to rampant violations of transportation norms and regulations. Motorized vehicles must be examined after 10 years of usage, according to the Motor Vehicle Act; however, the Regional Transport Office (RTO) occasionally administers the act. The lack of tough exams, low costs, and the introduction of intermediaries to facilitate the issuing of driving licenses have resulted in a decline in driver skill and competency (Bertrand et al., 2007). This is a significant contributor to the growing difficulties of traffic discipline, air pollution (Badami & Iyer, 2006), traffic-related accidents and safety (Shah et al., 2022), and so on in most Indian cities.

11.3.2 Disintegrated Institutional Frameworks

For commuters to have a smooth and enjoyable travel experience, urban transportation systems must execute various duties in a well-coordinated way. It's true that the way institutions are set up in India right now means that different groups at the national, state, and local levels do diverse things without always working together. The transportation department is in charge of urban transportation planning in some Indian states; in others, urban development or municipal administration is in charge (Indian Institute for Human Setttlements, 2015). However, there is a critical shortage of vertical and horizontal integration across these entities at the federal, state, and municipal levels, rendering responsibility incredibly difficult. Urban transportation and land use plans don't seem to be planned and linked with the same goal. Inadequate authority at the municipal level is another problem. In general, municipal authorities are insufficient to carry out efficient city governance, either owing to a lack of technical expertise within urban administrations or due to a poor income and reliance on state and central governments for financial demands. Though India's emerging urban transportation concerns are comparatively recent, they are significant. But current official commands prioritize other sectorial matters over urban transportation. For instance, the Indian Railways chose against establishing urban rail transportation, and because there wasn't enough money for separate agencies, the Ministry of Urban Development (MOUD) took over similar systems in other cities. Similarly, police view traffic enforcement and management tasks as secondary to criminal control. Municipalities, meanwhile, prioritize water supply and garbage disposal above urban transportation difficulties, resulting in no one entity being liable or authorized for addressing urban transportation challenges and issues effectively.

11.3.3 Impact of Misrepresentation of Land Market on the Development of Transportation Infrastructure

The increased cost of land rights, combined with laborious and tedious processes, is a significant obstacle to building integrated urban transportation infrastructure. In 2008, land acquisition issues accounted for almost 70% of most infrastructure project delays (3iNetwork, 2009). Local zoning and development control laws cause the real estate market to be very unbalanced. This limits the amount of land that can be used for commercial, industrial, or residential purposes. A substantial proportion of public property keeps enormous tracts of well-located land out of the market. Complicated and time-consuming rural to urban land transition laws raise the purchase cost. Several properties have been subjected to litigation as a result of laws such as the Urban Land Ceiling and Regulation Act (ULCRA), keeping them out of the supply of developable land (The Ministry of Urban Development, 2015). The Development Control Regulations (DCR) laws on floor area ratio (FAR) and floor space index (FSI) are excessively low in comparison to worldwide standards (FSI in Mumbai is restricted to 1.33) (Indian Institute for Human Setttlements, 2015). Landowners are given incentives to give up their land so that infrastructure can be built, and exceptions to these laws are worked out in a way that is very selective and unclear (Narain, 2009). An attempt to establish well-planned settlements beyond the current city boundaries with the goal of ultimately relocating the main activity centers has achieved moderate success. There is insufficient transportation infrastructure to accommodate these newly planned suburban townships and the surrounding households. As a result of such practices and uncontrolled expansion, the Indian suburbs are characterized by the accumulation of industrial expansion, waste, and unharmonious land uses. All of these uncontrolled expansions of metropolitan communities have deteriorated the villages both physically and socially. Suburbanization has also developed along key roads leading from Indian cities to the countryside. This sort of low-density, spread-out decentralization makes providing adequate public transportation services to such locations extremely difficult.

11.3.4 Deficiency in Inclusive Design Standards for Transport Infrastructure

For many years, the Indian Road Congress (IRC) has been the authoritative body on highway and urban road development in India, dictating both architectural standards and technical instructions. Public works departments (PWDs) and other municipal agencies responsible for roads and buildings all voluntarily follow the IRC's guidelines. To a large extent, this is because towns and public works agencies do not see any value in adhering to IRC standards and therefore do not insist that contractors do so.

This means that most urban roads are poorly planned and poorly implemented, and that the functional requirements of urban roads are not being met. Disorganized and uncontrolled traffic, a leading cause of traffic accidents and fatalities, occurs when just a section of the right-of-way is established. Many city-led efforts, especially in Delhi and Bengaluru, have been started to fill the gap left by the lack of guidelines for designing roads in cities. The Unified Traffic and Transportation Infrastructure (Planning and Engineering) Centre (UTTIPEC) in Delhi developed city-specific street plans, such as areas for three-wheeler stops and vending machines, lighting for pedestrians that takes into account the shade of nearby trees, and so on. These plans also account for the road network, water permeability, and other urban factors. Delhi is the first city in India to have legally recognized street design standards that specify how to make roads accessible to people with different abilities. Janaagraha has taken on the mission of creating street-design principles and launching a pilot project to construct 50 roads according to standards in Bangaluru. There is a pressing need to remedy these deficiencies since there are so few such programmes.

11.3.5 Availability of Consistent Transport Data

In the absence of a database with scientific management and analysis of urban transportation statistics, the capacity to design efficient urban transportation plans and evaluate the impacts of various initiatives in cities has been severely impeded (The Ministry of Urban Development, 2015). Because the vast majority of data is acquired either as part of specialized research or with a particular goal in mind, even the quality and reliability of the data that is publicly available are now in dispute. In addition, the data that is accessible is dispersed among several organizations, which might make it challenging to acquire it at times. The inability to gather data on a consistent basis is a barrier for both the process of strategic planning and the formulation of public policy. In any event, the data is not updated often enough to allow for in-depth research and accurate projections. It seems that this issue is widespread in Indian cities, which makes it more difficult to enhance public transportation. In order to ensure that data can be used for research, planning, development, and training, it is essential that the process of data collection be standardized and institutionalized and that data be gathered on a consistent basis. Only in this way can one be certain that data can be utilized for these purposes.

11.4 ADAPTATIONS REQUIRED FOR ACHIEVING SUSTAINABLE URBAN TRANSPORTATION IN INDIA

Any policy-based adaptation and reform about urban transportation should aim to provide services that can last for a long time. It is obvious that the challenge is to find, put in place, and keep tabs on a coordinated set of policy initiatives that effectively handle particular challenges. Many urban transportation organizations work together in a coordinated manner. After a comprehensive evaluation of expert recommendations and a study of worldwide guiding principles, policy measures deemed possibly helpful are outlined in the following sub-sections.

11.4.1 Readjusting the Regulatory and Legal Framework

In India, the regulatory and legal framework enables the concept of sustainable urban transportation. Each state should enact comprehensive urban transport laws to explain who is accountable for what for public transportation, land use and public transportation integration, safety, non-motorized transportation (NMT), and intermediate public transport (IPT). The federal government may do this by drafting model laws that the states could then adapt to their own requirements. Finally, metropolitan and municipal governments should seize control of their own public transit networks. If passed, this legislation would require all metropolitan areas with populations greater than one million to develop and implement a comprehensive mobility plan (CMP). In addition, the law should outline the goals and objectives of CMPs. Each state and union territory should enact the necessary state legislation to establish a unified metropolitan transport authority and outline its governance structure, responsibilities, and jurisdiction. Intervention in land use and transportation development, such as land management, built form, transport planning and engineering, and institutional and financial frameworks, must be founded in the law. Thus, it is proposed that the present regulatory and legal framework governing urban management be updated. The Town and Country Planning Acts must be amended to promote more mixed-use and compact development and less segregation of land uses and rigid zoning. Good fit and revisions must be applied to redevelopment control laws and building rules to close any potential gaps. For rules and regulations to be obeyed, enforcement must be centralized and increased.

11.4.2 Transformation of Institutions

New concepts and integrated strategies for sustainable transportation need strong institutional and governance backing. Parliamentary will, strong leadership, openness, enough resources, and transparency are all required for the timely execution of successful legislative proposals that ultimately secure public confidence. The skills and expertise of planning agencies in creating appealing visions of urban futures are also critical to the whole process. Besides that, individuals and communities must be ordered to guarantee that investments and planning choices are mutually supportive. It thus entails establishing a forum for non-state actors and city inhabitants to discuss major urban transportation choices that affect human lives in some way. Money and resources should be channelled towards training and capacity-building of relevant individuals so as to equip them to face the multifaceted issues of the urban transportation. Synchronization between municipalities and within municipalities is critical for the establishment of fully integrated urban transportation networks for cities. This good governance offers a geographical framework for organizing infrastructure development and public transport service well within different areas of a city. Municipal authorities must be enhanced with administrative control capabilities as well as fundraising capacity to pay transportation projects and managed services. It is possible that the goals of both the central government and the state governments in India can be integrated into the process of urban transport development and management through the creation and implementation of a unified metropolitan transport authority (UMTA) within major Indian metropolitan cities (Ministry of Housing and Urban Affairs et al., 2016).

11.4.3 Effective Planning and Allocation of Resources

Access to available resources is crucial for the UMTA to operate efficiently and fulfil its role in urban transport coordination. Public funding, a pool of experienced and trained workers, and regularly updated information for use in decisions and planning count as resources.

11.4.3.1 Public Financing for the Development of Urban Transport Projects

Investing in the right kind of infrastructure is crucial for establishing viable transportation solutions in the long run. Steps should be taken gradually to rectify the existing imbalance between spending on public transportation and road development projects geared towards motorized transport. More resources should be allocated towards increasing non-motorized and high-capacity public transportation projects to offset the existing emphasis on roads and highways. It is essential that urban transportation be financed and priced as a system as well. As urban local bodies' (ULB) resources are inadequate to leverage such massive capital investment, the current way of funding significant urban infrastructure projects is via capital grants from the centre or state. A variety of methods may be used to raise money for public transportation initiatives in cities:

- Making use of the private sector for financial support via public private partnerships (PPPs)
- Implementing the National Urban Transport Development Fund outlined within the upcoming Five-Year Plan
- Providing tax break eligibility to the private sector for their projects if they are ready to submit to audits of their finances and operations by the government

11.4.3.2 Government Agency and System Capacity Enhancement to Compete for Top Talent

The second crucial aspect is providing the government with the necessary institutional and individual levels of professional knowledge. The term "capacity building" refers to efforts made to improve municipal services by enhancing the knowledge and expertise of existing municipal authorities and creating new, highly trained employees with college degrees. Training for current municipal authorities should concentrate on improving their knowledge, abilities, and insight into the necessary concerns surrounding urban transportation. To maximize the efficacy of the training and skill-building programme, states must be required to quickly establish a specialized organization for urban transport within every city and, at the state level, deploy administrators to be designated to these organizations, deliver training, and then assign trained staff to the appropriate positions upon their return.

11.4.3.3 Innovation and Knowledge Creation

All relevant parties, such as the general public, require access to a trustworthy data source in order to establish effective urban transport policies and plans and evaluate their effects. Along the way, the MOUD has built up a Knowledge Management and Database Center (KMC) within the Institute of Urban Transport India (IUT) in Delhi. Their goal is to establish a repository for planning, exploration, and training from all Indian cities and to create a state-of-the-art library facility. It has also been suggested that every state build its own version of the KMC and library in the capital. In order to maintain its usefulness for research and decision-making, the data acquisition and handling mechanism must be standardized and kept updated on a regular basis. The MOUD has set up urban transport centres of excellence (CoEs) to train a new generation of experts in the industry. CoEs should be tasked with updating and maintaining the database on a consistent basis, as well as ensuring that it is accessible to everybody.

11.4.3.4 Reforms within Existing Planning Practices

Existing plans and practices of urban development with transport planning must be aligned with the Comprehensive Urban Transport Act (CUTA), which requires the legislative blueprints listed as follows to be prepared in an integrated fashion as part of the formal planning system:

- The most in-depth urban transport and land use planning document is the ward-level **Local Transport Plan (LTP)**, which is developed every ten years and amended every five years. LTPs must be drafted by ward committees with the assistance of UMTA. The LTP process allows the UMTA to experiment with trip orientations (trip destinations) and residential locations (trip origins) and make recommendations to improve them, in addition to implementing a variety of public transportation measures with local demand management to ensure efficient use of roads, seamless coordination of public transportation, and the right mix of advancement patterns and types.
- From the standpoint of city-wide transportation optimization, UMTA must develop a **Comprehensive Mobility Plan (CMP)** that compares land use patterns in the current planning system to mobility and land use initiatives projected within the LTP, and then selects an ideal design of land use and transportation incorporation through commitments of stakeholders and citizens. The CMP's proposal on an urban development plan must be incorporated into a revised master plan if it differs from the one currently in place. In cities without an existing master plan, creating a CMP is the first step in creating one.
- The competent planning authority should continue to create master plans in accordance with the Town and Country Planning Act of that state. Yet, it must be created so that the CMP is an important element of the master plan in each of these legal proposals from the act are consistent.

11.5 CONCLUSION AND POLICY IMPLICATIONS

It is critical to realize that transportation is a derived need resulting from people's desire to satisfy their required financial or social contacts. Private automobiles, public transportation, and NMT are merely means to an end. This vision sees cities and mobility networks as instruments for promoting desirable social goals, with transportation serving as a facilitator. This may be accomplished via compact city forms and mixed-use communities, which drastically minimize commute distances and, in certain cases, travel demands. Compact cities serve not just to bring activity centres closer together, but they also offer safe and efficient pedestrian and bicycle corridors, as well as economical, elevated public transportation alternatives.

To sum up, sustainable mobility is a critical facilitator of economic progress and has the ability to alleviate inequality in Indian cities. This is an important takeaway from the previous point. The comprehensive coordination of urban transportation and land use planning is essential in order to maximize efficiency, increase interconnection, and improve the operation of Indian cities via the use of multi-modal, environmentally friendly transportation. Traditional methods, which prioritize spending public money and resources on personal transportation over public forms of transportation, are not going to solve urban transportation problems such as traffic jams, road accidents, urban pollution, and other issues related to urban transportation. It is imperative that the state provide more financial resources for the construction of NMT and robust public transportation. There is a further risk that urban transportation will be seen as an essential support for the economy as a whole and the price structure. According to the discussion in this chapter, sustainable urban transport systems in Indian cities will only be possible to realize if institutions that are resilient, incorporated, and collaborative are established, and these institutions must also be facilitated by clearly defined responsibilities, statutory processes, economic freedom, and professional competence to effectively improve city accessibility. Structures must be put in place to ensure that these organizations are transparent to their members, subject to frequent oversight, and accountable to the people they serve. This is perhaps the most crucial aspect. This is not possible unless there is strong political will and persistent pressure from the general public for things to change.

Since sustainable transportation requires a comprehensive multi-sectoral strategy, following are some of the primary tactics and policy alternatives that municipal governments may examine in order to transform the city into one that is increasingly sustainable:

1. Integrate land-use and transportation planning procedures, as well as associated institutional frameworks, at the urban level.
2. Introduce a new public transportation project that must bring suitable land-use laws, establish multi-use development and medium-to-high densities inside communities, offer people-oriented local access, and aggressively promote transit-oriented development (TOD).
3. Solicit advances in information and communication technology (ICT) to eliminate needless transit in urban corridors.

4. Incorporate non-motorized transportation (NMT) elements into transit master plans and optimize NMT infrastructure spending, such as expansions of facilities for cycle-riders and pedestrians, the enlargement of intermodal connectivity facilities, and the implementation of broad street design principles wherever possible.
5. Enhance community transit services, together with higher eminence, lower cost of services on special infrastructure besides with city's key circulation corridors and links to feeder transit services in neighbourhoods.
6. Decrease the urban modal share for privately owned motorized vehicles through Transportation Demand Management (TDM) strategies such as paying for traffic, safety, and environmental costs, with the goal of gradually reducing price distortions that favour commuting, motorization, and expansion.
7. Encourage the development of environmentally friendly transportation fuels and technologies, such as increasing sales of renewable power cars, battery technologies, and natural gas.
8. Design and create municipal charging infrastructure for electric and plug-in hybrid cars, as well as participate in carpooling programmes to minimize automobile usage. Monitor fuel quality and tailpipe emissions regulations for all types of vehicles.
9. Ensure that national rules about air quality and noise are followed, as recommended by the WHO. Also, make sure that monitoring and reporting are followed to reduce the number of days with high levels of particulate matter and other harmful gases, especially in areas with a lot of traffic.
10. Use low-carbon transportation options that are good for the environment and help the country's energy security.
11. Set up and fund the institutions that will work on sustainable transportation and land-use policies and their implementation. These institutions will do things like exploration and expansion on environmental friendly transportation and endorse good governance for major transportation projects.

REFERENCES

3iNetwork. (2009). *India Infrastructure Report 2009 Land—A Critical Resource for Infrastructure* (pp. 1–283). Oxford University Press. http://www.indiaenvironmentportal.org.in/files/IIR2009.pdf

Badami, M. G., & Iyer, N. V. (2006). Motorized two-wheeled vehicle emissions in India: Behavioral and institutional issues. *Transportation Research Record*, *1954*, 22–28. https://doi.org/10.3141/1954-04

Balakrishnan, K., Dey, S., Gupta, T., Dhaliwal, R. S., Brauer, M., Cohen, A. J., Stanaway, J. D., Beig, G., Joshi, T. K., Aggarwal, A. N., Sabde, Y., Sadhu, H., Frostad, J., Causey, K., Godwin, W., Shukla, D. K., Kumar, G. A., Varghese, C. M., Muraleedharan, P., . . . & Dandona, L. (2019). The impact of air pollution on deaths, disease burden, and life expectancy across the states of India: The global burden of disease study 2017. *The Lancet Planetary Health*, *3*(1), e26–e39. https://doi.org/10.1016/S2542-5196(18)30261-4

Benjamin, S. (2008). Occupancy Urbanism: Radicalizing politics and economy beyond policy and programs. *International Journal of Urban and Regional Research*, *32*(3), 719–729. https://doi.org/10.1111/j.1468-2427.2008.00809.x

Bertrand, M., Djankov, S., Hanna, R., & Mullainathan, S. (2007). Obtaining a driver's license in India: An experimental approach to studying corruption. *Quarterly Journal of Economics*, *122*(4), 1639–1676. https://doi.org/10.1162/qjec.2007.122.4.1639

Estache, A. (2007). Infrastructures et développement: une revue des débats récents et à venir. *Revue d'économie du développement*, *15*, 5–53. https://doi.org/10.3917/edd.214.0005

Ghude, S. D., Jena, C., Chate, D. M., Beig, G., Pfister, G. G., Kumar, R., & Ramanathan, V. (2014). Reductions in India's crop yield due to ozone. *Geophysical Research Letters*, *41*(15), 5685–5691. https://doi.org/10.1002/2014GL060930

Gurjar, B. R. (2021, April 5). Air pollution in India: Major issues and challenges. *The Energy and Resources Institute*. www.teriin.org/article/air-pollution-india-major-issues-and-challenges

Indian Institute for Human Setttlements. (2015). *Challenges and Recommendations: IIHS RF Paper on Urban Transport*. http://iihs.co.in/knowledge-gateway/wp-content/uploads/2015/07/RF-Working-Paper-Transport_edited_09062015_Final_reduced-size.pdf

Joshi, R. (2014). *Mobility Practices of the Urban Poor in Ahmedabad (India)*. University of the West of the England (Issue October, 2014). https://core.ac.uk/download/pdf/323890023.pdf

Kanaujia, A., Bhati, M., Studies, D., Sandhiya, L., & Nishad, S. N. (2022, January). Air pollution in India: A critical assessment and suggestive pathways for clean air. *CSIR-NIScPR Discussion Paper Series*, 1–47. https://niscpr.res.in/includes/images/discussionpapers/CLEAN-AIR-POLLUTION-2022-01.pdf

Mathur, O. P. (2010). *Slum-Free Cities: Natioanl Urban Poverty Reduction Strategy 2010–2020* (pp. 1–70). The National Institute of Public Finance and Policy (NIPFP). http://sa.indiaenvironmentportal.org.in/files/Final Poverty Rep.pdf

Ministry of Housing and Urban Affairs, SUTP, & Deloitte Touche Tohmatsu India. (2016). Operations Document for Unified Metropolitan Transport Authority (UMTA). *Unified Metropolitan Transport Authority-Hyderabad* (Issue May). https://mohua.gov.in/upload/uploadfiles/files/UMTA_v13.pdf

Ministry of Road Transport & Highways. (2018). Road Accidents in India 2018. In *Government of India*. https://morth.nic.in/sites/default/files/Road_Accidednt.pdf

Ministry of Road Transport & Highways (MoRTH). (2021). *Road Accidents in India 2021*. In *Government of India*. https://morth.nic.in/sites/default/files/RA_2021_Compressed.pdf

The Ministry of Urban Development. (2015). Report on Indian Urban Infrastructure and Services. In *The Ministry of Urban Development, India*. https://doi.org/10.1093/acprof:oso/9780199454136.003.0004

Narain, V. (2009). Growing city, shrinking hinterland: Land acquisition, transition and conflict in Peri-Urban Gurgaon, India. *Environment and Urbanization*, *21*(2), 501–512. https://doi.org/10.1177/0956247809339660

OECD. (1996). Towards sustainable transportation. *OECD Proceedings*, Vancouver. https://www.oecd.org/greengrowth/greening-transport/2396815.pdf

Paladugula, A. L., Kholod, N., Chaturvedi, V., Ghosh, P. P., Pal, S., Clarke, L., Evans, M., Kyle, P., Koti, P. N., Parikh, K., Qamar, S., & Wilson, S. A. (2018). A multi-model assessment of energy and emissions for India's transportation sector through 2050. *Energy Policy*, *116*, 10–18. https://doi.org/10.1016/j.enpol.2018.01.037

Pandey, A., Brauer, M., Cropper, M. L., Balakrishnan, K., Mathur, P., Dey, S., Turkgulu, B., Kumar, G. A., Khare, M., Beig, G., Gupta, T., Krishnankutty, R. P., Causey, K., Cohen, A. J., Bhargava, S., Aggarwal, A. N., Agrawal, A., Awasthi, S., Bennitt, F., . . . & Dandona, L. (2021). Health and economic impact of air pollution in the states of India: The global burden of disease study 2019. *The Lancet Planetary Health*, *5*(1), e25–e38. https://doi.org/10.1016/S2542-5196(20)30298-9

Samal, S. R., Gireesh Kumar, P., Cyril Santhosh, J., & Santhakumar, M. (2020). Analysis of traffic congestion impacts of urban road network under Indian condition. *IOP Conference Series: Materials Science and Engineering*, *1006*(1). https://doi.org/10.1088/1757-899X/1006/1/012002

Shah, J., Bhatt, K., Trivedi, P., & Easa, S. (2022). *Road Safety Conditions and Management in India: Challenges and Opportunities*, 3–23. https://doi.org/10.1007/978-981-16-8837-9_1

Sharma, D., & Mauzerall, D. (2022). Analysis of air pollution data in india between 2015 and 2019. *Aerosol and Air Quality Research*, *22*(2), 1–20. https://doi.org/10.4209/aaqr.210204

Steg, L. (2007). Sustainable transportation: A psychological perspective. *IATSS Research*, *31*(2), 58–66. https://doi.org/10.1016/S0386-1112(14)60223-5

Trivedi, P., & Shah, J. (2022a). Identification of road crash severity ranking by integrating the multi-criteria decision-making approach. *Journal of Road Safety*, *33*(2), 33–44.

Trivedi, P., & Shah, J. (2022b). Road accident hazard prevention by applying the haddon matrix. In C. Ghosh & Kolathayar S. (eds) *A System Engineering Approach to Disaster Resilience* (Vol. 205, pp. 247–257). Springer. https://doi.org/10.1007/978-981-16-7397-9_18

United Nations. (2014). Shanghai manual—A guide for sustainable urban development in the 21st century. In *Shanghai 2020 World Exposition Exicutive Committee—United Nations*. https://doi.org/10.3141/2243-05

Verma, A., Harsha, V., & Subramanian, G. H. (2021). Evolution of urban transportation policies in India: A review and analysis. *Transportation in Developing Economies*, *7*(2), 1–15. https://doi.org/10.1007/s40890-021-00136-1

Section 4

Sustainable Construction

12 Applications of Civil Engineering in Disaster Risk Reduction

N Vinod Chandra Menon, Sreevalsa Kolathayar and Sreekeshava K S

12.1 INTRODUCTION

Engineering solutions are needed to ensure that the structures are able to withstand the adverse impact of disasters, extreme events and climate change. Civil engineering, structural engineering and geo-technical engineering expertise is required to estimate the multi-hazard profile of geographies, along with the toolkits for problem solving by analysing the data related to the geo-morphology and hydro-morphology of specific geographies. Civil engineering applications for disaster risk reduction cover a wide range of knowledge systems which help in understanding the complex nature of the multi-hazard risk and vulnerability of the building stock. Civil engineering applications are essential for strengthening the multi-hazard preparedness as well as risk reduction and mitigation strategies. Disaster typologies such as geological disasters (earthquakes, tsunamis, landslides, volcanic eruptions) and hydro-meteorological disasters (floods, tropical cyclones, hurricanes, tornadoes, cloud burst, wild fires, drought, etc.) adversely affect and damage buildings, public infrastructure and critical infrastructure assets. The governments have formulated National Building Codes (NBCs) and other safety regulations to ensure that buildings, critical infrastructure and lifeline structures are built to withstand disasters, including low-frequency, high-impact disasters in geographical areas which are prone to natural hazards. There are building bylaws and regulations which prohibit the construction of buildings in floodplain zones, in coastal areas and on unstable slopes. The building plans are approved by engineers of urban local bodies and local self-government institutions in urban, peri-urban and rural areas, respectively, after confirming that they comply with the multi-hazard-resilient building codes to protect the buildings from damage or destruction in the event of any disaster or unforeseen extreme event.

Sreevalsa Kolathayar, Inderjit Pal, Siau Chen Chian and Arpita Mondal have edited a comprehensive volume of authoritative papers on the risk, vulnerability and exposure of communities to multiple hazards and how civil engineering applications can assist and facilitate the development processes of sustainable and resilient communities (Kolathayar et al., 2022). It is hoped that the faculty members imparting engineering education will incorporate the best practices of disaster risk reduction

DOI: 10.1201/9781032686899-16

for designing and developing multi-hazard-resilient building stock and resilient critical infrastructure, saving lives and protecting assets from damage and collapse in disasters and extreme events.

12.2 DISASTER RISK REDUCTION

The United Nations Office for Disaster Risk Reduction (UNDRR) observes that "disaster risk reduction (DRR) is aimed at preventing new and reducing existing disaster risk and managing residual risk, all of which contribute to strengthening resilience and therefore to the achievement of sustainable development". It further clarifies that "DRR is the policy objective of disaster risk management, and its goals and objectives are defined in disaster risk reduction strategies and plans" (UNDRR, 2017). In the earlier years, the International Decade for Natural Disaster Reduction (IDNDR) during the 1990s and the International Strategy for Disaster Reduction (ISDR) were treating disaster reduction though the emphasis shifted to disaster risk management, risk governance and finally to disaster risk reduction with the ISDR graduating as the United Nations Office for Disaster Risk Reduction (UNDRR), with its head also designated as the Special Representative of the Secretary General (SRSG). In the recent years of the 21st century, there has been a growing realisation that climate change–induced hydro-meteorological disasters are occurring with increasing frequency, creating adverse impacts and mounting economic damage. The COVID-19 (SARS Cov-2) global pandemic in 2020–2024 also exposed the fragility of the public health delivery systems in several countries across continents and highlighted the importance of strengthening multi-hazard preparedness, disaster risk reduction and emergency response capacities at the global, regional, national and provincial levels.

12.3 RISK GOVERNANCE

The Global Assessment Report 2022 and the midterm review of the Sendai Framework for Disaster Risk Reduction 2015–2030 pointed out the need for strengthening the risk governance and improving the skill sets of the stakeholder groups to prepare for, respond to and recover from disasters. The Global Assessment Report (GAR) Special Report 2023 "Mapping the resilience of the Sustainable Development Goals" analysed the resilience deficit across all goals, ensuring the balance between People (Social), Planet (Environment) and Prosperity (Economy) (UNDRR, 2023a). In the GAR Special Report 2023, Governance refers to "the regimes, arrangements, structures, strategies and processes by which rules, laws and policies are agreed upon and made, and collective decisions are taken and implemented" (UNDRR, 2023a). Risk governance continues to be a weak area which needs to be strengthened to face disasters, extreme events and climate change.

12.4 UNDRR MIDTERM REVIEW REPORT

The UNDRR's midterm report on the implementation of the Sendai Framework for Disaster Risk Reduction in 2023 observed that

> to accelerate the implementation of the Sendai Framework towards 2030, Member States must further commit to the creation of adaptive governance arrangements that support vertically and horizontally integrated understanding and management of risks across all sectors, domains, scales, and are reflective of the broadened scope of hazards and risks.
>
> (UNDRR, 2023b)

It further suggested that adaptive governance must necessitate "the shift in the locus of responsibility and accountability for preventing risk creation and reducing existing risk, away from a single centralized agency, to coordinated, risk-informed decision making and investments that involve all stakeholders" (UNDRR, 2023b). The increasing frequency of disasters, extreme events and climate change indicate the need for a whole-of-society approach for multi-stakeholder engagement to strengthen multi-hazard preparedness, risk reduction, emergency response and recovery. Civil engineers have an important role in these activities as frugal innovations are required to ensure that the building stock and critical infrastructure and lifeline infrastructure are built to withstand high-impact disasters and reduce the loss of lives, disruption of livelihoods and the mounting economic damage caused by disasters.

12.5 CIVIL ENGINEERING APPLICATIONS IN GEOLOGICAL DISASTERS

The building stock and critical infrastructure such as roads, flyovers, dams, electrical installations, water supply installations, telecommunication infrastructure, airports and railway stations, etc. are damaged and destroyed by geological disasters such as earthquakes, tsunamis, landslides, volcanic eruptions, etc. Multi-hazard risk identification and risk assessment will help in preparing risk reduction plans and mitigation efforts to safeguard the building stock and critical infrastructure from collapse, damage and destruction.

Rapid visual screening (RVS) is a methodology adopted to analyse the structural safety of buildings to withstand earthquakes of high magnitudes. Non-destructive testing can also be undertaken to explore the structural integrity of buildings to withstand earthquakes of severe intensity. Base isolation techniques are also adopted to strengthen the multi-hazard resilience of multi-storied buildings. Micro-zonation is carried out to understand the risk and vulnerability of cities to earthquakes.

12.6 CIVIL ENGINEERING APPLICATIONS IN HYDRO-METEOROLOGICAL DISASTERS

Houses, government offices, critical infrastructure, public infrastructure and lifeline structures such as hospitals, schools, colleges, university buildings and utilities of essential services such as power, water supply, telecommunications, fire and emergency services, etc. can get adversely affected when hydro-meteorological disasters such as floods, cyclones, cloud bursts and extreme events happen. In cyclone-prone areas, civil engineers have successfully demonstrated that tying the roofs to the lintel beams and walls with braces will be able to save the thatched and tiled roofs from being blown away in high windspeeds. Ensuring slope stability with vetiver grass and planting saplings in discarded rubber tyres on unstable slopes have been found to prevent soil runoff and soil erosion (Meena and Chatterjee, 2023). Paving roads and pavements with natural fibres such as jute, recycled plastic, etc. have also been useful as frugal innovations. In flood-prone areas, civil engineers construct embankments, canals and culverts to regulate the flow of water so that they do not inundate human settlements and damage houses and crops through submergence.

12.7 CRITICAL INFRASTRUCTURE PROTECTION

Critical infrastructure protection is an integral component of disaster risk reduction approaches as the uninterrupted functioning of critical infrastructure such as power, water supply, dams, telecommunications and transport infrastructure and lifeline infrastructure such as hospitals, emergency operations centres (EOCs), fire stations, etc. is mission critical in disasters and extreme events. Critical infrastructure protection must be the core of any risk governance framework. Governments must design, develop and implement appropriate risk transfer instruments such as insurance, reinsurance and risk pool funds with the collaboration of the international financial institutions and Fortune 500 companies. Large numbers of electric lamp posts fall down and disrupt power supply during cyclones. The phasing out of electric lamp posts and putting the power distribution network underground has been proposed like the fibre-optic cables which are laid underground in most cities for establishing a telecommunication network which can withstand the adverse impact of disasters and extreme events.

12.8 PROTECTION OF LIFELINE STRUCTURES AND SOCIAL INFRASTRUCTURE

The structural safety of lifeline structures such as hospitals, schools and government offices must be assessed by civil engineers, structural engineers and geo-technical engineers in earthquake-prone areas. Bridges, flyovers, dams, airports and railway stations must also be assessed for their ability to withstand earthquakes of high magnitudes. The Bureau of Indian Standards (BIS) has formulated the NBC and several safety regulations to ensure the protection of lifeline structures in hazard-prone areas.

12.9 SAFETY AUDIT OF EXISTING BUILDING STOCK AND SOCIAL INFRASTRUCTURE

In India, the National Disaster Management Authority (NDMA) of the Government of India had launched a National School Safety Project in high-risk districts which are prone to earthquakes. Rapid visual screening of the selected school buildings were conducted, and efforts were made to carry out seismic strengthening and retrofitting of vulnerable school buildings.

12.10 RETROFITTING AND SEISMIC STRENGTHENING

Vulnerable buildings and lifeline structures in earthquake-prone areas can be assessed for their structural integrity, and seismic strengthening and retrofitting can be undertaken by trained civil engineers. The techniques and standards for seismic strengthening and retrofitting are also disseminated to civil engineers, builders and contractors through training programmes for improving their knowledge and skills to make the buildings resilient to geological and hydro-meteorological hazards.

12.11 NON-DESTRUCTIVE TESTING

In the case of aging structures, the seismic strengthening and retrofitting can be carried out after ascertaining the structural integrity of the building to withstand high-magnitude earthquakes by carrying out non-destructive testing.

12.12 SEISMIC MICROZONATION

According to Sitharam, James and Kolathayar, seismic microzonation or

> Seismic Zonation is a process of dividing a large region into small zones based on the expected level of earthquake hazard. Seismic zonation helps to identify vulnerable regions and also provide necessary outputs for the earthquake resistant design. Hence it is very much required in the modern world in order to minimise the casualty and economic losses during an earthquake.
>
> (Sitharam et al., 2018)

The authors observe that

> the basis of seismic zonation is to model the rupture mechanism at the source of an earthquake, evaluate the propagation of waves through the earth to the top of the bedrock, determine the effects of local soil profile and thus develop a hazard map indicating the vulnerability of the area to potentials seismic hazards.
>
> (Sitharam et al., 2018)

They describe the findings of seismic zonation of the Kalpakkam Nuclear Power Plant (NPP) site, Jabalpur, Delhi, Sikkim Himalaya and Guwahati, Bangalore, etc. and explain the local site effects and liquefaction susceptibility, etc. (Sitharam et al., 2018).

12.13 MONITORING DEFORMATIONS IN CRITICAL INFRASTRUCTURE

The deformations in critical infrastructure can be monitored through Interferometric Synthetic Aperture Radar (InSAR), Differential Interferometric Synthetic Aperture Radar (DinSAR) and Persistent Scatterer Interferometric Synthetic Aperture Radar (PSinSAR), and risk reduction and mitigation efforts initiated by civil engineers, structural engineers and geo-technical engineers. The deformations before, during and after disasters can help in strengthening the preparedness for, response to and recovery from disasters and extreme events. Satellite imagery and remote sensing can help in identifying vulnerable structures such as buildings and heritage monuments which may be facing the risk of collapse, subsidence, etc., along with PSinSAR, DinSAR and InSAR assisted investigations and analysis. The subsidence of Joshimath in Uttarakhand was observed through PSinSAR technique by researchers of the Indian Institute of Technology (IIT) Ropar, Punjab and also confirmed by the Indian Space Research Organisation (ISRO).

12.14 BASE ISOLATION

Base isolation techniques are applied by placing flexible bearings or pads made with layers of rubber and lead in the foundations to protect the super-structures of multi-storied buildings in earthquake-prone areas. The base isolators are dampers which dissipate the impact of earthquakes by cushioning the structure from swaying and collapsing in the event of an earthquake. Elastomeric pads, sliding plates or inverted pendulums are used as base isolators. An overview of the practice of applications of energy dissipation systems for seismic strengthening is provided with specific use cases in Symans et al. (Symans et al., 2008).

12.15 DRR IN ENGINEERING EDUCATION

In the education of civil engineers, structural engineers and geo-technical engineers, there is a critical imperative for incorporating DRR techniques and processes, as the building stock and critical infrastructure in developed countries and developing countries are expanding at a very rapid pace. Most countries are facing the dynamic pressures of increasing trends in urbanisation accompanied by the creation of large real estate building stock and critical infrastructure. The faculty members and students of engineering colleges and technical institutions must be equipped with the knowledge, tools and techniques of multi-hazard-resilient construction practices. In India, the Government of India had launched two flagship projects called the National Programme for Capacity Building of Engineers in Earthquake Risk Management (NPCBEERM) and the National Programme for Capacity Building for Architects in Earthquake Risk Management (NPCBAERM) and trained large numbers of engineers and architects.

12.16 FOG CATCHERS FOR WATER CONSERVATION

Many countries are facing the rapid decline of groundwater tables because of the indiscriminate extraction of groundwater through borewells, hand pipes, etc., even drilling for water by exploding rocks with dynamite. Water tankers are providing even drinking water in cities which are facing acute water shortage and the drying up of groundwater aquifers. Fog catchers in Peru and Morocco have received global attention by harvesting water from fog by putting up large numbers of vertical mesh nets to induce water droplets to flow into a trough for distributing further to human settlements.

12.17 ICE STUPAS IN LADAKH, INDIA

The innovations of Sonam Wangchuk to conserve the water in snow glaciers during the winter months by constructing ice stupas in Ladakh have helped the farmers in several villages to get water for irrigating their agricultural fields in the summer months. As climate change threatens the lives and livelihoods of farmers, and while glacier melting in the Himalayas has raised several concerns, such innovations need to be studied and replicated in countries facing inclement weather with very heavy snowfall and the availability of glacial lakes. Sonam Wangchuk had also helped the release of water from glacial lakes by puncturing the moraines to prevent the collapse of glacial lakes and sudden-onset glacial lake outburst floods (GLOFs). These frugal innovations help in saving lives, protecting livelihoods and safeguarding assets in disaster-prone areas.

12.18 RAPID VISUAL SCREENING

In the United States, the Federal Emergency Management Agency (FEMA) published in 1988 the methodology for assessing the structural integrity of buildings through a Handbook on Rapid Visual Screening of Buildings for Potential Seismic Hazards (FEMA, 1988a) and Supporting Documentation (FEMA, 1988b) with the support of the Appropriate Technology Council, which have been revised through several editions in 2002 and 2015 (FEMA, 2002a, 2002b, 2015a, 2015b). The rapid visual screening (RVS) methodology evaluates the structural integrity and seismic safety of a large stock of buildings rapidly at low cost with minimal access to the buildings and without resorting to non-destructive testing, etc. The RVS methodology was envisaged to identify weak structures that needed more detailed testing to determine the need for seismic strengthening and retrofitting. This approach was essential in the case of protecting critical infrastructure and public infrastructure such as hospitals, schools, government buildings, etc.

The National Disaster Management Authority (NDMA), Government of India also published a Primer on Rapid Visual Screening in October 2020 (NDMA, 2020).

12.19 GOOD PRACTICE DOCUMENTATION

There is an increasing urgency for documenting the good practices of civil engineering applications for disaster risk reduction and for widely disseminating the same for creating greater public awareness among stakeholder groups. The experience-sharing interactions among civil engineers, structural engineers, geo-technical engineers, architects, builders and contractors will be helpful in ensuring that the building stock and critical infrastructure are constructed to withstand the adverse impact of disasters. The National Disaster Management Authority (NDMA), Government of India has formulated several National Disaster Management Guidelines for earthquakes, tsunamis, floods, urban flooding, cyclones, landslides, etc., and these guidelines highlight the need for ensuring that disaster risk reduction is integrated into the creation and development of multi-hazard-resilient building stock and resilient critical infrastructure for which civil engineers have a very prominent role in developed and developing countries.

BIBLIOGRAPHY

FEMA, 1988a, *Rapid Visual Screening of Buildings for Potential Seismic Hazards: A Handbook*, FEMA 154, Prepared by the Applied Technology Council for the Federal Emergency Management Agency, Washington, DC.

FEMA, 1988b, *Rapid Visual Screening of Buildings for Potential Seismic Hazards: Supporting Documentation*, FEMA 155, Prepared by the Applied Technology Council for the Federal Emergency Management Agency, Washington, DC.

FEMA, 2002a, *Rapid Visual Screening of Buildings for Potential Seismic Hazards: A Handbook*, Second Edition, FEMA 154, Prepared by the Applied Technology Council for the Federal Emergency Management Agency, Washington, DC.

FEMA, 2002b, *Rapid Visual Screening of Buildings for Potential Seismic Hazards: Supporting Documentation*, Second Edition, FEMA 155, Prepared by the Applied Technology Council for the Federal Emergency Management Agency, Washington, DC.

FEMA, 2015a, *Rapid Visual Screening for Potential Seismic Hazards: A Handbook*, Third Edition, FEMA P-154, prepared by the Appropriate Technology Council for the Federal Emergency Management Agency, Washington, DC.

FEMA, 2015b, *Rapid Visual Screening of Buildings for Potential Seismic Hazards: Supporting Documentation*, Third Edition, FEMA P-155, Prepared by the Applied Technology Council for the Federal Emergency Management Agency, Washington, DC.

Kolathayar, S., I. Pal, S.C. Chian and A. Mondal (Eds), 2022, *Civil Engineering for Disaster Risk Reduction*, Springer Nature, Singapore.

Meena, P.K. and K. Chatterjee, 2023, “Influence of Pore Pressure Parameter on Seismic Stability Analysis of Geosynthetic Reinforced Soil Slope,” in Zhussupbekov, A., Sarsembayeva, A. and Kaliakin, V.N. (Eds) *Smart Geotechnics for Smart Societies*. CRC Press, Kazakhstan.

NDMA, 2020, *A Primer on Rapid Visual Screening (RVS)*, Consolidating Earthquake Safety Assessment Efforts in India, https://ndma.gov.in/sites/default/files/PDF/Technical%20Documents/RVS-Doc-11-2020.pdf

Sitharam, T. G., James, N., & Kolathayar, S. (2018). *Comprehensive seismic zonation schemes for regions at different scales* (1st ed.) [PDF]. doi:10.1007/978-3-319-89659-5

Symans, M.D., F.A. Charney, A.S. Whittaker, M.C. Constantinou, C.A. Kircher, M.W. Johnson and R.J. McNamara, 2008, “Energy Dissipation Systems for Seismic Applications: Current Practice and Recent Developments,” *Journal of Structural Engineering*, Vol. 134, No. 1.

UNDRR, 2017, UNDRR: Annual Report.

UNDRR: Global Assessment Report GAR, 2022, *Our World at Risk: Transforming Governance for a Resilient Future*, Geneva.

UNDRR, 2023a, UNDRR: Annual Report 2023, *Accelerating Resilience for All*.

UNDRR, 2023b, UNDRR: Regional Assessment Report on Disaster Risk Reduction 2023, Europe and Central Asia.

13 Towards Net-Zero Carbon Emissions

Embracing Sustainability in the Construction Industry through Recycled Concrete Aggregates

Jagdish H Godihal

13.1 INTRODUCTION: BACKGROUND AND DRIVING FORCES

In today's era, the construction and demolition (C&D) sector confronts a monumental challenge annually generating an astounding 890 million tonnes of waste in Europe alone. This staggering figure highlights the urgency of our collective responsibility to address the environmental impact of such practices. Alarming statistics reveal that approximately 42% of Australia's waste stream is intertwined with construction and demolition waste (C&DW), out of which concrete waste constitutes a staggering 81%. These patterns are mirrored globally, with Hong Kong and Japan contributing 38% and 16% of their total waste outputs to C&DW, respectively (Tam et al., 2010). Equally concerning is the report indicating that in the United States, the year 2017 witnessed the generation of an overwhelming 569 million tonnes of C&DW. The issue extends beyond continents, as even South Africa grapples with the menace, with C&DW comprising 21% of its overall waste composition (Ghanbari et al., 2017).

As we confront the paradox of waste proliferation amid a voracious demand for new construction, it becomes apparent that transformative measures are essential. Remarkably, while construction activities churn out this waste, the industry extracts a colossal three billion tons of raw materials annually for manufacturing construction materials. Thus, the clarion call for sustainability resonates louder than ever. It becomes not just an option but an imperative to incorporate waste materials into construction endeavors, aligning with a more sustainable trajectory (Muzenda, 2014).

Distinct strategies emerge across different nations to curb waste generation and foster reuse. Hong Kong, for instance, spearheads the effort through its Construction Waste Disposal Charging Scheme (CWDCS), targeting the pervasive issue of illegal

DOI: 10.1201/9781032686899-17

dumping. Noteworthy strides are made on a global scale, with recycling plants boasting capacities ranging from 1,500 to 3,500 tonnes/day in the United States and Europe, making use of cutting-edge technologies and sophisticated recycling machinery for C&DW. In countries with fewer resources, a pragmatic approach surfaces in the form of mobile recycling plants. This innovative solution, with a recycling capacity of 800 tonnes/day, seamlessly shifts to demolition sites, underscoring its economic viability (Mak et al., 2019).

The intricacies of the issue are highlighted by India, where the dissonance between waste generation and recycling capacity is stark. Astonishingly, the country produces an estimated 150 million tonnes of C&DW annually, yet its official recycling capacity stands at a mere 6,500 tonnes per day—amounting to a mere fraction of the waste generated. A disconcerting reality emerges as we observe the disparity between projections and actions, with only 13 out of the expected 53 cities in India having established recycling facilities for C&DW by the year 2020 (BBMP, 2016). This incongruity underscores the intricate challenges of aligning intent with action, demanding more concerted efforts from all quarters. In this pursuit of sustainability and carbon neutrality, the construction industry stands at a critical juncture. The mission to embrace recycled concrete aggregates and optimize waste management practices beckons as a transformative imperative.

The construction industry's urgent need for sustainable practices is underscored by its significant contribution to C&DW. This chapter focuses on India, where urban areas witness considerable C&DW, primarily composed of concrete, which presents a valuable opportunity for recycling into recycled concrete aggregates (RCA). Emphasizing the advantages of RCA utilisation, the chapter highlights increased protection against seepage, reduced costs through the elimination of mining, diminished environmental impact, and enhanced appeal to governments and customers. Notably, the use of RCA preserves crucial natural resources like gravel, water, coal, and oil while minimizing landfill space wastage. Comparing the environmental impact of natural aggregates involving land excavation and resource extraction, the chapter highlights that recycled aggregates offer a more sustainable option. The extraction and processing of natural materials adversely affect the environment, causing soil degradation, water scarcity, biodiversity loss, ecosystem damage, and contributing to global warming. Recycled aggregates prove economically viable by presenting a nearly 40% lower long-term cost per ton of coarse RCA compared to coarse natural aggregate. Furthermore, the environmental benefits of RCA are approximately 97% higher. Promoting the commercial production of RCA from waste concrete emerges as an imperative and cost-effective solution for the construction industry.

The chapter further investigates (C&DW) management practices at national and international levels. Utilising Autodesk Green Building Studio, the analysis of carbon emissions from clay brick and concrete masonry buildings underscores the environmental and cost benefits of recycling C&DW with recycled aggregates. Project managers and decision-makers must comprehend the cost-benefit dynamics of C&DW management to foster effective waste management plans. The chapter focuses on a case study of Bengaluru, India's fifth-largest metropolitan city, renowned as the 'Silicon Valley' for its tech-driven growth. By examining the city's

C&DW management, the study uncovers that the official estimate of 4000–4250 tonnes/day by the Bruhat Bengaluru Mahanagara Palike (BBMP) underestimates the actual waste generated due to extensive development efforts by government and private developers. It provides insights into the practicality and environmental relevance of employing RCA in construction. With a remarkable 22.32% cost decrease compared to natural aggregates, this approach proves instrumental in creating an eco-friendly construction industry that addresses the growing challenges of sustainable waste management. The construction industry's environmental footprint is a pressing concern, making the transition toward net-zero carbon emissions imperative.

13.2 THE TRANSFORMATION OF RECYCLED CONCRETE AGGREGATES (RCA) INTO SUSTAINABLE CONSTRUCTION MATERIALS

This is a critical step in realizing the potential of circular economy principles and achieving net-zero carbon emissions. This section explores the conversion processes and their impact on the environment, economy, and social dimensions.

Conversion Processes:

1. *Crushing and Grading*: The initial step involves crushing the recycled concrete into various sizes, depending on the intended application. Proper grading ensures that the resulting aggregates meet specific performance requirements.
2. *Cleaning and Removal of Contaminants*: Contaminants such as residual mortar, paints, or other construction debris are removed through mechanical or chemical processes. Effective cleaning enhances the quality and performance of the resulting material.
3. *Mix Design Optimization*: Designing concrete mixtures that accommodate the properties of RCA is essential. Adjustments in water-cement ratio, admixture usage, and aggregate proportions contribute to achieving the desired structural and durability characteristics.
4. *Admixture Utilization*: Incorporating chemical admixtures can enhance the workability, strength, and durability of concrete containing RCA. Admixtures also mitigate the potential negative effects of impurities in the recycled material.

Environmental Impact:

- *Positive Impact*: The conversion of RCA into sustainable construction materials reduces the demand for virgin aggregates, thereby lessening the environmental degradation caused by quarrying and resource extraction.
- *Energy Savings*: The use of recycled materials requires less energy compared to processing virgin aggregates, resulting in reduced carbon emissions and overall energy consumption.

Economic Factors:

- *Cost Savings*: Utilizing RCA as a sustainable material can lead to cost savings due to reduced material acquisition and disposal fees.
- *Market Stabilization*: Wider adoption of RCA can influence aggregate prices by stabilizing supply-demand dynamics and potentially lowering costs.

Social Aspects:

- *Job Creation*: The recycling process, along with the increased demand for sustainable construction materials, can contribute to job creation in recycling facilities, construction sites, and related sectors.
- *Community Engagement*: The integration of recycled materials reflects a commitment to environmental stewardship, enhancing a construction company's reputation and engaging the local community.

Challenges:

- *Quality Control*: Ensuring consistent quality of recycled aggregates poses challenges due to variations in input materials and processing methods.
- *Perception and Acceptance*: Some stakeholders might be cautious about using recycled materials due to concerns about structural integrity and durability.

The conversion of RCA into sustainable construction materials holds promise in aligning with environmental, economic, and social goals. By adopting efficient processing methods and addressing challenges, the construction industry can capitalize on the benefits of utilizing RCA, contributing to a more sustainable and responsible built environment.

13.3 OBJECTIVES AND METHODOLOGY

The foremost aims of the study encompass an in-depth exploration of the prevailing landscape and patterns in international and domestic construction and demolition practices. Concurrently, the study embarks on a comprehensive investigation into the far-reaching ramifications of C&DW on both the environment and the social fabric, as elucidated through a meticulous review of existing literature. The procedural framework guiding this inquiry finds its elucidation in Figure 13.1. The methodology involves a case study in Bengaluru, where data on construction waste generation and carbon emissions are collected.

13.4 GLOBAL C&D WASTE MANAGEMENT LANDSCAPE

The predicament of managing waste stemming from construction and demolition activities has, undoubtedly, assumed global proportions. Countries of considerable magnitude, including the likes of the USA, Australia, and China, have embarked on multifaceted strategies to grapple with this multifarious issue. The relentless march of urbanization invariably fuels an upsurge in construction undertakings, inevitably leading to a dual effect: the voracious consumption of raw materials and the

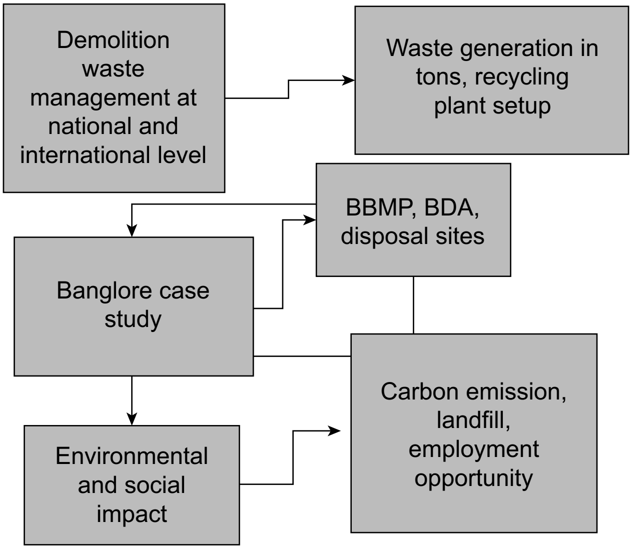

FIGURE 13.1 Methodology adopted for the study.

concurrent emergence of copious C&D waste. An illustrative example lies in China, where the staggering magnitude of C&D waste generation oscillates between 1.6 to 2.5 billion tonnes (Di Maria et al., 2018). In a parallel narrative, Brazil contributes to this global challenge, amassing approximately 100 million tonnes of C&D waste. Regrettably, a substantial fraction of this waste is relegated to unsanctioned spaces—the fringes of sidewalks, roadsides, canals, and lakes—where the environment suffers dire consequences due to these unauthorized disposal practices (Rosado et al., 2019).

13.5 NATIONAL DYNAMICS OF C&D WASTE

Within the borders of India, the narrative of C&D waste echoes a dynamic strain of challenges. The country bears witness to an annual generation of C&D waste encompassing a spectrum of 112 to 431 million tonnes. Intriguingly, a significant revelation emerges: a mere fraction of the anticipated 53 cities were poised to usher in recycling facilities to recuperate materials from C&D waste by the year 2017. However, reality paints a different canvas, as a mere 13 cities have managed to translate this aspiration into action by the year 2020 (Jain et al., 2018). The landscape is further punctuated by rising transportation costs, a direct consequence of inadequate recycling plant infrastructure. Moreover, the extensive traversal of materials like fly ash and M sand precipitates the emission of CO_2. Illuminating this quandary, the Building Material Promotion Council casts light on an alarming figure—a recycling capacity of a meager 6,500 tonnes per day, constituting a paltry percentile. As this narrative unravels across the diverse cities of India, Figure 13.2 offers a graphic portrayal of the varying degrees of C&D waste generation.

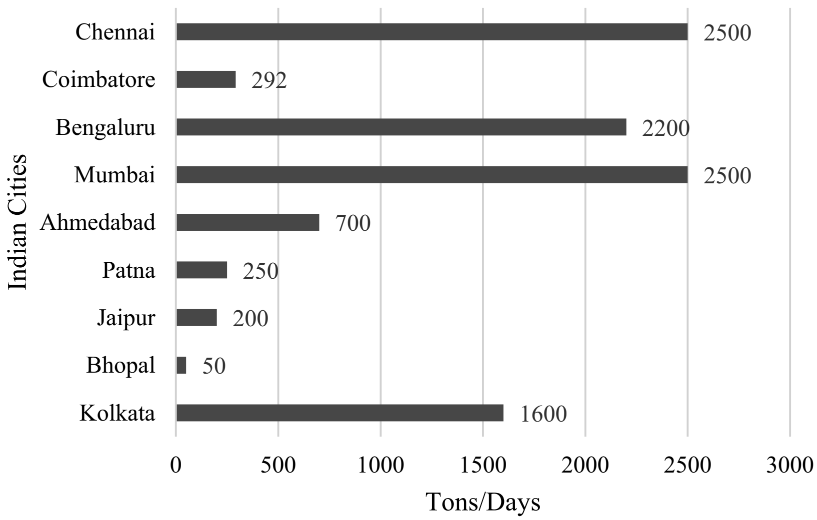

FIGURE 13.2 C&DW generation in different cities in India.

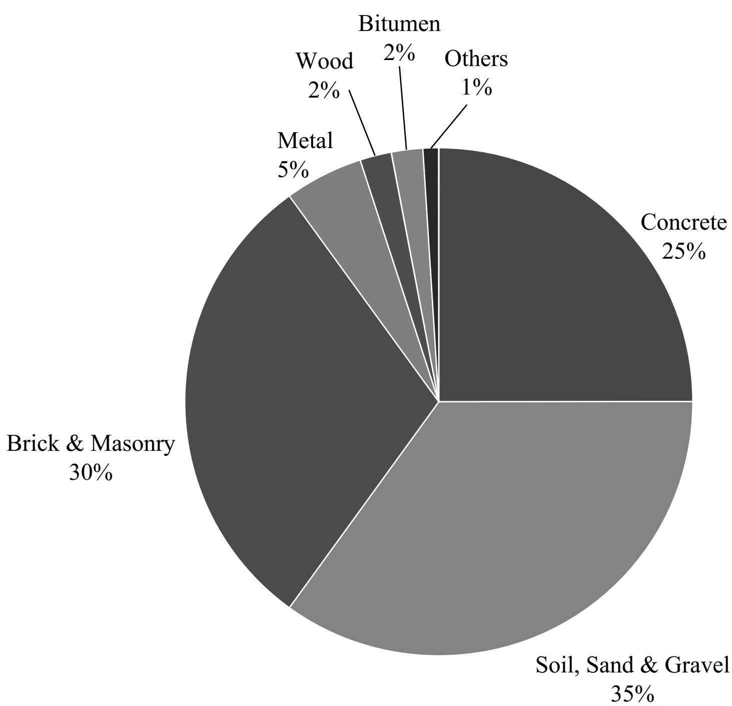

FIGURE 13.3 C&D waste composition in India.

According to Figure 13.2, the urban landscapes of Chennai and Mumbai emerge as prolific generators of debris, whereas Bhopal stands as the exception with the least contribution to this predicament. Within this spectrum, the bustling city of Bengaluru asserts its presence, contributing a formidable 2200 tonnes of waste daily. Further insight into the composition of this C&D waste reveals an intricate tapestry. As delineated by the Bruhat Bengaluru Mahanagara Palike (BBMP), the constituent elements of this waste exhibit a nuanced distribution. Soil, sand, and gravel coalesce to form a substantial portion, representing 35% of the composition, while materials such as bitumen, wood, and metal emerge as minor players in the broader context of the data provided. To encapsulate this vivid mosaic, Figure 13.3 casts light on the array of C&D waste constituent materials, providing a visual representation of their proportions.

13.6 CASE STUDY: C&D WASTE MANAGEMENT IN BENGALURU

Nestled within the urban fabric of India, Bengaluru, the country's fifth-largest metropolis, holds the distinguished moniker of 'Silicon Valley' due to its pivotal role in nurturing the growth of information technology enterprises. In the intricate dance of civic and infrastructural management, the Bruhat Bengaluru Mahanagara Palike (BBMP) emerges as the custodian, steering the course of progress through its dedicated council. Intriguingly, the narrative takes on new dimensions as we delve into the realm of C&D waste management, bearing relevance in the context of Bengaluru's urban sprawl. The intricate web of statistics weaves itself into Figure 13.4, vividly portraying the magnitude of C&D waste production each day within Bengaluru's bustling confines. This city's tale serves as an emblematic microcosm, unveiling the complexities and nuances that underscore the broader discourse on waste management.

The Bangalore Development Authority (BDA) is in charge of the city's major planning and zoning regulations. The information was gathered from several case studies on the BBMP website. The waste is projected to be 2500–3500 tonnes per day, according to numerous case studies conducted by various firms. Table 13.1 shows the C&D waste generation by activity.

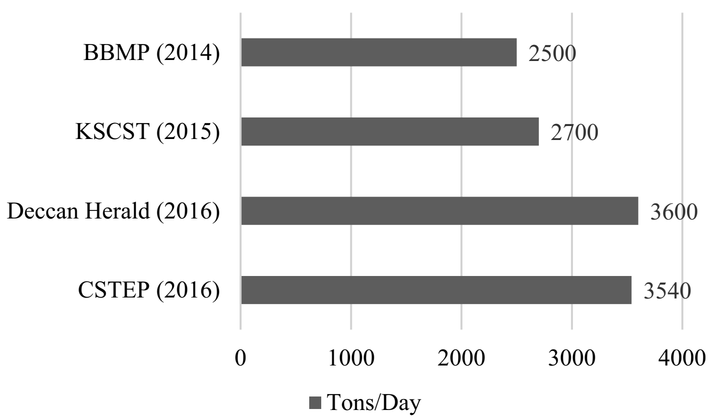

FIGURE 13.4 Bengaluru case study from different organizations in the years 2014–2016.

TABLE 13.1
C&DW Generation by Activity

Activity	Rate of Generation (waste/area)
Construction	40 Kg/m^2
Repair	50 Kg/m^2
Demolition	450 Kg/m^2

The mantle of overseeing the city's pivotal planning and zoning regulations rests upon the BDA. Drawing from a tapestry of case studies found on the BBMP website, a comprehensive repository of information was curated. Within this wealth of data, a prevailing pattern surfaces, projecting daily waste generation ranging from 2500 to 3500 tonnes, as evidenced by a multitude of case studies orchestrated by diverse firms. Navigating this labyrinth of statistics, Table 13.1 comes to the fore, delineating the spectrum of C&D waste generation classified by distinct activities. In this table, a nuanced narrative unfolds, illuminating the differential contributions of various undertakings to the tapestry of waste creation.

13.6.1 Present Designated BBMP Disposal Sites in Bengaluru

Within the dynamic landscape of Bengaluru, the generation of waste emerges as a quantifiable yet multifaceted phenomenon. A precise depiction of this scenario is revealed through distinct metrics: for every square meter of construction, 40 kilograms of waste emerge; in the realm of renovation, this figure amplifies to 50 kilograms for every cubic meter; meanwhile, the process of demolition begets a substantial 450 kilograms of debris for every cubic meter. These numerical insights, akin to brushstrokes on a canvas, contribute to the vivid portrait of waste generation that paints the city's ever-evolving urban panorama.

The intricate choreography of managing C&D waste across Bengaluru unfolds against the backdrop of specifically designated disposal sites. These sites serve as vital conduits for channeling waste generated from all four distinct zones of the city. As orchestrated by the BBMP, a meticulous blueprint guides this process, steering the C&D waste towards eight predetermined dumping sites. This orchestration of waste management takes tangible form within Table 13.2, an illustrative canvas that unveils the geography of these eight disposal sites in Bengaluru. With each site endowed with its capacity and status, this table provides a snapshot of its utilization within the present context, painting a vivid picture of the city's waste management infrastructure.

In Bengaluru, the landscape of disposal sites is marked by the operational presence of Mallasandra and Srinivasapura. These two sites stand as active players within the city's waste management orchestration, serving as conduits for the deposition of C&D waste. In contrast, the other disposal sites remain dormant, their silence echoing the absence of C&D waste being directed towards them. Within this tableau, Mallasandra unfolds across an expanse of 30 acres, while

TABLE 13.2
Active and Inactive Disposal Sites in Bengaluru

Sl. No.	Name of the Site	Area in Acres	Nearby Zone	Status
1	Mallasandra	30	R.R. Nagar/West	Active
2	Kadu Agrahara	18	Mahadevpura	Inactive
3	Srinivasapura and Kogilu	10	Yelahanka	Active
4	Gollahalli	60	Bommanahalli and South	Inactive
5	Kannur	50	East	Inactive
6	Guddadahalli	46	Dasarahalli	Inactive
7	Mittaganahall	10	East/Mahadevpura	Inactive

TABLE 13.3
List of Some SCUs Present in Bengaluru

Name of SCU	Tons/Day	Location
Vinayaka Stone Crushers	1000	Magadi Road (West Bengaluru)
Rock Crystals	1000 (Currently operating at 10% of its capacity)	Chikkajala, Bengaluru
Aishwarya Stone Crushers	<1000	Kumbalgodu area, Mysore Road
Proman Infrastructure Services Pvt. Ltd.	<1000	Bidadi, Bengaluru

the Srinivasapura site occupies a more modest 10-acre terrain. These figures provide spatial context to the operational areas of these disposal sites, contributing to the broader understanding of Bengaluru's efforts in managing its waste landscape.

13.6.2 Stone-Crushing Units (SCUs) in Bengaluru

Beyond the urban pulse of Bengaluru, a distinctive facet of the city's landscape emerges in the form of stone-crushing units (SCUs). These units, situated on the outskirts, are integral players in the dynamics of the region. The stage is set within Table 13.3, a comprehensive enumeration of these SCUS that dot the periphery of the city.

In this tabulated narrative, a spectrum of names comes to life, each associated with a distinct crushing capacity. Vinayaka Stone Crushers and Rock Crystals stand as towering entities, boasting a formidable crushing capacity of 1000 tonnes per day. In contrast, Aishwarya Stone Crushers and Proman Infrastructure tread a more modest path, each equipped with a capacity of under 1000 tonnes per day. These figures paint a vivid picture of the operational landscape of SCUs in Bengaluru's periphery, revealing their unique roles in the city's trajectory.

13.6.3 Energy Analysis Employing Revit 2020.2 and Autodesk Green Building Studio

The synergy of Revit 2020.2 and Autodesk Green Building Studio (GBS) culminates in a sophisticated energy analysis paradigm. Revit functions as an orchestrator, harmonizing project outputs and assimilating diverse data streams, encompassing computer-aided design (CAD) inputs. The present study has been carried out using Revit 2020.2, which undertook the creation of architectural blueprints spanning dimensions both imperial (30’ x 40’) and metric (3m x 4m). The design genesis mandates the incipient generation of a bespoke project file, followed by the pivotal decision of adopting either metric or imperial measurement units. The meticulous edifice assembly entails judicious selections: foremost, a choice amongst architectural wall types, trailed by a granular delineation of material composition and dimensions. Further configuration emerges from architectural floor menus, instating dimensionality and specifying material attributes. Roof genesis unfolds upon venturing into the roof module, encompassing material preference, area demarcation, and the pivotal designation of default material typology. Material attributes and dimensions attain formal articulation through the window settings, setting the stage for analytical profundity.

Navigating into the analysis continuum, one traverses the energy optimization domain. The acme of this architectural tango is embodied by the initiation of an energy analytical model, realized via the “create energy analytical model” prompt. This multifaceted orchestration culminates with the curation of an energy analysis file, elegantly transcribed into the gbXML format.

13.6.4 Energy Analysis (Carbon Emissions) within Autodesk Green Building Studio

The saga of energy analysis unfurls seamlessly into Autodesk GBS, casting this analytical pursuit in a broader arena. The preceding groundwork, scribed with precision within Revit 2020.2, furnishes the blueprint for the energy analysis model, delineating its appellation, edifice typology, and temporal framework (Autodesk Green Building Studio User Guide, 2023).

Within the tapestry of GBS, the commencement of a novel project eventuates after the architectural inception etched by Revit. Herein, the geospatial connotation assumes significance, leading to the formal instantiation of the project canvas. Integration of the Revit gbXML artifact transpires within the interface’s actions nexus, culminating in the triggering of consequential outcomes via file execution.

13.6.5 Energy Analysis Findings for the 30' x 40' Blueprint

The denouement of this discourse rests upon the revelation of energy analysis findings for an architectural magnum opus spanning dimensions of 30 feet by 40 feet. This chapter pivots upon the exposition of estimated CO_2 emissions inherently embedded within the design ethos, concurrently unearthing the latent potential for attaining carbon neutrality.

The sculpted insights emanating from Autodesk GBS spotlight a remarkable discourse. Within a concrete block manifestation of the 30’x40’ paradigm, a prodigious deduction of net CO_2 emissions materializes at –10.3 tonnes, as elegantly encapsulated by Figure 13.5. In parallel, the clay brick variant advances an even more conscientious environmental narrative, portraying net CO_2 emissions at an astonishing –13.2 tonnes, vividly depicted by Figure 13.6.

This data highlights the pre-existing CO_2 emissions in the absence of design interventions or elements aimed at curtailing carbon output, like the integration of renewable energy sources. In specific cases, the concrete material exhibits a prospective for on-site carbon reduction, measured at –21.7 tonnes for concrete and –22.6 tonnes for clay brick. This negative value underscores the potential for eliminating carbon emissions by adopting renewable energy solutions instead of traditional utility-based electricity sources. Moreover, an intriguing facet emerges through the concept of natural ventilation potential, which showcases the carbon offset achievable by leveraging natural cooling methods, thereby circumventing electricity-intensive mechanical cooling systems. For instance, concrete holds a natural ventilation potential of –0.6 tonnes, whereas clay brick surpasses this with –1.5 tonnes of potential carbon reduction. The integration of on-site biofuels introduces yet another avenue for carbon mitigation, elucidated by the negative values of –7.0 tonnes for concrete and –2.7 tonnes for clay brick. This articulates the tangible environmental advantage attainable by

Carbon Footprint

Base Run Carbon Neutral Potential ?

Annual CO_2 Emissions	tons
❶ Base Run	19.0
Onsite Renewable Potential	-21.7
Natural Ventilation Potential	-0.6
Onsite Biofuel Use	-7.0
Net CO_2 Emissions	-10.3

FIGURE 13.5 Net carbon emissions for concrete blocks.

Carbon Footprint

Base Run Carbon Neutral Potential ?

Annual CO_2 Emissions	tons
❶ Base Run	13.6
Onsite Renewable Potential	-22.6
Natural Ventilation Potential	-1.5
Onsite Biofuel Use	-2.7
Net CO_2 Emissions	-13.2

FIGURE 13.6 Net carbon emissions for clay bricks.

substituting traditional fossil fuel sources like natural gas, fuel oil, or propane with on-site biofuels.

A study conducted by Marian Sabau et al. in 2021 underscores the role of recycling aggregates in diminishing CO_2 emissions. Their investigation encompasses diverse mix proportions denoted by labels A, B, C, and D, each evaluated for distinct concrete properties. Among these, scenario A emerges as the exemplar, with the composition C75-S25-RA100-L-F22 (75% cement, supplementary cementitious material, 100% recycled aggregates). The study highlights that the transition from RCA to natural concrete aggregates (NCA) at varying percentages and the incorporation of supplementary cementitious materials (SCM) have significant implications on global warming potential (GWP), quantified at 3,308 $kgCO_2$ for certain scenarios.

13.7 UNVEILING THE ENVIRONMENTAL IMPLICATIONS

Within the intricate tapestry of C&D waste, a diverse array of materials emerges, each with its unique journey of impact on the environment. Segregation and redirection for reuse/recycling are the tenets that govern materials like metals, wood, glass, and plastics, effectively minimizing their environmental footprint. However, a starkly different narrative emerges for C&D debris encompassing concrete, bricks, and tiles, which frequently end up in landfills, triggering a cascade of adverse effects upon the environment. Under the scrutiny of life-cycle assessment (LCA) studies, a resounding verdict resonates—recycling emerges as the preferred pathway. Nevertheless, it's pertinent to note that the environmental credits accrued from these studies are primarily attributed to the recycling of metals and wood, leaving a gap in our understanding of the broader environmental implications of C&D debris recycling. The act of landfilling C&D debris casts a shadow of environmental impacts while recycling scenarios manifest environmental benefits (Ram et al., 2020).

Delving further, the intricate dance of environmental and geochemical impacts of RCA production surfaces, replete with insights that mirror the profound influences of cement content, aggregate production, transportation, and waste landfills. A sensitivity study, painting with a palette of SCM and varying ratios of natural-to-recycled aggregate content, unveils nuanced findings. A spectrum of carbon emissions, ranging from 323 to 332 kgCO_2 per cubic meter, emerges for cement-only NCA. Notably, this exploration highlights that RCA, endowed with strength akin to structural members, can eclipse conventional concrete in terms of lower carbon emissions. This revelation underscores their potential as an alternative to achieve global sustainability benchmarks in construction (Sabău et al., 2021).

A field study further adds texture to this evolving narrative, unfurling the energy consumption trajectories associated with the production of NCA and RCA. The energy consumed to produce one tonne of NCA and RCA is charted at 21,112 KJ/tonne and 16,178 KJ/tonne, respectively. The promise of RCA shines through, with a notable 30.5% reduction in energy consumption compared to NCA. A sensitivity analysis deepens our understanding, establishing that the energy consumed to produce RCA remains lower than that of NCA within a maximum distance of 13.5 km. As the spotlight falls on machinery-involved diesel consumption, an intriguing dimension emerges—cost savings complement the prospects of RCA usage (Ittyeipe et al., 2020).

13.8 REVELATION OF SOCIETAL IMPLICATIONS

The resonance of C&D activities reverberates beyond the realm of mere waste generation, casting its shadow upon both the environment and human lives. Within this expansive tapestry, a jarring truth takes shape—C&D waste contributes to a staggering 20% to 30% of total solid waste globally, with concrete and masonry constituting a dominant 70% to 80%. The implications are profound, demanding that the management of C&D waste ascend as a linchpin in cultivating a sustainable environment. Amidst the backdrop of population surges and economic strides, catalyzed by re-development endeavors, India's construction sector has burgeoned. This transformation has been accompanied by the surge of urbanization and industrialization. However, the silver lining is juxtaposed with environmental challenges stemming from the escalating tide of C&D waste. Amidst these complexities, the study of C&D waste's environmental impacts emerges as a pivotal endeavor, delving into the challenges and prospective solutions in India's urban solid waste management landscape (Shen et al., 2004; Gayakwad and Sasane, 2015).

The potential of C&D waste doesn't end with its challenges; it extends into a vista of possibilities. The reclamation of this waste for low-compressive strength applications, such as footpaths and roadside kerbs, harbours the promise to channel 215,000 tonnes of C&D waste, simultaneously circumventing AUD11.8 million in landfill charges, as proposed by the Australia Council. The horizon broadens further, envisioning a new era of RCA with high compressive strength, a prospect that could redefine the construction landscape. The forecasted surge of residential housing projects, estimated to require around 380,000 m^3 of concrete, opens up the potential to divert half a million tonnes of C&D waste from landfills, should this innovative approach find traction.

The tale of structural performance gains depth with the emergence of 100% RCA, fortified by a 10% infusion of fly ash, boasting a robust compressive strength of 40 MPa—a clear indicator of its potential application in high-strength concrete formations (Shaikh et al., 2019). The implications cascade further, proposing the creation of approximately 13 recycling companies in Perth, each with the potential to convert around 0.87 million tonnes of C&D waste into recycled aggregates for both high- and low-compressive applications. In this act of transformation, employment opportunities burgeon, potentially engaging around 40 western Australians annually. This narrative paints a picture of transformation beyond waste—a prospect of sustainable growth, societal impact, and environmental harmony.

13.9 DISCUSSION

Through insights from the findings of the literature and the Bengaluru case study, it becomes evident that RCA play a significant role in achieving net-zero carbon emissions. The case study reveals that buildings constructed with RCA showcase nearly 25% lower carbon emissions compared to those using traditional aggregates. The discussion emphasizes the alignment between the literature's focus on RCA and the practical results observed in the Bengaluru case study. It also addresses challenges related to quality control and supply chain management.

The combined insights from the literature and the case study highlight the potential of such strategies, calling for collaboration among stakeholders to accelerate the transition to a more sustainable construction industry:

- *Holistic C&D Waste Management*: The bedrock of sustainable waste management rests upon the enhancement of C&D waste practices at every juncture. This pursuit encompasses both local and global efforts, demanding a collective commitment.
- *Empowering Bangalore's Transformation*: A pivotal stride for Bengaluru entails initiating the mechanism for C&D waste disposal, catalyzing the seamless transition from dumping sites to recycling facilities. This movement will usher in a new era of waste management efficiency.
- *Strategic Spatial Planning*: The quest to minimize both economic and environmental losses incurred during transportation necessitates a calculated approach. The strategic placement of stone-crushing units at intervals of 10 to 15 kilometers emerges as a key strategy.
- *Symbiotic Production*: The tapestry of sustainability extends beyond a singular dimension. To embrace this philosophy, the production of RCA products should align with the geographical presence of recycling units.

This harmonious dance seeks to achieve a balance among environmental, economic, and societal pillars.

- *A Trio of Benefits through Recycled Aggregates*: Pioneering the use of recycled aggregates as a substitute for natural aggregates within concrete is a monumental step. This act carries a triad of benefits: curbing carbon emissions, optimizing wasteland utilization, and opening avenues for new employment opportunities.

13.10 CONCLUSION

The study underscores the importance of sustainable construction waste management and the potential of recycled concrete aggregates in mitigating environmental impacts. The findings provide valuable insights for project managers, decision-makers, and policymakers in the construction industry. The integration of recycled materials not only contributes to environmental preservation but also offers substantial cost savings. However, challenges related to sourcing, quality control, and awareness need to be addressed for widespread adoption. Hence, promoting the utilization of recycled concrete aggregates emerges as a feasible and impactful strategy for creating an eco-friendly construction industry.

REFERENCES

Autodesk Green Building Studio User Guide (2023). Retrieved from www.autodesk.com/green-building-studio/user-guide

BBMP. (2016). *Guidelines for Construction and Demolition Waste Management*. https://site.bbmp.gov.in/documents/Guidelines%20For%20Construction%20And%20Demolition%20Waste%20Management.pdf

Bruhat Bengaluru Mahanagara Palike (BBMP). (2020). *Construction and Demolition Waste Management Report*. https://site.bbmp.gov.in/departmentwebsites/swm/Construction%20&%20Demolition%20Waste.html

Di Maria, A., Eyckmans, J., and Van Acker, K. (2018). Down cycling versus recycling of construction and demolition waste: Combining LCA and LCC to support sustainable policy making. *Waste Management*, 75, 3–21.

Gayakwad, H. P., and Sasane, N. B. (2015). Construction and demolition waste management in India. *Development*, 10, 12.

Ghanbari, M., Abbasi, A. M., and Ravanshadnia, M. (2017). Economic and environmental evaluation and optimal ratio of natural and recycled aggregate production. *Advances in Materials Science and Engineering*, 2017.

Ittyeipe, A. V., Thomas, A. V., and Ramaswamy, K. P. (2020). Comparison of the energy consumption in the production of natural and recycled concrete aggregate: A case study in Kerala, India. *IOP Conference Series: Materials Science and Engineering*, 989(1), 012011.

Jain, S., Singhal, S., and Jain, N. K. (2018). Construction and demolition waste (C&DW) in India: Generation rate and implications of C&DW recycling. *International Journal of Construction Management*, 1–13.

Mak, T. M., Chen, P. C., Wang, L., Tsang, D. C., Hsu, S. C., and Poon, C. S. (2019). A system dynamics approach to determine construction waste disposal charge in Hong Kong. *Journal of Cleaner Production*, 241, 118309.

Muzenda, E. (2014). A discussion on waste generation and management trends in South Africa. *International Journal of Chemical, Environmental and Biological Sciences*, 2, 105–112.

Ram, V. G., Kishore, K. C., and Kalidindi, S. N. (2020). Environmental benefits of construction and demolition debris recycling: Evidence from an Indian case study using life cycle assessment. *Journal of Cleaner Production*, 255, 120258.

Rosado, L. P., Vitale, P., Penteado, C. S. G., and Arena, U. (2019). Life cycle assessment of construction and demolition waste management in a large area of São Paulo State, Brazil. *Waste Management*, 85, 477–489.

Sabău, M., Bompa, D. V., and Silva, L. F. (2021). Comparative carbon emission assessments of recycled and natural aggregate concrete: Environmental influence of cement content. *Geoscience Frontiers*, 12(6), 101235.

Shaikh, F. A., Nath, P., Hosan, A., John, M., and Biswas, W. K. (2019). Sustainability assessment of recycled aggregates concrete mixes containing industrial by-products. *Materials Today Sustainability*, 5, 100013.

Shen, L. Y., Tam, V. W., Tam, C. M., and Drew, D. (2004). Mapping approach for examining waste management on construction sites. *Journal of Construction Engineering and Management*, 130(4), 472–481.

Tam, V. W. Y., Tam, L., and Le, K. N. (2010). Cross-cultural comparison of concrete recycling decision-making and implementation in the construction industry. *Waste Management*, 30(2), 291–297.

14 Potential of Agricultural Residues as Sustainable Resources for Civil Engineering Applications

Narendra Reddy

14.1 INTRODUCTION

Achieving net zero carbon emissions in the construction and building industry is a major target for countries across the globe. Although the construction industry accounts for 13%–15% of the global GDP, it is also responsible for more than 40% of the total energy used and for about 30% of the total annual greenhouse gas emissions (Pervez et al., 2021). Several strategies are being adopted at the national, international and local levels to mitigate the effects of building and construction on the environment. For example, a report by Karlsson et al. indicates that net zero emissions could be achieved by 2045 in the Swedish road construction industry by using recycled steel, aggregates, etc., developing alternate binders, electrification and carbon capture in the steel and cement industry, etc. (Karlsson et al., 2020). Similarly, various waste materials such as scarp tyres, glass, coal waste, fly ash, concrete waste and/or wood waste can be used in bituminous pavement construction and reduce the use of virgin materials, which leads to increased sustainability and reduced pollution (Sizirici et al., 2021; Vishnu and Singh, 2020). Such efforts could lead to the reduction in greenhouse gas (GHG) emissions by as much as 90% (Sizirici et al., 2021).

Cultivation of agricultural crops generates considerable amounts of byproducts and coproducts that are generally discarded as waste and are either burnt or buried. Although these residues are inevitably generated, contain valuable polymers and are available at low cost, they have limited applications. In fact, the unscientific disposal of the residues is a major cause of environmental and health pollution (Koul et al., 2022). Major efforts are being made to reduce the disposal of agricultural residues and find applications to increase their value. Concepts such as circular economy and biorefineries are being aggressively pursued and adopted to reduce the disposal of the residues and add value (Duque-Acevedo et al., 2020a, 2020b; Awasthi et al., 2022).

Composites are unique structures that provide the opportunity to tailor the properties for specific applications. Metal, polymer, fiber-reinforcers and cementitious composites have been extensively used in the construction industry (Mohan et al., 2021; Li et al., 2022; Mosallam et al., 2022; Hamidi and Aslani, 2019). Recently, considerable

DOI: 10.1201/9781032686899-18

efforts have also been made to utilize agricultural residues for composites used in civil engineering applications. For example, composites containing hemp fibers and hemp residues are being used on a commercial scale as an alternative to aggregated concrete. The hemp-reinforced concrete called “hemp crete” has been successfully adopted on a commercial scale (Abdellatef et al., 2020; Kore and Sudarsan, 2021). Similarly, bagasse was used as reinforcement for cement along with lime. Composites with compressive strength of 2.6 MPa and bending strength of 2.1 MPa were obtained (Souza et al., 2022).

In addition to the low cost and large availability, agricultural residues have unique properties that make them ideal for construction and building applications. For instance, banana fibers, sisal fiber and even groundnut shells have high thermal and noise insulation properties. Similarly, coproducts such as chicken feathers and sheep wool have low density and also insulation properties preferred for building applications. In our previous studies, we have reported the use of various agricultural residues and coproducts for developing false ceiling tiles as a replacement for the gypsum-based tiles (Guna et al., 2019; Sheng et al., 2022; Aramwit et al., 2023). The gypsum-based tiles have poor strength and are also easily susceptible to moisture and are non-biodegradable. Hence, we have used several agricultural residues to develop composites as replacements for false ceiling tiles and also insulation panels. In this chapter, we present the process of making the biocomposites and the properties of the biocomposites obtained from various agricultural residues for insulation applications. The properties of the composites obtained have been compared with commercially available gypsum and also to medium-density particleboards.

14.2 MATERIALS AND METHODS

14.2.1 Materials

The agricultural residues such as straw, stems, leaves and husks were collected from farms near our institution. The residues were collected and used for developing the composites without any major chemical or physical treatment to ensure low processing cost and also to maintain the inherent features of the raw materials. Composites were developed using either gypsum or polypropylene (PP) as the matrix. Gypsum was purchased from local vendors and PP was purchased from KT International, Mumbai, India. Commercially available gypsum-based false ceiling tiles and medium-density particleboards were purchased from local vendors.

14.2.2 Producing the Composites

Agricultural residues reinforced gypsum composites: Agricultural residues including rice husk, coffee husk, coconut coir, groundnut shells, etc. were selected to reinforce gypsum and obtain composites. The residues were combined with the gypsum in various proportions by mixing them in water. The mixture was cast into molds and allowed to cure for about 24 hours. Later, the composites formed were dried and cured before using for testing. Various thicknesses and densities of composites were obtained by varying the weight per unit area, thickness and proportion of the matrix and reinforcement.

Polypropylene reinforced with agricultural residues: In the second approach, the residues were combined with PP as the matrix. Desired ratios of the residues and PP were placed in layers and stacked to form a sandwich-type prepreg. This sandwich was compression molded at 160–170°C for 3–5 minutes at predetermined pressure. After compression, the mold was cooled to room temperature, and the composites obtained were collected and stored for further analysis. The thickness, weight/unit area, time and temperature of treatment were varied to obtain composites with the desired properties. The composites obtained were conditioned at different temperatures and humidity and tested for their properties.

14.2.3 Testing the Composites

Composites were cut into the required shape and size for determining the properties. Tensile and flexural tests were done as per ASTM D638–14. Thermal conductivity was analyzed as per ISO 8301:1991 and sound absorption according to ASTM E1052–12. Further, flame resistance was measured according to the UL standard. For all tests, at least 10 samples were tested, and the average and ±one standard deviation is reported. Further, statistical analysis using ANOVA was also performed to determine the significant differences in the values obtained between samples.

14.3 RESULTS AND DISCUSSION

14.3.1 Tensile and Flexural Properties of the Composites

Figure 14.1 provides a comparison of the tensile and flexural strength of composites obtained from agricultural residues as reinforcement and polypropylene as matrix

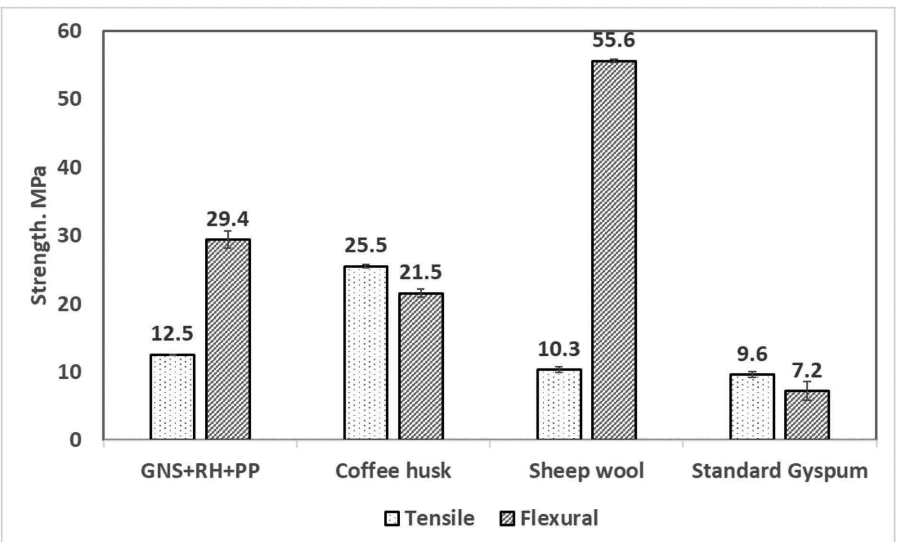

FIGURE 14.1 Tensile and flexural strength of polypropylene (PP) composites reinforced with various agricultural residues. The properties are compared with false ceilings made from gypsum having similar density that are available on the market. The composites were made using 70–80% reinforcement and 20% matrix.

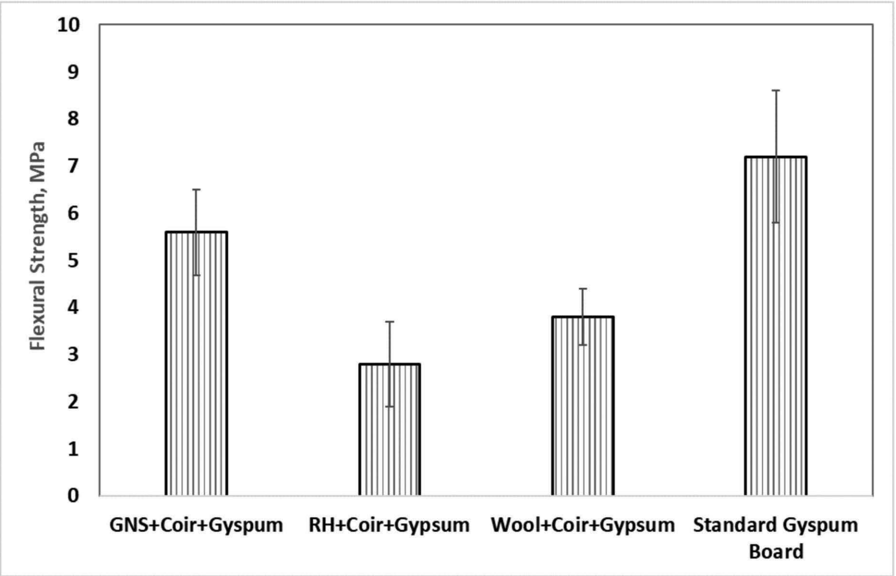

FIGURE 14.2 Comparison of the flexural strength of gypsum reinforced with different agricultural residues and standard gypsum-based ceiling tiles. The composites were made using 70–80% reinforcement and 20% matrix.

in comparison to the commercially available gypsum boards. Considerable difference can be observed in the strength depending on the type of residue used. Tensile strength of the coffee husk composites is highest compared to sheep wool or the groundnut shell (GNS) and rice husk (RH) hybrid composite. However, flexural strength of the sheep wool reinforced composites is nearly twice that of the coffee husk and hybrid composites. Both the tensile and flexural strength of the composites developed are considerably higher compared to the commercially available gypsum boards. Not only PP, even gypsum reinforced with the agricultural residues provide composites with flexural strength similar to that of the commercial gypsum boards (Figure 14.2). The extent of improvement in properties of the composites can be controlled by varying the type of reinforcement and the properties desired for specific applications.

14.3.2 Thermal Conductivity of the Composites

Materials used for thermal insulation applications are suggested to have thermal conductivity of less than 0.1 W/mK. As seen from Table 14.1, composites obtained from the different residues have a varying range of conductivity. The lowest conductivity is obtained from the sheep wool reinforced composites, which is understandable since wool has natural insulation abilities. A combination of wool and coir with gypsum as binder showed considerably high conductivity. The extent of conductivity will not only depend on the inherent properties of the reinforcement but also on the

TABLE 14.1
Thermal Conductivity of Composites Obtained from Various Agricultural Residues

Reinforcement Type	Thermal Conductivity (W/mK)
GNS+RH+PP	0.193± 0.017
Coffee Husk	0.052–0.105
Sheep Wool	0.058–0.083
GNS + Coir + Gypsum	0.12± 0.4
RH + Coir + Gypsum	0.09 ± 0.03
Wool + Coir + Gypsum	0. 305± 1.3
Standard Gypsum Board	0.170± 0.014

Note: Either PP or gypsum was used as the matrix in comparison to commercially available gypsum boards. The composites were made using 70–80% reinforcement and 20% matrix.

TABLE 14.2
Extent of Sound Absorption Possible with Composites Reinforced with Different Agricultural Residues

Composite	Sound Absorption Coefficient
GNS+RH+PP	0.2–0.4
Coffee Husk	0.2–0.9
Sheep Wool	0.86
GNS + Coir + Gypsum	0.10–0.75
RH +Coir + Gypsum	0.25–0.55
Wool + Coir + Gypsum	0. 15–0. 35
Standard Gypsum Board	0.4–0.6

The composites were made using 70–80% reinforcement and 20% matrix.

density, thickness, presence of pores in the composites, etc. Compared to commercially available gypsum, most of the composites meet or exceed the requirements for thermal conductivity.

14.3.3 Acoustic Absorption

Composites obtained in this study have the necessary acoustic absorption properties. As seen from Table 14.2, sound absorption coefficients up to 0.9 can be obtained by varying the type of residue used. Coffee husk–reinforced composites had the highest absorption, close to the ideal level of 1.0. However, wool and GNS/RH composites have relatively low absorption because of the lack of voids and pores that can absorb or dissipate sound.

14.3.4 Flame Resistance

Most agricultural residues are inherently flammable, and hence composites containing the residues have flammability rating between V1–V2 compared to V0 for the gypsum boards. However, composites made from wool and husks have ratings of V0 and V1 depending on the ratio of the reinforcement and density of the composites. Using 1–3% flame retardants such as ammonium polyphosphate have provided composites with complete flame resistance (V0) similar or better than that of the gypsum boards.

14.4 CONCLUSIONS

Agricultural residues are not only renewable, sustainable and low-cost sources for developing composites for civil engineering applications, but they also provide unique properties not possible by using gypsum. Residues such as wool and rice husk have excellent thermal insulation and even sound absorption properties. The technology proposed in this research study enables using agricultural residues in their original form, and multiple residues can be used to develop hybrid composites that meet the specific requirements. Composites developed in this study meet or exceed the properties of the gypsum-based false ceiling tiles available on the market. However, further studies on improving the processability and enhancing the flame resistance of the composites are necessary before the composites could be used for commercial applications.

REFERENCES

Abdellatef, Yaser, Mohammad Amil Khan, Asif Khan, Mehdi Iftekharul Alam, and Miroslava Kavgic. "Mechanical, thermal, and moisture buffering properties of novel insulating hemp-lime composite building materials." *Materials* 13, no. 21 (2020): 5000.

Aramwit, Pornanong, Desmond Daniel Chin Vui Sheng, Goutam Krishna Moorthy, Vijaykumar Guna, and Narendra Reddy. "Rice husk and coir fibers as sustainable and green reinforcements for high performance gypsum composites." *Construction and Building Materials* 393 (2023): 132065.

Awasthi, Mukesh Kumar, Raveendran Sindhu, Ranjna Sirohi, Vinod Kumar, Vivek Ahluwalia, Parameswaran Binod, Ankita Juneja et al. "Agricultural waste biorefinery development towards circular bioeconomy." *Renewable and Sustainable Energy Reviews* 158 (2022): 112122.

Duque-Acevedo, Mónica, Luis J. Belmonte-Ureña, Francisco J. Cortés-García, and Francisco Camacho-Ferre. "Recovery of agricultural waste biomass: A sustainability strategy for moving towards a circular bioeconomy." *Handbook of Solid Waste Management: Sustainability through Circular Economy* (2020b): 1–30.

Duque-Acevedo, Mónica, Luis J. Belmonte-Ureña, José A. Plaza-Úbeda, and Francisco Camacho-Ferre. "The management of agricultural waste biomass in the framework of circular economy and bioeconomy: An opportunity for greenhouse agriculture in Southeast Spain." *Agronomy* 10, no. 4 (2020a): 489.

Guna, Vijaykumar, Manikandan Ilangovan, Chunyan Hu, Krishna Venkatesh, and Narendra Reddy. "Valorization of sugarcane bagasse by developing completely biodegradable composites for industrial applications." *Industrial Crops and Products* 131 (2019): 25–31.

Hamidi, Fatemeh, and Farhad Aslani. "Additive manufacturing of cementitious composites: Materials, methods, potentials, and challenges." *Construction and Building Materials* 218 (2019): 582–609.

Karlsson, Ida, Johan Rootzén, and Filip Johnsson. "Reaching net-zero carbon emissions in construction supply chains—analysis of a Swedish road construction project." *Renewable and Sustainable Energy Reviews* 120 (2020): 109651.

Kore, Sudarshan D., and J. S. Sudarsan. "Hemp concrete: A sustainable green material for conventional concrete." *Journal of Building Material Science* 3, no. 2 (2021): 1–7.

Koul, Bhupendra, Mohammad Yakoob, and Maulin P. Shah. "Agricultural waste management strategies for environmental sustainability." *Environmental Research* 206 (2022): 112285.

Li, Xuemei, Di Qin, Yidan Hu, Waqas Ahmad, Ayaz Ahmad, Fahid Aslam, and Panuwat Joyklad. "A systematic review of waste materials in cement-based composites for construction applications." *Journal of Building Engineering* 45 (2022): 103447.

Mohan, Harish T., Karingamanna Jayanarayanan, and K. M. Mini. "Recent trends in utilization of plastics waste composites as construction materials." *Construction and Building Materials* 271 (2021): 121520.

Mosallam, A. S. (2014). Polymer Composites in Construction: An Overview. *SOJ Materials Science & Engineering*, 2(1), 01–25. doi:10.15226/sojmse.2014.00107

Pervez, Hamza, Yousaf Ali, and Antonella Petrillo. "A quantitative assessment of greenhouse gas (GHG) emissions from conventional and modular construction: A case of developing country." *Journal of Cleaner Production* 294 (2021): 126210.

Sheng, Desmond Daniel Chin Vui, Nagesh Saragondlu Ramegowda, Vijaykumar Guna, and Narendra Reddy. "Groundnut shell and coir reinforced hybrid bio composites as alternative to gypsum ceiling tiles." *Journal of Building Engineering* 57 (2022): 104892.

Sizirici, Banu, Yohanna Fseha, Chung-Suk Cho, Ibrahim Yildiz, and Young-Ji Byon. "A review of carbon footprint reduction in construction industry, from design to operation." *Materials* 14, no. 20 (2021): 6094.

Souza, Patrícia P. L. de, Rute Eires, and Raphaele Malheiro. "Sugarcane bagasse as aggregate in composites for building blocks." *Energies* 16, no. 1 (2022): 398.

Vishnu, T. B., and Kh Lakshman Singh. "A study on the suitability of solid waste materials in pavement construction: A review." *International Journal of Pavement Research and Technology* 14 (2021): 625–637.

15 Mortars for Thin Joint Masonry Utilising Recycled Materials for Sustainability and Circularity

S M Basutkar, Ashwin M Joshi, Md Imran Ahmed, Namratha Bharadwaj and M V Renukadevi

15.1 INTRODUCTION

Mortars are the binding materials used in the construction of masonry. Their composition comprises a homogeneous blend of cementitious materials along with inert fine aggregate fraction and water. The selection and composition of mortar are pivotal in masonry construction, as they have a significant impact on various characteristics, including strength, durability, and resistance to rain. The behaviour of masonry construction is greatly influenced by the characteristics of mortar in a fresh and hardened state. The characteristics like consistency (workability) and water retentivity of mortar in fresh states are of most importance, as it assists during construction of the masonry bed joint. The hardened mortar characteristics, including bond strength, drying shrinkage, porosity, and stress-strain behaviour of mortar, significantly affect the performance of masonry strength.

In the field, conventional or normal masonry construction comprises bed joint thickness of 12–15 mm [1]. Use of such masonry practice demands a large volume of conventional materials, which are energy intensive and create greater impact on environment. An innovative technique named *thin joint masonry construction* has been widely practiced in the West, which recommends the use of bed joint thickness of 0.5–3 mm [2]. The compressive strength of these mortars ranges from 10–15 MPa. This technique proves to be effective for construction of low-rise masonry, resulting in large savings in mortar materials and providing a sustainable environment. This thin joint masonry demands mortars made with particle size of fine aggregate less than 1 mm [2]. Use of conventional sand for production mortars for thin jointed masonry requires additional segregation, which results in time and economic constraints. However, it is possible to develop mortars for thin bed joints in masonry construction with alternate materials containing particle size of maximum 1 mm resulting from recycling. It is noteworthy to mention the masonry unit properties especially of bricks

DOI: 10.1201/9781032686899-19

in the developed economies have compressive strength in the order of about 60 MPa. However, for developing countries, the compressive strength for locally produced table-moulded bricks lies in the range of 7–10 MPa. For such bricks, suitable mortars can be developed for thin jointed masonry using conventional fine aggregates and its alternatives. In this way, one can ensure circularity in construction.

Over the years, extensive construction activities have exploited conventional materials, leading to depletion of natural resources and consumption of non-renewable fossil fuels. These actions have considerable implications and have done irreparable damage to the environment, like emission of greenhouse gases, depletion of the ozone layer, and promoting global warming and climate changes. Thus, there is no haziness about the fact that immediate action should be taken in this field, primarily to reduce use of natural resources and energy consumption, and to encourage the use of eco-friendly and sustainable materials leading to a sustainable environment. The various alternate construction materials like natural soil, manufactured sand, marble fines, granite fines, masonry waste, and concrete waste are used for developing mortars. The application of such mortars and an industrial product in the development of thin bed joint masonry is explored in this chapter to promote sustainable construction.

15.2 MATERIALS

15.2.1 Natural Soil (S)

Soil is a naturally occurring material which is abundantly available. The utilisation of soil as a building material has been in practice since ancient times and is considered to be eco-friendly, cost-effective, and efficient to practice with minimal impact on the environment. A wide variety of soil is available, thus in the process of selecting soil as a construction material, factors like type and constituents of soil are of utmost importance. Ancient construction employed soil as fine aggregates in making mortars with different binders. Mortars for thin jointed masonry construction can be developed using fine soils with an appropriate amount of silt and clay content. The properties of soil used for evaluation of thin joint masonry behaviour is presented in Table 15.1

15.2.2 Manufactured Sand (M Sand)

Manufactured sand or M sand is the most popular alternative widely used in the construction process as a substitute to conventional river sand. The sand size particles are acquired by means of a crushing aggregate process in a stone-crushing plant. The properties of M

TABLE 15.1
Characteristics of Soil

	Gradation of Soil (%)					
Soil Type	**Gravel**	**Sand**	**Silt**	**Clay**	**G_s**	**References**
Type-I	-	40	40	20	2.52	[1]
Type-II	-	28	35	37	2.35	[3]
Type-III	-	32	55	13	-	[4]

sand vary considerably depending on the source of the parent material. The shape of particles must be given significant consideration during the production process to avoid the accumulation of charges on edges, leading to improper bonding with the binders.

15.2.3 Granite Fines or Powder (GF)

Granite fines (GF) is a byproduct produced in granite factories while cutting huge granite rocks and polishing slabs. GF debris is generally in the form of slurry produced by granite industries. GF generally contains a large portion of silt-size particles of the order 65–80% [5]. India has about 15% of the world's stone deposits [6]. There are also about 350 granite cutting and polishing industries [5]. These resources generate a considerable amount of granite sludge. Research in the recent past [5, 6] has shown that fines generated from stone-polishing industries can be used as sand replacement in mortar, concrete, and masonry units. Effective utilisation of these industrial waste materials will resolve environmental problems of their disposal.

15.2.4 Marble Fines or Powder (MF)

Marble fines (MF) is the waste generated during marble polishing in marble industries. MF mainly consists of calcite and other minerals like mica, quartz, pyrite, etc. [7]. India is among the leading producers of marble products. The state of Rajasthan has about 1100 MT of marble deposits, with 1200 marble processing units generating five to six million tonnes of marble waste annually [8]. The application of marble waste as a resource will not only reduce the environmental effects of disposing of marble waste, but also lead to conserving natural resources. Marble waste has also shown its potential to be utilised as fine aggregates in concrete production [8]. Recent investigations indicate the pozzolanic behaviour of marble waste in cementitious products.

15.2.5 Ready-Mix Mortar

'Fixoblock', a ready-mix product, is widely used as jointing material in masonry nowadays. The premix consists of a mixture of cement, sand, and admixture ready to be used on-site with the addition of water. It serves as a highly effective jointing material between masonry units, since application of only 3 mm with '*Fixoblock*' achieves a bond strength comparable to conventional mortar of 12–15 mm thickness. It should be noted that adequate mixing is required to be administrated before application. The addition of moisture depends upon the consistency of paste required.

15.2.6 Construction and Demolition (C&D) Waste

Construction and demolition (C&D) waste are the wastes generated during construction and demolition of structures after their serviceable life. It usually contains demolished materials from masonry wall, concrete slab, plastering mortars, etc. This type of waste can be recycled and reused as recycled aggregates in the construction operations after the proper sorting, crushing, and screening processes. Considerable studies have been conducted in producing building products like concrete and allied products [9].

The properties of various alternate materials used as fine aggregates in making mortars for thin joint masonry are presented in Table 15.2. It is interesting to

TABLE 15.2
Characteristics of Materials

Materials	FM	Zone	G_s	WA (%)	Dry Density (g/cc)	References
MS	2.2–2.6	II	2.59–2.62	1.6–3.6	-	[3, 11]
NS	2.53	II	2.66	-	-	[1]
GF	1.083–1.2	IV	2.16–2.5	-	1.17–1.2	[11, 12]
MF	1.25	-	2.31	-	1.2	[11]
CW	-	II	2.51	5.44	-	[13]
MW	-	II	2.57	6.32	-	

note that natural sand and manufactured sand were categorised in Zone-II, as shown in Figure 15.1a. Granite and marble fines contain a large amount of fine (silt and clay-sized) particles and was beyond Zone-IV of the Indian standard code of practice IS 383–2016 [10]. The grain size distribution of various fine aggregates and its alternatives are presented in Figure 15.1a and Figure 15.1b.

15.3 MORTAR PROPERTIES

The constituent of mortar and its proportioning plays a significant role in the development of strength. The water-to-cement ratio have a greater contribution in attaining the desired strength and improving the workability of mortar during masonry construction. In comparison to conventional cement-sand mortars, use of soil, C&D waste, and fines from granite and marble industrial waste demands more water due to the presence of clay and fine particles with high water absorption capacity. Water absorption of mortar is a property that is often not accounted for. However, water absorption defines the voids in mortar composites and leads to moisture movement through mortar joints. This moisture holding and movement lead to aesthetics distortion of masonry elements and facilitate mold growth. Conventional cement sand mortar exhibits water absorption of 5–10% [14]. Somanath et al. also reported a similar range of water absorption limits for GF-based mortars [14]. A stiff lump of paste was obtained for 100% flow for fines-based mortar, improving the workability. Along with this, rapid hardening of paste was observed at low water-to-cement ratios (w/c). Use of soil and C&D waste often accounts for considerable variation in water absorption. This value may range from 5–27% depending upon the absorption capacity of fine aggregate, cement content in the mortar, and the percentage replacement of natural aggregate by alternative substitute. The w/c for each mortar combination is selected depending upon the consistency of mix required; generally, w/c corresponding to a flow of 100–115% was selected [15]. The characteristics of various alternate mortars explored are presented in Table 15.3.

15.3.1 Compressive Strength

The compressive strength of mortar combinations was evaluated on specimens of sizes specified by IS 10086:1982 - RA 2008 [16]. Flow of 150–175% was maintained for mortars containing granite fines. A total of 20 mortars were explored, using various alternatives to conventional fine aggregates. These mortars were categorised as soil, granite fines, marble fines, and C&D waste fines-based mortars. The compressive strength of

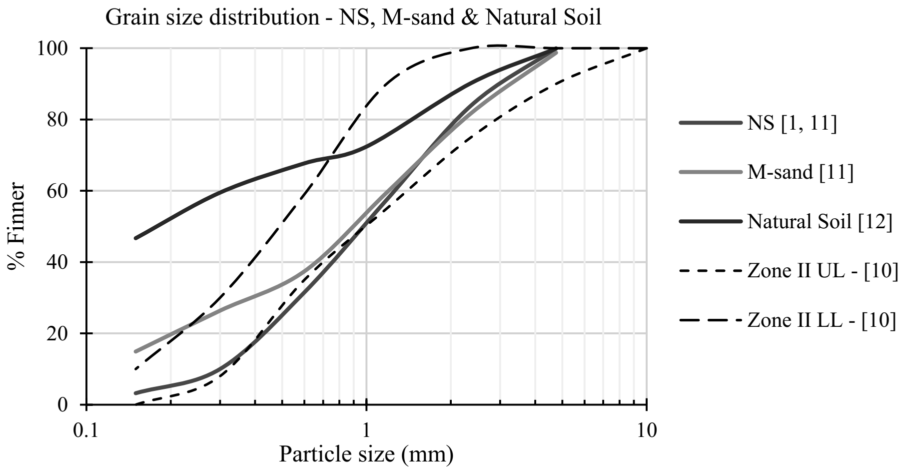

FIGURE 15.1A Grain size distribution of natural sand, M sand, and natural soil.

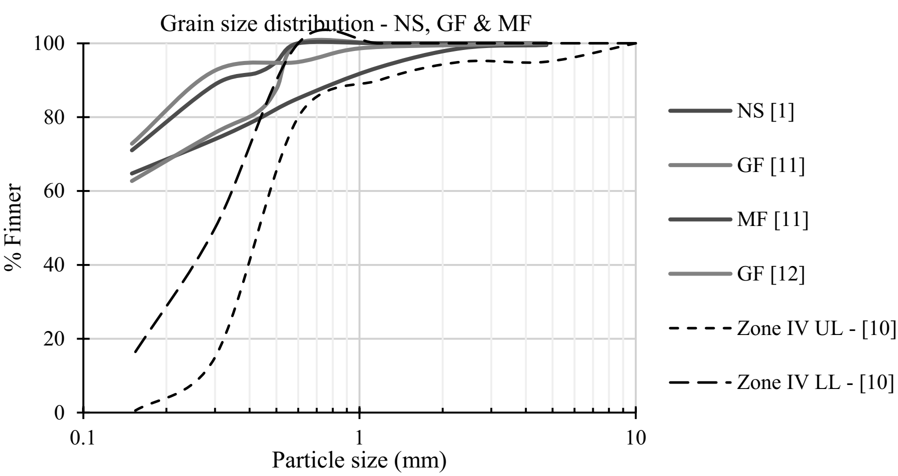

FIGURE 15.1B Grain size distribution of natural sand, granite fines, and marble fines.

mortars for thin joint masonry was also dependent on cement content in the mix and constituent materials. The detailed designation and characteristics of mortars explored are presented in Table 15.3. Series A and B mortars were made with soil containing clay of 20%. However, Series C and D mortars contained clay of 37%. Soil-based mortars exhibited contrasting variations in their strength characteristics. This is mainly due to the presence of silt and clay content in the soil used as fine aggregates in mortars. More studies are required to investigate the strength properties of mortars for thin joint masonry made with modified soil suitable for manufactured compressed earth blocks. The clay and silt content in such soils are often restricted to 10–15% and 30–35%, respectively.

Despite a higher flow percentage of GF-based mortars, compressive strength was found to vary 7.52 to 16.31 MPa. Mortars samples (F, G, and I) comprise

TABLE 15.3
Characteristics of Different Mortar Combinations

Designation	Constituents of Mortar	Proportion	w/c	CS (MPa)	Reference
A	C: L: S: P	1:1:2	1.50	11.29	[1]
B	C: L: S: P	1:1:1.5		14.13	
C	C: L: S: P	1:1:1	-	2.50	[3]
D	C: L: S: P	1:1:2		2.19	
E	C:GF	1:1	0.79	16.31	[4]
F	C:GF	1:2	1.17	11.47	
G	C:S:GF	1:1:1	1.06	12.27	
H	C:S: GF	1:1:2	1.45	7.52	
I	C: S: FA: GF	1:1:1:1	2.45	12.27	
J	C: NS	1:6	1.28	4.31	
K	C:GF	1:3	1.40	13.36	[11]
L	C:MF	1:3	1.20	13.54	
M	C:MS	1:6	1.38	13.66	
N	Fixoblock	-	0.23	13.56	
O	C:MS	1:4	0.80	16.02	[13]
P	C: MS+CW	1:4 (0.7+0.3)	0.80	13.38	
Q	C: MS+CW	1:4 (0.5+0.5)	0.90	12.96	
R	C: MS+MW	1:4 (0.7+0.3)	0.90	16.15	
S	C: MS+MW	1:4 (0.5+0.5)	0.90	11.34	
T	C: MS+CW+MW	1:4 (0.4+0.3+0.3)	0.88	17.58	
H1	CLNS	1:1/4:3		10.00	[17]
H2	CLNS	1:1/4:4		7.50	
M1	CNS	01:05:00		5.00	
M2	CLNS	01:01:06		3.00	

constituents like granite fines, granite fines–soil, and granite fines–soil–fly ash resulted in comparable compressive strength in the range of 11.47 to 12.72 MPa. In addition, use of soil and fly ash along with granite fines showed improved ease in handling of mortar. Madhusudhan [11] investigated the properties of 1:3 (binder: fine aggregate) proportioned mortar. The fine aggregates used in mortars were natural sand, marble waste, and M sand. The compressive strength of mortar was around 13 MPa. A commercial ready-mix mortar called *Fixoblock* was also explored, resulting in a similar compressive strength of 13.56 MPa. Use of C&D waste as fine aggregate in 1:4 proportion mortar was explored [13]. The concrete waste and masonry waste varied from 30%, 50%, and combined 60% as replacement to conventional fine aggregate. Substitution of 30% and combined 60% of concrete waste resulted in higher compressive strength as compared to mortar made with conventional fine aggregates. All of the mortars explored were compared with different grades of masonry mortars as specified by IS 1905–1987 [17]. Figure 15.2 shows that various mortars investigated resulted in higher compressive strength as compared to conventional mortar.

15.4 MASONRY PROPERTIES

The performance of thin joint masonry has been assessed on stack bonded and English bonded prisms, while ensuring the height/diameter (h/d) ratio between 2–5, in accordance with the guidelines mentioned in IS 1905:1987 [17]. A comparison of strength characteristics of normal masonry with 12 mm bed joint thickness and thin joint masonry with bed joint thickness of 3–6 mm is discussed in the following section. The characteristics of different masonry prism evaluated were tabulated in Table 15.4.

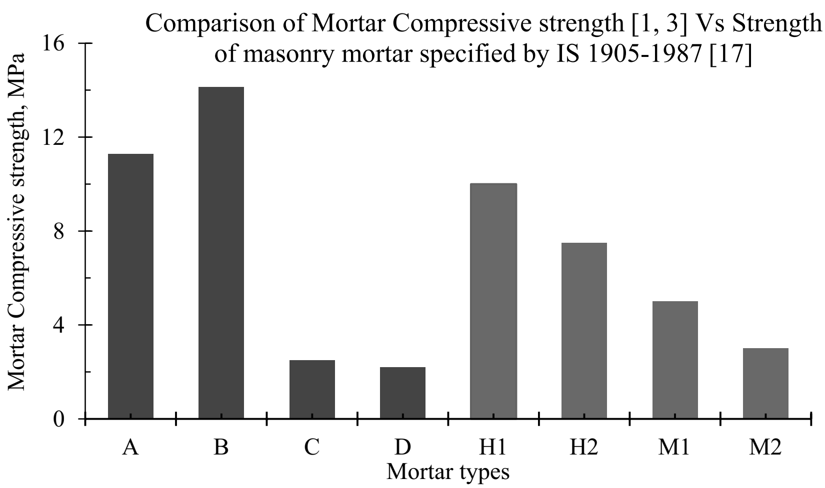

FIGURE 15.2A Soil-based mortars.

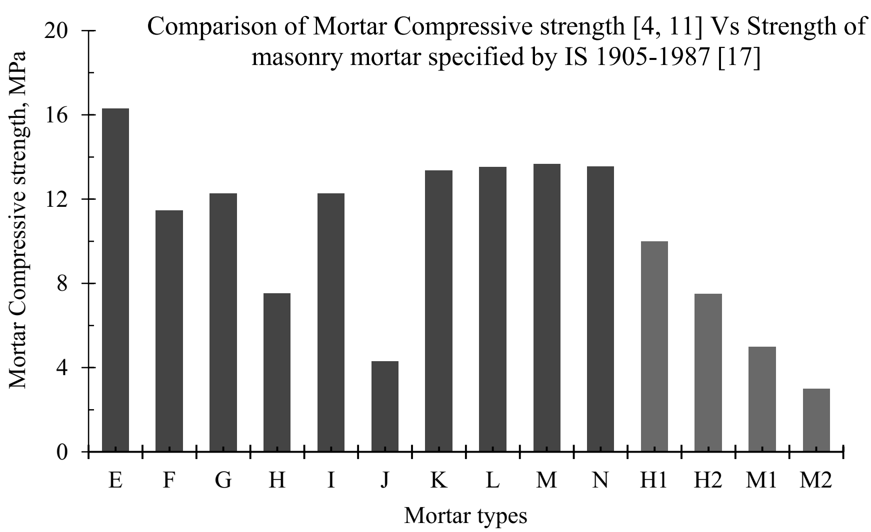

FIGURE 15.2B Granite fines and marble fines-based mortars.

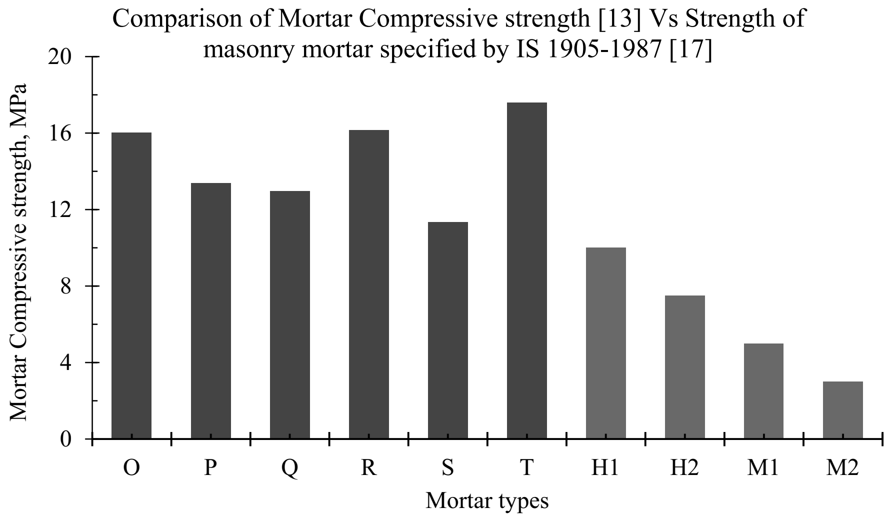

FIGURE 15.2C C&D waste-based mortars.

TABLE 15.4
Characteristics of Thin Joint Masonry Prism

Designation	fm (MPa)	fb (MPa)	h/t	CS (MPa) SBP	CS (MPa) EBP	FS (MPa)	Reference
A	11.29	8.53	2.15	4.05	-	-	[1]
B	14.13		2.15	4.35	-	-	
C	2.50	6.18	-	-	2.22	-	[3]
D	2.19		-	-	2.43	-	
E	16.31	5.92	1.77	-	1.67	0.13	[12]
F	11.47		1.76	-	1.70	0.20	
G	12.27		1.87	-	1.45	0.19	
H	7.52		1.87	-	1.09	0.14	
I	12.27		1.88	-	1.19	0.14	
E	16.31	8.99	1.77	-	4.93	0.26	
F	11.47		1.76	-	3.65	0.31	
E	16.31	14.64	1.77	-	4.66	0.35	
F	11.47		1.76	-	5.39	0.30	
K	13.36	4.64	2.09	-	1.10	-	[11]
L	13.54		2.11	-	1.44	-	
M	13.66		2.11	-	1.32	-	
N	13.56		2.02	-	1.90	-	
O	16.02	5.93	-	2.33	1.36	0.14	[13]
P	13.38		-	1.89	1.38	0.06	
Q	12.96		-	2.35	3.22	0.09	
R	16.15		-	1.84	4.30	0.15	

(*Continued*)

TABLE 15.4 (*Continued*)
Characteristics of Thin Joint Masonry Prism

Designation	fm (MPa)	fb (MPa)	h/t	CS (MPa) SBP	EBP	FS (MPa)	Reference
S	11.34		-	1.34	2.82	0.04	
T	17.58		-	1.77	3.24	0.05	

fm—mortar strength, fb—unit strength, CS—Compressive strength, FS—Flexural strength, SBP—Stack bonded prism, EBP—English bonded prism, h/t ratio for English bonded prisms was 2.00–2.71 and for stack bonded prism was 4.00–4.5

15.4.1 Compressive Strength of Prism

The strength of masonry prism is influenced by various parameters, including strength of masonry unit, h/d ratio, moisture absorption of masonry unit, thickness of mortar joint, and the ratio of elastic modulus of mortar and masonry unit. Masonry compressive strength is significantly influenced by unit strength more than mortar strength. Masonry compressive strength with conventional bed joint thickness can be evaluated using equation (1), whereas prism compressive strength of thin bed joint masonry can be evaluated using equation (2) as per the Euro code:

$$f_k = k.f_b^{\alpha}.f_m^{\beta} \tag{15.1}$$

$$f_k = k.f_b^{0.70} \text{ to } k.\ f_b^{0.85} \tag{15.2}$$

where f_k_Compressive strength of masonry prism, f_b—Unit strength, f_m—Mortar strength, k,α,β—Constants depending upon type of masonry and type of bonding [18].

From equation 15.2, it can be observed that when the mortar strength is not greater than 20 MPa or twice the strength of unit, compressive strength of thin joint masonry is governed by unit strength only. Increase in brick strength improved the masonry compressive strength of thin jointed and normal masonry. Compressive strength of thin jointed masonry increased by 32–48% for brick strength up to 8 MPa. This increment in masonry compressive strength was 24–16% higher for high-strength bricks, i.e., f_b greater than 10 MPa. Like thin jointed masonry, increment in masonry compressive strength with increase in brick strength was observed for normal masonry. However, the slope of increment of normal masonry was 32% lower than that for thin jointed masonry, as shown in Figure 15.3a. Masonry efficiency, the ratio of masonry strength to unit strength, was found to increase marginally for thin jointed masonry with an increase in brick strength. Whereas, in the case of normal masonry, masonry efficiency reduced as the brick strength increased, as shown in Figure 15.3b. The strength of mortar does not have a significant role in the development of masonry strength. However, it is desirable to have a good strength of mortar for efficient binding of masonry units.

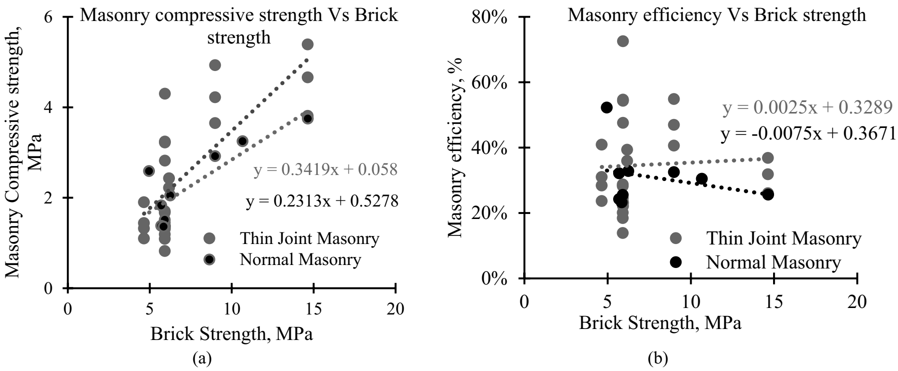

FIGURE 15.3 Variation of masonry compressive strength and masonry efficiency with brick strength.

15.4.2 Flexural Strength of Prism

Flexural strength of masonry prism evaluates the modulus of rupture, which represents the bond strength of masonry units. The bond strength of masonry prism is significantly influenced by the surface texture of masonry units and the type of mortar utilised [1]. Figure 15.4 shows the variation of flexural bond strength of normal masonry and thin joint masonry. It can be clearly seen from Figure 15.4a, for mortars strength ranging 6–12 MPa, an increase in bond strength is around 5.5–6.26% for every 2 MPa increase in mortar strength. The strength of the masonry unit has a major influence in determining the failure pattern of masonry prism. The higher strength masonry unit showed block failure, while mortar joint failure was observed for the masonry unit with comparable lower strength [12], as shown in Figure 15.4b. However, the rate of strength increment of thin joint mortar was higher than the normal masonry. The flexural strength of thin joint masonry prism was evaluated as per ASTM standards C 1072 [19]. The detailed characteristics were presented in Table 15.4.

15.5 ENERGY ANALYSIS

Energy of building components mainly depends on its constituent materials like cement, aggregates, and building units. Burnt clay bricks and cement are the most energy-intensive materials. Embodied energy of aggregate mainly depends on the distance of its procurement. Table 15.5 presents the embodied energy of various basic building materials [20]. Embodied energy per cubic meter of mortar was evaluated and presented in Table 15.6.

Maximum embodied energy was observed for cement-lime-soil mortar followed by mortar made with granite fines. This increase in embodied energy is due to the presence of higher cement content in these mortar proportions. The least energy requirement was exhibited by cement–natural sand mortar of proportion 1:6. However, if the ratio of embodied energy to compressive strength of mortar is observed, cement-rich mortars exhibit lower values as compared to mortars with high sand fractions. Use of cement-rich mortars enhances bond strength characteristics of masonry. This thin jointed mortar will substantially reduce the energy in building components when energy-efficient

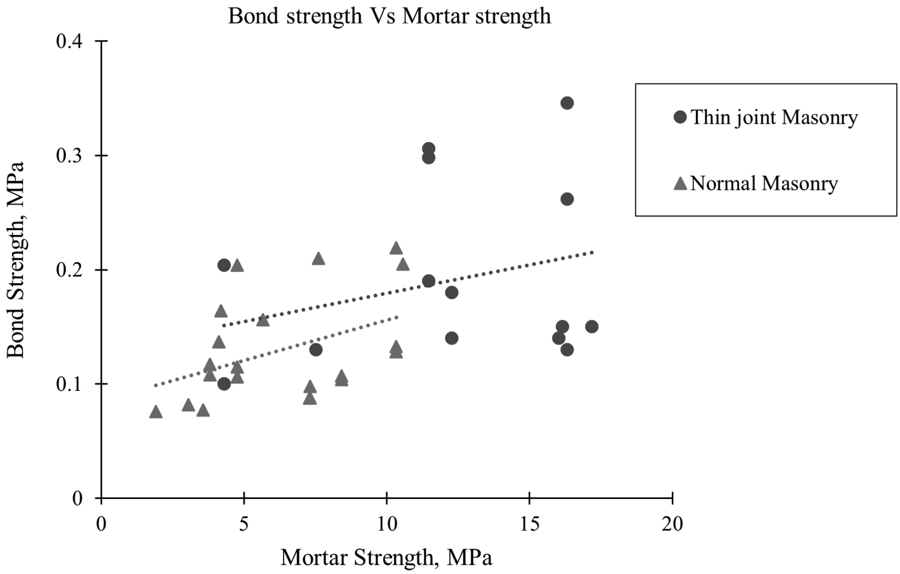

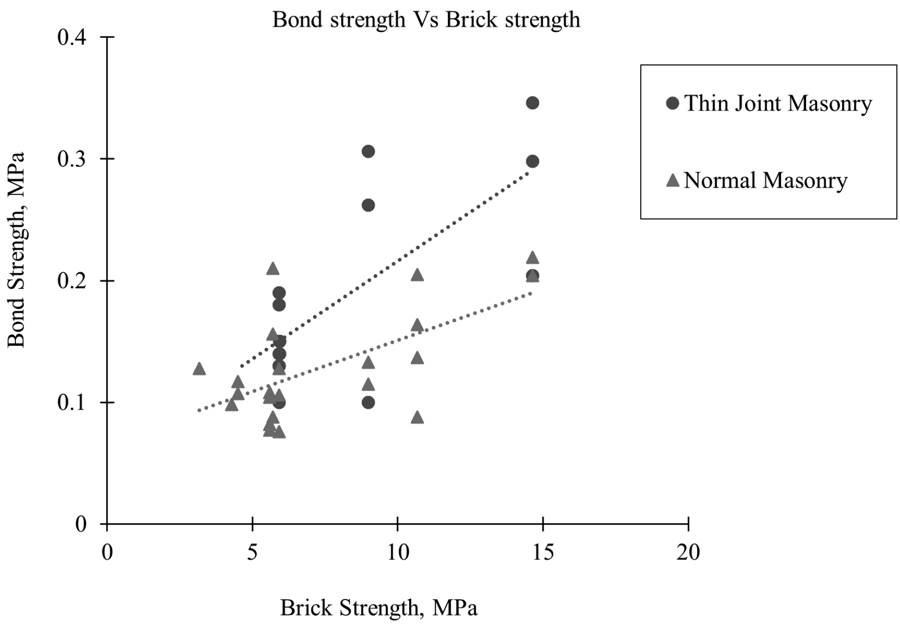

FIGURE 15.4 Variation of bond strength of masonry prism with mortar strength and brick strength.

and engineered building units are utilised. A comparison of energy utilised for 1 m^3 of stretcher-bonded wall constructed using stabilised mud blocks and hollow clay blocks is analysed. The energy is calculated for wall built using 5-mm and 12-mm-thick bed joint, and details are presented in Table 15.7. It was noted that thin jointed stabilised

TABLE 15.5
Embodied Energy of Basic Building Materials

Material	EE (MJ/unit)
Cement, kg	3.60
M sand, kg	0.20
CW or MW, kg	0.11
Lime, kg	2.50
GF, kg	0.01
MF, kg	0.01
Soil, kg	0.01
Hollow clay block, unit	16.70
SMB, unit	2.85

TABLE 15.6
Embodied Energy per Cubic Meter of Mortar

Vol. of mortar = 1 m^3

Mortar	Proportion	Energy (MJ)	CS (MPa)	Energy/Strength
C:GF	01:02	1686.40	11.47	147.03
C:MF	01:03	1267.38	13.54	93.60
C:MS+CW	01:04	1223.60	12.96	94.41
C:MS+MW	01:04	1221.50	11.34	107.72
C:MS	01:06	1020.00	13.66	63.67–236.65
C:NS	01:06	847.99	4.31	49.36–196.75
C:L:S	1:1:1.5	2603.87	14.13	184.28

TABLE 15.7
Embodied Energy of Masonry Wall with Various Mortar Combinations and Masonry Units

		EE (MJ) Bed joint: 5mm		EE (MJ) Bed joint: 12mm			
		Masonry Unit		Masonry Unit		% Savings	
Constituents	Proportion	SMB	Clay block	SMB	Clay block	SMB	Clay block
C: GF	01:02	974.34	1559.16	4302.63	1729.07	77.35	9.83
C: MF	01:03	916.87	1498.11	4180.51	1588.98	78.07	5.72
C: MS+CW	01:04	911.56	1489.43	4085.27	1572.73	77.69	5.30
C: MS+MW	01:04	911.56	1489.43	4085.27	1572.73	77.69	5.30
C: MS	01:06	883.10	1459.00	4105.60	1507.00	78.49	3.19
C: NS	01:06	860.64	1433.39	4056.47	1451.47	78.78	1.25
C: L:S	1:1:1.5	1044.82	1644.69	4460.05	1905.78	76.57	13.70

mud block masonry resulted in energy savings of more than 75% as compared to 12 mm bed joint masonry. This reduction is due to the low embodied energy of stabilised mud block. Hollow clay block masonry with 4–6 mm bed joint thickness resulted in 5–10% savings in energy as compared to 12–15 mm bed joint masonry construction when mortars made with waste materials are used. Use of conventional aggregates for making mortars results in a marginal energy savings of 1.25–3.19%.

15.6 CONCLUSIONS

Based on the studies reported, the following conclusions are derived. Industrial waste such as C&D waste, granite fines, marble fines, and many others can be used in making mortars for masonry. Soil-based mortars exhibited considerable variations in the strength and absorption characteristics due to the presence of silt and clay content. Mortars of proportion 1:3 and 1:4 (cement: fine aggregate) made with industrial waste resulted in enhanced compressive strength compared to conventional mortars applicable to both thin jointed and normal masonry.

Masonry properties viz. compressive strength are governed by unit strength in thin joint masonry, thus use of high-strength engineered units will facilitate faster construction and uniform joint thickness. Masonry compressive strength and masonry efficiency of thin joint masonry was superior for thin joint masonry as compared to normal masonry. Flexural strength of thin joint masonry was also found to increase with an increase in brick-and-mortar strength. For every 4 MPa increase in mortar strength, an increment in flexural bond strength of 0.02 MPa and 0.028 MPa was observed for thin joint masonry and normal masonry, respectively. And for every 5 MPa increase in brick strength, an increase in bond strength by 0.081 MPa and 0.042 MPa was observed for thin joint masonry and normal masonry, respectively. Energy savings up to 75% was noted with thin jointed masonry wall construction using stabilised mud block. Hollow clay blocks used in wall construction using thin bed joints results in 5–10% energy savings when mortars made with recycled aggregates are used. Use of conventional units like non-modular burnt clay bricks does not lead to any savings in energy or reduced carbon emissions.

REFERENCES

1. Kamplimath S M, Joshi AM (2015) Alternatives to Conventional Cement-Sand Mortar for Sustainable Masonry Construction. *Emerging Trends on Sustainable Construction—National Level Conference*, 2015. http://doi.org/10.2139/ssrn.3350341
2. EURO Code 6 (2005) *Design of Masonry Structures—Part—1–1: General Rules for Reinforced and Under Reinforced Masonry Structures*. November 2005. https://eurocodes.jrc.ec.europa.eu/EN-Eurocodes/eurocode-6-design-masonry-structures
3. Atlur SM (2013) *A Study on Behaviour of Thin Jointed Brick Masonry*. MTech Thesis, Visvesvaraya Technological University
4. Basutkar S, Renukadevi MV, Jagadish KS (2016) Use of Cementitious Pastes for Thin Joint, Sandless, Brick Masonry. *Bulletin of ACCE (I) Association of Consulting Civil Engineers (India), Bangalore*, January–March, Volume 1,(34-48).
5. Jagadish K, Amalkar M, Ambarish K, Jagadish KS (2011) Effect of Granite Fines on Strength of Hollow Concrete Blocks. *International Journal of Advanced Engineering Technology* 2(4):475–479, eISSN 0976-3945

6. Lakhani R, Kumar R, Tomar P (2014) Utilization of Stone Waste in the Development of Value-Added Products: A State-of-the-Art Review. *Journal of Engineering Science and Technology* 7:180–187
7. Mhamal AA, Savoikar PP (2023) Use of Marble and Granite Dust Waste as Partial Replacement of Fine Aggregates in Concrete. In: *IOP Conference Series: Earth and Environmental Science*. Institute of Physics
8. Vardhan K, Siddique R, Goyal S (2019) Influence of Marble Waste as Partial Replacement of Fine Aggregates on Strength and Drying Shrinkage of Concrete. *Construction and Building Materials* 228. https://doi.org/10.1016/j.conbuildmat.2019.116730
9. Joshi AM (2020) *Studies on Strength and Elastic Properties of Masonry Products Using C&D Waste*. PhD Thesis, Visveswaraya Technology University. http://doi.org/10.13140/RG.2.2.32359.78243
10. Indian Standards IS 383 (2016) *Coarse and Fine Aggregate for Concrete—Specification*. Bureau of Indian Standards, New Delhi
11. Madhusudhan A (2016) *Experimental Study on Behaviour of Different Types of Mortars on Strength of Brick Masonry with Reduced Joint Thickness*. MTech Thesis, Visvesvaraya Technological University
12. Basutkar SM (2018) *Influence of Joint Thickness and Slenderness on the Strength of Brick Masonry*. PhD Thesis, Visvesvaraya Technological University
13. Harsha B (2017) *Behavior of Masonry with Reduced Joint Thickness Using Different Mortar Proportions with Demolished Concrete and Masonry Waste as Partial Replacement to Fine Aggregate*. MTech Thesis, Visvesvaraya Technological University
14. Basutkar SM, Manjunath A, Renukadevi MV, Jagadish KS (2014) Effective Utilization of Demolished Brick Masonry in Building Products. In: *9th International Masonry Conference*. Guimaraes
15. Indian Standard IS 2250 (1981) *Code of Practice for Preparation and Use of Masonry Mortars*. Bureau of Indian Standards, New Delhi
16. Indian Standard IS 10086 (1982) *Specification for Moulds for Use in Tests of Cement and Concrete*. Bureau of Indian Standards, New Delhi
17. Indian Standard IS 1905 (1987) *Code of Practice for Structural Use of Unreinforced Masonry*. Bureau of Indian Standards, New Delhi
18. Jagadish KS (2015) *Structural Masonry*. I K International Publishing House Pvt. Ltd
19. ASTM C 1072 (2022) *Standard Test Methods for Measurement of Masonry Flexural Bond Strength*, ASTM International, West Conshohocken. https://cdn.standards.iteh.ai/samples/114156/caee6a6a2076434fab2f1a189d297646/ASTM-C1072-22.pdf
20. Jagadish KS, Reddy BVV, Rao KSN (2017) *Alternative Building Materials and Technologies*, Second edition. New Age International (P) Limited Publishers.

16 Environmental Impact of Cement and Fly Ash Geopolymer as a Sustainable Construction Material

Poonam Shekhawat, Gunwant Sharma, Rao Martand Singh and Jitendra Singh Yadav

16.1 INTRODUCTION

Portland cement is the typical binding material applied in civil engineering works. A prodigious quantity of concrete is required for the ongoing construction of grand infrastructure projects. Consequently, the utilization of concrete by communities around the world acquires second rank after water (Davidovits 2013). However, the cement industry emits greenhouse gas carbon dioxide (CO_2) and harmful smokes in huge extents into the atmosphere. Additionally, the production of Portland cement is a highly energy-exhaustive process that is mostly consumed during the manufacturing of clinker.

Furthermore, the major problem associated with soft soil is structural damage in lightweight structures due to significant changes in volume caused by wetting and drying of clay. An uplift force is applied on the foundation by swelled clay particles during the wet period. This condition is called edge heave condition, as demonstrated in Figure 16.1a, while shrink at the edge and settlement of foundation occur during the dry period, and the consequence is known as the edge-shrink effect. Moreover, a rise of foundation from the center occurs due to capillary action caused by collected moistness under the foundation center. This time-dependent phenomenon is termed center heave condition, as demonstrated in Figure 16.1b. Generally, soft soil is stabilized with a non-eco-friendly conventional stabilizer, i.e., cement. Therefore, it is a challenge for the geotechnical engineer to increase the mechanical properties of soft soil by using eco-friendly stabilization and reinforcement methods at a reasonable price.

For global sustainable development, enlarged release of greenhouse gases in the air is not tolerable both socially and environmentally, as specified in the World Earth Summit organized in Rio de Janeiro, Brazil, in 1992 and subsequently in Kyoto,

DOI: 10.1201/9781032686899-20

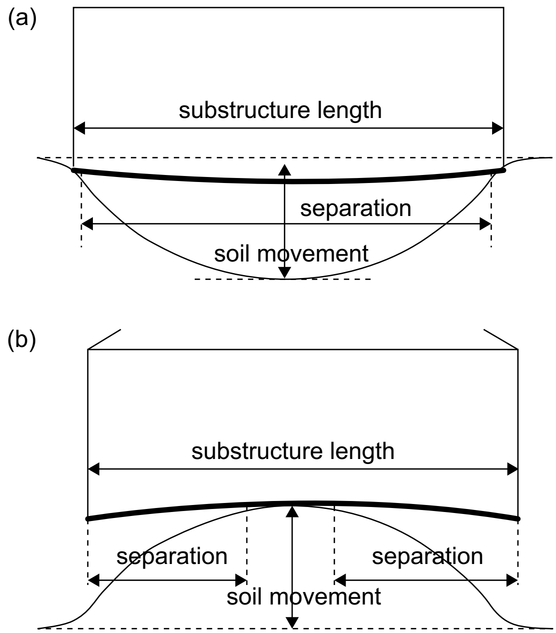

FIGURE 16.1 Demonstration of critical soft soil swell-shrink ground conditions: (a) edge heave condition and (b) center heave condition.

Japan, in 1997. Furthermore, decreasing global warming by lessening the greenhouse gas released into the air is the aim of the worldwide agreement called the Kyoto Protocol, accepted in 1997 in Kyoto, Japan. The Kyoto Protocol has applied numerous emission reduction goals to the countries globally (Malhotra 1999). Following this point of view, the global warming phenomenon should be considered more seriously, and attempts should be made to decrease the consequences.

To overcome the concerns related to the construction industry, a novel, greatly durable, strong, and advanced binding material with a considerably small carbon footprint, called "geopolymer", has been offered as a valid substitute to traditional Portland cement.

16.2 GEOPOLYMER

Geopolymers are three-dimensional aluminosilicate constituents that strengthen by the aid of heat treatment at temperatures less than 100°C (Davidovits 1991). A precursor material comprising alumina and silicate, an alkaline component, and thermal curing are essential to generate geopolymers. When the raw precursor material containing aluminosilicate interacts with the alkaline reagent, an amorphous to a semi-crystalline substance is created within a complex chemical procedure, termed geopolymerization. Relying on the accessibility of calcium ion from a precursor material viz. iron blast furnace slag, class C fly ash, etc., strengthening of this semi-crystalline substance or geopolymer binder can also be attained at ambient temperature.

The conversion of a raw precursor material into a geopolymer matrix can be concise in three stages. During the first stage, the suspension of the amorphous aluminosilicate precursor material in the alkaline liquid yields a supersaturated mix of SiO_2 and Al_2O_3. In the second stage, while water is discharged slowly in the process, a gel structure is created through the development of big links by polycondensation of oligomers in the aqueous stage. Lastly, in the third stage, a three-dimensional geopolymer matrix is formed due to an increased gel network.

The difference between the manufacturing of cement and the production of geopolymer binder is that hardening of Portland cement occurs through hydration of calcium silicate into calcium disilicate and lime, whereas hardening of geopolymer binder occurs through polycondensation of oligomers into a cross-linked network of polymers, as shown in Figure 16.2. The curing of geopolymer binders occurs more rapidly than does Portland cement. Most of the strength of a geopolymer binder is gained within 24 hours, although they set slowly enough that they can be mixed at a batch plant and delivered in a concrete mixer. As described earlier, Portland cement is a severe atmospheric contaminant, whereas using blended types of cement with coal fly ash ingredients reduces the CO_2 emissions by 10%–15%. On the other hand, typically geopolymer lessens CO_2 releases by 40%–90% (Davidovits 2013).

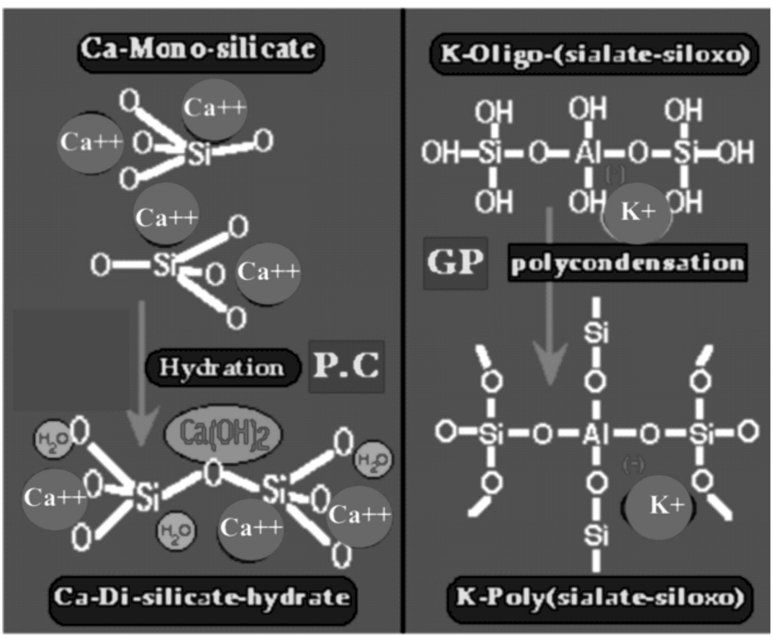

FIGURE 16.2 Difference between chemistry of Portland cement and chemistry of geopolymer binder.

Geopolymer binders are mechanically strong and possess a high-temperature resistance along with high resistance against chemical attack (Albitar et al. 2017; Valencia Saavedra and Mejía de Gutiérrez 2017). These properties are extremely significant for use in transportation infrastructure, construction, and offshore applications. However, when geopolymer binder is used in pavement construction, other performances like durability along with mechanical strength are a priority. In this thesis, the geotechnical aspects of the geopolymer have been studied for mainly its application in pavement construction, which is also an innovative method to check the performance.

Numerous aluminosilicate-based precursors have been proposed for geopolymerization viz. metakaolin, fly ash, slag, etc. Using these precursors individually in geopolymerization causes various issues, for example, fly ash–based geopolymer requires heat curing to achieve the mechanical strength, which is slightly unfavorable for field conditions, whereas slag-based geopolymers have a very fast setting time. Moreover, metakaolin-based geopolymer significantly affects the workability of the mix. On the other hand, a blended geopolymer based on two precursor materials appears to have high efficacy to overcome these issues.

16.3 FLY ASH

The industrial byproducts and municipal discard removal are the main concerns in emerging nations like India. Both types of discards have provoked numerous ecological problems as they are frequently disposed into a landfill. Instead, lack of land and natural reserves led to lack of landfill sites with elevated price due to quick urbanization. In this situation, the application of such discards in construction should be encouraged so as to avert the greatest waste from landfills. Consequently, it will aid in the waste reduction initiative, presently operating in India by decreasing the load on landfills.

Fly ash (FA), created from coal burning, is an industrial byproduct. FA is usually applied as a precursor in production of geopolymer. Each year about 480 million tons of FA is produced worldwide, whereas in India, more than 100 million tons of coal FA is being produced yearly (Sivakumar and Mahendran 2014). This is an enormous quantity of waste being created. FA is being utilized as a partial substitute in cement because of the pozzolanic characteristic. Furthermore, FA comprises minerals such as alumina and silica, which are important in the geopolymerization process. Therefore, FA can be a suitable alternative for construction material.

FA is the most widespread pozzolan and is found widely applied in universal construction material. It is acknowledged that the quality of concrete is significantly improved by the addition of FA. With the increased production of FA in upcoming years due to increased demand for power generation, disposal of FA is going to be a bigger issue. Additionally, dumping a large volume of FA into a landfill can contaminate the environment. Therefore, utilizing such waste pozzolanic material as a precursor to producing a geopolymer binder will benefit the environment.

FA, a discard of coal burning, is the most used raw precursor material for geopolymerization. Boiler operation situations in power plants and characteristics of coal influence the composition of an individual particle of FA. Major chemical

TABLE 16.1
Major Properties of Class F Fly Ash Used by Different Authors

Major Constituent	Xu and Van Deventer (2002)	Sindhunata et al. (2006)	Kua et al. (2016)	Zhao et al. (2019)	Sukmak et al. (2019)
SiO_2	46.20%	50.01%	67%	59.74%	53.93%
Al_2O_3	30.30%	27.97%	24%	27.51%	20.19%
CaO	4.31%	3.48%	1.59%	1.45%	5.38%
LOI	2.00	1.39	-	2.66	5.01
D_{50}	8.47 μm	12.4 μm	36 μm	16 μm	
Specific gravity	2.39	2.34	2.4	-	2.10

configuration and typical characteristics of FA are summarized in Table 16.1, as documented by the various investigators.

FA can be categorized into two classes depending on the calcium content: Class C fly ash with high calcium content and Class F fly ash with the low calcium content. Class C fly ash is acquired from burning lignite and sub-bituminous coals, whereas burning of bituminous coal provides Class F fly ash.

Due to the presence of higher CaO content, geopolymerization of Class C fly ash led to the early development of C-S-H even after curing in ambient conditions (Shekhawat et al. 2020, 2022). Therefore, geopolymers made from Class C fly ash have a rapid setting time compared to geopolymers made from Class F fly ash. Rapid setting of a geopolymer is not ideal for its development, hence the inclusion of a retarder is always required in Class C fly ash. On the other hand, in order to obtain high compressive strength, Class F-based geopolymers are required to be cured at temperatures 40°C–95°C, although the reactivity of Class F fly ash can be increased by reducing the particle size.

The surface features and particle shape of fly ash can be studied by using the scanning electron microscopy (SEM) technique. Various SEM images of fly ash used by researchers in their research work have been shown in Figure 16.3.

FA particles are spherical, generally hollow, and have a smooth surface. These particles are glassy or vitreous due to the presence of amorphous minerals. This vitreous phase could be related to the presence of iron, calcium, and alkali elements, primarily sodium in a low-calcium FA. Moreover, variation in the chemical composition of the vitreous phase was also noticed for different FA particles and even point to point within one particle.

FA has been utilized as a source material in geopolymerization in the majority of investigations due to the presence of amorphous alumina and silica. Out of 125 formulations of precursors for geopolymer and blended geopolymers reported in recent reviews, 65% were based on FA as a precursor, as shown in Figure 16.4. The percentage incorporation of any other two precursors individually or together is below 15%. Therefore, it can be concluded that FA is the most widely accepted precursor material due to its properties and availability.

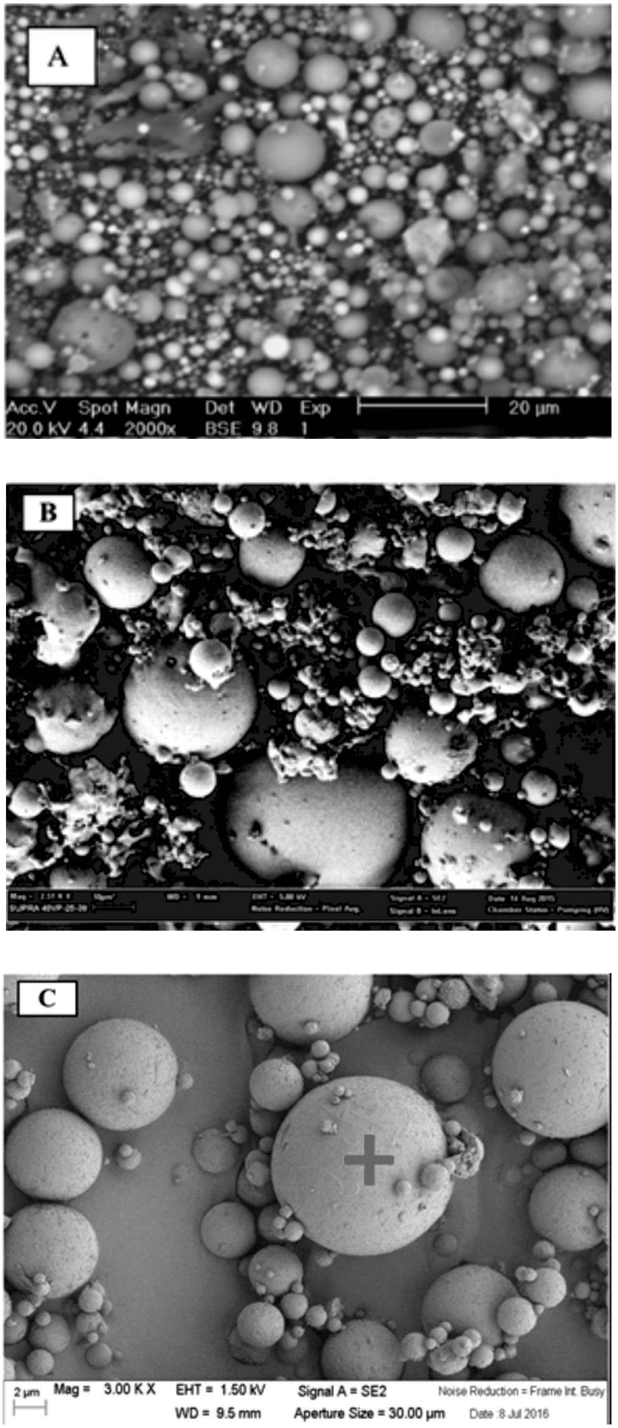

FIGURE 16.3 SEM images of fly ash used by various researchers.

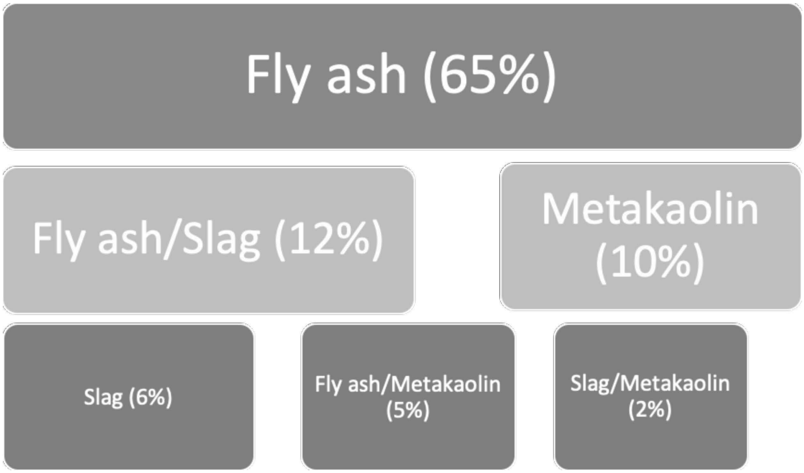

FIGURE 16.4 Percentage distribution of incorporation of precursors fly ash, metakaolin, and slag in geopolymerization in recent reviews.

16.4 USABILITY OF FLY ASH GEOPOLYMERS

The possible applications of FA geopolymers suggested by the researchers are as follows:

- As a cementitious binder for the production of concrete structural members (Palomo et al. 1999; Guo et al. 2010; Ravikumar et al. 2010; Yang et al. 2017; Chen et al. 2018)
- Developing fire-resistant concrete (Mustafa Al Bakri et al. 2013)
- As a green composite material to be used as bearing masonry units (Sukmak et al. 2015; Horpibulsuk et al. 2016; Malkawi et al. 2016; Bezerra et al. 2019)
- For the production of heavy-duty bricks (Ezzat et al. 2016)
- For manufacturing of lightweight concrete (Tekin 2016)
- As a high-quality subgrade, sub-base, and base material in road construction projects (Kua et al. 2016; Hoy et al. 2017; Tahir et al. 2019; Xiao et al. 2020)
- For self-compacting rammed earth construction (Cristelo et al. 2012)
- For geopolymer-treated subgrade materials (Phetchuay et al. 2014; Sukprasert et al. 2019)
- For the production of soil–fly ash geopolymer brick (Leong et al. 2018)
- For manufacturing unfired lightweight masonry units using geopolymer-stabilized soft soil (Sukmak et al. 2019)

16.5 CONCLUSIONS

Geopolymerization is a procedure of polycondensation that includes the dissolution of alumina and silica from a source with the occurrence of a certain alkaline activator. Usually, discarded raw FA is employed as a precursor in geopolymerization, which is harmful to our health and ecological system. The voluminous consumption of this hazardous discard is possible either in concrete industries or for soil stabilization. The application of these wastes in developing geopolymers also assists in reducing CO_2 emissions from the construction industry. Consequently, the novel practice of geopolymerization ultimately results in sustainable development and cleaner production of the cementitious binder.

REFERENCES

Albitar, M., Mohamed Ali, M.S., Visintin, P., and Drechsler, M., 2017. Durability evaluation of geopolymer and conventional concretes. *Construction and Building Materials*, 136, 374–385.

Bezerra, A.C. da S., França, S., Magalhães, L.F. de, and Carvalho, M.C.R. de, 2019. Alkaline activation of high-calcium ash and iron ore tailings and their recycling potential in building materials. *Ambiente Construído*, 19 (3), 99–112.

Chen, Z., Li, J.S., Zhan, B.J., Sharma, U., and Poon, C.S., 2018. Compressive strength and microstructural properties of dry-mixed geopolymer pastes synthesized from GGBS and sewage sludge ash. *Construction and Building Materials*, 182, 597–607.

Cristelo, N., Glendinning, S., Miranda, T., Oliveira, D., and Silva, R., 2012. Soil stabilisation using alkaline activation of fly ash for self compacting rammed earth construction. *Construction and Building Materials*, 36, 727–735.

Davidovits, J., 1991. Geopolymers: Inorganic polymeric new materials. *Journal of Thermal Analysis*, 37 (8), 1633–1656.

Davidovits, J., 2013. Geopolymer Cement a review. *Geopolymer Science and Technics*, 21, 1–11.

Ezzat, M., Khater, H.M., and Nagar, A.M. El, 2016. Enhanced characteristics of alkali activated slag/grog geopolymer bricks. *International Journal of Scientific & Engineering Research*, 7 (2), 230–243.

Guo, X., Shi, H., and Dick, W.A., 2010. Compressive strength and microstructural characteristics of class C fly ash geopolymer. *Cement and Concrete Composites*, 32 (2), 142–147.

Horpibulsuk, S., Suksiripattanapong, C., Samingthong, W., Rachan, R., and Arulrajah, A., 2016. Durability against wetting-drying cycles of water treatment sludge-fly ash geopolymer and water treatment sludge-cement and silty clay-cement systems. *Journal of Materials in Civil Engineering*, 28 (1), 1–9.

Hoy, M., Rachan, R., Horpibulsuk, S., Arulrajah, A., and Mirzababaei, M., 2017. Effect of wetting—drying cycles on compressive strength and microstructure of recycled asphalt pavement—Fly ash geopolymer. *Construction and Building Materials*, 144, 624–634.

Kua, T.A., Arulrajah, A., Horpibulsuk, S., Du, Y.J., and Shen, S.L., 2016. Strength assessment of spent coffee grounds-geopolymer cement utilizing slag and fly ash precursors. *Construction and Building Materials*, 115, 565–575.

Leong, H.Y., Ong, D.E.L., Sanjayan, J.G., and Nazari, A., 2018. Strength development of soil—fly ash geopolymer: Assessment of soil, fly ash, alkali activators, and water. *Journal of Materials in Civil Engineering*, 30 (8), 04018171.

Malhotra, V.M., 1999. Making concrete 'greener' with fly ash. *Concrete International*, 21 (5).

Malkawi, A.B., Nuruddin, M.F., Fauzi, A., Almattarneh, H., and Mohammed, B.S., 2016. Effects of alkaline solution on properties of the HCFA geopolymer mortars. *Procedia Engineering*, 148, 710–717.

Mustafa Al Bakri, A.M., Abdulkareem, O.A., Kamarudin, H., Khairul Nizar, I., Rafiza, A.R., Zarina, Y., and Alida, A., 2013. Microstructure studies on the effect of the alkaline activators of fly ash-based geopolymer at elevated heat treatment temperature. *Applied Mechanics and Materials*, 421, 342–348.

Palomo, A., Grutzeck, M.W., and Blanco, M.T., 1999. Alkali-activated fly ashes: A cement for the future. *Cement and Concrete Research*, 29, 1323–1329.

Phetchuay, C., Horpibulsuk, S., Suksiripattanapong, C., Chinkulkijniwat, A., Arulrajah, A., and Disfani, M.M., 2014. Calcium carbide residue: Alkaline activator for clay-fly ash geopolymer. *Construction and Building Materials*, 69, 285–294.

Ravikumar, D., Peethamparan, S., and Neithalath, N., 2010. Structure and strength of NaOH activated concretes containing fly ash or GGBFS as the sole binder. *Cement and Concrete Composites*, 32 (6), 399–410.

Shekhawat, P., Sharma, G., and Singh, R.M., 2020. Durability analysis of eggshell powder—flyash geopolymer composite subjected to wetting—drying cycles. *Journal of Engineering, Design and Technology*, 18 (6), 2043–2060.

Shekhawat, P., Sharma, G., and Singh, R.M., 2022. A comprehensive review of development and properties of flyash-based geopolymer as a sustainable construction material. *Geotechnical and Geological Engineering*, 40 (11), 5607–5629.

Sindhunata, Van Deventer, J.S.J., Lukey, G.C., and Xu, H., 2006. Effect of curing temperature and silicate concentration on fly-ash-based geopolymerization. *Industrial and Engineering Chemistry Research*, 45 (10), 3559–3568.

Sivakumar, M., and Mahendran, N., 2014. Strength and permeability properties of concrete using fly ash (FA), rise husk ash (RHA) and egg shell powder (ESP). *Journal of Theoretical and Applied Information Technology*, 66 (2), 489–499.

Sukmak, P., Kunchariyakun, K., Sukmak, G., Horpibulsuk, S., Kassawat, S., and Arulrajah, A., 2019. Strength and microstructure of palm oil fuel ash—fly ash—soft soil geopolymer masonry units. *Journal of Materials in Civil Engineering*, 31 (8), 04019164.

Sukmak, P., Silva, P. De, Horpibulsuk, S., and Chindaprasirt, P., 2015. Sulfate resistance of clay-portland cement and clay high-calcium fly ash geopolymer. *Journal of Materials in Civil Engineering*, 27 (5), 1–11.

Sukprasert, S., Hoy, M., Horpibulsuk, S., Arulrajah, A., Rashid, A.S.A., and Nazir, R., 2019. Fly ash based geopolymer stabilisation of silty clay/blast furnace slag for subgrade applications. *Road Materials and Pavement Design*, 1–15.

Tahir, M.F.M., Abdullah, M.M.A.B., Hasan, M.R.M., and Zailani, W.W.A., 2019. Optimization of fly ash based geopolymer mix design for rigid pavement application. In: *5th International Conference on Green Design and Manufacture, AIP Conference Proceedings 2129*, 020144.

Tekin, I., 2016. Properties of NaOH activated geopolymer with marble, travertine and volcanic tuff wastes. *Construction and Building Materials*, 127, 607–617.

Valencia Saavedra, W.G., and Mejía de Gutiérrez, R., 2017. Performance of geopolymer concrete composed of fly ash after exposure to elevated temperatures. *Construction and Building Materials*, 154, 229–235.

Xiao, R., Polaczyk, P., Zhang, M., Jiang, X., and Zhang, Y., 2020. Evaluation of glass powder-based geopolymer stabilized road bases containing recycled waste glass aggregate. *Transportation Research Record*, 2674 (1), 22–32.

Xu, H., and Van Deventer, J.S.J., 2002. Geopolymerisation of multiple minerals. *Minerals Engineering*, 15 (12), 1131–1139.

Yang, T., Zhu, H., and Zhang, Z., 2017. Influence of fly ash on the pore structure and shrinkage characteristics of metakaolin-based geopolymer pastes and mortars. *Construction and Building Materials*, 153, 284–293.

Zhao, M., Zhang, G., Htet, K.W., Kwon, M., Liu, C., Xu, Y., and Tao, M., 2019. Freeze-thaw durability of red mud slurry-class F fly ash-based geopolymer: Effect of curing conditions. *Construction and Building Materials*, 215, 381–390.

Section 5

Frugal Innovations

17 Biotechnological Approaches for Reaching Zero Waste from Agro-Food Wastes

G Deepika and Ravi-Kumar Kadeppagari

17.1 INTRODUCTION

The zero-waste concept has been adopted in various fields, including agriculture, mining, manufacturing, transportation and urban development. A zero-waste approach has to be sustainable, and it should make the earth a better place in which to live. Though this approach is excellent and should be a futuristic approach, the majority of zero-waste methods are focused on resource recovery, reuse and recycling, which does not yield new products nor valorize the material. Different wastes generated during manufacturing, construction activities, domestic activities, agriculture and food processing activities will harm the environment. Also electronic waste, plastic materials and sewage are posing serious ecological problems. Various chemical and physical approaches have been used to address problems created due to waste. However, these methods again generate accessory wastes, harmful chemicals and emissions, which are not good for the environment. In this context, biotechnological approaches are more promising.

Biotechnological methods are more sustainable and environmentally friendly while reaching zero waste. Biofuels have long been used as a source of energy, and biofuels have been produced from the food, urban and agricultural wastes. Recently, enzymes have been used for the production of bioethanol from lignocellulosic waste. This is one of the promising biotechnological approaches for producing eco-friendly fuel from plant biomass, which is available in huge amounts and discarded as waste. Also, hydrogen has been explored as a green alternative fuel to fossil oils, and it was produced by eco-friendly dark fermentation by utilizing organic substrates and microorganisms. Used cooking oil as a source of biodiesel has been attracting many people since it generates less emissions.

Wastes contain valuable materials, and they should be viewed as salvageable resources while adopting zero-waste approaches. Bioconversion methods like bioremediation, biopulping, biosorption, biofiltration and bioleaching were utilized in order to obtain precious products like metals, industrial chemicals, bioactive compounds, etc. from various wastes. These conversion technologies utilize various organisms and enzymes. They are also utilized in different fermentation methods in order to transform different agricultural and food wastes into valuable biochemicals,

DOI: 10.1201/9781032686899-22

biofuels, biopolymers, etc. These biotransformation technologies will facilitate the circular economy. The biopolymers obtained can be utilized for making packaging materials that are biodegradable. This will reduce our dependency on synthetic plastics, which are a serious threat to the environment. Recently, utilization of microbes and their enzymes for the degradation of synthetic plastics was attempted at small scales. Also, microbes were explored for the production of bioplastics. However, these efforts were not successful at commercial scale due to higher costs.

In this chapter, we have focused on some of the recent developments on biotechnology-driven zero-waste approaches. They are integrated methods for the production of biofuels and biodegradable plastics, anaerobic co-digestion process for treating different wastes simultaneously, utilization of immobilized enzymes for valorization of waste, photobiological reactors for remediation of wastewaters, zero-waste biorefineries for driving a circular economy, bioremediation by utilizing biofunctionalized nanomaterials, microbial fuel cells for reaping bioenergy, utilization of waste cooking oil as biodiesel, biosorbents from microbial and agricultural wastes, and more.

17.2 BIOTECHNOLOGICAL APPROACHES FOR REACHING ZERO WASTE FROM AGRO-FOOD WASTES

17.2.1 Anaerobic Co-digestion

In mono-digestion, biogas will be produced from a single kind of feedstock, where as in the co-digestion process, two different feedstocks will be used in the digester in order to produce biogas. Co-digestion was used initially for balancing the carbon to nitrogen (C/N) ratio of feedstocks since some are rich in carbon and few are rich in nitrogen content. During this process, one can alter the composition of the feed or waste to obtain the optimum C/N ratio depending on the waste composition and microbial consortium. Wastewater treatment plants across the globe are shifting towards this co-digestion process for increasing the output of biogas. One plant at Mesa, Arizona, USA, successfully used solid food waste and sewage sludge for evaluating the co-digestion process. Also, sewage sludge was co-digested with restaurant waste that was rich in lipid.

Biogas is a major contributor towards achieving the goals of a zero-emission economy since it will burn clean and reduce carbon emissions. Wastewater treatment plants in Australia have generated 187 GW of electricity per year through biogas, and they have generated additional electricity of 5.5 GW by adopting an anaerobic co-digestion process [1]. Hence, diverting organic waste from urban areas, restaurants and landfills will lead towards achieving the target of zero carbon emissions by 2040.

17.2.2 Integrated Methods for the Production of Biofuels and Biodegradable Plastics

Bioethanol or bioplastics can be produced from organic waste in a fermentation process by utilizing specific microorganisms. Hence, organic waste is considered as a valuable renewable source. The physical and chemical characteristics of polyhydroxyalkanoates (PHAs), aliphatic polyesters and polylactides are similar to those of synthetic plastic. Hence they are called bioplastic polymers. PHAs are produced by using bacteria [2, 3]. Organic wastes of starch, molasses, food and dairy, and wastewater were promising during the simultaneous production of bioenergetic materials (biohydrogen and biomethane) and biopolymers [2].

Purple non-sulfur bacteria such as *Rhodopseudomonas palustris*, *R. sphaeroides*, *Rhodospirillum rubrum* and *Bacillus spp.* will simultaneously produce PHA and hydrogen when nutrients are limited [2, 4]. Fermentation will be carried out at two stages while transforming the glucose into PHA and hydrogen by using *Bacillus spp.* Batch fermentation was carried out for an initial three days by using *B. thuringiensis* EGU45 and *B. cereus* EGU44, and 1.67–1.92 mol of hydrogen was produced per mol glucose. During a later two days, a PHB yield of 11.3% was obtained [5]. More studies need to be carried out by using integrated processes.

17.2.3 Immobilized Enzymes for Valorization of Waste

It is disadvantageous to use free enzymes for industrial purposes since they will have less stability and be lost in the process. Application of enzymes has gone up in many sectors, including production of biofuels, food processing, biomedical, laundry, pharmacy, transformation of agro-industrial waste, etc. [6]. Enzyme molecules are immobilized onto or into bigger inert structures by using different methods like adsorption covalent bonding, encapsulation, etc. Protease enzymes can be used for converting protein-rich wastes (poultry, dairy, soy bean, oil seeds) into valuable polymer precursors. Immobilized trypsin can be used for hydrolyzing whey protein, which is generated as a dairy waste. Immobilized aspartic protease was reported to hydrolyze concentrates of whey protein into peptides having antioxidant properties [7]. Amylase enzyme produced by the immobilized cells of *S. cerevisiae* and *Aspergillus awamori* could lead to the cassava starch hydrolysis and ethanol production in the liquid-air culture system [8]. Immobilized pectinase was highly resistant to acidic conditions, and pineapple juice was clarified by using this enzyme [9]. Stability of the pectinase was improved by immobilizing it on the nanoporous activated carbon that was functionalized [10]. Lipases of *Rhizomucor miehei* and *Candida antarctica* were immobilized onto functionalized silica, and this enzyme system was used for treating waste cooking oil to obtain higher levels of biodiesel [11]. In another study, aromatic esters were synthesized by using lipase that was immobilized on activated carbon [12].

17.2.4 Photobiological Reactors for Remediation of Wastewaters

Photobiological reactors are promising for degrading the harmful compounds present in wastewaters. Different microbiological agents like immobilized *Aspergillus niger*, alkali or oil degrading bacteria, cyanobacteria, yeast, *Halomonas spp.*, algae, and photosynthetic and acidogenic bacteria are used in these reactors. Different methods like photo-enhanced degradation, photo-activated degradation, photocatalytic degradation and photo-fermentation were used with these reactors. The strains *Pseudomonas aeruginosa* strain B, *Rhodococcus erythropolis* G2 and *Achromobacter piechaudii* O1 showed 38%, 84% and 93% degradation of hexadecane in the polluted waters, respectively [13]. Species of cyanobacteria and microalgae will grow efficiently in wastewater, and they can be exploited for the production of biofertilizers, bioactive molecules and biofuel in the reactors or ponds for the sustainable agriculture and environment [14]. Textile dye effluents were anaerobically degraded by using species of *Halomonas* [15]. Algae and bacteria were used together in the photo sequence batch reactor for removing nitrogen from wastewater [16].

17.2.5 Zero-Waste Biorefineries for Driving a Circular Economy

Excessive use of fossil fuels led to a tremendous increase in the concentration of greenhouse gases, which in turn led to grave climatic changes. With similar use of fossil fuels, CO_2 levels will increase to 40 and 50 Gt by 2030 and 2050, respectively [17]. Hence, one has to depend on other sources to meet energy demands and for reducing carbon footprint. In this context, biorefineries are promising and sustainable for meeting energy demands with a reduced carbon footprint. One such biorefinery is the one that converts food waste into biodiesel or biogas. Another is the one that converts lignocellulosic waste into bioethanol. Algal biorefineries are used to sequester CO_2 into biomass, and algal species like *Laminaria japonica*, *Undaria pinnatifida* and *Porphyra* are used [18]. The biomass will be converted into sugars, biochar and biogas, and sugars will be fermented into bioethanol and CO_2, which in turn will be sequestered into biomass. Here, products will have end use or will be cycled back as substrates, leading to a circular economy. Finally, nothing will be discarded as waste into the environment.

17.2.6 Bioremediation by Utilizing Biofunctionalized Nanomaterials

Integrating biomaterials with nanoparticles will lead to the formation of biofunctionalized nanomaterials, which can be used for potential environmental applications. Enzymes, biopolymers, nucleic acids and biosurfactants are the biomaterials commonly used for functionalizing nanoparticles. Chitosan was integrated with magnetic nanoparticles and used for neutralizing metals in polluted water. It forms chelates with metal ions, which will be attached on the surface of chitosan, and chelates can be separated by applying a magnetic field. A cellulose acetate film coated with TiO_2 could be able to remove methylene blue dye from polluted waters [19]. Lead-specific metalloprotein was cross-linked with calcium alginate nanoparticles and used to recover lead from industrial effluents [20]. Magnetic nanoparticles were encapsulated with chitosan, then laccase enzyme was conjugated to chitosan. This biofunctionalized material was used for removing dyes and hydrocarbons from the polluted water. A biosensor fabricated by using urease enzyme and nanoparticles of ZnO was used for detecting urea in the polluted water [21]. Soy protein with iron-based nanoparticles was used for removing different oil-based pollutants [22].

17.2.7 Microbial Fuel Cells for Reaping Bioenergy

Microbial fuel cells (MFCs) are promising for the generation of electricity and biohydrogen. These MFCs can also be used for wastewater treatment and biosensor development. These cells are promising for zero waste and a circular economy. Different carbon sources in the wastewater can be converted into electricity by using MFCs [23]. The main components of these cells, i.e., electrodes, membrane and microbes, will dictate the performance and cost of MFCs [24]. Glucose, sucrose, acetate, complex substrate, lactate, marine sediment, wastewater or sewage sludge was used in the single- or double-chambered MFC to generate electricity [25]. Maximum power density of 6000 mW/m^2 was obtained in single-chamber MFC with sewage sludge. Different bacterial species with (*Klebsiella*, *Proteus*, *Gluconobacter*, *Streptococcus*, etc.) or without mediator (*Desulfomonas*, *Geobacter*, *Aeromonas*, *Pichia*) were used for generating electricity in MFCs. However, these cells should be scaled up to commercial levels.

17.2.8 Utilization of Waste Cooking Oil as Biodiesel

Nowadays, waste cooking oil has been explored as a feedstock for the production of biodiesel, which has a distinct advantage over petroleum-based biodiesel in terms of emissions. Biodiesels will extensively reduce the emission of particulate matter and toxic substances in the environment. They will reduce pollution without compromising on the values of heat of combustion. Different processing technologies were adopted for converting vegetable oils into biodiesel [25], and the transesterification step will reduce the viscosity of vegetable oils, which will be favorable for biodiesel production. Used cooking oils can also be used for producing bioasphalt, bioplasticizer, solvents, polyhydroxy alkanoates, green lubricants, biosurfactants, liquid detergents, etc.

17.3 CONCLUSIONS

Zero-waste technologies are promising for a circular economy and sustainable environment. Biotechnological methods are eco-friendlier and more sustainable for achieving zero waste. Hence, biorefineries are more viable for a circular economy, which can drive us towards a sustainable planet. However, these zero-waste technologies are currently at small scale, though a few of them are scaled up to a commercial level. Hence, more zero-waste technologies should be scaled up to commercial scale in order to create a circular economy faster and prevent further environmental damage.

REFERENCES

1. Strazzbosco, A., Kenway, S.J., and Lant, P.A. (2020). Quantification of renewable electricity generation in the Australian water industry. *Journal of Cleaner Production* 254: 120119.
2. Pagliano, G., Ventorino, V., Panico, A., et al. (2017). Integrated systems for biopolymers and bioenergy production from organic waste and by-products: A review of microbial processes. *Biotechnology for Biofuels* 10: 113. http://doi.org/10.1186/s13068-017-0802-4.
3. Lu, J., Tappel, R.C., and Nomura, C.T. (2009). Mini-review: Biosynthesis of poly (hydroxyalkanoates). *Polymer Reviews* 49 (3): 226–248. https://doi.org/10.1080/15583720903048243.
4. Saharan, B.S., Grewal, A., and Kumar, P. (2014). Biotechnological production of polyhydroxyalkanoates: A review on trends and latest developments. *Chinese Journal of Biology* 80: 29–84.
5. Patel, S.K.S., Singh, M., and Kalia, V.C. (2011). Hydrogen polyhydroxybutyrate producing abilities of Bacillus spp. from glucose in two stage system. *Indian Journal of Microbiology* 51: 418–423.
6. Bilala, M., and Iqbalb, H.M.N. (2019). Sustainable bioconversion of food waste into high-value products by immobilized enzymes to meet bio-economy challenges and opportunities: A review. *Food Research International* 123: 226–240.
7. Rocha, G.F., Kise, F., Rosso, A.M., et al. (2017). Potential antioxidant peptides produced from whey hydrolysis with an immobilized aspartic proteases from Salpichroa origanifolia fruits. *Food Chemistry* 237: 350–355.

8. Roble, N.D., Ogbonna, J., and Tanaka, H. (2020). Simultaneous amylase production, raw cassava starch hydrolysis and ethanol production by immobilized Aspergillus awamori and Saccharomyces cerevisiae in a novel alternating liquid phase—air phase system. *Process Biochemistry* 95: 115–121.
9. Mohammadi, M., Mokarram, R.R., Shahvalizadeh, R., et al. (2020). Immobilization and stabilization of pectinase on an activated montmorillonite support and its application in pineapple juice clarification. *Food Bioscience* 36: 100625.
10. Mahesh, M., Arivizhivendhan, K.V., Maharaja, P., et al. (2016). Production, purification and immobilization of pectinase from Aspergillus ibericus onto functionalized nanoporous activated carbon (FNAC) and its application on treatment of pectin containing wastewater. *Journal of Molecular Catalysis B: Enzymatic* 133: 43–54.
11. Babaki, M., Yousefi, M., Habibi, Z., et al. (2017). Process optimization for biodiesel production from waste cooking oil using multi-enzyme system through response surface methodology. *Renewable Energy* 105: 465–472.
12. Brito, M.J.P., Bauer, L.C., Santos, M.P.F., et al. (2020). Lipase immobilization on activated and functionalized carbon for the aroma ester synthesis. *Microporous and Mesoporous Materials* 309: 110576.
13. Mehdi, H., Mohammad, A., Hamid, T., et al. (2013). Isolation and characterization of alkane degrading bacteria from petroleum reservoir waste water in Iran (Kerman and Tehran provenances). *Marine Pollution Bulletin* 73 (1): 300–305.
14. Jay, S.S., Arun, K., and Mani, S. (2019). Cyanobacteria: A sustainable and commercial bio-resource in production of bio-fertilizer and bio-fuel from waste waters. *Environmental and Sustainability Indicators* 3–4: 100008.
15. Balamurugan, B., Thirumarimurugan, M., and Kannadasan, T. (2011). Anaerobic degradation of textile dye bath effluent using Halomonas sp. *Bioresource Technology* 102 (10): 6365–6369.
16. Huijun, J., and Quiyan, Y. (2018). Nitrogen removal in photo sequence batch reactor using algae-bacteria consortium. *Journal of Water Process Engineering* 26: 108–115.
17. Pires, J.C.M., and da Cunha Goncalves, A.L. (eds.) (2019). *Bioenergy with Carbon Capture and Storage: Using Natural Resources for Sustainable Development*. Academic Press.
18. Pandey, A., Lee, D.J., Chang, J.S., et al. (eds.) (2018). *Biomass, Biofuels, Biochemicals: Biofuels from Algae*. Elsevier.
19. Wittmar, A., Thierfeld, H., Köcher, S., and Ulbricht, M. (2015). Routes towards catalytically active TiO2 doped porous cellulose. *RSC Advances* 5 (45): 35866–35873.
20. Keshav, V., Franklyn, P., and Kondiah, K. (2019). Recombinant fusion protein PbrD cross-linked to calcium alginate nanoparticles for Pb remediation. *ACS Omega* 4 (16): 16816–16825.
21. Eghbali, M., Farahbakhsh, A., Rohani, A., and Pour, A.N. (2015). Urea biosensor based on immobilization of urease on ZnO nanoparticles. *Oriental Journal of Chemistry* 31 (2): 1237–1242.
22. Zhang, W. (2009). Soy proteins and/or soy derivatives with zero-valent iron compositions and use for environmental remediation. *US Patent 7,507,345 B2*, filed 23 August 2007 and issued 24 March 2009.
23. Naveen Kumar, M. (2017). Design of BFS in up flow mode using synthetic wastewater for the optimization of microorganisms. *International Journal of Latest Engineering Research and Applications* 2: 1–9.
24. Hu, J., Zhang, Q., Lee, D.J., et al. (2018). Feasible use of microbial fuel cells for pollution treatment. *Renewable Energy* 129: 824–829. https://doi.org/10.1016/j.renene.2017.02.001
25. Hussain, C.M., and Kadeppagari, R.-K. (eds.) (2022). *Biotechnology for Zero Waste: Emerging Waste Management Techniques*. WILEY-VCH GmbH.

18 Need for Detailed Landslide Inventory Maps and Landslide Databases in Indian Context

Minu Treesa Abraham and Neelima Satyam

18.1 INTRODUCTION

A 'landslide' can be defined as any mass movement (earth, rock or debris) in the downslope direction, under the influence of gravity (Cruden and Varnes 1996). Landslides can be triggered due to multiple factors, such as heavy rainfall, earthquakes, volcanic activities, snow melting and other anthropogenic factors. The triggering factors can result in multiple landslide types, depending upon the topographical and hydro-geological settings of the affected area. The most widely followed landslide classification is the one proposed by Varnes (Varnes 1978) and its update by Hungr et al. (2014). The classification is primarily based on the type of failure and then based on the material involved. Thus, the movements of rock or earth or debris in the form of fall, topple, slide, spread, flow or any slope deformations can be termed landslides. In practice, most landslides occur as a combination of two or more types, and it is difficult to classify the landslide into a single category. Locating and mapping of landslide events are of utmost significance, as the data is highly useful in landslide hazard zonation of the region (Guzzetti et al. 2012). It is well accepted that occurrence of landslides follows previous landslides, and the topographical and hydro-geological settings of historical landslides can be used to identify similar locations. The collection of location, date of occurrence (if known), type of landslide and other details about the landslide can be termed as landslide inventory mapping (Pašek 1975). Such maps are prepared for different purposes and are one of the most important inputs in landslide hazard assessment. The inventory maps can be used to record the extent of landslide hazard in an area, ranging from small watersheds or valleys (Santangelo et al. 2015) to the whole country (Trigila et al. 2010). Once the data is collected, it can be used as an initial step in assessing the landslide hazard and risk (van Westen et al. 2006; Abraham et al. 2021a, 2021b), as they will provide relevant information regarding the relationship between occurrence of landslides and the topographical and geological settings of the region. The inventory maps provide critical information to the process of landscape evolution as well (Parker et al. 2011).

DOI: 10.1201/9781032686899-23

It is well accepted that landslides do not occur at random locations and are the result of physical processes making a slope unstable. Thus, the processes can be modelled mathematically, and the stability of slopes can be calculated deterministically using process-based approaches (Baum et al. 2008; Alvioli and Baum 2016), or such locations can be identified using historical data, through statistical or machine learning approaches (Pradhan 2010). Even in the case of process-based models, landslide inventory maps are necessary to evaluate the performance of the model. Thus, landslide inventory maps of the past and the present are the keys to identify the landslide-prone areas in the future. This is based on the assumption that the conditions that led to slope instabilities in the past will lead to the same situations in the future (Guzzetti et al. 2012).

Preparation of landslide inventory maps in many countries is a task designated to government agencies and, in recent days, the availability of remote sensing data has made the procedure much easier. The primary assumption in mapping landslides is that the landslides leave recognizable signs, which helps in the identification, classification and mapping in the field and through the interpretation of aerial and satellite images (Guzzetti et al. 2000). The classification is done using the morphological signature of a landslide (Cruden and Varnes 1996), assuming the same type of mass movements will result in similar signatures. Identifying these signatures from aerial or satellite-based sources is a difficult task, and utmost care should be taken while classifying the landslides using these sources (Guzzetti et al. 2012).

Geomorphological field mapping is the oldest and most widely practiced approach for preparing landslide inventories, but the intensive field-based data collection is now mostly replaced by aerial and satellite-based images. The field mapping approach has many limitations due to the size of the landslide. Mapping is not easy when the size of a landslide is large and it is difficult to see the whole picture in the field, whereas visual interpretation of aerial or satellite images can overcome these limitations. The latter approach is easier and can be carried out with the help of an expert. However, when the studied region has very thick vegetation, small-scale landslides might not get noticed in satellite images. This significantly affects the completeness of an inventory map. The extent of the study area, characteristics of the available imagery and the purpose of the inventory map determine the method to be adopted for landslide inventory mapping. When aerial surveys cannot be conducted immediately after the hazard, then one has to rely on satellite-based data alone to map the landslides; also when the extent is too large, field mapping will be a difficult task. The cloud cover of monsoon season makes it difficult to get clear images immediately after the disaster. In this study, we have mapped the landslides that happened along the road stretch between 9.621° N, 76.847° E and 9.584° N, 76.885° E, on 16 October 2021, through field mapping and through visual interpretation of satellite images. The field mapping was carried out three days after the event, to locate and classify the landslides. Later, satellite images were also used for mapping, and a comparison was made to understand the advantages and limitations of both approaches.

18.2 STUDY AREA

Rainfall-induced landslides are a critical concern for hilly regions across the world, and they result in critical socio-economic setbacks in different parts of India (Bulzinetti et al. 2021; Satyam and Abraham 2021, 2022). Kerala is one of the southernmost states of India, running along the western coast. Among the 14 districts in the state, 13 are parts of Western Ghats (Gadgil et al. 2011), the most prominent orthographic feature of peninsular India (Kuriakose 2010). The study area belongs to the state of Kerala, between 76.83° E and 76.89° E longitudes and 9.57° N and 9.53° N latitudes. The landslide inventory map is prepared along a road stretch between 9.621° N, 76.847° E and 9.584° N, 76.885° E (Figure 18.1). The 9.54-km-long stretch was affected by several landslides due to heavy rains on 16 October 2021. The study area is part of the catchment basin of Pullakayar (Figure 18.2), and all the drainage paths along the road are tributaries of this river. Farther downstream, Pullakayar joins with another river and flows together as the Manimala River. Multiple debris flows and shallow landslides created havoc in the river basin on 16 October 2021. The debris flows and flash flooding in the river destroyed hundreds of houses and seven bridges, leaving many people homeless. Many debris flows happened in the region in t 2018, and a major debris flow of 2.6 km runout happened on 6 September 2020, at the upstream side of Pullakayar, where the stream originates, initiating the process of drainage divide in the basin. However, these events went unnoticed as there were no casualties associated with them. One major debris flow happened on the considered road stretch, which resulted in the loss of six lives. The area is very close to the administrative boundaries of two landslide-prone districts of the state, Kottayam and Idukki. The regions on the western side of Pullakayar belong to Kottayam district and on the east, it is Idukki district.

The charnockite group dominates the geology of the region. Medium to coarse-grained charnockite, dark grey quartz and granite are observed in the region. Soil along the road has both cohesive and frictional properties, formed by weathered laterite. The colour of soil varies from red to dark brown, indicating the presence of

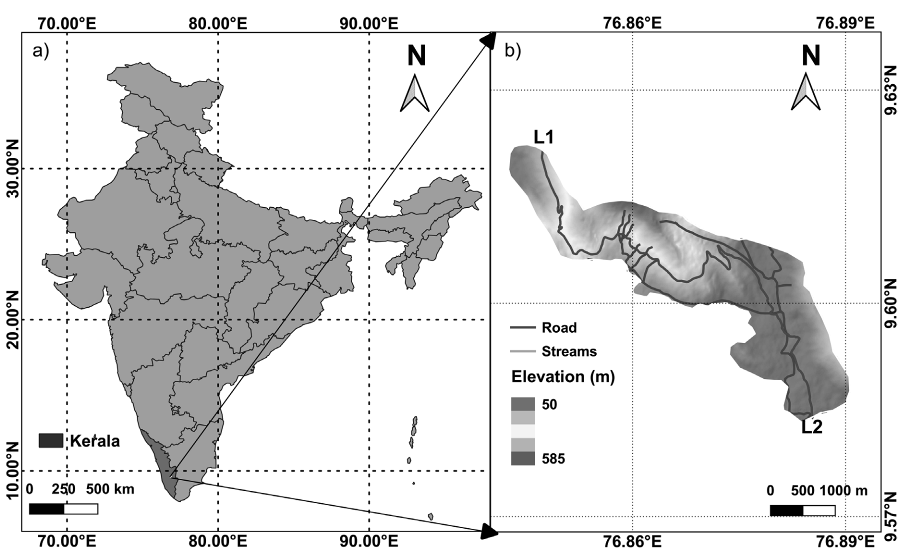

FIGURE 18.1 Study area location map: (a) map of India, and (b) road stretch and stream layers overlaid onto an elevation map of the region.

organic content. Granite is exposed at several locations along the road stretch. As observed from Figure 18.1, the elevation of the region varies from 50 m to 585 m in a short span, resulting in steep topography. The variation in elevation is significant in the first 7 km of the stretch, and most failures have occurred in the same span.

The location has experienced very heavy rainfall on 15 and 16 October 2021, and per the records of the India Meteorological Department, the rainfall at nearby town Peermedu on 16 October was 240.5 mm. The rainfall was continuous for around 8 hours and 30 minutes, indicating an intensity of 28.23 mm/h, which is much higher than the critical rainfall thresholds defined for the region (Abraham et al. 2021c). Extremely heavy rainfall triggered multiple landslides along the road stretch and, in this study, an attempt was made to prepare landslide inventory maps, using both field mapping and satellite images.

18.3 LANDSLIDE INVENTORY DATA

18.3.1 Field Mapping

The inventory data consists of landslide type, locations, and morphological signatures. The visibility issues using both approaches are also discussed. Most failures are shallow landslides, while debris flows are also recorded along the preexisting flow paths. The road crosses the drainage channels at multiple locations, and the natural flow path is obstructed due to the construction activities (Figure 18.2). The landslide locations identified during field visit are marked in Figure 18.2. As the crown points of most landslides were not accessible at the field, locations are marked at the nearest points accessible from the road.

Cut slopes along the roadside without proper lateral support have failed in multiple modes and disrupted the transportation facilities. A total of 56 landslides were located during the field visit, and were numbered from LS 1 to LS 56, based on their occurrence, from L1 to L2, and the directions, left and right are also mentioned with respect to the direction from L1 to L2. The landslides LS 1, LS 2 and LS 3 are located very near each other. As it can be observed from Figure 18.1, the left side of the road is at higher elevation and the right side at lower elevation at the initial portions. And hence, most failures up to LS 52 have happened along the left side of the road. Beyond the location of LS 52, the elevation reduces considerably, and the failures have happened on the right side of the road.

The landslides LS 1, LS 2 and LS 3 are located very near to each other. LS 1 has a height of around 3 m from the road level, and the layered bedrock is exposed after the failure (Figure 18.3). LS 2 and LS 3 are located on either side of a house, where the retained earth has failed. At LS 1, highly weathered bedrock is exposed and has two distinct scarps. At LS 3, the failure is rotational, and the rock is not exposed. The stretch between LS 4 to LS 8 has failed continuously along the left side of the road, and the failures are located close to each other (Figure 18.3). LS 4 and LS 5 are very shallow failures of around 1.5 m height from the road level. The vegetation is very heavy at these locations, which makes it difficult to be viewed in aerial or satellite-based images. LS 4 has two scarps, and the failure is rotational. LS 6 and LS 7 have two different scarps, and the failed mass converged and got deposited together on the roadside. Both failures are rotational, and at LS 6, the failed material is composed of

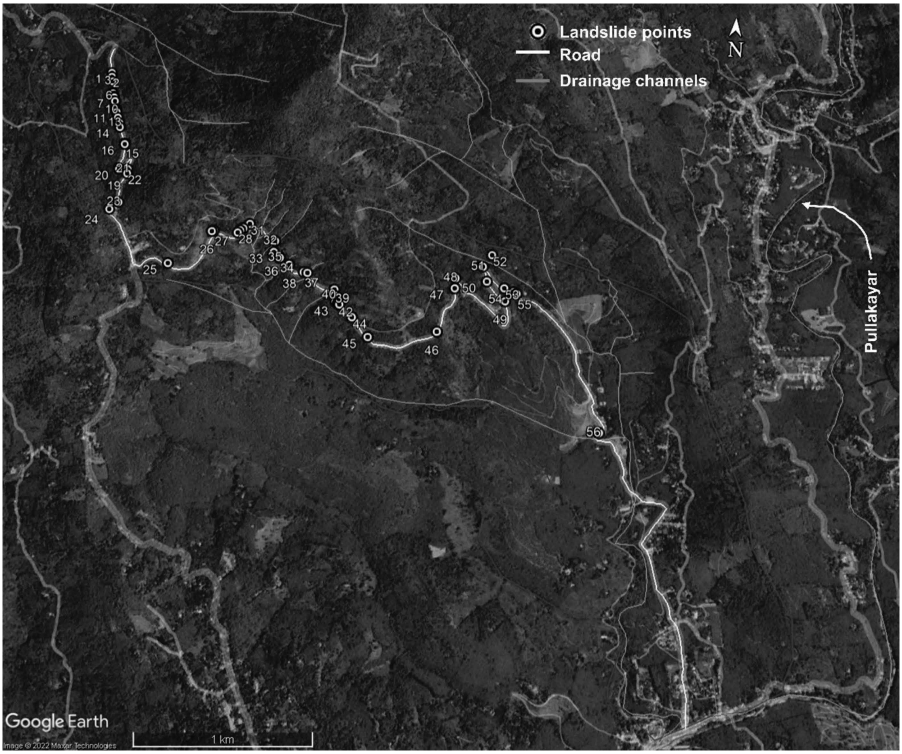

FIGURE 18.2 Landslide inventory data, overlaid on pre-event Google Earth image.

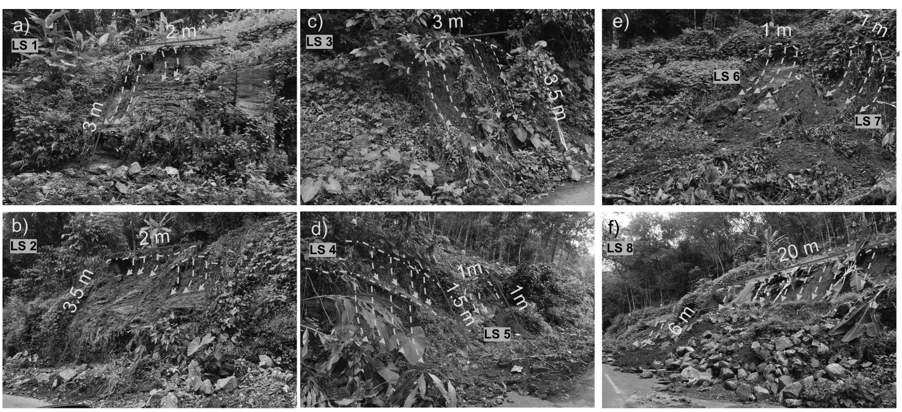

FIGURE 18.3 Landslides at locations 1 to 8: (a) LS 1, (b) LS 2, (c) LS 3, (d) LS 4, LS 5, (e) LS 6, LS 7 and (f) LS 8.

both soil and rock, while LS 7 is a case of earth slide. LS 8 is a long failure on the left side of the road, where the masonry retaining wall of an agricultural land has failed. The failure is translational, and the bedrock is not exposed, but the rubbles used for masonry have also failed along with the soil mass.

LS 9 and LS 10 are also on the left side of the road, very near to LS 8. Both failures are very similar to each other, in terms of dimensions and failure time. Both soil and weathered rock pieces have failed in the case of LS 9, while in the case of LS 10, the failed mass is soil (Figure 18.4). Immediately after LS 9 and LS 10, LS 11 is also on the left side of the road. The landslide has two separate scarps, one 3 m wide and one around 1 m wide. The failure is translational, and the material is composed of soil and weak lateritic rock pieces. The first debris flow of the study area is LS 12, which crosses the road and flows down further downstream. The location of the crown and the zone of deposition are not visible from the road. The bedrock is clearly exposed in this zone of erosion near the road, and the material that got deposited in the road was removed immediately to make the traffic open. LS 14 is the second debris flow in the considered stretch, and LS 13 is a shallow landslide where soil is exposed, between LS 12 and LS 14. Similar to LS 12, bedrock is visible in the upper portions of LS 14, but the amount of debris deposited along the road is more in the case of LS 14.

LS 15 and LS 16 are located immediately after a house, and LS 14 is just before the house. LS 15 is also a debris flow, and the debris got deposited along the way to the house and had blocked the road. No failure has happened below the road level at LS 15. LS 16 is a rotational failure very near to the debris flow location. The bedrock is exposed here, and from Figure 18.4 and Figure 18.5, it can be understood that a granite layer is available at very shallow depths from the surface. LS 17 and LS 18 are located very near to each other, and LS 18 is a clear rotational failure with a very minor flow path. Bedrock is also exposed at LS 18.

More shallow failures were recorded along the road, and LS 19 and LS 20 are located around 200 m from the location of LS 18. Both LS 19 and LS 20 are shallow failures with rotational slip surfaces. The location has deposits of boulders of around 0.6 m × 0.6 m × 0.5 m dimension, along the roadside. The fragmented rocks are exposed at LS 20, as shown in Figure 18.6, while the material detached at LS 19 is lateritic soil. A translational failure is observed in LS 21, where the failure has

FIGURE 18.4 Landslides at locations 9 to 13: (a) LS 9, LS 10, (b) LS 11, (d) LS 12—runout path above road level, (d) LS 12—runout path below road level, (e) LS 13.

FIGURE 18.5 Landslides at locations 14 to 18: (a) LS 14—runout path above road level, (b) LS 14—runout path below road level, (c) LS 15, (d) LS 16 and (e) LS 17, LS 18.

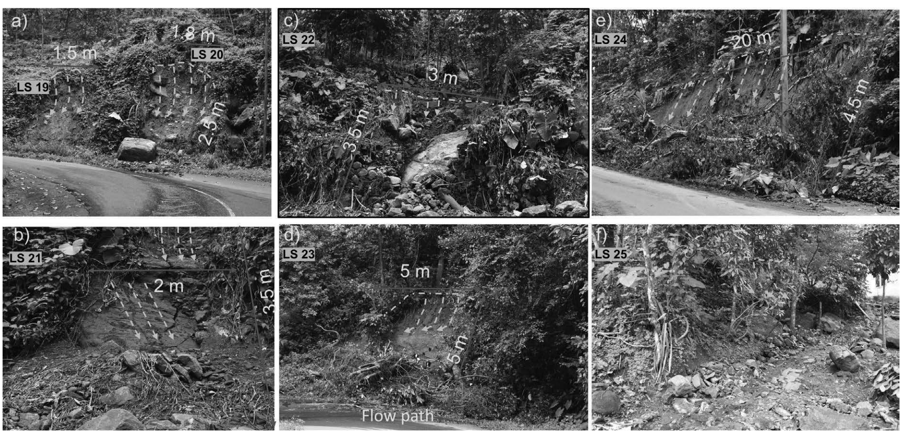

FIGURE 18.6 Landslides at locations 19 to 23: (a) LS 19, LS 20, (b) LS 21, (c) LS 22, (d) LS 23, (e) LS 24 and (f) LS 25.

occurred along a joint plane. Cracked rocks are exposed at the location. LS 22 is located very near to LS 21, where the masonry retaining wall has failed, exposing the bedrock. The exposed rock is jointed, and the failed material is partially deposited along the failure and may get eroded during further rainfall. LS 23 is located around 370 m away from the location of LS 22, along the road. The soil has failed with a rotational slip surface, and the location has an active flow path passing across the road. There are higher chances of further debris flows along this path. LS 24 is a 20-m-long translational failure with a single scarp. Even though the thickness of failed material is very less, around 0.6 m, a few trees are uprooted in the failure. LS 24 is a minor failure that happened around 700 m away from the location of LS 23. The scarp is located around 10 m away from the road, and the failed material is deposited along the mud road on the left side of the road.

LS 26 and LS 27 are located around 400 m away from the location of LS 25. LS 26 is a shallow rotational failure where jointed rocks are exposed, and LS 27 is a debris flow. The flow path of LS 27 is preexisting, and the material got deposited because of a new failure (Figure 18.7). LS 28, LS 28 and LS 29 are three shallow failures located very near to each other. At LS 28 is a rockslide with a translational slip surface. The layered rock has disintegrated into small pieces upon failure. Sedimentary layers are visible at the exposed surface. LS 29 and LS 30 have similar modes of failure, with two significant scarps. A thick layer of soil of around 1 m thickness has failed in both cases with rotational slip surface. The mobilization of failed mass at LS 29 is partially restricted by the roots exposed at the location. LS 31 and LS 32 are two debris flows that have happened through preexisting paths. The crowns are not visible from the road, and the deposited material is composed of fragmented rock pieces and soil.

The landslides LS 33, LS 34, LS 35 and LS 36 are located within a 140 m stretch. The failures are shallow and are poorly visible from the road, due to vegetation cover. The failure is translational in the case of LS 33. The face failure has a depth of 1 m, and the failed mass got deposited along the slope itself. The thickness of failed mass is around 60 cm at LS 33, and the same is around 30 cm at LS 34 and LS 35. LS 34 and LS 35 are also slope face failures with circular slip surfaces. At LS 36, the mode of failure is partially translational and partially rotational. The slope is almost vertical at the location, and there are high chances of retrogression. LS 37 and LS 38 happened around 100 m away from the location of LS 36, and a house is located between the failures (Figure 18.8). LS 37 is a rotational earth slide, which happened on the slope face, with the location of scarp around 5 m above the ground level of the house. The slope vertically retains earth behind the house, and there are chances

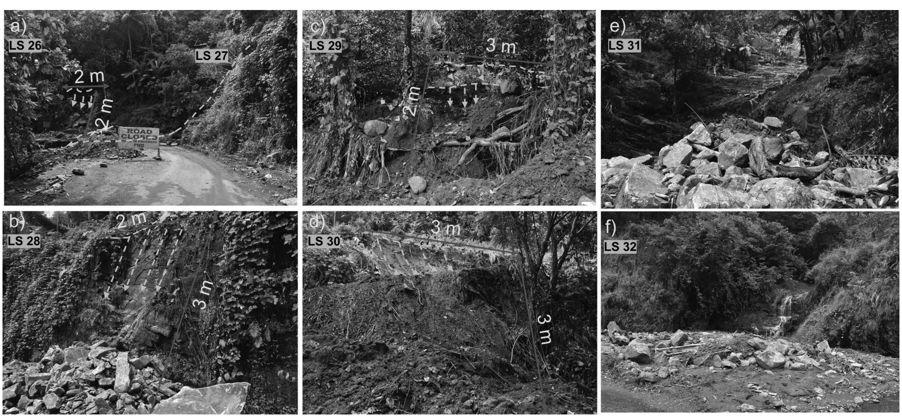

FIGURE 18.7 Landslides at locations 24 to 32: (a) LS 26, LS 27, (b) LS 28, (c) LS 29, (d) LS 30, (e) LS 31 and (f) LS 32.

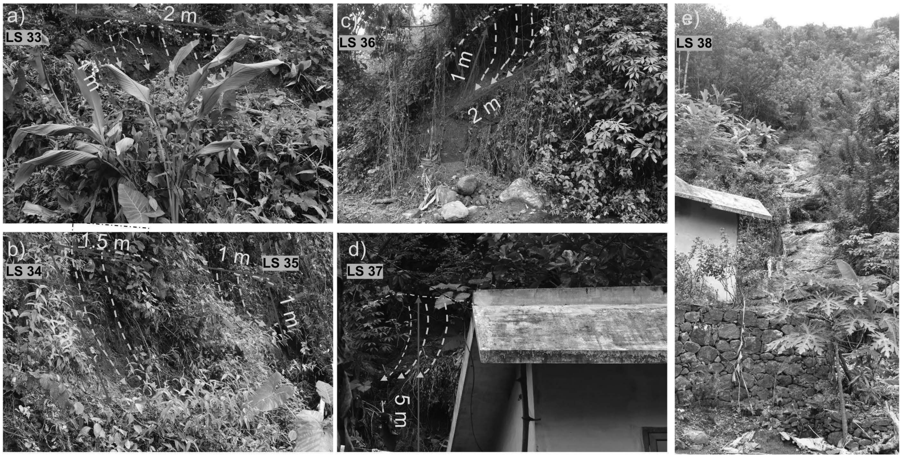

FIGURE 18.8 Landslides at locations 33 to 38: (a) LS 33, (b) LS 34, LS 35, (c) LS 36, (d) LS 37, and (e) LS 38.

of further erosion at the location. LS 38 has occurred along a preexisting path where rock is exposed. The material, including cobbles and fine material, got deposited along the road and have travelled further downstream, to reach the river.

LS 39 and LS 40 are located 50 m apart from each other. LS 39 is a debris flow, through a preexisting path. Bedrock is exposed on the upper side of the road, and minor damages have happened to the retaining wall along the road (Figure 18.9). The deposited mass had completely blocked the road and was removed immediately. LS 40 is a shallow failure with partially rotational and partially translational failure. The exposed soil mass is loose and is prone to erosion.

Around 50 m away from LS 39, three failures were marked very near to each other, LS 41, LS 42 and LS 43. LS 41 has three different scarps, and bedrock is exposed at the failure through one scarp, as observed in Figure 18.10, indicating the possibility of further failure along the layer of separation of loose soil and bedrock. At LS 42, a highly fragmented rock has failed along a joint plane, further exposing the stratified bedrock. Granite is exposed at LS 43 also, where soil has failed along a rotational slip surface (Figure 18.10). LS 44 is a retaining wall failure, where the masonry got detached from the retained earth along a translational surface, and the soil mass has failed in the orthogonal direction along a rotational surface. LS 45 is located around 180 m away from the location of LS 44. The failure occurred along a vertical slip surface, very near to a granite quarry.

LS 46 has happened 375 m away from the location of LS 45, where organic silty soil has failed along a rotational slip surface. Granite bedrock is exposed very near to this location, and medium to large-sized rock pieces are deposited very near to the failure. LS 49 is another shallow toe failure with a rotational and translational slip surface and three different scarps (Figure 18.11). The failed material is composed of soil and weathered rock pieces, and dense laterite is exposed along the failure surface. LS 48 has a clear translational slip surface, and loose soil detached from the

FIGURE 18.9 Landslides at locations 39 and 40: (a) LS 39—runout path above road level, (b) LS 39—runout path below road level and (c) LS 40.

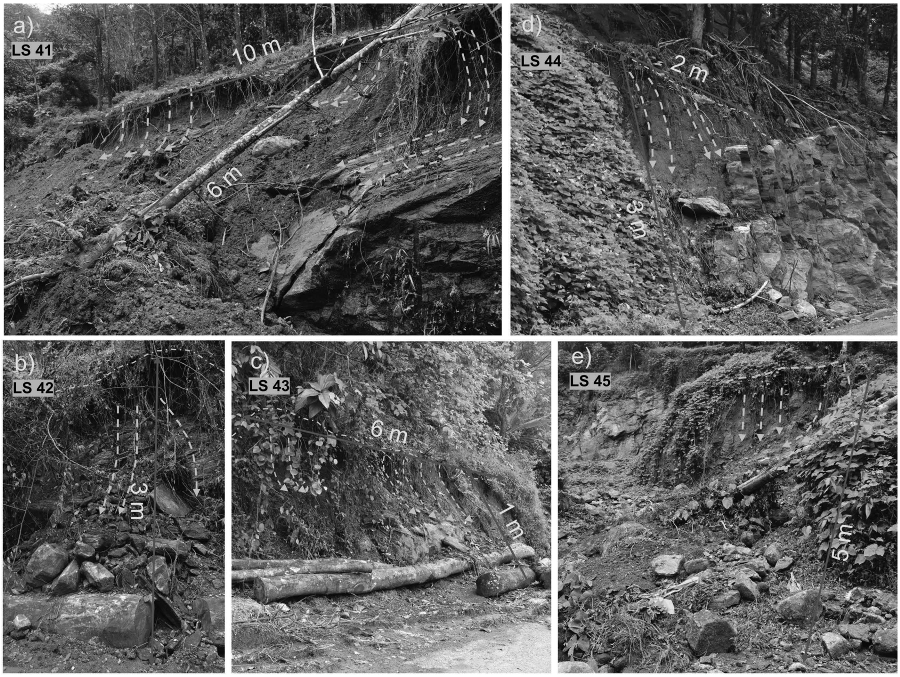

FIGURE 18.10 Landslides at locations 41 to 44: (a) LS 41, (b) LS 42, (c) LS 44, (d) LS 44, and (e) LS44.

FIGURE 18.11 Landslides at locations 46 to 51: (a) LS 46, (b) LS 47, (c) LS 48, (d) LS 49, (e) LS 50 and (f) LS 51.

slope, obstructing the road. LS 49 has a circular slip surface, where soil is detached, and weathered laterite is exposed at several locations. LS 50 is a combination of multiple shallow failures, where weathered laterite is exposed. LS 51 is very similar to LS 49, where the soil is detached from the dense laterite, along a rotational slip surface.

LS 52 is the most critical landslide along the path, a debris flow which claimed six lives from the same family. The house was destroyed, and all the members were inside the house during the event. The location is Kaavali, a debris slide has progressed at a flow, and joined the channel downstream (Figure 18.12) around 1 pm on 16 October 2021. The failed mass is deposited along the flow path, and there are high chances of further runoff-triggered debris flows due to the loose debris deposits. Fragmented rocks and boulders are deposited along the stream.

The road runs parallel to the stream from the location of LS 52. LS 53 is located parallel to the zone of deposition of LS 52, where thick regolith deposits are observed. All three failures are located nearby and have rotational slip surfaces through which soil has failed (Figure 18.13). The road was blocked by landslides on both sides of LS 52, which delayed the rescue operations. LS 53 to LS 56 have occurred in the stretch which connects the location of LS 52 to the nearby town. LS 56 is a riverbank failure, which happened due to flash floods. The debris deposits have raised the water level in the river, damaging several culverts, bridges and riverbanks.

18.3.2 Visual Interpretation of Satellite Images

The satellite images from passive sensors during daytime after the disaster were used for visual interpretation and detection of landslides. High vegetation cover and clouds during monsoons are the major challenges in detecting landslides using satellite images. The vegetation regrowth is very fast in the region, which protects the exposed soil from further erosions. The case studies conducted by the authors for

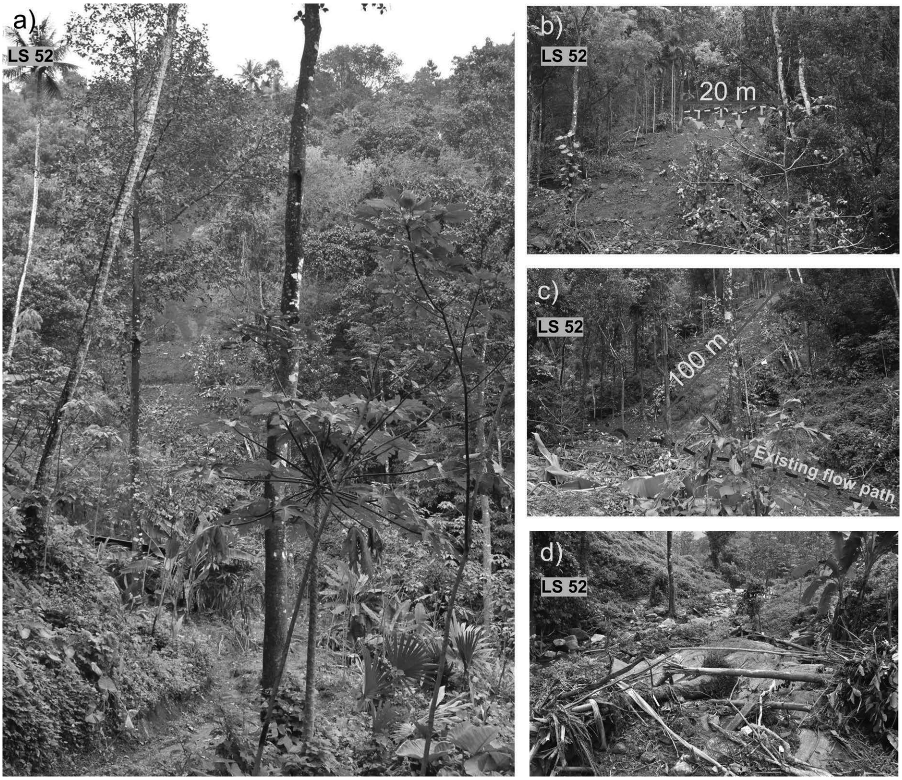

FIGURE 18.12 Landslides at location 52: (a) view of LS 52 from road, (b) crown area of LS 52, (c) runout path of LS 52 and (d) runout path of LS 52 flowing along with the stream.

large debris flow locations in Western Ghats have indicated that the deposited debris along the flatter region also gets stabilized and covered with vegetation within a year, in this region. The images from Sentinel-2 L2A, Landsat 8 T1, Landsat 8 T2 and Landsat 7 RT from 16 October to 31 December 2021 were continuously evaluated to detect the landslides. The natural colour images with bands B04, B03 and B02 were used for the interpretation. The images were collected from a Landviewer portal (Landviewer 2021), with a quality of 5 m per pixel. The list of images, sun elevation and cloudiness are reported in Table 18.1.

Two scenes from Sentinel 2 cover the road stretch, and hence two images are available on the same day. The images from 15 December 2021 were found useful in detecting landslides, as the cloud cover was lesser. On 9 December 2021, even though an image with 10% cloud cover was available, it had cloud cover above the study area and was not much useful. Both Sentinel images on the same day had provided very similar images except in the case of 29 December. Among the 54 landslides identified from the field mapping, only three were clearly visible in the satellite images. The three debris flows, LS 27, LS 31 and LS 52, were visible from the satellite images. While LS 52 is clearly visible, the runout zone below the road

FIGURE 18.13 Landslides at locations 53 to 56: (a) LS 53, (b) LS 54, (c) LS 55 and (d) LS 56.

level is visible in the case of LS 27 and LS 31. Some other major debris flows were also detected in the considered region, as shown in Figure 18.14, which are away from the road stretch.

The results from satellite images were used to calculate the dimension of the debris flows. Mapping debris flows from the field is extremely difficult, particularly due to their massive size. The dimensions are difficult to measure at the field. The satellite images were helpful in detecting the failures away from the road as well. The images have also provided a better picture about the location and distances between different landslide locations. Furthermore, some more major debris flows that happened in the region were mapped using the satellite images, because a wider area can be investigated in a short span of time using this approach, and the debris flows identified are marked in Figure 18.14.

Figure 18.14 shows a larger area when compared to the road stretch, and four more debris flows are identified in the region. Two of them are catastrophic events, resulting in loss of lives. All these debris flows have happened through existing flow paths or paths with very high value of flow accumulation, forming new tributaries

TABLE 18.1
Details of Post-Event Satellite Images

Sl No	Name of Sensor	Date	Sun Elevation (degrees)	Cloudiness (%)
1	Sentinel 2 L2A	20 October 2021	64	67
2	Sentinel 2 L2A	20 October 2021	63	71
3	Landsat 7 RT	20 October 2021	47	74
4	Sentinel 2 L2A	25 October 2021	62	56
5	Sentinel 2 L2A	25 October 2021	62	63
6	Landsat 8 T1	28 October 2021	59	32
7	Sentinel 2 L2A	30 October 2021	61	100
8	Sentinel 2 L2A	30 October 2021	61	100
9	Sentinel 2 L2A	04 November 2021	60	99
10	Sentinel 2 L2A	04 November 2021	59	96
11	Landsat 7 RT	05 November 2021	44	65
12	Landsat 8 T2	13 November 2021	55	23
13	Sentinel 2 L2A	14 November 2021	57	94
14	Sentinel 2 L2A	14 November 2021	57	100
15	Sentinel 2 L2A	19 November 2021	56	56
16	Sentinel 2 L2A	19 November 2021	56	73
17	Sentinel 2 L2A	24 November 2021	55	100
18	Sentinel 2 L2A	24 November 2021	55	100
19	Landsat 8 T1	29 November 2021	51	96
20	Sentinel 2 L2A	29 November 2021	54	100
21	Sentinel 2 L2A	29 November 2021	54	99
22	Sentinel 2 L2A	04 December 2021	53	96
23	Sentinel 2 L2A	04 December 2021	53	78
24	Sentinel 2 L2A	09 December 2021	52	10
25	Sentinel 2 L2A	09 December 2021	53	52
26	Landsat 8 T1	15 December 2021	49	23
27	Sentinel 2 L2A	19 December 2021	51	0
28	Sentinel 2 L2A	19 December 2021	52	12
29	Sentinel 2 L2A	24 December 2021	51	0
30	Sentinel 2 L2A	24 December 2021	51	1
31	Sentinel 2 L2A	29 December 2021	51	2
32	Sentinel 2 L2A	29 December 2021	51	0

to the river. The debris flow affected area and the reported casualties are listed in Table 18.2.

The debris flow events DF X3, LS 52 and DF X4 have resulted in loss of lives while others resulted in flash floods in the rivers. All events till DF X4 have happened in Pullakayar basin itself, while the events LS 12, LS 27 and LS 31 have damaged the road, and DF X1 and DF X2 have not created any direct impacts, other than the debris deposits to the stream network. These roads were inaccessible during the time

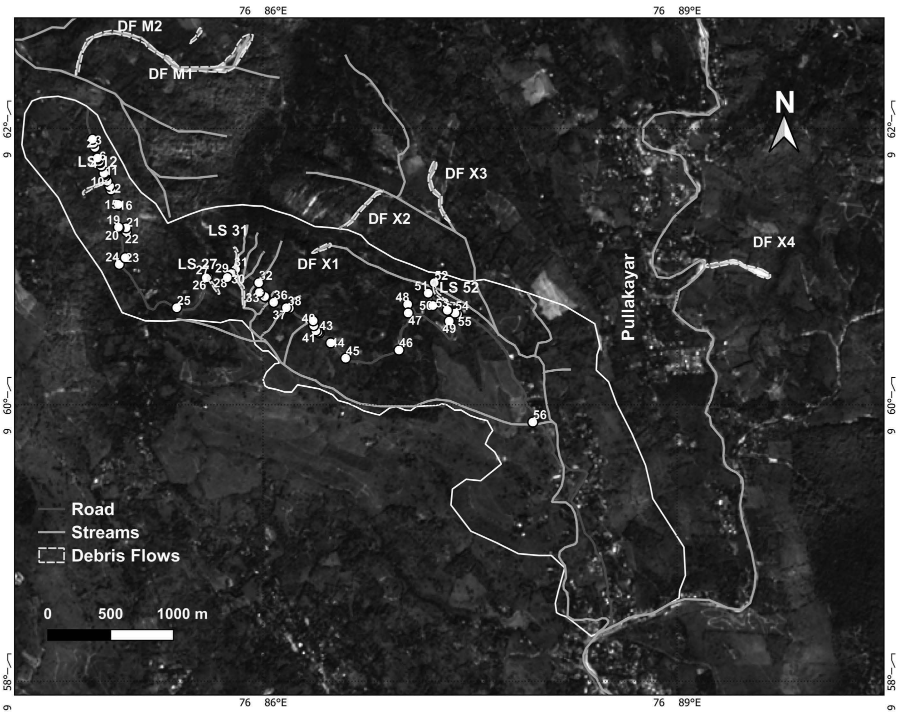

FIGURE 18.14 Debris flows marked using satellite images, overlaid on Sentinel 2 L2A image on 29 December 2021.

TABLE 18.2
Details of Debris Flows Mapped from Satellite Images

Sl No.	Name	Location	Approximate Area (m²)	Runout Length (m)	Casualties
1	LS 12	Kuzhumpally	4000*	200*	Nil
2	LS 27	Cholathadom	3000*	160*	Nil
3	LS 31	Cholathadom	9500	500	Nil
4	DF X1	Kaavali	4000	170	Nil
5	DF X2	Kaavali	9500	400	Nil
6	LS 52	Kaavali	5000	270	6
7	DF X3	Plappally	14000	550	4
8	DF X4	Poovanji	18000	550	7
9	DF X5	Poonjar	68000	1800	Nil
10	DF X6	Poonjar	3000	150	Nil

*These debris flows were partially visible, and the mentioned lengths are measured below the road level.

of field visit and were restored later. Even though LS 52 is smallest in terms of magnitude when compared with the other debris flows, the event resulted in the death of six persons from the same family. Landslides are often neglected when no casualties are reported, making the inventories incomplete, which will lead to incorrect hazard mapping and susceptibility zonation. DF X5 and DF X6 happened in another river basin (Meenachil) and have not contributed to the floods in Pullakayar basin. The event DF X5 is the largest in terms of magnitude of the event and has very high similarities to the debris flow of 6 September 2020, reported in Pullakayar basin. This event indicates further chances of drainage divide in Meenachil basin as well, and the need to be alert for the coming monsoon seasons. Extensive field studies must be conducted to investigate the shallow landslides that have occurred near all these debris flows and to prepare a complete landslide inventory map for the region.

18.4 DISCUSSION

From the study, it is evident that there exists a critical gap between the satellite-based landslide inventory maps and the field data. Collecting all data points and conducting detailed field investigations can aid in landslide hazard assessment and thereby disaster management. Among the 56 landslides, 47 were found to be shallow landslides, and the remaining nine were debris flows. Figure 18.15 shows the distribution of landslides along each kilometer stretch of the road. It can be observed from Figure 18.15 that the maximum number of landslides have happened in the first 1 km, and 17 out of 20 in this stretch were shallow landslides. In the stretch from 3 km to 4 km, debris flows outnumber shallow landslides, and the stretch has multiple active flow paths, as observed from Figure 18.14. The distribution is more or less uniform in the other stretches till 7 km, and beyond 7 km, only one landslide has happened, which is at a distance of 8 km.

The material involved in failure is classified into three categories: soil only (S), debris material including both soil and rock (SR), and soil and a mix of cobbles and boulders (SB). The term soil in this context indicates particles varying from silt to gravel, with high organic content. Boulders are also rock pieces, with diameters more than 300 mm average diameter as per Indian Standards, and cobbles are particles with average diameter between 80 to 300 mm. Here the classification SB indicates a mix of soil with cobbles and boulders, and the larger particles are from a failed retaining wall, or a construction. On the other hand, SR indicates a mixture of soil with pieces of detached rock material, from a larger rock. According to size, these pieces are also cobbles or boulders, but different terminology is used to indicate whether the rock pieces are part of bedrock or manually constructed masonry retaining walls. Two such failures have occurred along the road, LS 8 and LS 44. No rockfalls or rockslides are observed along the path, and the fragmented rock had failed along with soil mass in the considered study area. Among the 56 landslides, 32 have both soil and rock particles, including the two SB failures, and in the remaining 24 cases, only soil has failed.

While comparing the field mapping and satellite mapping results, it can be observed that both are unavoidable parts of landslide inventory preparation. Even though the field visit was conducted immediately after the event, the vegetation had

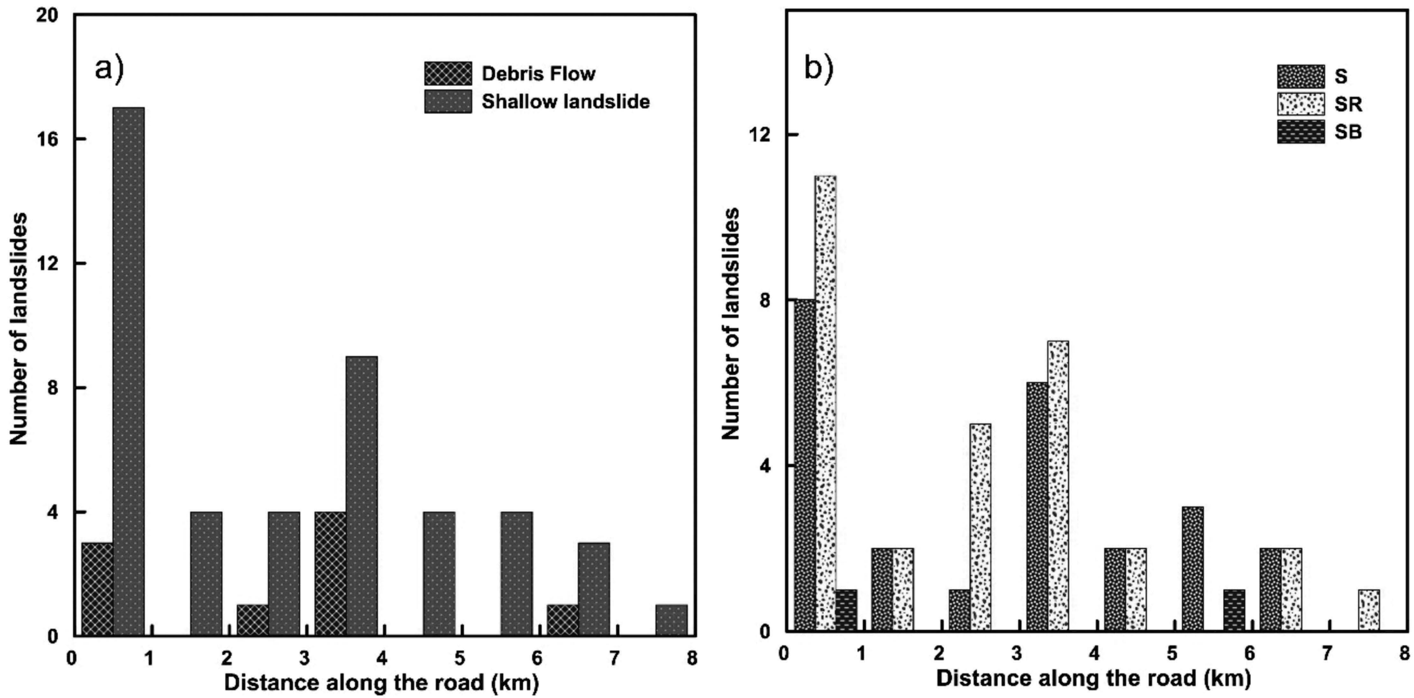

FIGURE 18.15 Landslides along the road: (a) classification based on type of failure and (b) material involved.

already started covering the failures, making them invisible from the road. The fast rate of regrowth of vegetation will make it difficult to map the dimensions of landslides correctly, even after a few months from the occurrence of landslides. The vegetation cover also makes it difficult to detect landslides from satellite images, especially in the case of cut slope failures that has been observed in this study. The failures are mostly vertical and are not visible from the satellite images. In the case of massive landslides like debris flows, satellite images are more helpful than field mapping. The dimensions of landslides can be measured easily from the images, and the flow path can be better understood from satellite images. The high cloud cover makes it difficult to map the landslides using satellite images during monsoon season, and the inventory can be completed only once the vision is clear. This will delay the preparation of inventory, and hence aerial surveys can be conducted as an alternate option. Aerial images can be taken closer to the failures and can be effectively used for mapping the landslides. In the study area, the length of road stretch and presence of trees made aerial survey a difficult option, as the vehicles flying above the height of trees also cannot detect the shallow failures effectively.

From the results, it can be understood that field mapping alone makes it difficult to map large landslides correctly, and satellite images alone may result in incomplete landslide inventory data, with many shallow landslides undetected. Also, in regions with heavy vegetation, the landslide scars will get easily covered by vegetation, and the mapping should be carried out immediately after the disaster. With the advancements in computational facilities, landslide inventory data is the most crucial input for landslide hazard assessment and landslide susceptibility studies. The reliability of all the data-driven approaches primarily depends upon the quality and completeness of the inventory data, and hence it is suggested that field mapping should be conducted immediately after the failure, and satellite-based images should be used to get more details about the failures.

18.5 CONCLUSIONS

Landslide inventory data is a crucial input in the process of landslide hazard assessment, and the completeness of inventory data determines the quality of all models prepared for landslide hazard assessment. The landslides happened along the road stretch between 9.621° N, 76.847° E and 9.584° N, 76.885° E, on 16 October 2021. The road connects Poonjar and Kootickal towns in Kottayam district, in the South Indian state of Kerala. The landslides were mapped by both field mapping and visual interpretation of satellite images, and the results were compared to understand the advantages and limitations of both approaches.

A total of 56 landslides were detected from field investigation, and the details regarding dimensions, type of failure and material involved are collected from the field. Among the 56 landslides, nine were debris flows for which measuring the dimensions was extremely difficult in the field. A total of 32 satellite images were available for the study area after the event (till 31 December 2021), from Sentinel-2 L2A, Landsat 8 T1, Landsat 8 T2 and Landsat 7 RT sensors, but only seven images captured after 15 December 2021 were useful for the preparation of inventory. Only three debris flows were spotted from the satellite images, among the 56 landslides detected from the field, which raises serious concerns on the completeness of satellite-based landslide inventories of highly vegetated regions. The images were helpful in estimating the size and flow paths of the three debris flows detected, which was almost impossible from the field. Some more debris flows that happened in the region away from the road stretch were also mapped from the images.

From the results, it is suggested that both field-based and satellite-based investigations should be carried out after the occurrence of landslides, for getting reliable landslide inventory data. Both methods have their own strengths and limitations, and only an integrated approach can deliver quality landslide inventory maps. Data collection initiatives should be centralised and should be more people centric, such that the inventory data can be collected from the field with the support of common people.

REFERENCES

Abraham MT, Satyam N, Jain P, Pradhan B, Alamri A (2021b) Effect of spatial resolution and data splitting on landslide susceptibility mapping using different machine learning algorithms. *Geomat Nat Hazards Risk* 12(1):3381–3408. https://doi.org/10.1080/19475705.2021.2011791

Abraham MT, Satyam N, Lokesh R, et al. (2021a) Factors affecting landslide susceptibility mapping: Assessing the influence of different machine learning approaches, sampling strategies and data splitting. *Land* 10:989. https://doi.org/10.3390/land10090989

Abraham MT, Satyam N, Rosi A, et al. (2021c) Usage of antecedent soil moisture for improving the performance of rainfall thresholds for landslide early warning. *Catena* 200:105147. https://doi.org/10.1016/j.catena.2021.105147

Alvioli M, Baum RL (2016) Parallelization of the TRIGRS model for rainfall-induced landslides using the message passing interface. *Environ Model Softw* 81:122–135. https://doi.org/10.1016/j.envsoft.2016.04.002

Baum RL, Savage WZ, Godt JW (2008) *TRIGRS—A Fortran Program for Transient Rainfall Infiltration and Grid-Based Regional Slope-Stability Analysis, Version 2.0*. U.S. Geological Survey, Reston, Virginia. https://pubs.usgs.gov/of/2008/1159/downloads/pdf/OF08-1159.pdf

Bulzinetti MA, Abraham MT, Satyam N, Pradhan B, Segoni S (2021) Combining rainfall thresholds and field monitoring data for development of LEWS. *EGU21–2072*. https://doi.org/10.5194/egusphere-egu21-2072

Cruden D, Varnes D (1996) Landslide types and processes. In: Turner AK, Schuster RL (eds) *Landslides, Investigation and Mitigation, Special Report*. Transportation Research Board, Washington, DC, pp. 36–75

Gadgil M, Krishnan BJ, Ganeshaiah KN, et al. (2011) *Report of the Western Ghats Ecology Expert Panel (WGEEP)*. Submitted to the Ministry of Environment and Forests, Government of India.

Guzzetti F, Cardinali M, Reichenbach P, Carrara A (2000) Comparing landslide maps: A case study in the Upper Tiber River Basin, Central Italy. *J Environ Manag* 25:247–263. https://doi.org/10.1007/s002679910020

Guzzetti F, Mondini AC, Cardinali M, et al. (2012) Landslide inventory maps: New tools for an old problem. *Earth Sci Rev* 112:42–66. https://doi.org/10.1016/j.earscirev.2012.02.001

Hungr O, Leroueil S, Picarelli L (2014) The Varnes classification of landslide types, an update. *Landslides* 11:167–194. https://doi.org/10.1007/s10346-013-0436-y

Kuriakose SL (2010) *Physically-Based Dynamic Modelling of the Effect of Land Use Changes on Shallow Landslide Initiation in the Western Ghats of Kerala, India*. University of Twente, Enschede, The Netherlands

Landviewer (2021) *EOS Landviewer*. https://eos.com/landviewer/. Accessed 31 Dec 2021

Parker RN, Densmore AL, Rosser NJ, et al. (2011) Mass wasting triggered by the 2008 Wenchuan earthquake is greater than orogenic growth. *Nat Geosci* 4:449–452. https://doi.org/10.1038/ngeo1154

Pašek J (1975) Landslide inventory. *Int Assoc Eng Geol Bull* 12:73–74

Pradhan B (2010) Application of an advanced fuzzy logic model for landslide susceptibility analysis. *Int J Comput Intell Syst* 3:370–381. https://doi.org/10.1080/18756891.2010.9727707

Santangelo M, Gioia D, Cardinali M, et al. (2015) Landslide inventory map of the upper Sinni River Valley, Southern Italy. *J Maps* 11:444–453. https://doi.org/10.1080/17445647.2014.949313

Satyam N, Abraham MT (2021) Development of landslide early warning using rainfall thresholds and field monitoring: A case study from Kalimpong. In: Garg A, Solanki CH, Bogireddy C, Liu J (eds) *Proceedings of the 1st Indo-China Research Series in Geotechnical and Geoenvironmental Engineering* (pp. 153–173). Springer, Singapore. https://doi.org/10.1007/978-981-33-4324-5_11

Satyam N, Abraham MT (2022) Forecasting landslides for disaster risk reduction: Process-based approaches and real-time field monitoring. In: Kolathayar S, Pal I, Chian SC, Mondal A (eds) *Civil Engineering for Disaster Risk Reduction* (pp. 147–167). https://doi.org/10.1007/978-981-16-5312-4_11

Trigila A, Iadanza C, Spizzichino D (2010) Quality assessment of the Italian landslide inventory using GIS processing. *Landslides* 7:455–470. https://doi.org/10.1007/s10346-010-0213-0

van Westen CJ, van Asch TWJ, Soeters R (2006) Landslide hazard and risk zonation—Why is it still so difficult? *Bull Eng Geol Environ* 65:167–184. https://doi.org/10.1007/s10064-005-0023-0

Varnes DJ (1978) Slope movement types and processes. In: Schuster RL, Krizek RJ (eds) *Landslides, Analysis and Control, Transportation Research Board, Special Report* No. 176, pp. 11–33.

19 Monitoring of Melt Ponds and Supra-Glacial Lakes over Nivlisen Ice Shelf, East Antarctica, Using Satellite-Based Multispectral Data

Geetha Priya M, Raghavendra K R, Dhanush S, Rakshita C, Mahesh B and Deva Jefflin A R

19.1 INTRODUCTION

The melt ponds and supra-glacial lakes (SGLs) are hydrological features that are formed on the surface of an ice sheet/ice shelf/glacier due to the melting of snow and ice. They are characterized by the accumulation of meltwater in a depression (ponding mechanism), resulting in the formation of an SGL on a prolonged basis (Lindbäck et al. 2019). Despite being temporary in nature, melt ponds and SGLs can exhibit considerable variation in depth, size, and spatial distribution, with few lakes spanning several kilometres in length and diameter, which can reach depths of several meters. SGLs typically experience a seasonal cycle of forming and draining, with most lakes re-freezing or draining during the Austral summer. Nevertheless, certain SGLs have been documented undergoing a drainage process, wherein the water flows into the glacier's surface through moulins, crevasses, melt channels, or any other drainage features. This process has the potential to influence the dynamics of the underlying ice (Banwell et al. 2014). The presence of melt ponds (MPs) and SGLs can reduce the reflectivity of the glacier's surface, leading to increased absorption of solar radiation and intensifying surface melt (Alley et al. 2018). This, in turn, can lead to a warming effect on the surrounding ice column and potentially contribute to ice shelf destabilization (Banwell, MacAyeal, and Sergienko 2013). The feedback mechanisms that link SGL formation, surface albedo, and ice shelf dynamics are complex and depend on several factors, including the lake's size, depth, and spatial distribution, as well as atmospheric conditions such as temperature and radiation.

DOI: 10.1201/9781032686899-24

The development and interplay of SGLs on ice shelves carry substantial implications for the stability of these ice shelves, as noted by Horwath et al. (2006). This phenomenon can have a buttressing effect on the flow of inland ice. The Nivlisen Ice Shelf, which is located in eastern Antarctica, in Dronning Maud Land, was considered for the present study. The area encompasses a significant expanse of the eastern region of Antarctica, featuring a coastline that spans over 2000 kilometers (Horwath et al. 2006). The area is distinguished by extensive ice shelves, which are intermixed with numerous ice rises and rumple zones. The primary objective of the current study is to examine the spatiotemporal patterns in the distribution and development of MPs and SGLs over the course of two Austral summers.

19.2 STUDY AREA

The Nivlisen Ice Shelf, located in central Dronning Maud Land (cDML), East Antarctica, is positioned between the Lazarev and Vigrid ice shelves (Figure 19.1). It is also fed by Potsdam Glacier (Lindbäck et al. 2019). It has an approximate area of 7300 square kilometers and extends roughly 80 kilometers along the north-south axis into the Lazarev Sea and 130 kilometers along the east-west axis. The persistence of bare ice in the southeastern region of the ice shelf is upheld by the presence of Katabatic winds and is moving at an average rate of 80 my^{-1} (Lindbäck et al. 2019). The ice shelf is connected to an ice-free zone known as Schirmacher Oasis, which is along the Princess Astrid Coast (Pande et al. 2017). The Nivlisen Ice Shelf is undergoing substantial melting during Austral summer, resulting in the formation of SGLs. The presence of increased

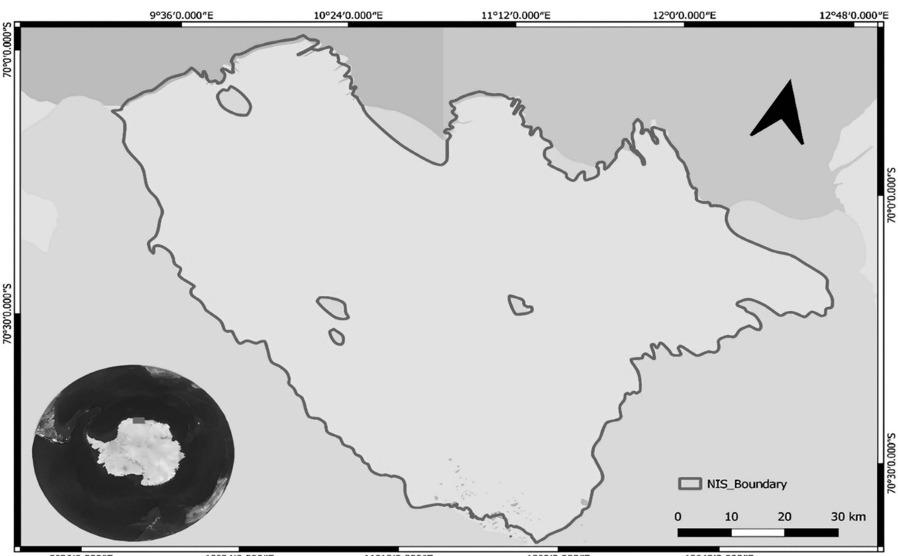

FIGURE 19.1 Study area—Nivlisen Ice Shelf (NIS), located at 70.3 °S, 11.3°E.

MPs and SGLs in the Nivilisen Ice Shelf increases its vulnerability to hydrofracturing, as noted by Robel and Banwell in 2019. As a result, this location is of utmost importance for investigating the various processes and factors contributing to ice loss in the Antarctic ice shelf, as emphasized by Lindbäck et al. in 2019. The Nivilisen Ice Shelf has been chosen as the focus of the current study due to the noticeable rise in the occurrence of MPs and SGLs in the ice shelf region in recent years.

19.3 MATERIALS AND METHODS

19.3.1 Data Acquisition and Preprocessing

The multispectral data from the Landsat-8 and 9 satellites were obtained from the USGS Earth Explorer for the Austral summer of the years 2021–2022 and 2022–2023 with minimum/no cloud cover. The Landsat-8 was launched on 11 February 2013 with Operational Land Imager (OLI) and Thermal Infrared Sensor (TIRS) sensors, which have 11 bands with a swath of 185 km x 180 km and spatial resolution of 15–100 m. The Landsat-9 was launched on 27 September 2021 with the Operational Land Imager 2 (OLI-2) and Thermal Infrared Sensor 2 (TIRS-2) sensors, with the same swath and resolution as Landsat-8 (Masek et al. 2020). The list of data used is shown in Table 19.1, with a data gap for December 2021 due to cloud cover. The pre- and post-processing of the datasets were carried out in open-source software Quantum GIS (QGIS), as shown in Figure 19.2.

The satellite data acquired is initially in digital number (DN) format, and to utilize it effectively, it needs to undergo a conversion process into top of atmosphere (TOA) reflectance. This conversion, specifically for the visible bands (red and blue), is achieved through the dark object subtraction (DOS1) method using equations 19.1 and 19.2 (Zhang, He, and Wang 2010):

$$\rho' = M_{Rf} Q_{Cal} + A_{Rf} \tag{19.1}$$

TABLE 19.1
List of Landsat-8/9 Datasets Used

Sl No.	Scene ID	Date of Acquisition	Path and Row Number
1.	LC08_L1GT_166110_20211107_20211117_02_T2	07/11/2021	166 & 110
2.	LC08_L1GT_165110_20211116_20211125_01_T2	16/11/2021	165 &110
3.	LC08_L1GT_166110_20220126_20220204_02_T2	26/01/2022	166 & 110
4.	LC08_L1GT_166110_20220227_20220309_02_T2	27/02/2022	166 & 110
5.	LC08_L1GT_165110_20221103_20221114_02_T2	03/11/2022	165 & 110
6.	LC09_L1GT_165110_20221127_20221127_02_T2	27/11/2022	165 & 110
7.	LC09_L1GT_165110_20221213_20221213_02_T2	13/12/2022	165 & 110
8.	LC08_L1GT_165110_20230106_20230110_02_T2	06/01/2023	165 & 110
9.	LC09_L1GT_165110_20230215_20230215_02_T2	15/02/2023	165 & 110

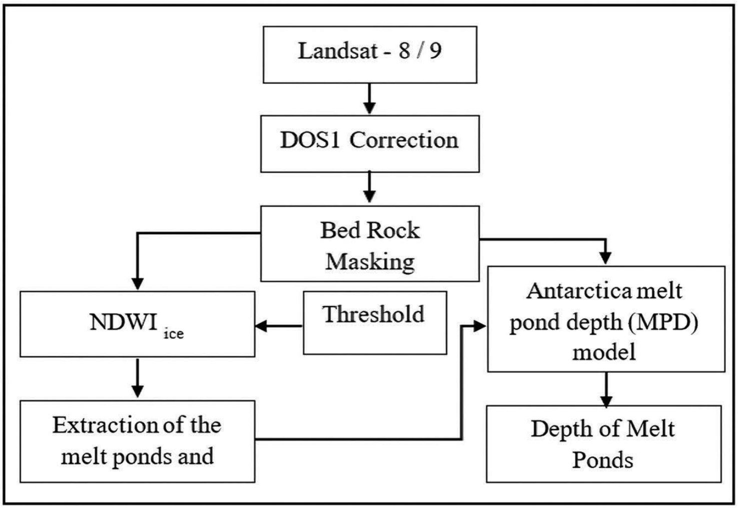

FIGURE 19.2 Process flow followed to obtain the depth of MPs and SGLs using melt pond depth model.

$$\rho = \frac{\rho'}{cos(\theta_{SZ})} = \frac{\rho'}{cos(\theta_{SE})} \quad (19.2)$$

where ρ′ & ρ are top of atmosphere reflectance (TOA) without and with sun angle correction respectively, M_{Rf}—band-specific multiplicate rescaling factor, A_{Rf}—band-specific additive rescaling factor, Q_{Cal}—the imagery in DN format, θ_{SZ} represents zenith angle of the sun, and θ_{SZ} is sun elevation angle. The bedrock masking was applied to the TOA blue and red bands.

19.3.2 Mapping of Melt Ponds and SGLs

To delineate the MPs and SGLs present on the ice shelf, we employed a modified version of the Normalized Difference Water Index ($NDWI_{ICE}$), as outlined in equation 19.3. This adapted $NDWI_{ICE}$ is specifically designed for icy environments and enhances the spectral contrast between unfrozen water and the relatively dry snow/ice surfaces (Shelf et al. 2020).

In order to identify the extent of MPs and SGLs coverage on the ice shelf, we applied a threshold value of 0.25 to the $NDWI_{ICE}$. To fine-tune this threshold and accurately capture the water features visible in the false color composite imagery, we incrementally adjusted it by 0.01. Subsequently, we determined the areas occupied by the MPs and SGLs by analyzing the vectorized raster data following the thresholding process:

$$NDWI_{ICE} = \frac{(BLUE_{Ref} - RED_{Ref})}{(BLUE_{Ref} + RED_{Ref})} \quad (19.3)$$

where $BLUE_{Ref}$ and RED_{Ref} represent the TOA reflectance of the visible bands blue and red, respectively.

19.3.3 Lake Depth Estimation

A melt pond model based on multispectral data (equation 9.4) was employed to calculate the depth (D_L) of MPs and SGLs (Shelf et al. 2020; Geetha Priya et al. 2022). This model operates on the principles of radiative transfer, simulating how light interacts with the water column, the lake bottom, and the surrounding environment. It relies on the rate at which light attenuates in water, which depends on water's absorption and scattering characteristics, to deduce the water column's depth. Additionally, this approach necessitates knowledge of the albedo of the lake bottom, which represents how the lake bottom reflects light at various wavelengths.

$$D_L = \frac{\left[\ln\left(L-R\right)-ln\left(W-R\right)\right]}{A} \tag{19.4}$$

where L is the reflectance from lake peripherals, R is the reflectance exhibited by optically deep water, W is the reflectance exhibited by the water bodies, and A represents the attenuation constant.

The D_L was computed by taking an average of two pixels buffer around the blue ponds/lakes. The average difference between employing an R value of zero and utilizing R values obtained from the lakes within the scenes is found to be within a 10% margin. Therefore, the R value was assumed to be zero. The red band was used to estimate the depth, as the water bodies reflect the red band spectrum when compared to blue. Red band reflectance was considered for W due to the spectral signature of water bodies. An attenuation constant of 0.7507 was considered for both the OLI1 and OLI2 sensors (Masek et al. 2020).

19.4 RESULTS AND DISCUSSION

The process flow outlined in section 19.3 was used to estimate the depth of the MPs and SGLs situated on the ice shelf. A pixel-based volume estimation was carried out for each MP and SGL using the depth estimated from the MPD model. The study was conducted during the Austral summers of 2021–2022 and 2022–2023. For representation purpose, the model-based results for MPs and SGLs on 6 January 2023 is shown in Figure 19.3. The distribution of SGLs and MPs across the NIS demonstrates a tendency to cluster, with a notable accumulation of ponds primarily observed in the grounding zone. In contrast, MPs and SGLs are notably scarce near the calving front of the ice shelf, although surface melt rates are at their peak in this area.

The results were scrutinized in correlation with the weather data sourced from the Meteostat database (https://meteostat.net/en/station/). The database provides extensive weather data for numerous weather stations and locations around the world. Figure 19.4 illustrates the temperature and precipitation trends in the study region, as acquired from Meteostat for the Austral summers of both 2021–2022 and

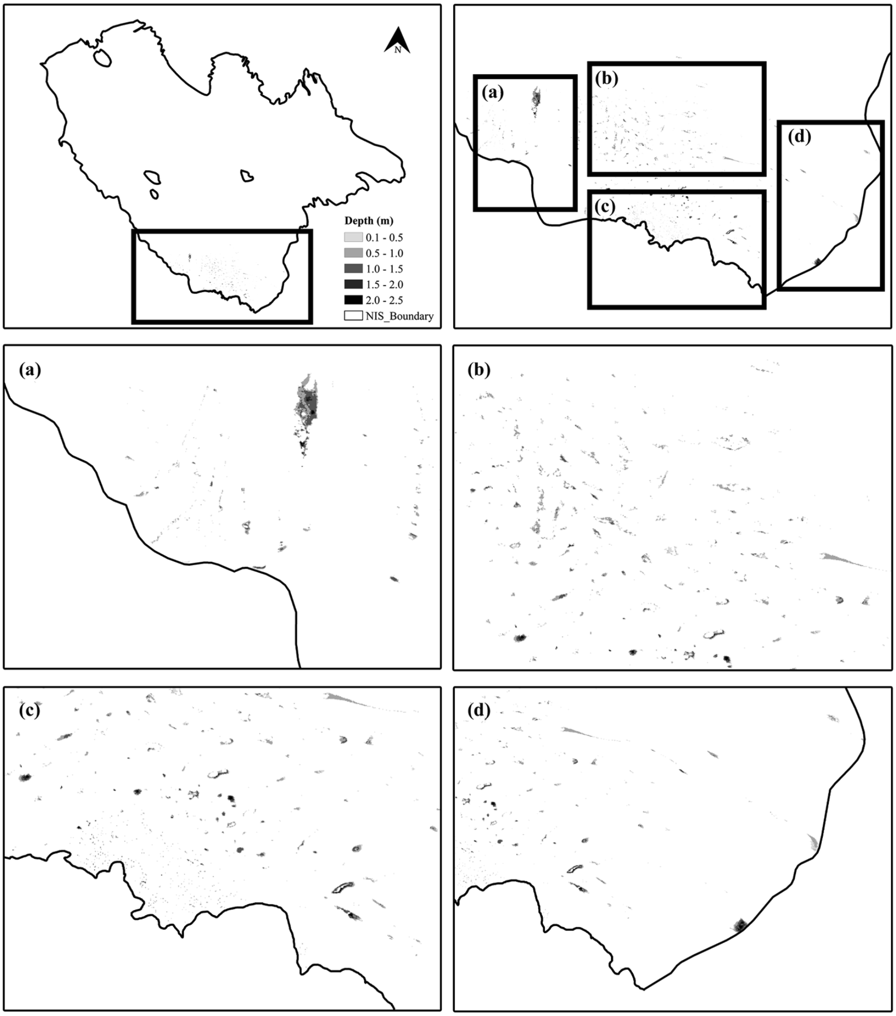

FIGURE 19.3 MPD model-based results over NIS for 6 January 2023.

2022–2023, with a data gap in February 2023. Table 19.2 and Figure 19.5 provide the estimated average depth, area, and volume of the MPs and SGLs.

The MPs and SGLs average and maximum depth had increased from November 2021 to January 2022 due to a rise in temperature from -9.1^0C to -3^0C, with an overall area of 536.87 km^2 during January 2022, which is a peak melting time. In February 2022, it is observed that the area of MPs and SGLs reduced by 24 km^2 approximately due to the refreezing (offset of summer). It is also observed that there is a subsequent reduction in volume at the end of January 2022, which is possibly due to the draining of water (internal cracks and drainage channels). During November 2022 to January 2023, the depth estimates of the MPs and SGLs scaled up by 2.5 m maximum due to temperature increment from -10.3^0C to -4.7^0C (Figure 19.4a). The

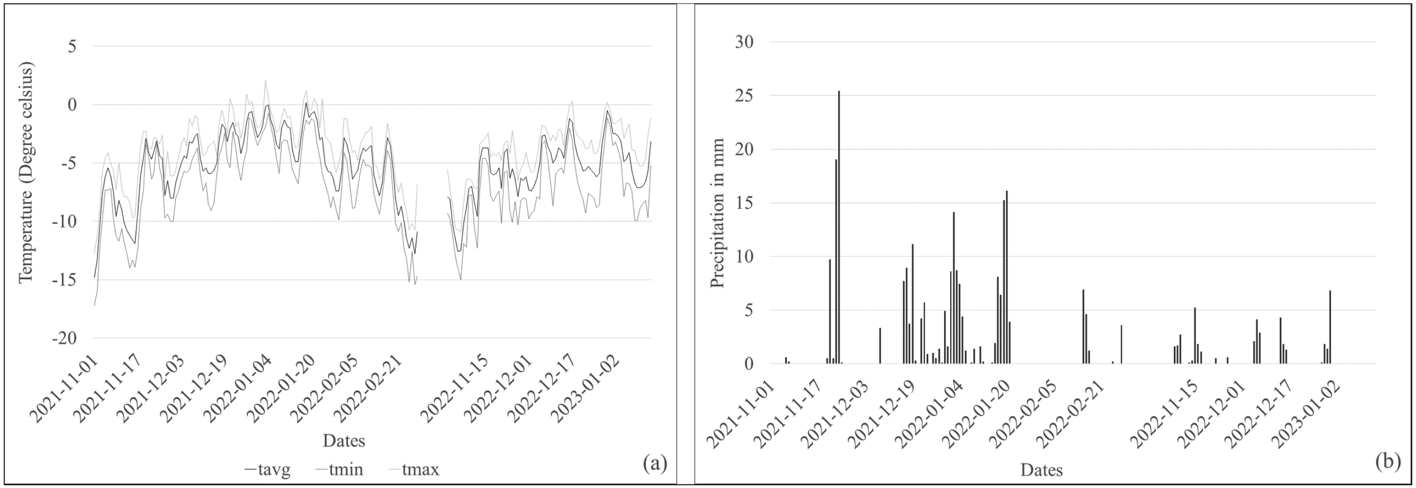

FIGURE 19.4 Meteostat weather data during Austral summer: (a) temperature profile, (b) precipitation.

TABLE 19.2
Melt Ponds and SGLs Depth, Area, and Volume

Parameters		Austral Summer 2021–2022				Austral Summer 2022–2023				
		7 Nov	**16 Nov**	**26 Jan**	**27 Feb**	**03 Nov**	**27 Nov**	**13 Dec**	**6 Jan**	**15 Feb**
Depth (m)	Average Depth	0.0003	0.0021	0.0178	0.0043	0.0021	0.0001	0.0002	0.0026	0.0007
	Maximum Depth	1.0000	1.0324	1.4359	1.0231	1.0025	0.5216	0.6008	2.4932	1.4325
	Minimum Depth	0.0374	0.0237	0.0363	0.0426	0.0728	0.0742	0.0632	0.0010	0.0008
Area (km^2)		21.32	65.37	536.87	512.96	1902.11	2003.51	2105.33	237.09	143.45
Volume (m^3)		1488.46	1708.09	1964.90	741.94	2044.04	2147.81	2572.20	3134.61	577.21

depth of the SGLs was observed to be reduced from 1 m to 0.6 m from 3 November 2022 to 16 December 2022, which is possibly due to precipitation of 4.1 mm (Figure 19.4b) recorded during 5–6 December. The SGL refreezing started post December 2022, so a decrement in the area was observed from November 2022 to January 2023. The volume of the SGLs reduced post January 2023 due to the drainage mechanism.

Generally, during the December and January months of Austral summer, the total surface area of the MPs and SGLs present over the NIS undergoes an overall expansion, culminating in a maximum value during late December and early January (Shelf et al. 2020). Subsequently, there was a progressive reduction in the estimated lake area during the end of the melt season, which attains a minimum value during late February. During the late December to early January period, the ice shelf typically exhibits the deepest lakes. This temporal pattern aligns with the seasonal fluctuations in both lake depth and the overall lake area, as these factors are closely linked to the melting and freezing processes occurring within the ice shelf during this specific period.

The maximum depth of the MPs and SGLs is increased by four times in comparison of January 2022 to January 2023, from 1.4359 m to 2.4932 m, respectively. During the Austral summer 2021–2022, the maximum lake area recorded was 519 km^2, and for the Austral summer 2022–2023, the maximum lake area recorded was 2105 km^2, i.e., there is an increase in the total area by four times.

The following observation was made for the Austral summer 2021–22 (Figure 19.5a):

- The number of MPs and SGLs was found to increase during November 2021–January 2022 from 5–60 with a gradual increase in area.
- The pond draining mechanism has been observed during post-November 2021 as the average depth and volume have decreased.
- The process of freeze-up for MPs and SGLs commenced in late February 2022, leading to a subsequent decrease in both the surface area and volume of these lakes.

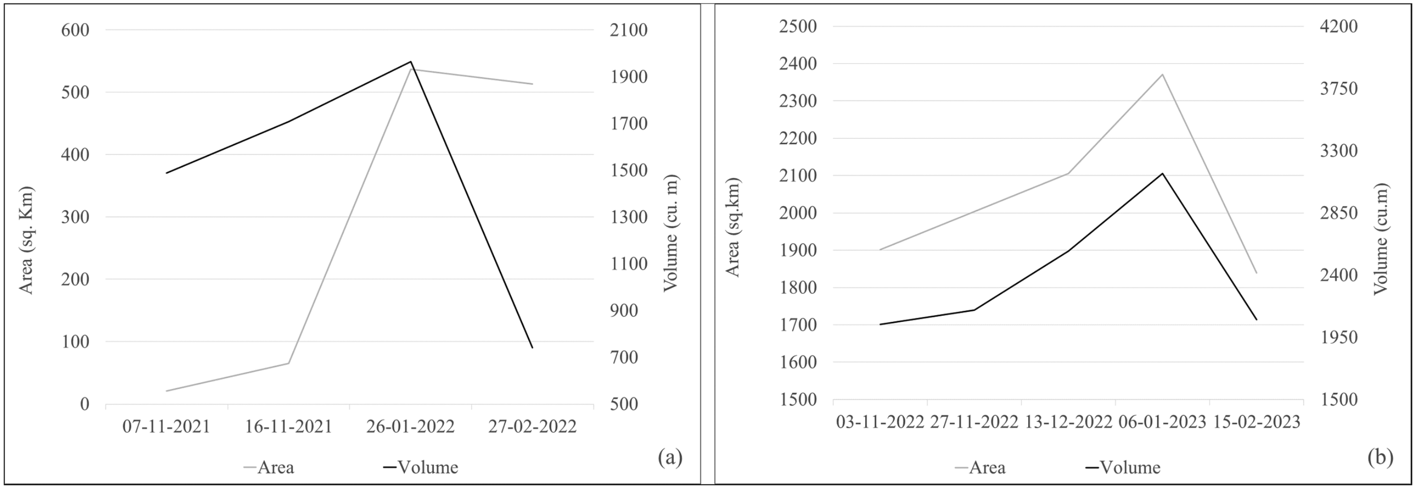

FIGURE 19.5 Area and volume profile of melt ponds and SGLs for (a) Austral summer 2021–22 and (b) Austral summer 2022–23.

The following observation was made for the Austral summer 2022–23 (Figure 19.5b):

- The number of MPs and SGLs was found to increase during November 2022–January 2023 from 10–80 with a gradual increase in area.
- The pond draining mechanism has been observed during post-December 2022 as the average depth and volume have decreased.
- The refreezing of MPs and SGLs started in mid-February 2023.

The MPs and SGLs over ice shelves can have potential impacts on global sea level rise, marine ecosystems, and circulation patterns of the ocean. As the planet continues to warm, the formation of MPs and SGLs is likely to increase, leading to further influences on the Earth's systems. Hence, it is important to monitor and understand the effects of MPs and SGLs on ice shelves and the environment, to mitigate their impacts and inform climate change policies.

The observation shows that lakes on the ice shelf disappear through three primary mechanisms: supra-glacial drainage occurring through channels, englacial drainage taking place within the firn layer, and surface refreezing or snowfall-induced burial. Among these mechanisms, refreezing or burial by snowfall is the most common way that lakes disappear at the end of the melt season. This is typically due to the presence of (past) frozen lake scars, which appears similar to refrozen lakes. The primary process behind the disappearance of lakes often involves the development of ice 'lids' originating from the lake centres. These lids gradually expand, eventually enveloping the entire lake surface and causing the cessation of further thawing.

The physical processes that govern these mechanisms of lake disappearance are complex and may depend on several factors, including the thickness and thermal properties exhibited by the ice shelf, the distribution and volume of the MPs and SGLs, and the local meteorological conditions.

The results obtained through modelling have been confirmed and validated through on-site data collected during the 42nd Indian Scientific Expedition to Antarctica (42-ISEA), which took place from November 2022 to February 2023. This validation was carried out specifically on a melt pond within the cDML area. The melt pond is located at 110 45′ 6.79" E and 700 46′ 22.46" S near Maitri Indian research base at Schrimacher Oasis, cDML. Melt pond depth has been measured physically at six different ground validation point (GVP) locations around the water surface, as shown in Figure 19.6. Depth measurements derived from the MPD model are compared with GVPs and found to be in very good correlation, making the MPD model more intuitive and robust for Antarctica melt pond and SGL studies.

19.5 CONCLUSION

Meltwater can have a significant impact on an ice shelf, as it can contribute to the breakup and destabilization of the ice shelf. This study aims to monitor the dynamics of MPs and SGLs on the surface of the NIS in Dronning Maud Land, East Antarctica, using a newly developed MPD model. The model has been used to analyse the depth and volume of the MPs and SGLs from Landsat-8/9 datasets during the Austral summer of 2021–2022 and 2022–2023. Based on the results, it is observed that the estimated maximum depth of the MPs and SGLs has increased by 1.5 times, and the

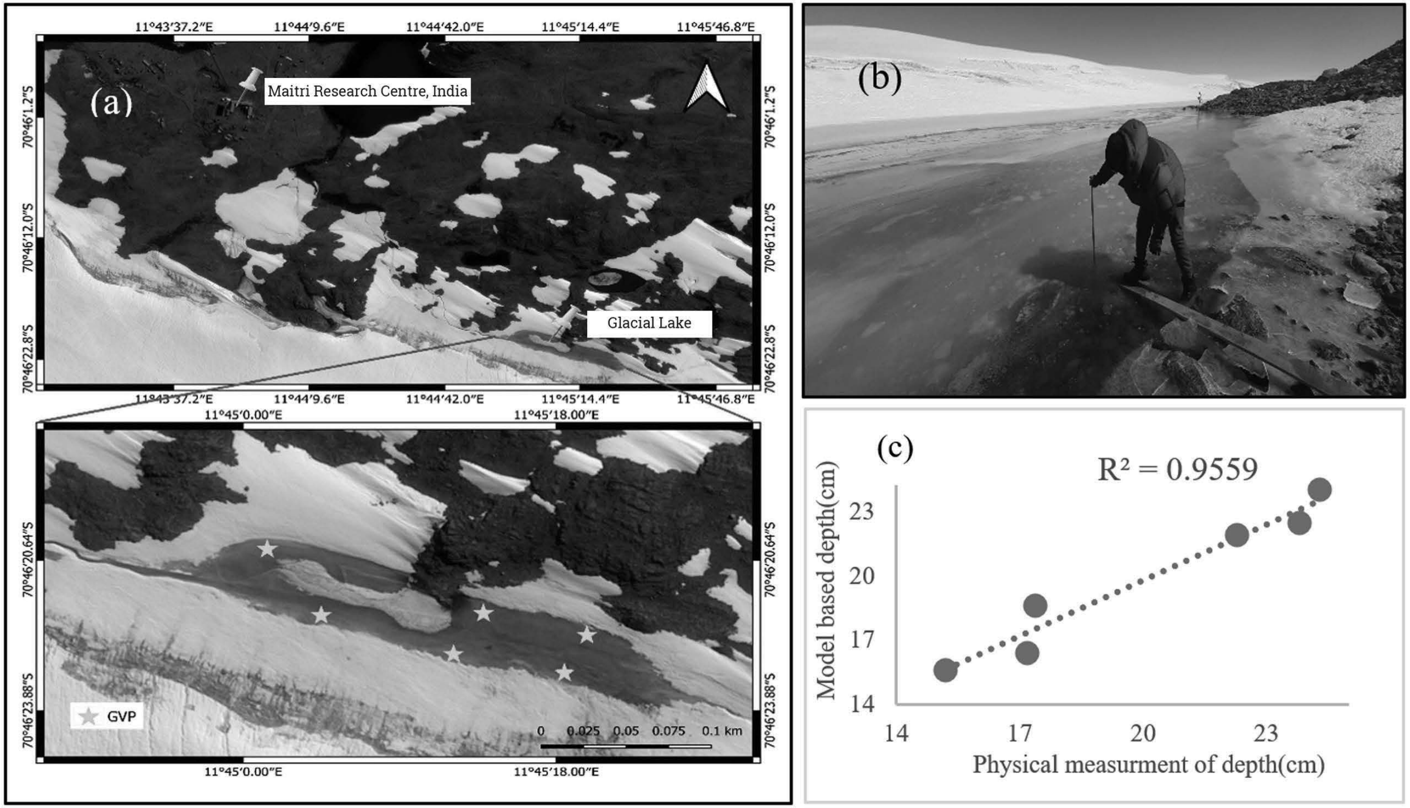

FIGURE 19.6 Ground truth validation: (a) GVP locations; (b) manual depth estimation by CIIRC team in cDML on 13 December, 2022; (c) correlation of depths estimated from MPD model and manual depth.

volume of meltwater has increased eight times during January 2023 in comparison to January 2022, while the average depth remained constant. In essence, the influence of meltwater on an ice shelf hinges on factors such as the quantity and dispersion of the water, alongside the general state and resilience of the ice shelf. As climate change leads to increased melting of ice sheets, the impacts of meltwater are becoming a growing concern for scientists and policymakers.

19.6 ACKNOWLEDGMENT

The authors express their sincere gratitude for the valuable support and collaboration provided by PTICL and Dr. Krishna Venkatesh, Director of CIIRC—Jyothy Institute of Technology in Bengaluru. Additionally, the authors appreciate the logistical assistance extended by the National Centre for Polar and Ocean Research, Ministry of Earth Sciences, Government of India, as part of the Indian Scientific Expedition to Antarctica (ISEA), which enabled them to conduct this research.

REFERENCES

Alley KE, Scambos TA, Miller JZ, et al. (2018) Quantifying vulnerability of Antarctic ice shelves to hydrofracture using microwave scattering properties. *Remote Sens Environ* 210:297–306. https://doi.org/10.1016/j.rse.2018.03.025

Banwell AF, Caballero M, Arnold NS, et al. (2014) Supraglacial lakes on the Larsen B ice shelf, Antarctica, and at Paakitsoq, West Greenland: A comparative study. *Ann Glaciol* 55:1–8. https://doi.org/10.3189/2014AoG66A049

Banwell AF, MacAyeal DR, Sergienko OV. (2013) Breakup of the Larsen B Ice Shelf triggered by chain reaction drainage of supraglacial lakes. *Geophys Res Lett* 40:5872–5876. https://doi.org/10.1002/2013GL057694

Geetha Priya M, Deva Jefflin AR, Luis AJ, Bahuguna IM (2022) Estimation of surface melt induced melt pond depths over Amery Ice Shelf, East Antarctica using Multispectral and ICESat-2 data. *Disaster Adv* 15:1–8. https://doi.org/10.25303/1508da01008

Horwath M, Dietrich R, Baessler M, et al. (2006) Nivlisen, an Antarctic ice shelf in Dronning Maud Land: Geodetic-glaciological results from a combined analysis of ice thickness, ice surface height and ice-flow observations. *J Glaciol* 52:17–30. https://doi.org/10.3189/172756506781828953

Lindbäck K, Moholdt G, Nicholls KW, et al. (2019) Spatial and temporal variations in basal melting at Nivlisen ice shelf, East Antarctica, derived from phase-sensitive radars. *Cryosphere* 13:2579–2595. https://doi.org/10.5194/tc-13-2579-2019

Masek JG, Wulder MA, Markham B, et al. (2020) Landsat 9: Empowering open science and applications through continuity. *Remote Sens Environ* 248. https://doi.org/10.1016/j.rse.2020.111968

Pande A, Sivakumar K, Sathyakumar S, et al. (2017) Monitoring wildlife and their habitats in the southern ocean and around Indian research stations in Antarctica. *Proc Indian Natl Sci Acad* 83:483–496. https://doi.org/10.16943/ptinsa/2017/48958

Robel AA, Banwell AF (2019) A speed limit on ice shelf collapse through hydrofracture. *Geophys Res Lett* 46:12092–12100. https://doi.org/10.1029/2019GL084397

Shelf SI, Arthur JF, Stokes CR, et al. (2020) Distribution and seasonal evolution of supraglacial lakes on shackleton ice shelf, East Antarctica. *The Cryosphere* 14:4103–4120.

Zhang Z, He G, Wang X (2010) A practical DOS model-based atmospheric correction algorithm. *Int J Remote Sens* 31:2837–2852. https://doi.org/10.1080/01431160903124682

Index

Note: Page numbers in *italics* indicate figures, and page numbers in **bold** indicate tables in the text

C

D

E

F

Q

R

S

T

U

W

X

Z